DARK ENERGY PHENOMENA IN COSMOLOGY

A thesis submitted to

DELHI TECHNOLOGICAL UNIVERSITY

in partial fulfillment of the requirements of the award of the degree of

DOCTOR OF PHILOSOPHY

in

APPLIED MATHEMATICS

by

MILAN SRIVASTAVA, M.Sc.

under the supervision of

Dr. Chandra Prakash Singh, Ph.D.

Associate Professor

DEPARTMENT OF APPLIED MATHEMATICS

DELHI TECHNOLOGICAL UNIVERSITY

(Formerly Delhi College of Engineering)

BAWANA ROAD, DELHI-110 042, INDIA.

September, 2018 **Enroll. No. : 2K13/Ph.D./AM/02**

DECLARATION

I declare that the research work reported in this thesis entitled "**Dark Energy Phenomena in Cosmology**" for the award of the degree of *Doctor of Philosophy in Mathematics* has been carried out by me under the supervision of *Dr. Chandra Prakash Singh*, Associate Professor, Department of Applied Mathematics, Delhi Technological University, Delhi, India.

The research work embodied in this thesis, except where otherwise indicated, is my original research. This thesis has not been submitted by me earlier in part or full to any other University or Institute for the award of any degree or diploma. This thesis does not contain other person's data, graphs or other information, unless specifically acknowledged.

Date : **(Milan Srivastava)**

CERTIFICATE

On the basis of declaration submitted by **Ms. Milan Srivastava**, student of Ph.D., I hereby certify that the thesis titled **"Dark Energy Phenomena in Cosmology"** submitted to the Department of Applied Mathematics, Delhi Technological University, Delhi, India for the award of the degree of *Doctor of Philosophy in Mathematics*, is a record of bonafide research work carried out by her under my supervision.

I have read this thesis and that, in my opinion, it is fully adequate in scope and quality as a thesis for the degree of Doctor of Philosophy.

To the best of my knowledge the work reported in this thesis is original and has not been submitted to any other Institution or University in any form for the award of any Degree or Diploma.

(Dr. Chandra Prakash Singh)
Associate Professor & Supervisor
Department of Applied Mathematics
Delhi Technological University
Delhi, India.

(Dr. Sangita Kansal)
Professor & Head
Department of Applied Mathematics
Delhi Technological University
Delhi, India.

ACKNOWLEDGEMENTS

This thesis becomes a reality with the kind support and help of many individuals. I would like to extend sincere thanks to all of them.

Foremost, I want to offer this endeavor to our **God Almighty** for the wisdom he bestowed upon me, the strength, the peace of mind and good health in order to finish this Ph.D. work.

I submit my heartiest gratitude to my respected supervisor Dr. Chandra Prakash Singh, Associate Professor, Department of Applied Mathematics, Delhi Technological University (DTU), Delhi, India for his inspiring guidance and continuous support of my Ph.D. study and related research, for his patience, motivation, and immense knowledge. It is indeed a great pleasure for me to work under his supervision. His guidance has helped me in all the time of research and writing of this thesis.

I place on record, my sincere gratitude to Prof. Sangita Kansal, Head, Department of Applied Mathematics, DTU, for providing me the necessary facilities and constant encouragement during the progress of the work.

I extend my sincere thanks to Prof. H. C. Taneja, Dean (Academic, PG), DTU for his constant support and guidance. I also take this opportunity to record our sincere thanks to all the faculty members of the Department for their help and encouragement.

I am extremely grateful to Prof. Shri Ram, Ex. Head, Department of Mathematics, IIT, BHU, Varanasi, and Prof. S. G. Ghosh, CTP, JMI, New Delhi for their valuable guidance and encouragement extended to me during Ph.D. work.

I gratefully acknowledge the academic branch and administration of DTU for providing the environment and facilities to carry out my research work. I also express my thanks to office staffs of the Department for their all kind of support.

I would like to thank Dr. Vijay Singh, Dr. Virendra Kumar, Dr. Pankaj Kumar and Mr. Ajay Kumar for valuable discussions on the subject matter and for their support. My thanks and appreciations also go to my friends who have willingly help me out with their abilities.

I humbly extend my thanks to all concerned persons who have not been mentioned here but supported, encouraged and inspired me during my Ph.D. work.

I gratefully acknowledge University Grants Commission (UGC), Government of India, for providing fellowship (JRF and SRF) that made my Ph.D. work possible.

While writing the thesis, I have consulted many standard books and references. I am indebted to the authors of these books and references.

Last but not the least, I would like to express my gratitude towards my family: my parents and my brother for supporting me spiritually throughout my Ph.D. work and my life in general. Thank you all.

Date : **(MILAN SRIVASTAVA)**

Place : Delhi, India.

Dedicated

to

My Family

Contents

Preface

Important observational developments in the last two decades have much enlarged the scope of cosmological studies. Therefore, cosmology has become a precision science to understand early as well as late time evolutionary behaviour of the Universe. The rapid development in observational cosmology which started during late 1990s shows that the Universe passes two phases of cosmic acceleration:

The first cosmic accelerated phase, which is known as the inflationary phase as proposed by Alan Guth in 1981, is believed to have occurred prior to the radiation-dominated era. Inflationary phase is basically a short period of rapid expansion in the very early Universe, at the end of which the description of the standard big bang model is applied. The inflationary scenario actually means a period of phase transition which is controlled by a scalar field. The scalar field may contribute to the negative pressure and once the phase transition is over, the scalar field decays away and the inflationary expansion terminates. This phase not only resolves the flatness and horizon problems, but also explains a nearly flat spectrum of temperature anisotropies observed in Cosmic Microwave Background (CMB).

The second cosmic accelerated phase, which is known as the late time acceleration, is assumed to have started after the matter-dominated phase. This recent transition from decelerating phase to the accelerating phase has been observed by a number of observations such as the measurements of SNe Ia, CMB, Large Scale Structures (LSS), Baryon Acoustic Oscillations (BAO),Wilkinson Microwave Anisotropy Probe (WMAP) and very recent Planck Collaboration. These observations predict that some unknown matter with negative pressure gives rise to this late time cosmic acceleration, which is popularly known as “Dark Energy”. It is a hypothetical type of energy that fills all of space and is responsible to increase the expansion rate of the Universe. Nowadays, the quest to understand this cosmic acceleration is the most competitive challenge in the current cosmology. To explain the accelerated expansion, the modern

cosmology requires two outstanding concepts: (i) the matter which does not interact with the electromagnetic force - known as dark matter (DM) and (ii) the hypothetical energy that is responsible to increase the expansion rate of the Universe, known as dark energy (DE).

Nowadays, the study of dark energy models are of great interest in general theory of relativity as well as in modified theories of gravitation. This thesis is devoted to investigate both isotropic Friedmann-Robertson-Wlaker (FRW) and anisotropic Bianchi models in general theory of relativity and modified theories of gravitation, namely, Brans–Dicke, $f(R,T)$ gravity theory. The holographic dark energy is also a possible choice to explain current acceleration of the Universe. It has been investigated that bulk viscosity may be one of the possible candidate to explain such phenomena of the Universe. A theoretical approach has been followed to understand the cosmic acceleration in the framework of these theories of gravitation.

The central problem investigated in this thesis is the role of scalar field and bulk viscosity in explaining the dark energy phenomena in cosmology. In doing this we have studied holographic dark energy with and without bulk viscosity. The thesis entitled **"Dark Energy Phenomena in Cosmology"** comprises eight chapters. The bibliography and the list of publications have been given at the end of the thesis.

Chapter 1 offers a general introduction of the study in general relativity. It includes the brief overview of the cosmology with tensor calculus to build the cosmological models. Some important cosmological parameters, which describe the physical and the geometrical properties of the Universe, have been discussed. The concept of DE and DM with equation of state parameter have been discussed. The exotic matter like scalar field and its energy-momentum tensor has been described briefly. The bulk viscosity has been introduced in the model to explore the possible candidate for an accelerating Universe. The holographic dark energy and new holographic dark energy have been discussed for explaining the concept of DE. The modified theories of gravitation like Brans–Dicke theory and modified $f(R,T)$ gravity theory have been discussed in detail. The purpose of this chapter is to provide the motivation of the work carried out in the thesis.

Chapter 2 deals with the dynamics of non-interacting and interacting holographic dark energy models in Brans–Dicke theory. We have considered the future event horizon as an infrared cutoff. The field equations have been solved by assuming the Brans–Dicke scalar field as a logarithmic form of scale factor instead of gener-

al power-law form of scale factor. This assumption gives the time-dependent value of the deceleration parameter which explains the phase transition of the evolution of the Universe. We have noticed that the model is able to explain the early time inflation as well as late time acceleration. It has also been observed that in late time the crossing of phantom divide line may be possible for the equation of state parameter. The model is more appropriate to achieve a less acute coincidence problem in non-interacting model whereas a soft coincidence can be achieved if coupling parameter in interacting model has small value. The content of this work has been published as a research paper entitled "**Cosmological evolution of non-interacting and interacting holographic dark energy model in Brans-Dicke theory**, *International Journal of Geometric Methods in Modern Physics*, **15**, 1850124 (2018)".

In **chapter 3**, we have explored bulk viscosity as a candidate of DE. Viscous new holographic DE model has been discussed with Ricci scalar as an infrared cutoff, proposed by Granda and Oliveros. It is thought that the negative pressure caused by the bulk viscosity can behave as a DE component and drive the acceleration of the Universe. We have presented four possible solutions of the model based on the choice of the different forms of the bulk viscosity. The solutions for scale factor as well as deceleration parameter have been obtained to discuss the evolution of the Universe. We have also studied two independent geometrical diagnostics: statefinder pair and *Om*, to discriminate this model with other available DE models. The content of this chapter has been published as a research paper entitled, "**Viscous cosmology in new holographic dark energy model and the cosmic acceleration**, *European Physical Journal C* **78**, 190 (2018)".

Chapter 4 is the extension of above work in $f(R,T)$ gravity theory. We have investigated constant bulk viscous new holographic DE model in $f(R,T)$ gravity theory. From the viewpoint of the fluid description and the current observational data, there is no reason for excluding the imperfect fluid due to the presence of bulk viscosity. We have obtained the solution for both cases, without viscous and with constant viscous new holographic DE models. In the model without viscosity, the scale factor has the form as power-law type and deceleration parameter is constant so this model can not explain the phenomena of phase transition. In constant viscous model, the scale factor is of exponential type. In early time it expands with decelerated rate whereas in late time it expands with accelerated rate. The expansion rate depends on the coefficient of bulk viscosity. The phase transition of the Universe from deceleration to acceleration has

been observed as the deceleration parameter is time-dependent. We have studied statefinder and *Om(z)* diagnostics for viscous new holographic DE in $f(R,T)$ gravity to compare this model with the other available DE models. The thermodynamics and the local entropy have been discussed for this model. The model preserves the validity of the second law of thermodynamics as the bulk viscous coefficient is always positive during the evolution of the Universe. We have also discussed the finite-time future singularity and found that the model shows the Type I (Big-Rip) singularity and Type III singularity. The content of this chapter has been published in the form of research paper entitled "**New holographic dark energy model with constant bulk viscosity in modified $f(R,T)$ gravity theory**, *Astrophysics and Space Science* **363**, 117 (2018)".

In **chapter 5**, we extend our work with a most general form of bulk viscosity in new holographic DE in $f(R,T)$ gravity. We have classified all possible evolutions with different parameters constraints. Some analysis have been carried out by plotting the graph between scale factor with time. The phase transition from deceleration to acceleration is observed at early or late time depending on bulk viscous coefficients. We have also discussed the nature of deceleration parameter. Statefinder and *Om(z)* diagnostics have been carried out for viscous new holographic dark energy model. The nature of bulk viscous coefficient has been discussed through the graph which shows that it is positive for a range of viscous term. The entropy and the generalized second law of thermodynamics has been investigated. We have observed that the generalized second law of thermodynamics always valid under certain restrictions on bulk viscous coefficients. The content of this chapter is submitted for publication in the form of research paper entitled "**Evolution and thermodynamics of new holographic dark energy with bulk viscosity in modified $f(R,T)$ gravity**; [arXiv:1804.05693 [gr-qc]]".

In **chapter 6**, we have investigated the spatially homogeneous and anisotropic Bianchi-I model with a minimally coupled scalar field. A non-interacting combination of scalar field and perfect fluid as a source of matter components has been considered. To solve the system of equations, an exponential form of average scale factor with scalar field has been assumed. We have considered the solution for two cases: flat potential and exponential potential. Explicit form of average scale factor, energy density and pressure of the scalar field and perfect fluid, and their respective equation of state parameters have been obtained. Other geometrical and physical parameters like expansion scalar, deceleration parameter, anisotropy parameter, and shear scalar

have been calculated and their physical interpretations have been discussed. In flat potential and exponential potential models we have obtained power-law scale factor which expands with decelerated rate. We have found the scalar field as logarithmic form. The scalar potential decreases with time and vanishes in late time. We have observed that the universe is expanding but rate of expansion , measure of anisotropy and shear scalar decrease to zero and become isotropic in late time. This chapter is based on a published research paper entitled "**Minimally coupled scalar field cosmology in anisotropic cosmological model**, *Pramana Journal of Physics* **88**, 22 (2017)".

Chapter 7 deals with the dynamical evolution of a homogeneous and anisotropic Bianchi-V model filled with perfect fluid and scalar field. These two sources are assumed to be non-interacting. We have assumed that the average scale factor and scalar potential are of exponential functions of scalar field. We have used the observational data to find the parameters used in the model. The role of scalar field through the variable equation of state parameters are studied. It has been observed that equation of state parameters change from phantom region to quintessence region for small values of parameters, respectively. We have concluded that the model shows phantom behavior in early time and quintessence in late time evolution. For large values of parameters, it varies in quintessence region only. We have also studied the statefinder parameters and obtained that the model behaves like ΛCDM or $SCDM$ depending on the values of parameters. This chapter has been published in a research paper entitled "**Dynamics of Bianchi V anisotropic model with perfect fluid and scalar field**, *Indian Journal of Physics* **91**, 1645 (2017)".

At the last, we summarize what results have come out in this thesis. We have also presented the future scope of the current work. As we have seen that the bulk viscosity may play a vital role in explaining the dark energy phenomena, therefore, the further investigation is needed to understand the role of bulk viscosity. The investigation carried out in the present work provides the explanation of early as well as late time evolution of the Universe. It would be interesting to investigate in modified theory with different exotic matter of content which could possibly solve the problems related to the late time evolution of the Universe.

Finally, the bibliography and list of author's publications have been given at the end of the thesis.

List of Figures

List of Tables

Chapter 1

Introduction

The introductory chapter includes the brief overview of the cosmology which explains the evolution of the Universe. In this chapter, we discuss general theory of relativity, early time inflation, late-time acceleration and the modified theory of gravity, especially the Brans–Dicke theory and $f(R,T)$ theory. The cosmological parameters and the geometrical parameters of cosmological models are also explained. The viscosity mechanism in cosmology is discussed. This chapter also includes the motivation of the thesis work.

The origin and evolution of the Universe are two of the most actively researched areas in cosmology. Cosmologists convince that the Universe came into existence at a definite moment in time, some 13.6 billion years ago, in the form of a super hot, super dense fireball of energetic radiation known as the **Big Bang** event. Recent cosmological observations have completely changed the prospective of the researchers about the understanding of the Universe. The Universe which is expanding with an accelerated rate, is the most important observational result of the modern cosmology, which was first discovered by Hubble in 1929 [1]. Let us start this chapter with the brief introduction of the Einstein's general theory of relativity [2].

1.1 General theory of relativity

There are two fundamental theories in physics which study the behavior of matter: Newtonian theory of gravitation which describes the behavior of one mass point on the other, and the electrodynamics describing the behavior of charged matter in the presence of electromagnetic fields. The theory of relativity is divided into two parts: Special theory of relativity (STR) which had its origin in the development of electrodynamics, and General theory of relativity (GTR) which is the relativistic theory of gravitation. The STR leads with the systems known as inertial systems, that is, the systems which move in uniform rectilinear motion relative to one another. According to this "All systems of co-ordinates are equally suitable for description of physical phenomena". Only two years after the publication of his STR, Einstein in 1907 wrote a paper attempting to modify Newton's theory of gravitation to fit STR. Einstein extended this principle to accelerated systems, i.e., the systems moving with accelerated velocity relative to one another, the theory of relativity is called **"general theory of relativity (GTR)"**, which was published by Albert Einstein in 1916. GTR explains that the force of gravity which we perceive arises from the curvature of space and time. The GTR is applicable to the laws of gravitation and explains it in a more refined manner than given by Isaac Newton.

General theory of relativity, with its fundamental feature of a dynamical space-time, offers a natural conceptual framework for cosmology. Furthermore, GTR can simply accommodate the possibility of a constant "vacuum energy density" giving rise to a repulsive gravitational force. Such an agent is the key ingredient of modern cosmo-

logical theories of the Big Bang (the inflationary cosmology) and of the accelerating Universe (having a dark energy). GTR successfully passes the solar system tests, and explains the perihelion of mercury and bending of light near the Sun. GTR is based on two main principles:-

- **The principle of general covariance:-** The laws of Physics retain their same form in all coordinate systems, i.e., the laws of physics remain covariant independent of the frame of reference. According to this principle the equations governing the laws of the physics must be expressed in the tensorial form.

- **The principle of equivalence:-** In a local experiment, the gravitational field can be obtained by a suitable accelerating frame of reference. In other words, an inertial observer is locally equivalent to a free-falling observer in a gravitational field. Any local experiment can't distinguish these two situations.

1.2 The Metric or line element

Einstein's general theory of relativity is a geometric theory of gravity. An expression which expresses the distance between two adjacent points is called a metric or line element. It also explains the space-time geometry. In GTR, one time coordinate ($x^0 = ct$) along with the three space coordinates (x^1, x^2, x^3) are used to represent the coordinates of the four dimensional space-time (x^μ, *i.e.*, x^0, x^1, x^2, x^3). The most general tensorial form of the line-element, ds^2 in general relativity, which is related to the coordinates dx^μ of the space-time manifold through metric tensor $g_{\mu\nu}$, is represented by

$$ds^2 = g_{\mu\nu}\, dx^\mu dx^\nu. \tag{1.2.1}$$

The Greek indices μ and ν run from 0 to 3 and $g_{\mu\nu}$ denotes the covariant form of the metric tensor of rank 2 and its components are the functions of coordinates x^μ subject to the restriction $g =$ determinant of $g_{\mu\nu}$, *i.e.*, $|g_{\mu\nu}| \neq 0$. Since the coordinate lines are orthogonal to each other, thus the diagonal metric is formed in an orthogonal coordinate system. In this thesis we use only orthogonal coordinate systems. The line-element $(1.2.1)$ represents the curved geometry of space-time. The metric tensor obeys the transformation law

$$g_{\bar{\mu}\nu} = \frac{\partial x^i}{\partial \bar{x}^\mu} \frac{\partial x^j}{\partial \bar{x}^\nu}\, g_{ij}, \tag{1.2.2}$$

where the quantities carrying bar correspond to the new coordinate system. The contravariant metric tensor $g^{\mu\nu}$ can be defined as

$$g^{\mu\nu} = \frac{\text{cofactor of } g_{\mu\nu} \text{ in } g}{g}. \tag{1.2.3}$$

The metric tensor $g^{\mu\nu}$ is reciprocal of $g_{\mu\nu}$. This is also a symmetric tensor of rank two and is called the conjugate metric tensor. Greek indices running from 0 to 3 has been used in this thesis for the summation convention and geometrized units are used.

1.3 Basic formalism

We start by the outline of the general relativity theory, setting speed of light (c) equals to one. With $g_{\mu\nu}$ being a fundamental tensor (metric tensor) we introduce the projection tensor

$$h_{\mu\nu} = g_{\mu\nu} + U_\mu U_\nu, \tag{1.3.1}$$

and rotation tensor

$$\omega_{\mu\nu} = h^\alpha_\mu h^\beta_\nu U_{(\alpha;\beta)} = \frac{1}{2}\left(U_{\mu;\alpha}h^\alpha_\nu - U_{\nu;\alpha}h^\alpha_\mu\right). \tag{1.3.2}$$

The expansion scalar is

$$\theta_{\mu\nu} = h^\alpha_\mu h^\beta_\nu U_{(\alpha;\beta)} = \frac{1}{2}\left(U_{\mu;\alpha}h^\alpha_\nu + U_{\nu;\alpha}h^\alpha_\mu\right), \tag{1.3.3}$$

and has the trace $\theta \equiv \theta^\mu_\mu = U^\mu_{;\mu}$. The shear tensor is

$$\sigma_{\mu\nu} = \theta_{\mu\nu} - \frac{1}{3}h_{\mu\nu}\theta, \tag{1.3.4}$$

which satisfies $\sigma^\mu_\mu = 0$. The fluid velocity is

$$U_{\mu;\nu} = \omega_{\mu\nu} + \sigma_{\mu\nu} + \frac{1}{3}h_{\mu\nu}\theta - A_\mu U_\nu, \tag{1.3.5}$$

where A_μ stands for the four-acceleration, namely $A_\mu = \dot{U}_\mu = U^\nu U_{\mu;\nu}$.

The above formalism is for a general geometry. In the following we will focus on Friedmann-Robertson-Walker (FRW) geometry, which is of main interest in cosmolo-

gy.

1.3.1 Homogeneous and isotropic metric

The most general representation of the curved space-time line-element is defined by (1.2.1) but it is being very difficult to study the cosmological models with this metric. Therefore, Friedmann [3] used cosmological principle to simplify the models. To build the standard cosmological model at a large scale in the framework of GTR, the cosmological principle (CP) is taken into consideration which is the most simplest assumption for it. In modern cosmology, the CP states that at a very large scale the distribution of the galaxies is uniform and the appearance of it is same at every direction. Thus, CP has two most important mathematical properties of the Universe: homogeneous and isotropic nature of the Universe at a very large scale ($\gg 100\,Mpc$) at each instant of cosmic time. This implies that the appearance of the Universe is same at every place and same in every direction too. It may change only along the time axis. Then the Universe has to be maximally symmetric as far as three dimensionally space is concerned. In case of homogeneous and isotropy [1], the line-element can be described by a simplest way as

$$ds^2 = dt^2 - a^2(t)\left[dx^2 + dy^2 + dz^2\right], \tag{1.3.6}$$

where we consider speed of light $c = 1$ throughout the thesis, $a(t)$ stands for the scale factor, depends on the cosmic time t, which is related to the expansion (possible contraction) of the Universe. The line-element (1.3.6) is called the flat Robertson-Walker metric (RW). It is called the Friedmann-Robertson-Walker (FRW) metric when the scale factor obeys the Einstein's field equations (see, section 1.4). In case of spherical coordinate system where $x^0 = t$, $x^1 = r\sin\theta\cos\varphi$, $x^2 = r\sin\theta\sin\varphi$, $x^3 = r\cos\theta$, the line-element (1.3.6) can be rewritten as [4]

$$ds^2 = dt^2 - a^2(t)\left[\frac{dr^2}{1-kr^2} + r^2(d\theta^2 + sin^2\theta d\varphi^2)\right], \tag{1.3.7}$$

where k represents the curvature of the spatial sections. It can have three values -1, 0 and $+1$ for open, flat and closed Universes, respectively, and $0 \leq \theta \leq \pi$ and

[1] Homogeneity means that space "looks the same everywhere" and spatial isotropy means that space "looks the same in every direction"

$0 \leq \varphi \leq 2\pi$. The FRW model (1.3.7) describes the time evolution of a homogeneous and isotropic Universe that gets larger in time as $a(t)$ increases and smaller as $a(t)$ decreases. All the information about the evolution of the Universe is contained in this one function determined by the Einstein's field equations. The coordinates $(t,\, r,\, \theta,\, \varphi)$ of FRW metric shows *comoving coordinates* [2]. Most of the thesis work are based on FRW line-element (1.3.6).

1.3.2 Homogeneous and anisotropic metric

Many observations, like Cosmic Microwave Background (CMB) [5] and Wilkinson Microwave Anisotropy Probe (WMAP) [6], confirm that the Universe is anisotropic, which is quiet interesting to know. Many theoretical models also confirm that initially the Universe was in anisotropic stage but in late-time of the evolution it corresponds to an isotropic one. Anisotropic model have a significant place in description of evolution of the early phase of the Universe. The Bianchi type models are spatially homogeneous cosmological models that in general are anisotropic. These models are the generalization of standard homogeneous and isotropic FRW models. Bianchi models I to IX present a middle way between FRW model and inhomogeneous and anisotropic Universe and thus important in modern cosmology. Bianchi type I - IX line elements are the most common anisotropic line-elements which are widely used [7]. The most simplest model among all the types of Bianchi is the Bianchi type-I (B-I). The line-element of the homogeneous and anisotropic B-I is defined as

$$ds^2 = dt^2 - A^2(t)dx^2 - B^2(t)dy^2 - C^2(t)dz^2, \tag{1.3.8}$$

where $A(t)$, $B(t)$ and $C(t)$ stand for the directional scale factors in the respective direction of the coordinate axes x, y, z, respectively. For the particular case when $A = B = C$, the line-element (1.3.8) reduces to flat FRW model (1.3.6), and if $A \neq B = C$ (or $A = B \neq C$ or $A = C \neq B$), the line-element (1.3.8) is said to be the locally-rotationally-symmetric (LRS) B-I model whereas $A \neq B \neq C$ gives totally anisotropic B-I model. Bianchi type-V (B-V) model is also one among all the homogeneous and anisotropic Bianchi types. The line-element of homogeneous and anisotropic B-V is described by

$$ds^2 = dt^2 - A^2(t)dx^2 - e^{2mx}[B^2(t)dy^2 - C^2(t)dz^2], \tag{1.3.9}$$

[2] Comoving means that the coordinate system follows the expansion of space, so that the space coordinates of objects which do not move remains the same.

where $A(t)$, $B(t)$ and $C(t)$ have their usual meanings and m is a constant.

1.4 Einstein's field equations

The key equation of general relativity is Einstein's field equations, which is relativistic equivalent of Poisson's equation of Newtonian dynamics. According to Newton's theory of gravitation the field equations in the presence of matter are given by [8]

$$\nabla^2\Phi = 4\pi G\rho, \tag{1.4.1}$$

where Φ is the gravitational potential, ρ is the density of matter and G is gravitational constant. Equation $(1.4.1)$ is the Poisson's equation which gives a mathematical relation between the gravitational potential Φ at a point in space and the mass density ρ at that point. Since in non-relativistic limit g_{00} plays the role of gravitational potential, therefore, Φ must be replaced by the metric tensor $g_{\mu\nu}$ in the relativistic theory of gravitation. Hence, from Eq. $(1.4.1)$ it follows that the left hand side must be expressed in terms of the second order derivatives of $g_{\mu\nu}$. As ρ is the density of matter which is one of the components of second rank energy-momentum tensor, the right hand side of $(1.4.1)$ must be expressed in terms of the material energy tensor $T_{\mu\nu}$ in relativistic theory of gravitation such that the divergence of $T_{\mu\nu}$ must vanishes. Thus, the generalization of $(1.4.1)$ for relativistic theory of gravitation can be written as

$$G_{\mu\nu} = R_{\mu\nu} - \frac{1}{2}g_{\mu\nu}R = \kappa T_{\mu\nu}, \tag{1.4.2}$$

where $G_{\mu\nu}$ is the Einstein tensor, $\kappa = 8\pi G$ with G as a Newton's gravitational constant and $R = g_{\mu\nu}R^{\mu\nu}$ is the Ricci scalar curvature with $R^{\mu\nu}$ as a Ricci curvature tensor. Equations $(1.4.2)$ are the required field equations in GTR in the presence of matter and represent the Einstein's field equations for naturally curved material world. Einstein's field equations give a mathematical relation between the metric of space-time at a point and the energy and the pressure at that space-time point. The trajectories of freely moving objects then correspond to geodesics curved space-time.

A gravitational action, known as Einstein-Hilbert (EH) action can also describe GTR and yield the Einstein's field equations. In general relativity, the action is usually assumed to be a function of metric tensor $g_{\mu\nu}$. On including the matter field, the

EH action for gravity proposed in 1915 by David Hilbert can be written as [4]

$$S = \int \left(\frac{1}{2\kappa} R + \mathscr{L}_m \right) \sqrt{-g}\, d^4x, \tag{1.4.3}$$

where $\mathscr{L}_m$ is the matter Lagrangian density of any matter fields. The action principle then requires the variation of this action with respect to the inverse metric $g^{\mu\nu}$ to vanish $\delta S = 0$. After mathematical calculations, we get same Einstein's field equations (1.4.2).

The right hand side of the Einstein's equations (1.4.2) represents the densities of energy and momentum which are the sources of space-time curvature and give the information about the energy density, momentum density, pressure. According to Einstein's theory the matter content is described by energy-momentum tensor which is also known as stress-energy tensor. It is represented by a quantity $T_{\mu\nu}$, which is a second-rank tensor and symmetrical. The energy-momentum tensor for a perfect fluid is

$$T_{\mu\nu} = (\rho + p)\, u_\mu\, u_\nu - p\, g_{\mu\nu}, \tag{1.4.4}$$

where ρ and p represent the energy density and pressure of the fluid, respectively and u^μ is the four-velocity vector such that $g_{\mu\nu} u^\mu u^\nu = 1$. $T_{\mu\nu}$ does not depend on θ and φ even though it is only a function of t due to spatial homogeneity. Thus, the distribution of matter content of the Universe only depends on t. Bianchi identity states that the Einstein tensor $G_{\mu\nu}$ has zero divergence, i.e., $G^{\mu\nu}{}_{;\nu} = \left(R^{\mu\nu} - \frac{1}{2} g^{\mu\nu} R \right)_{;\nu} = 0$. Then, from equation (1.4.2), we can say that $T^{\mu\nu}{}_{;\nu} = 0$, which is known as the conservation law of energy and momentum. This conservation law is physical requirement.

The energy-momentum tensor $T_{\mu\nu}$ is the sum of the stress-energy tensors for the various components of energy, baryons, radiation, neutrinos, dark matter and possible other forms. Einstein's formula (1.4.2) expresses that the energy densities, pressures and shears embodied by the stress-energy tensor determine the geometry of space-time, which, in turn, determine the motion of matter.

1.5 Friedmann cosmology

Let us now discuss a model describing a homogeneous and isotropic Universe for which the Robertson-Walker metric in Eq. (1.3.6) is given.

1.5.1 Friedmann equations

In 1922, a Soviet mathematician and meteorologist, Alexander A. Friedmann was the first person who mathematically predicted an expanding Universe [3]. He derived two independent field equations based on an isotropic and homogeneous Universe from Einstein's field equations (1.4.2) as

$$\frac{\dot{a}^2}{a^2} + \frac{k}{a^2} = \frac{8\pi G}{3}\rho, \tag{1.5.1}$$

$$\frac{2\ddot{a}}{a} + \frac{\dot{a}^2}{a^2} + \frac{k}{a^2} = -8\pi G p, \tag{1.5.2}$$

where an over dot is used to represent the differentiation with respect to cosmic time t. These equations were derived in 1922 by Friedmann, seven years before Hubble's discovery, at a time when even Einstein did not believe in his own equations because they did not allow the Universe to be static. Friedmann's equations did not gain general recognition until after his death, when they were confirmed by an independent derivation (in 1927) by Georges Lemaitre [9].

The expansion (or contraction) of the Universe is inherent to Friedmann's equations. Equation (1.5.1) shows that the rate of expansion, $\dot{a}$, increases with the mass density ρ in the Universe, and Equation (1.5.2) shows that it may accelerate.

We can obtain the following equation, known as 'acceleration equation' by subtracting (1.5.1) from (1.5.2), which is important in discussing the different evolutionary phases of the Universe.

$$\frac{\ddot{a}}{a} = -\frac{4\pi G}{3}(\rho + 3p). \tag{1.5.3}$$

The above equation is also called the Raychauduri equation. From equation (1.5.3), one can observe that for non-exotic perfect fluid (matter and radiation), we always get $\frac{\ddot{a}}{a} < 0$ which implies the non-static behavior of the Universe, i.e., the decelerated expansion of the Universe. But, initially Einstein just considered Friedman's equations as a mathematical curiosity and dismissed these equations and its non-static explanation about the evolution of the Universe. Even, in 1923 Eddington [10] pointed out that the Einstein Universe was unstable.

Further, in 1927, Georges Lemaître [9] independently concluded the same expanding nature of the Universe. Later, in 1929 it was experimentally confirmed by Edwin Hubble [1] that the nature of the Universe is expanding. After this, Einstein stated that introducing the cosmological constant, i.e., the $\Lambda-$ term, into the equations, was the

"biggest blunder of his life". Then, the Λ– term was abandoned for a long time. After some years Einstein's biggest blunder turned out to be strong candidate for the "dark energy" (the major constituent of the present Universe) in the later development of cosmology to explain the accelerating Universe.

1.5.2 Einstein Universe

Consider the static Universe proposed by Einstein. In case of static Universe, the scale factor $a(t)$ would be constant so that $\dot{a} = 0$ and $\ddot{a} = 0$ and the age of the Universe is infinite. Equations (1.5.1) and (1.5.2) then reduces to

$$k = \frac{8\pi G}{3}\rho_0 = -8\pi G p_0, \tag{1.5.4}$$

where ρ_0 stands for present energy density and p_0 stands for present pressure at present time $t = t_0$. Here, we consider $a(t_0) = 1$. In order that the energy density ρ_0 be positive today, k must be $+1$. This leads to the negative pressure.

Einstein corrected this in 1917 by introducing a constant Lorentz-invariant term $\Lambda g_{\mu\nu}$ into the equation (1.4.2). Equation (1.4.2) then becomes

$$R_{\mu\nu} - \frac{1}{2}g_{\mu\nu}R - \Lambda g_{\mu\nu} = 8\pi G\, T_{\mu\nu}, \tag{1.5.5}$$

where Λ is known as cosmological constant. The constant Λ is such that its effect is negligible for phenomena of the solar system or even in our own galaxy but becomes important when the Universe as a whole is considered. With this addition, Friedmann's equations take the form

$$\frac{\dot{a}^2}{a^2} + \frac{k}{a^2} - \frac{\Lambda}{3} = \frac{8\pi G}{3}\rho,, \tag{1.5.6}$$

$$\frac{2\ddot{a}}{a} + \frac{\dot{a}^2}{a^2} + \frac{k}{a^2} - \Lambda = -8\pi G p,. \tag{1.5.7}$$

A positive value of Λ curves space-time so as to counteract the attractive gravitation of matter. Einstein adjusted Λ to give a static solution, which is called the Einstein Universe. In the static case, Eq. (1.5.6) becomes

$$k - \frac{\Lambda}{3} = \frac{8\pi G}{3}\rho_0. \tag{1.5.8}$$

It follows that for a spatially flat Universe

$$\rho_\Lambda = \frac{\Lambda}{8\pi G} = -\rho_0. \tag{1.5.9}$$

But Einstein did not notice that the static solution is unstable. This flaw was only noticed by Eddington in 1930, soon after Hubble's discovery about the expansion of the Universe, in 1929. After that Einstein abandoned his static Universe and withdrew the cosmological constant. H he called this as the 'greatest blunder of my lifetime'.

The Eqs. (1.5.6) and (1.5.7) with a positive Λ is called the Friedmann-Lemaitre Universe or concordance model. Lemaitre noted that if the physics of the vacuum looks the same to inertial observer, its contribution to the energy-momentum tensor is the same as Einstein's cosmological constant Λ. The mathematical contents of Eqs. (1.5.6) and (1.5.7) are not changed if the Λ term moved to the right-hand side, where they appear as corrections to $T_{\mu\nu}$.

1.5.3 Energy conservation law

Let us discuss the conservation of energy-momentum tensor $T_{\mu\nu}$. Differentiating Eq. (1.5.1) with respect to time

$$\frac{d}{dt}(\dot{a^2} + k) = \frac{8\pi G}{3}\frac{d}{dt}(\rho a^2), \tag{1.5.10}$$

we obtain an equation of second order in the time derivative

$$2\dot{a}\ddot{a} = \frac{8\pi G}{3}(\dot{\rho}a^2 + 2\rho a\dot{a}). \tag{1.5.11}$$

Using (1.5.3) and multiplying by $1/a^2$ into (1.5.11), we obtain

$$\dot{\rho} + 3(\rho + p)\frac{\dot{a}}{a} = 0. \tag{1.5.12}$$

This equation does not contain Λ and k, but that is not a consequence of having started from Eqs. (1.5.1) and (1.5.2). If, instead, we start from Eqs. (1.5.6) and (1.5.7), we will get the same equation (1.5.12).

Note that all terms here have dimension of energy density per time. In other words, Equation (1.5.12) states that the change of energy density per time is zero, so we can interpret it as the local energy conservation law. In a volume element dV, ρdV

represents the local decrease of gravitational energy due to the expansion, whereas pdV is the work done by the expansion. Energy does not have a global meaning in the curved spacetime of general relativity, whereas work does. If different forms of energy do not transform into one another, each form obeys Equation (1.5.12) separately.

Equation (1.5.12) can also be derived through thermodynamic point of view. Let the total energy content in a comoving volume a^3 be

$$E = (\rho + p)a^3. \tag{1.5.13}$$

If the expansion is adiabatic, i.e., if there is no net inflow or outflow of energy, then

$$\frac{dE}{dt} = \frac{d}{dt}[(\rho + p)a^3] = 0. \tag{1.5.14}$$

If p does not vary with time, change in ρ and a compensate and equation (1.5.12) immediately follows.

1.5.4 Equation of state

Of the above three equations (1.5.1), (1.5.2) and (1.5.12), only two are independent, since equation (1.5.2) can be derived from Eqs. (1.5.1) and (1.5.12). Thus, we have a system of two independent equations in three unknowns, namely, $a(t)$, $\rho(t)$ and $p(t)$. To solve these unknowns, we need another equation. For this purpose, we use a barotropic equation of state (EoS); a mathematical relation between the pressure and energy density of the stuff that fills up the Universe and is given by

$$p = p(\rho). \tag{1.5.15}$$

In general, EoS can be dauntingly complicated. Condensed matter physicists frequently deal with substances in which the pressure is a complicated nonlinear function of the density. Fortunately, cosmology usually deals with dilute gases, for which the EoS is simple. For substances of cosmological importance, the EoS can be written in a simple linear form:

$$p = (\gamma - 1)\rho = \omega\rho, \tag{1.5.16}$$

where $\omega = (\gamma - 1)$ is a dimensionless number known as EoS parameter. In general relativity, γ is treated as a constant and its value lies in the range $0 \leq \gamma \leq 2$. In reality, the evolution of our Universe is complicated by the fact that it contains different com-

ponents with different EoS.

Using (1.5.16) into (1.5.12), we find a relation between energy density and scale factor as

$$\rho(a) \propto a^{-3(1+\omega)} = (1+z)^{3(1+\omega)}, \tag{1.5.17}$$

where z is the redshift. The value of ω follows from the adiabaticity condition. We shall here discuss its value in three cases of great importance.

Case I. A Matter-dominated Universe filled with nonrelativistic cold matter in the form of pressureless nonradiating dust for which $p = 0$. Then, from (1.5.16), we have $\omega = 0$, and energy density evolves according to $\rho \propto a^{-3} = (1+z)^3$. Inserting this into (1.5.1) for $k = 0$, we get $a \propto t^{2/3}$.

In matter-dominated Einstein-de Sitter Universe which is flat and $\Lambda = 0$, Friedmann equation (1.5.1) can be integrated to give

$$t(z) = \frac{2}{3H_0}(1+z)^{-3/2}. \tag{1.5.18}$$

The present age of the Universe at $z = 0$ would be

$$t_0 = \frac{2}{3H_0}. \tag{1.5.19}$$

Case II. A radiation-dominated Universe filled with an ultra-relativistic hot gas. In this case, the EoS parameter $\omega = 1/3$ so that the radiation density evolves as $\rho \propto a^{-4}$ for which we get $a \propto t^{1/2}$.

Case III. A vacuum-energy state corresponds to a flat, static Universe $(\dot{a} = 0, \ddot{a} = 0)$ without dust and radiation, but with a cosmological constant term where $p_\Lambda = -\rho_\Lambda$, $\omega = -1$ for which $a \propto e^{(\text{const.})\,t}$.

1.5.5 de Sitter Universe

Let us consider the flat homogeneous and isotropic Robertson-Walker metric in which the density of pressureless dust is constant, i.e., $\rho(t) = \rho_0$. The Friedmann equation (1.5.6) gives

$$\frac{\dot{a}}{a} = \sqrt{\frac{8\pi G}{3}\rho_0 + \frac{\Lambda}{3}} = H, \tag{1.5.20}$$

where Hubble parameter H is now constant. This is even true for $k \neq 0$ since due to constant density and a increases without limit, k/a^2 will be eventually negligible. The solution of above equation is given by

$$a(t) \propto e^{Ht}, \tag{1.5.21}$$

which is obviously exponentially expanding Universe. The above solution can be obtained for $p = \rho = 0$ where H is directly related to Λ. The same solution can be followed even if $\Lambda = 0$ and density is constant. This solution is the de Sitter solution for which Eddington described it as "motion without matter".

1.6 Cosmic Inflation

In this section, we will discuss the problems caused by the expansion of space-time: horizon problem associated with its size at different epochs, the flatness problem associated with its metric, the monopole problem related to topological defects and the entropy problem.

1. **The Horizon Problem:** The horizon problem which is also known as homogeneity problem, is a cosmological fine-tuning problem within Big Bang model. These problems were part of the main motivation for the original proposal of the idea of inflation. The horizon problem is the existence of background radiation with a high degree of isotropy (uniformity in all directions): the Cosmic Microwave Background (CMB)[3]. In every direction we observe the CMB to have the spectrum of a thermal blackbody with a temperature T_0 of 2.725 Kelvin, and departing from perfect isotropy only to one part in $100,000$.
   The Hot Big Bang is based on the cosmological principle which predicts that the Universe as a whole is spatially homogeneous and isotropic. The CMB is isotropic for every fundamental observer in the Universe, i.e., the present temperature of CMB is inferred to be everywhere 2.725 Kelvin. This implies that the distant opposite parts of the Universe would be in thermal equilibrium in the past. Since the radiation from two distant opposite parts could not possibly be causally connected to each other because information can not travel faster than the speed of light. Nor could the regions they traveled from even have been

[3]The CMB is called "background radiation" because it originates from cosmos and not from the discrete sources such as stars, quasars, etc.

in communication. Then, why are we measuring the same temperature in all directions with great accuracy?

2. **The Flatness Problem:** The geometry of the Universe is nearly flat determined by the CMB data. A Universe as flat as we see it today would require an extreme fine–tuning of conditions in the past, which would be an unbelievable coincidence. This strange coincidence is known as the flatness problem[4] of the standard cosmological model. This problem arises because we appear to live in a Universe that has an observed density parameter (Ω) very close to 1 or can say very close to critical density. There is no known reason for the density of the Universe to be so close to the critical density and this appears to be an unacceptably strange coincidence.
   We can understand it as, a flat Universe is one in which the amount of matter present is just sufficient to halt its expansion, but insufficient to re–collapse it. This would represent a very fine–balancing act. This seems like a truly remarkable coincidence and is known as the flatness problem.

3. **The Monopole Problem:** The Grand Unified theory (GUT) of particle physics predicts that in very early Universe magnetic monopoles were produced with high abundance. They are supposed to be extra ordinary massive, about 10^{16} GeV. Monopoles are highly stable particles and once they have been created, they are indestructible. Therefore, they would survive as relics in the present epoch. As we don't observe magnetic monopoles at present, this imposes a problem on the standard model of cosmology called the monopole problem.

4. **The Entropy Problem:** This is the restatement of the flatness problem and the horizon problem in a somewhat different form. The entropy in a given comoving volume stays constant in an adiabatic expansion. However, we have found that in the flatness problem this hypothesis led to fine tuning, whereas for the horizon problem it gave an extremely small size of homogeneity. It therefore appears that the trouble lies in entropy=constant: it could be resolved if the adiabatic assumption were violated at some stage and entropy boosted to its present value by an enormously large factor. It is obvious that this problem has the same origin as the horizon problem.

[4]The flatness problem is occasionally called the “age problem".

1.7 Inflation and the Accelerating Universe

Alan H. Guth [11] proposed an inflationary theory as a solution to the above discussed problems of standard cosmology, which is the most accepted theory. Inflationary theory suggests that the Universe underwent a phase of accelerated expansion very early in its history. The word inflation means a rapid expansion in the early Universe. The inflationary theory was based on Weinberg's grand unified theory (GUT) which suggests that the particle interactions possess certain symmetry. Linde [12, 13], Albrecht and Steinhardt [14] and Albrecht et al. [15] have also discussed and modified this theory. It was accepted in the scientific community due to its promising and elegant way to understand the very early Universe. According to this theory of inflation, the early Universe expanded exponentially fast for a fraction of a second after the Big Bang. This phase not only resolves the flatness and horizon problems, but also explains a nearly flat spectrum of temperature anisotropies observed in cosmic microwave background (CMB).

It is still not clear to scientists the cause of inflationary phase, however, the best guess being some kind of a negative "vacuum energy density" triggered by the separation of strong nuclear force from the other elementary forces at that time. The scalar field was supposed to initiate inflation, which decayed into radiation and matter to stop this scenario. The kinetic energy of the scalar field was dominant during inflation which allowed de Sitter like expansion of the Universe. Inflation happened for a very short time in the very early Universe and the Universe experienced a very rapid expansion in this duration. Due to very rapid expansion of the Universe during the time of inflation, the small size of the Universe was increased to a much larger size. Thus, the small size of the Universe which was able to achieve thermal equilibrium before inflation has been expanded to a greatly large size and it might even be larger than our observable Universe.

Thus, inflation provides the mechanism through which distant opposite sides of the Universe may have come close in very early times to establish thermal equilibrium. Therefore, the horizon problem has been solved. The monopole problem has also been resolved by inflation. The rapid expansion of the Universe during the inflationary era has diluted the density of magnetic monopoles. Therefore, we don't observe monopoles at the present time.

In addition to the flatness, horizon, and monopole problems, inflation naturally solves

the initial low entropy problem. As we know already, the energy of a vacuum stays constant despite the expansion. In this way, room for matter full of energy could have been created. If there is mechanism to convert vacuum energy into particles and radiation at some later stage, then the observed huge entropy will be created and the problem of entropy will be solved. Potentially, this mechanism works for any inflationary scenario, since the product ρa^3 is guaranteed to grow whenever $\ddot{a} > 0$.

Thus, the inflation resolves the problems of Hot Big Bang cosmology successfully. Inflation is an active field of research. In the literature, mainly scalar field theory and supersymmetry theory are being used to get inflation.

The rapid development in observational cosmology which started during late 1990s shows that the Universe passes two phases of cosmic acceleration: The first cosmic accelerated phase is the inflationary phase which has been discussed above. Before 1998, the cosmologists assured that the Universe was expanding with decelerated rate after a very short and rapid expansion (inflation). But, in 1998 two separate teams headed by Perlmutter et al. [16] and Riess et al. [17] who were working on the observations of distant Supernovae Ia (SN Ia) to measure the rate of expansion of the Universe, announced that our Universe is currently experiencing a phase of accelerated expansion. Thus, the second cosmic accelerated phase which is known as the late time cosmic acceleration, is assumed to have started after the decelerated phase. According to the theoretical point of view, the expansion of the Universe after the inflationary phase of the Universe had to be slow. This behaviour of the Universe, i.e., the phase transition from deceleration to acceleration, has been affirmed by many observational results such as Wilkinson Microwave Anisotropy Probe (WMAP) [6, 18], Planck collaboration [19], Sloan Digital Sky Survey (SDSS) [20], etc. This event has brought many challenges to the cosmologists. The observations show that the accelerating expansion of the Universe is due to a mysterious form of energy with negative pressure which is dubbed as “dark energy” (DE) [16, 17].

Nowadays, the DE has become one of the most active field in physics and astronomy. Many models have been proposed to describe this late time accelerated expansion of the Universe. There are two ways to discuss the acceleration of the Universe. First: one can consider an exotic type of energy content which could provide sufficient amount of negative pressure to observe the acceleration, which is known as the modification in the matter part of the Einstein equations and is called DE models of the Universe. Second: one can modify the geometric part of Einstein equations, which is known as modified theories of gravity models. Let us study the evolution of

the Universe based on these two concepts.

1.7.1 Dark Energy

In the early 1990s, the researchers were clear about the expansion of the Universe. The Universe might have enough energy density to stop its expansion and recollapse, it might have so little energy density that it would never stop expanding, but gravity was certain to slow the expansion as time went on. In 1998 the Hubble Space Telescope (HST) observations of very distant supernovae showed that, a long time ago, the Universe was actually expanding more slowly than it is today. So the expansion of the universe has not been slowing due to gravity, as everyone thought, it has been accelerating. No one expected this, no one knew how to explain it. But something was causing it.

To explain this phenomena, theorists came up with three sorts of explanations. It may be a result of a long-discarded "cosmological constant" which was introduced by Einstein in his theory of gravitation to obtain the static Universe. It may be some strange kind of energy-fluid that filled space. May be there is something wrong with Einstein's theory of gravity and a new theory could include some kind of field that creates this cosmic acceleration. Theorists still don't know what the correct explanation is, but they have given the solution a name which is known as "Dark energy" (DE). The Universe roughly contains 68% of DE where as dark matter makes up about 27% and rest 5% contains everything all normal matter.

The Standard ΛCDM model

The Lambda cold dark matter (ΛCDM) model of the Universe which contains cosmological constant Λ and cold dark matter (CDM) are known as the standard model of cosmology [21–25]. Cosmologists believe that dark matter (DM) comprises of cold slow moving particles that can not emit electromagnetic radiation or scatter light. The Lambda accounts for the presence of DE, a hypothetical force that appears to be accelerating the expansion of the Universe. Although ΛCDM model is compatible with observations very well, even this model is able to explain almost all the aspects of cosmic evolution like structure formation, black hole phenomenon, accelerated expansion etc., but still it has some theoretical problems, namely cosmic coincidence and fine–tuning.

Steinhardt [26] and Zlatev et al. [27] were the first who addressed the cosmic coincidence problem. According to the observations, at present the ratio of the DE and matter is of order unity. With respect to the standard model, very fine tuned initial conditions of the early Universe are required to observe this ratio of order unity. This means, it is like a coincidence that we are living in a time where the densities of DE and matter are of same order. The fine–tuning problem of the ΛCDM model is related to its observed value and theoretical value. The observations predict a very tiny value in comparison to the theoretical value of it which is about to 120 orders higher. It is a huge difference.

The ΛCDM model is the incarnation of our understanding about the origin of the Cosmos. It can also be understood as a model which is a parametrization of the Big Bang cosmological model in which the Universe contains a cosmological constant Λ, associated with DE, and cold dark matter (CDM). It is frequently referred as the standard cosmological model of Big Bang cosmology because it is the simplest model that provides a reasonably good account with the properties of the cosmos.

From $(1.5.5)$, we observe that in Einstein's modified equations the cosmological constant Λ was included in the left hand side, i.e., the geometric part of the equations. In the case of the standard cosmological model it has been considered as a candidate of the DE. Therefore, it could be introduced in the matter part of the equations, i.e., in the right hand side. Then, the modified form of the Einstein equations $(1.5.5)$ may be written as

$$R_{\mu\nu} - \frac{1}{2} g_{\mu\nu} R = 8\pi G \, (T_{\mu\nu} + T^{\Lambda}_{\mu\nu}), \tag{1.7.1}$$

where $T^{\Lambda}_{\mu\nu}$ stands for the energy-momentum tensor of the cosmological constant and its energy is supposed to be the energy of the space (vacuum) itself. It remains constant during the evolution. The energy-momentum tensor of the vacuum energy is defined as

$$T^{(vac)}_{\mu\nu} = -\rho_{\Lambda} g_{\mu\nu} = T^{\Lambda}_{\mu\nu}. \tag{1.7.2}$$

The vacuum energy density and cosmological constant have the relation $\rho_{\Lambda} = \frac{\Lambda}{8\pi G}$. For the cosmological constant the EoS parameter is $\omega = -1$. It can also be explained as, for ΛCDM model the pressure-energy relation is $p_{\Lambda} = -\rho_{\Lambda}$.

Dynamical Dark Energy Models

The fine–tuning and coincidence problems, occurred with the cosmological constant have led to the search for dynamical DE models [28]. A phenomenological solution of

these problems is to consider a time dependent cosmological term [29,30]. One of the simplest and probably the most common candidate of dynamical DE is 'quintessence' [27,31–38]. The concept of quintessence basically uses a scalar particle field [39,40]. Historically, scalar fields are used as the responsible candiadate for inflation [41]; to seed the primordial perturbation for structure formation during an early inflationary epoch; and as a candidate for cold dark matter, responsible for the formation of the actual cosmological structures [42].

Due to remarkable qualitative similarity between the present DE and primordial DE that derives inflation in the early Universe, the inflationary models based on scalar fields have also been applied for a description of the late time cosmic acceleration [27, 28, 34–36, 38, 43, 44]. Therefore, the scalar field cosmological models have acquired great popularity in recent decades. The outcomes from different observational data [45–49] also show a possibility of the existence of some strange kind of fields in the Universe such as the phantom field as proposed by Caldwell [50] having negative kinetic energy [51,52]. Some other candidates of such dynamical DE are the quintom (a combination of quintessence and phantom scalar fields) [53], tachyonic field [54–56], k-essence [56–58], Chaplygin gas [59, 60].

Nowadays, it is a common issue to make the use of such exotic matters as the responsible candidate to describe the late time acceleration of the Universe [28,38,54, 56, 60–62]. Apart from these DE candidates, some other candidates like holographic dark energy (HDE), new holographic dark energy, agegraphic dark enery (ADE) and new agegraphic dark energy, etc.

Scalar Field Cosmology

Instead of arguing about Λ, we could postulate the existence of a new kind of energy, described by a slowly evolving scalar field $\phi(t)$ that contributes to the total energy density together with the background (matter and radiation) energy density. This scalar field is assumed to interact only with gravity and itself. The natural and simple model for dynamical DE is the scalar field model [32, 43]. The cosmological models based on scalar fields have been discussed by many authors for explaining the possible early inflationary scenarios [11] as well as for describing the dark energy [63]. The dynamics of the evolution of the Universe is often realized by scalar field ϕ with a proper scalar potential $V(\phi)$. The self-interacting potential can act like an effective cosmological constant which drives a period of inflation. It depends on the specific form of the potential as a function of scalar field. It has been observed that the scalar

potential $V(\phi)$ in a scalar field cosmology has very important role as it radically affects the cosmological behavior.

The EH action of a Universe constituted with matter and a scalar field minimally coupled to gravity, in the system of units $8\pi G = 1 = c$, is

$$S = \int d^4x\sqrt{-g}\left[\frac{1}{2}R + \mathscr{L}_\phi + \mathscr{L}_m\right], \tag{1.7.3}$$

where, $\mathscr{L}_m$ is the total matter content in the Universe (including CDM) and $\mathscr{L}_\phi$ is the scalar field Lagrangian which is defined as

$$\mathscr{L}_\phi = -\frac{1}{2}\nabla^\delta\phi\nabla_\delta\phi - V(\phi), \tag{1.7.4}$$

where ϕ is the scalar field and $V(\phi)$ is the self -interacting scalar potential. The fluid energy density ρ_m and scalar field ϕ are functions of a time like coordinate t. In the scalar field cosmology, the Einstein field equations $(1.4.2)$ become as

$$R_{\mu\nu} - \frac{1}{2}g_{\mu\nu}R = T^{(m)}_{\mu\nu} + T^{(\phi)}_{\mu\nu}, \tag{1.7.5}$$

where $T^{(m)}_{\mu\nu}$ is the energy-momentum tensor of perfect fluid given in Eq. $(1.4.4)$ and $T^{(\phi)}_{\mu\nu}$ is the energy-momentum tensor associated with the scalar field ϕ, which is given by

$$T^{(\phi)}_{\mu\nu} = \nabla_\mu\phi\nabla_\nu\phi - \left[\frac{1}{2}\nabla^\delta\phi\nabla_\delta\phi + V(\phi)\right]g_{\mu\nu}. \tag{1.7.6}$$

The scalar field itself obeys the Klein-Gordon (wave) equation

$$g^{\mu\nu}\nabla_\mu\nabla_\nu\phi + \frac{dV(\phi)}{d\phi} = 0. \tag{1.7.7}$$

Here, ρ_ϕ and p_ϕ are respectively the energy density and pressure for the canonical scalar field, which are given by

$$\rho_\phi = \frac{\dot{\phi}^2}{2} + V(\phi), \qquad p_\phi = \frac{\dot{\phi}^2}{2} - V(\phi). \tag{1.7.8}$$

Clearly the pressure is always negative if the evolution is so slow that the kinetic energy density $\frac{1}{2}\dot{\phi}^2$ is less than the potential energy density. Under the assumption that all matter fields are minimally coupled to the metric $g_{\mu\nu}$, which means that the principle of equivalence is guaranteed.

Assuming negligible interaction between matter and scalar field, the conservation

equation for perfect fluid leads to

$$\dot{\rho_m} + 3H(1+\omega_m)\rho_m = 0, \tag{1.7.9}$$

and the evolution equation of the scalar field (1.7.7) gives

$$\ddot{\phi} + 3H\dot{\phi} + \frac{dV(\phi)}{d\phi} = 0, \tag{1.7.10}$$

which can be equivalently written as

$$\dot{\rho_\phi} + 3H(1+\omega_\phi)\rho_\phi = 0. \tag{1.7.11}$$

The energy density of scalar field decreases as $a^{-3(1+\omega_\phi)}$. The pressure and energy density of these scalar fields are connected by a relation $p_\phi = \omega_\phi \rho_\phi$, where, ω_ϕ is known as the EoS parameter of the scalar field. The parameter ω_ϕ can be expressed as

$$\omega_\phi = \frac{p_\phi}{\rho_\phi} = \frac{\dot{\phi}^2 - 2V(\phi)}{\dot{\phi}^2 + 2V(\phi)}. \tag{1.7.12}$$

It is well known from observational data that $-1 < \omega_\phi < -1/3$ gives the region for quintessence, $\omega_\phi = -1$ corresponds to the cosmological constant and $\omega_\phi < -1$ represents phantom region. Therefore, the conditions for acceleration are $\omega_\phi < -1/3$, $a(t) \propto t^d$ with $d > 1$ so that $p_\phi < 0$ or $\rho_\phi \propto a^{-2}$.

The potential $V(\phi)$ is not known and one must assume the specific form as a function of the scalar field ϕ. There are many such proposals available of this potential like power-law, exponential, zero, constant potentials etc. Hence, it is of interest to understand the early inflation and late time acceleration of the Universe with scalar fields along with the various form of scalar potentials.

Holographic Dark Energy

The most important issue of the modern cosmology is the origin of DE. The HDE, which possesses some significant properties of the quantum theory, has been proposed as a candidate for DE to explain the recent phase transition of the Universe. The origin of HDE contains more scientific approach in comparison to other DE candidates, and presents a better way to deal with the accelerated expansion. The HDE is based on the holographic principle proposed by Gerard 't Hooft [64].According to the holographic principle, the information contained in a volume of space can be rep-

resented as a hologram, which corresponds to a theory locating on the boundary of that space. It can also be stated as the number of degrees of freedom in a bounded system should be finite and has a relation with the area of its boundary. Soon after, Leonard Susskind [65] gave a precise string-theory interpretation of this principle. Moreover, in 1999, Juan Maldacena [66] proposed the famous AdS/CFT correspondence, which is the most successful realization of the holographic principle. Now, it is widely believed that the holographic principle should be a fundamental principle of quantum gravity. Therefore, as the most fundamental principle of quantum gravity, holographic principle may play an important role in solving the DE problem.

For a system with size L and ultraviolet (UV) cutoff Λ without decaying into a black hole, it is required that the total energy in a region of size L should not exceed the mass of a black hole of same size, thus $L^3\rho_\Lambda \leq LM_P^2$, where M_P is the reduced Planck mass which is equal to $M_P^2 = 1/8\pi G$. In 2004, after applying the holographic principle to the DE problem, Miao Li [67] proposed a new DE model, called holographic dark energy (HDE) model. In this model, the energy density of DE only relies on two physical quantities on the boundary of the Universe: one is the reduced Planck mass M_p and another is the cosmological length scale L. Li assumed that the largest infrared (IR) cutoff to saturate the inequality imposed by black hole formation and obtained the density of HDE as

$$\rho_h = 3d_1^2 M_p^2 L^{-2}, \tag{1.7.13}$$

where d_1^2 is a dimensionless constant which is taken to be of the order of unity and L represents the IR cutoff. It means that there must be a duality between UV cutoff and IR cutoff. Therefore, the UV cutoff is related to the vacuum energy and IR cutoff is related to the large scale of the Universe. The large scale of the Universe can be taken as, for example Hubble horizon, particle horizon or event horizon [67, 68]. It has been shown that HDE model is favored by the latest observational data including the sample of Type Ia supernovae (SNe Ia), the shift parameter of the cosmic microwave background (CMB), and the baryon acoustic oscillation (BAO) measurement [69].

Li [67] discussed three choices for the length scale L which is supposed to provide an IR cutoff. The first choice is to identify L with the Hubble radius, H^{-1}. In the formalism of HDE, the Hubble horizon is a most natural choice for the IR cutoff, but Hsu [68] in general relativity and Xu et al. [70] in Brans–Dicke (BD) theory have shown that the Hubble horizon as an IR cutoff is not a suitable candidate to explain the recent accelerated expansion. The second option is the particle horizon radius but it

also does not give an accelerated expansion. The third choice is the identification of L with the radius of the future event horizon which gives the desired result, namely a sufficiently negative EoS to obtain an accelerated Universe. Soon after, it was shown by Pavón and Zimdahl [71] that if there is an interaction between two dark components of the Universe, the identification of L with the Hubble horizon, $L = H^{-1}$, may give a suitable EoS for DE. It was also shown that it necessarily implies a constant ratio of the energy densities of the two components regardless of the details of the interaction. Nojiri and Odintsov [72] have studied a generalized model of HDE and found that a unified model of the Universe may be achieved. The authors also claimed that the coincidence problem may be resolved in a generalized HDE model. Thus, HDE models may also alleviate the cosmic coincidence problem which provides an advantage of HDE models over the other DE models.

The HDE model is the first theoretical model of DE inspired by the holographic principle, and is in good agreement with the current cosmological observations at the same time. This makes HDE a very competitive candidate of DE. In recent years, the paradigm of HDE has drawn a lot of attention and has been widely studied.

New Holographic Dark Energy

As the origin of the HDE is still unknown, Granda and Oliveros [73] proposed a new IR cutoff for HDE, known as new holographic dark energy, which besides the square of the Hubble scale also contains the time derivative of the Hubble scale. As suggested by Granda and Oliveros in paper [73] the energy density of HDE with the new IR cutoff is given by

$$\rho_d = 3(\alpha H^2 + \beta \dot{H}), \tag{1.7.14}$$

where α and β are the dimensionless parameters, which must satisfy the restrictions imposed by the current observational data. Wang and Xu [74] found the best-fit values in order to make this cutoff to be consistent with observational data as $\alpha = 0.8502^{+0.0984+0.1299}_{-0.0875-0.1064}$ and $\beta = 0.4817^{+0.0842+0.1176}_{-0.0773-0.0955}$ with 1σ and 2σ errors in flat model. In this thesis work we shall take $\alpha = 0.8502$ and $\beta = 0.4817$.

The advantage is that this new HDE model depends on local quantities and avoids the causality problem appearing with event horizon IR cutoff. The authors, in their other paper [75], reconstructed the scalar field models for HDE by using this new IR cutoff in flat Friedmann-Robertson-Walker (FRW) Universe with only DE content. Karami and Fehri [76] generated the results of ref. [73] for non-flat FRW Universe.

Malekjani et al. [77] have studied the statefinder diagnostic with new IR cutoff proposed in [73] in a non-flat model. Sharif and Jawad [78] have investigated interacting new HDE model in non-flat Universe. Debnath and Chattopadhyay [79] have considered flat FRW model filled with mixture of dark matter and new HDE, and have studied the statefinder and Om diagnostics. Oliveros and Acero [80] have studied new HDE model with a non-linear interaction between the DE and dark matter (DM) in flat FRW Universe.

Although, the DE models explain the recent accelerated expansion of the Universe very well and also accommodate the observations but the origin and evolution of DE is still mysterious and unknown. Many other problems like the fine–tuning problem, coincidence problem etc. associated with DE models compel us to think beyond the standard model and other DE models.

Undoubtedly, the DE models are the most popular explanation of the current epoch of the accelerating Universe, but they do not seem to be as well motivated theoretically as one would desire. Therefore, the mystery is continued with the existence and nature of such exotic matters. In the absence of an evidence for the existence of DE, there leaves a space to explore other possible ways to alleviate the most crucial problem of cosmic acceleration.

1.7.2 Modified Theories of Gravity

Let us discuss theories of gravity which are the candidates both for inflation and for the present accelerated expansion. The modified theories of gravity are just an extension of the GTR to study the behaviour of the Universe. The idea of an alternative theory to Einstein's GTR is not new in the literature. A large number of models within modified theories can explain the DE phenomena. After Einstein's GTR, the first modification has done by Weyl [81] in 1919 who proposed the scale invariant theory, and in 1923, Eddington's theory of connections [10] was presented. The Kaluza-Klein theory [82, 83] and string theory [84, 85] are examples of higher dimensional theories, and scalar tensor theories [86, 87] are example of extra fields included in the field equations. In last two decades, considerable developments have been made in the study of the most potential candidate of quantum gravity, which is string theory. Another well established and extensively studied theories of gravity are the scalar-tensor theories, in which the model Newton's constant G is more often taken as a variable. One of the most simplest and well studied scalar-tensor theory is Brans-Dicke (BD)

scalar-tensor theory.

The well known modification of GTR is done by replacing Ricci scalar R by a general function $f(R)$, known as $f(R)$ gravity. This concept to modify GTR using higher order terms of scalar curvature R have been performed by Utiyama and De Witt [88] in 1962. In 1980, Starobinsky [89] came up with an inflationary model using the higher order corrections to GTR which has became a successful model of inflation. In 1970, Buchdahl [90] was the first who considered the general function $f(R)$ in the EH action and presented a more general model of modified gravity. This theory is consistent with the observations [91–93].

A number of modified theories of gravity are available in the literature namely, $f(R)$ theories [93–97], Gauss-Bonnet $f(G)$ theory [98, 99], Brans-Dicke theory [100, 101], Brane World gravity [102, 103], Horava-Lifshitz gravity [104, 105] and $f(T)$ theory [106, 107], $f(R,T)$ theory [108, 109]. In recent years the modified gravity models have become an active area of the research. However, none of these presents a complete theory of gravity [110] which can completely solve the mysteries of the Universe. However, the search for a complete theory of gravity continues. In this thesis, we have done some work in the framework of Brans–Dicke scalar–tensor theory and modified $f(R,T)$ gravity theory to analyse the different evolutionary behaviour of the Universe. Let us discuss about these two theories in details.

Brans–Dicke Theory

In theoretical physics, the Brans–Dicke (BD) theory of gravitation (sometimes called the Jordan–Brans–Dicke theory) is a theoretical framework to explain gravitation. The BD theory was proposed by Brans and Dicke [100] in 1961. It describes the gravitation through spacetime metric ($g_{\mu\nu}$) and a massless scalar field (ϕ). It is a modification or rather generalization of the GTR. It is considered as a viable alternative to GTR. The pioneering study on scalar-tensor theories was carried out by Brans and Dicke [100] to incorporate Mach's principle into gravity which is known as Brans–Dicke (BD) theory. This was the first gravity theory in which the dynamics of gravity was described by a scalar field while spacetime dynamics was represented by the metric tensor. In the BD theory, it is to be noted that $\phi = (8\pi G)^{-1}$, and this scalar field couples to gravity with a coupling parameter w. Since the BD theory passes the experimental tests from the solar system [111] and provides an explanation of the accelerated expansion of the Universe, it is worthwhile to discuss dark energy models in this framework.

The canonical form of the (Jordan frame) Brans–Dicke action is

$$S_{BD} = \int d^4x\sqrt{-g}\left(-\phi R + \frac{w}{\phi}\nabla^\mu\phi\ \nabla_\mu\phi + \mathscr{L}_m\right), \tag{1.7.15}$$

where ϕ is a time-dependent scalar field called BD scalar field and w is the BD constant known as coupling constant. One important point about BD theory is its varying gravitational constant, G. In BD gravity the $G_{eff}^{-1} = 2\pi\phi^2/w$, where G_{eff} is the effective gravitational constant as long as the scalar field ϕ varies slowly.

The variation of the action (1.7.15) with respect to the metric tensor, $g_{\mu\nu}$ yield the following field equations

$$R_{\mu\nu} - \frac{1}{2}g_{\mu\nu}R = \frac{8\pi}{\phi}T_{\mu\nu} + \frac{w}{\phi^2}\left(\partial_\mu\phi\partial_\nu\phi - \frac{1}{2}g_{\mu\nu}\partial_\sigma\phi\partial^\sigma\phi\right) + \frac{1}{\phi}\left(\nabla_\mu\nabla_\nu\phi - g_{\mu\nu}\Box\phi\right). \tag{1.7.16}$$

The wave equation for scalar field is given by

$$\Box\phi = \frac{8\pi}{8+3w}T. \tag{1.7.17}$$

In the above field equations, w is dimensionless coupling constant, $T = T_\mu^\mu$ the trace of energy-momentum tensor, $\Box$ is the d'Alembert operator or covariant wave operator, $\Box\phi = \partial_\delta\partial^\delta\phi$.

This theory [101, 112, 113] is widely used to study the inflationary epoch of the Universe. A second order thermodynamic viscous model in the framework of BD theory has been discussed by Banerjee and Beesham [114]. The exact solutions of the FRW model have been obtained by the authors under the power–law form of BD scalar field. This theory has also been used by Ram and Singh [115] to study the flat FRW model with variable EoS parameter. In 1998, Liddle et al. [116] have studied the transition from the radiation to the matter dominated epoch and constrained the BD parameter using microwave anisotropy and large–scale structure data in Jordan–Brans–Dicke theory. This BD theory is also used to investigate the emergent Universe model by Campo et al. [117] in 2007. Early time cosmology with particle creation was studied by Singh [118] to analyze its thermodynamical effect in open thermodynamical systems within the framework of BD theory. The various aspects of black hole have been investigated in BD theory in Refs. [119–123].

Nowadays, BD theory has got interest to explain the accelerated expansion due to its association with string theory and higher dimensional theories. This theory

describes the latest acceleration of the Universe and verifies the observational data as well [124–126]. DE models like HDE model, new agegraphic DE model, Ricci DE model etc. have been discussed to explain the accelerated expansion, cosmic coincidence problem, etc. in BD theory.

$f(R,T)$ Gravity

Since the modification of the gravitational theory is a way to overcome the problems of DE and accelerating Universe but it is not an easy task because there may be a numerous way to deviate from GTR. Even the EH action in GTR has a additive structure in Ricci scalar R and matter Lagrangian $\mathscr{L}_m$, both of which have very different conceptual levels without any interaction between them. However, there is no any fundamental guiding principle for considering the matter and geometry to be additive. Moreover, a more generalised EH action requires a general coupling between matter and geometry.

The generalised $f(R)$ gravity was introduced by Bertolami et al. [126] in 2000 by assuming the maximal coupling between the curvature term R and the matter Lagrangian density. In 2008, this model was extended by Harko [127] for the case of the arbitrary couplings in both geometry and matter. Further in 2010, Harko and Lobo [128] presented $f(R,\mathscr{L}_m)$ gravity theory where the gravitational Lagrangian is an arbitrary function of the Ricci scalar R and matter Lagrangian density $\mathscr{L}_m$.

The $f(R,T)$ gravity theory was proposed by Harko et al. [108] as an extension of the $f(R)$ theories, for which besides geometrical correction terms, proportional to the Ricci scalar R, one has also material correction terms, proportional to the trace of the energy-momentum tensor T. The $f(R,T)$ gravity presents a maximal coupling between geometry and matter. Following the Harko et al. [108], the EH action for $f(R,T)$ gravity is written as

$$S=\frac{1}{2}\int d^4x\sqrt{-g}[f(R,T)+2\mathscr{L}_m], \tag{1.7.18}$$

where $f(R,T)$ is the function of Ricci scalar, R and trace of energy-momentum tensor, T, and $\mathscr{L}_m$ represents the matter Lagrangian density. If $\mathscr{L}_m$ depends only on the metric components and not on its derivatives, one has, for the energy-momentum tensor, $T_{\mu\nu}$ the following [129]

$$T_{\mu\nu}=-\frac{2}{\sqrt{-g}}\frac{\delta(\sqrt{-g}\mathscr{L}_m)}{\delta g^{\mu\nu}}, \tag{1.7.19}$$

so that $T=g^{\mu\nu}T_{\mu\nu}$.

Varying the action $(1.7.18)$ with respect to $g_{\mu\nu}$, we obtain the field equations of $f(R,T)$

theory as

$$f_R(R,T)R_{\mu\nu}-\frac{1}{2}f(R,T)g_{\mu\nu}+(g_{\mu\nu}\Box-\nabla_\mu\nabla_\nu)f_R(R,T)=T_{\mu\nu}-f_T(R,T)(T_{\mu\nu}+\ominus_{\mu\nu}), \tag{1.7.20}$$

where f_R and f_T denote the partial derivatives of $f(R,T)$ with respect to R and T, respectively, ∇_μ is the covariant derivative, $\Box\equiv\nabla_\mu\nabla^\mu$ is the d'Alembert operator, and $\ominus_{\mu\nu}$ is defined by

$$\ominus_{\mu\nu}\equiv g^{ij}\frac{\delta T_{ij}}{\delta g^{\mu\nu}},\qquad i,j=0,1,2,3. \tag{1.7.21}$$

Using (1.7.19) into (1.7.21), we obtain

$$\ominus_{\mu\nu}=-2T_{\mu\nu}+g_{\mu\nu}\mathscr{L}_m-2g^{\varsigma\tau}\frac{\partial^2\mathscr{L}_m}{\partial g^{\mu\nu}\partial g^{\varsigma\tau}}. \tag{1.7.22}$$

It has been suggested that the $f(R,T)$ gravity depend on a source term and this source term is a function of the matter Lagrangian $\mathscr{L}_m$. Therefore, the choice of $\mathscr{L}_m$ will decide the field equations of the model. Let us take matter lagrangian $\mathscr{L}_m=-p$, then from Eq. (1.7.22), we obtain

$$\ominus=-2T_{\mu\nu}-pg_{\mu\nu}. \tag{1.7.23}$$

As $f(R,T)$ gravity depends on the source term, various theoretical models may be obtained for different choices of matter source. In this thesis, we have assumed the form $f(R,T)=R+f(T)$. With this assumption, the Eq. (1.7.20) become as

$$R_{\mu\nu}-\frac{1}{2}Rg_{\mu\nu}=T_{\mu\nu}-(T_{\mu\nu}+\ominus_{\mu\nu})f'(T)+\frac{1}{2}f(T)g_{\mu\nu}, \tag{1.7.24}$$

where a prime represents the differentiation with respect to T. Using (1.7.23), the field equations (1.7.24) become

$$R_{\mu\nu}-\frac{1}{2}Rg_{\mu\nu}=T_{\mu\nu}+(T_{\mu\nu}+pg_{\mu\nu})f'(T)+\frac{1}{2}f(T)g_{\mu\nu}. \tag{1.7.25}$$

Friedmann models in general relativity ensure the energy conservation through the continuity equation (1.5.12), which implies that $d(\rho V)=-pdV$. Here, $V=a^3$ is the volume scale factor of the Universe and the quantity ρV gives an account of the total energy. However, in modified gravity theories, one may get a different picture.

The $f(R,T)$ gravity has the intriguing property that once geometry-matter coupling

is introduced, the four-divergence of the energy-momentum tensor is nonzero. Taking into account the covariant divergence of (1.7.20), with the use of the mathematical identity of Eq. (20) of Ref. [130], we obtain for divergence of the energy-momentum tensor $T_{\mu\nu}$

$$\nabla^{\mu}T_{\mu\nu} = -\frac{f_T(R,T)}{1+f_T(R,T)}\left[(T_{\mu\nu}+\ominus_{\mu\nu})\nabla^{\mu}\ln f_T(R,T) + \nabla^{\mu}\ominus_{\mu\nu} - \frac{1}{2}g_{\mu\nu}\nabla^{\mu}T\right]. \quad (1.7.26)$$

Thus, one of the common features of this modified gravity is the non-conservation of the matter energy-momentum tensor. This extra terms is generated by the nonminimal geometry -matter coupling which is considered as particle production, with the gravitational field acting as a particle source.

Using the value of $\ominus_{\mu\nu}$, defined above, the energy non-conservation equation (1.7.26) for a perfect fluid $T_{\mu\nu} = (\rho+p)u_{\mu}u_{\nu} - pg_{\mu\nu}$ with energy density ρ, thermodynamical pressure p and normalized four velocity u^{ν}, satisfying the condition $u_{\nu}u^{\nu} = 1$, gives

$$\dot{\rho} + 3(\rho+p)H = -\frac{f_T(R,T)}{1+f_T(R,T)}\left[(\rho+p)\nabla_{\mu}\ln f_T(R,T) + \nabla_{\nu}\frac{\rho-p}{2}\right]. \quad (1.7.27)$$

Thus, the divergence of the energy-momentum tensor is nonzero. Let us interpret (1.7.27) from a thermodynamic point of view as describing adiabatic irreversible particle creation in a cosmological context. The above equation can be written as

$$\dot{\rho} + 3(\rho+p)H = (\rho+p)\,\Gamma, \quad (1.7.28)$$

where

$$\Gamma = -\frac{f_T(R,T)}{1+f_T(R,T)}\left[\nabla_{\mu}\ln f_T(R,T) + \nabla_{\nu}\frac{\rho-p}{2(\rho+p)}\right], \quad (1.7.29)$$

describes the particle creation rate.

The various evolutionary issues of the Universe have been discussed and studied under the framework of $f(R,T)$ gravity. Houndjo et al. [131] have investigated the cosmological model in $f(R,T)$ gravity for finite-time future singularities. Reconstruction of modified holographic Ricci dark energy have been studied with a particular form of $f(R,T)$ gravity in [109]. Thermodynamical aspects with apparent horizon in $f(R,T)$ gravity under the FRW Universe have been investigated by Sharif and Zubair [132]. Azizi [133] has presented a discussion over the wormhole geometries in $f(R,T)$ gravity and showed that in this modified gravity scenario, the effective stress–energy may be considered as a responsible candidate for violation of the null energy condition.

Considering the assumption that the conservation equation holds for $f(R,T)$ gravity, Chakraborty [134] has studied the energy conditions in this modified gravity theory both generally and a particular case of perfect fluid with constant EoS. Alvarenga et al. [135] have studied the evolution of scalar cosmological perturbations in the metric formalism in $f(R,T)$ gravity under the assumption that the considered model is modified in such a way that it guarantee the standard continuity equation. In a paper [136], authors have discussed the dynamics and stability of the model in $f(R,T)$ gravity. They showed that the model presents stability for both the de Sitter and power-law solutions for both the low-redshift and high-redshift regimes, and satisfies the observational data.

Along with the cosmological consequences, the solar system consequences of the $f(R,T)$ gravity have been investigated by Shabani and Farhoudi [137]. The study of $f(R,T)$ gravity models is not limited with the isotropic and homogeneous Universe, a number of authors have done a lot of work to observe the cosmological consequences in the anisotropic and homogeneous Universe under the framework of $f(R,T)$ gravity. Like, Fayaz et al. [138] have explored the discussion of HDE and new agegraphic DE in the anisotropic cosmological model under the framework of $f(R,T)$ gravity. Harko [130] generalized the conservation equation of $f(R,T)$ gravity by using the concept of irreversible matter creation in open thermodynamic systems. There are many authors who have considered the $f(R,T)$ gravity to discuss the consequences of the Universe and tried to give a fruitful outcome to understand the evolution of the the Universe. Many authors [139–142] have successfully explained the history of the Universe by reconstructing the $f(R,T)$ gravity with different matter content. Many other works have been carried out to discuss the evolutionary behaviour of the Universe in $f(R,T)$ gravity considering different energy contents and formalisms [143–150].

Thus, a number of pioneer papers in the literature have motivate us to analyse the evolutionary behaviour of the Universe in $f(R,T)$ gravity. In this thesis, we shall discuss new HDE in $f(R,T)$ gravity to investigate the different aspects of the evolution of the Universe.

1.8 Viscous Cosmology

The perfect fluid in cosmological models constitutes an idealized case, but not always. Many aspects of the evolution of the Universe have been explained by the

perfect fluid, still some processes can't be explained without the investigation of dissipative phenomena arising in the cosmic fluid. The concept of viscosity is introduced from fluid mechanics. From a hydrodynamics point of view the inclusion of viscosity concepts in the macroscopic theory of the cosmic fluid would appear most natural. It is due to shear and bulk viscosity characterized by shear viscosity parameter η and bulk viscosity parameter ζ. In viscous cosmology, shear viscosity comes into play in connection with spacetime anisotropy. A bulk viscosity usually functions in an isotropic Universe.

From a thermodynamical viewpoint the bulk viscosity in a physical system is appeared due to its deviation from the local thermodynamical equilibrium. In a cosmological setting, the bulk viscosity may arise when the cosmic fluid expands (or contracts) too fast so that the system does not have enough time to restore the local thermal equilibrium. The bulk viscosity, therefore, is a measure of the pressure required to restore equilibrium to a compressed of expanding system. It is natural for such a term to exist in expanding Universe anytime the fluid is out of equilibrium. Usually, in cosmology the restoration processes are taken to be so rapid that the recover of equilibrium is almost immediate. However, there is a finite time for the system to adjust to the change of EoS induced by particle decays. This leads to non-trivial dependence of pressure on density as Universe expands, and therefore a bulk viscosity.

Since, the evolution of the Universe involves a sequence of dissipative processes. These processes include bulk viscosity, shear viscosity and heat transport. The introduction of viscosity coefficients in cosmology has itself a long history. Its physical importance of these phenomenological parameters has traditionally been assumed to be weak. The general theory of dissipation in relativistic imperfect fluid was put on a firm foundation by Eckart [151] in 1940 and the full causal theory was developed by Israel and Stewart [152]. However, this theory faces causality problem as dissipative perturbations propagate at infinite speed. According to Eckart theory, if p denotes the thermodynamic pressure of matter content and cosmic fluid has viscosity then the effective pressure is given by

$$\tilde{p} = p - \Pi, \tag{1.8.1}$$

where, $\Pi = 3\zeta H$ is the viscous pressure which occur due to viscosity. Here, ζ is the coefficient of bulk viscosity. The homogeneous and isotropic FRW models have been considered in this thesis to study the viscous cosmological models. In the case of isotropic and homogeneous model, the dissipative process is modeled as a bulk vis-

cosity, see Refs. [153–160]. The viscosity concept in cosmology was first used by Misner [161] in 1968.

Eckart's theory is only the first order deviation from equilibrium and may has a causality problem. The full causal theory was developed by Israel and Stewart [152], which has been studied in the evolution of the early Universe. His causal theory of relativistic viscosity is nothing but a second-order dissipative thermodynamic theory. In this theory, the dissipative variables were included to describe non-equilibrium states due to which this theory is causal and stable. The full Israel-Stewart transport equation is given by [162]

$$\tau\dot{\Pi}+\Pi=-3\zeta H-\frac{\varepsilon\tau\Pi}{2}\left[3H+\frac{\dot{\tau}}{\tau}-\frac{\dot{\zeta}}{\zeta}-\frac{\dot{T}}{T}\right], \tag{1.8.2}$$

where τ denotes relaxation time associated with the dissipative effect. Scalar dissipation processes in cosmology may be treated via the relativistic theory of bulk viscosity. The effects of bulk viscosity in an expanding Universe is to reduce the equilibrium pressure. Therefore, sufficient large bulk viscous pressure could make the effective pressure negative. Thermodynamics states with negative pressure are meta stable and cannot be excluded by any law of nature. These states are connected with phase transitions. We know that there is a problem of singularity either in GTR or modified gravity models. Many authors [162–164] have shown that the bulk viscosity removes the initial singularity. Modified gravity models with bulk viscosity have been discussed in many ways to describe the evolution of the Universe. However, because of the simple form of Eckart theory, it has been widely used by several authors to characterize the bulk viscous fluid. The Eckart approach has been used in models explaining the recent acceleration of the Universe with bulk viscous fluid. Many authors [165–172] have studied the DE phenomenon as an effect of the bulk viscosity in the cosmic medium.

All the above cited works are pioneer papers on bulk viscosity which show that for an appropriate viscosity coefficient, an accelerating cosmology can be achieved without the need of a cosmological constant. At the late times, since we do not know the nature of the Universe content very clearly, concern about the bulk viscosity is reasonable and practical. To our knowledge, such a possibility has been investigated only in the context of the primordial Universe, concerning also the search of non-singular models. But many investigations show that the viscous pressure can play the role of

an agent that drives the present acceleration of the Universe. Therefore, the interest in viscosity theories in cosmology has increased in recent years, for various reasons, perhaps especially from a fundamental viewpoint.

1.9 Cosmological Parameters

Now before going further, it is useful to define some of the cosmological parameters because these parameters play a very important role in the study of the evolution of the Universe. Let us bring our attention towards some parameters which are used to study the cosmological phenomena in this thesis.

1.9.1 Hubble Parameter

The rate of expansion of the Universe is measured by the Hubble parameter. The Hubble parameter is denoted by $H(t)$ and is defined as

$$H(t) = \frac{\dot{a}(t)}{a(t)}, \tag{1.9.1}$$

where a as usual denotes the cosmic scale factor and an over dot defines a derivative with respect to time t. Note that Hubble parameter is not a constant. The Hubble constant is the Hubble parameter measured today- we denote it by H_0. The Universe contracts for negative values and expands for positive values of the Hubble parameter. Our Universe is expanding because we observe a positive value of the Hubble parameter. The present value H_0 has been obtained using various observational data. The latest data of the SDSS-III Baryon Oscillation Spectroscopic Survey gives $H_0 = 67.6^{+0.7}_{-0.6}\ km\, s^{-1} Mpc^{-1}$ [173].

The time-varying Hubble parameter $(1.9.1)$ measures the rate of change of the scale factor $a(t)$ and provides a way to link the observations with a proposed model using the scale factor. It is to be noted that we can expect the constant expansion rate throughout its history, $H(t) = H_0$ only in a empty space.

1.9.2 Critical density

The density of the Universe which is required for the Universe to be flat is known as the critical density of the Universe. It is denoted by ρ_c and is defined as

$$\rho_{\mathrm{c}} = \frac{3H^2}{8\pi G}\,. \tag{1.9.2}$$

Since critical density depends on Hubble parameter, hence the critical density also evolves with time. The present value of the critical density can be calculated from the known value of H_0.

1.9.3 Density parameter

It is very useful to express cosmological quantities and cosmic field equations in the terms of the density parameter Ω. It is defined as the ratio of the matter density of the Universe to the critical density of the Universe at the same time, that is,

$$\Omega = \frac{\rho}{\rho_{\mathrm{c}}} = \frac{8\pi G\rho}{3H^2}, \tag{1.9.3}$$

where ρ may be the density of matter, DE, scalar field etc. Although current research suggests that Ω is very close to 1, it is still of great importance to know whether Ω is slightly greater than 1, less than 1, or exactly equal to 1, as this reveals the ultimate fate of the Universe. If Ω is less than 1, the Universe is open and will continue to expand forever. If Ω is greater than 1, the Universe is closed and will eventually halt its expansion and recollapse. If Ω is exactly equal to 1 then the Universe is flat and contains enough matter to halt the expansion but not enough to recollapse it. Observations have shown that the present Universe is very close to a spatially flat geometry ($\Omega \simeq 1$).

The total energy content of the Universe may be divided in two parts, matter (Baryonic + Dark matter) and DE. The density of both are represented by ρ_m and ρ_Λ, respectively, and the total density given by $\rho = \rho_m + \rho_\Lambda$. The density parameters for matter and DE are given as

$$\Omega_m = \frac{\rho_m}{\rho_c}; \qquad \Omega_\Lambda = \frac{\rho_\Lambda}{\rho_c}, \tag{1.9.4}$$

where $\Omega = \Omega_m + \Omega_\Lambda$.

1.9.4 Deceleration Parameter

The deceleration parameter (DP) is the simplest cosmological parameter which is very useful parameter to discuss the behaviour of the Universe. The positive or negative sign of DP explains whether the Universe decelerates or accelerates, respectively. It is represented by q and is defined as

$$q = -\frac{a\ddot{a}}{\dot{a}^2}\,, \tag{1.9.5}$$

where a and the overdot have their usual meanings. Our Universe has experienced two phase transitions, early time inflation to decelerated expansion and decelerated expansion to late time accelerated expansion. When DP changes its sign from positive to negative or negative to positive, then it becomes more useful to explain the phase transition of the Universe.

1.10 Kinematical Parameters

We introduce some kinematical parameters of the observational interest in cosmology, which are helpful to study the homogeneous and anisotropic Universe.

1.10.1 Expansion Scalar

The expansion scalar represents the rate of expansion and is denoted by θ. In case of homogeneous and isotropic FRW model, it is defined as

$$\theta = u^{i}_{;\,i} = 3\frac{\dot{a}}{a} = 3H, \tag{1.10.1}$$

and in case of homogeneous and anisotropic models, it is defined as

$$\theta = \left(\frac{\dot{A}}{A} + \frac{\dot{B}}{B} + \frac{\dot{C}}{C}\right), \tag{1.10.2}$$

where A, B, C and overdot have their usual meaning.

1.10.2 Anisotropy Parameter

The anisotropy parameter is used to study the anisotropic behaviour of the Universe. It gives the measure of departure from isotropy, i.e., with this parameter we can observe at which phase the anisotropy is greater or lesser, or at which phase the anisotropy is removed from the Universe. This parameter is represented by A_p and is defined as

$$A_p = \frac{1}{3}\sum_{i=1}^{3}\left(\frac{H_i - H}{H}\right)^2, \tag{1.10.3}$$

where H_i $(i = 1,2,3)$ represent the directional Hubble parameters along x, y and z-axes, respectively. The Hubble parameter in the anisotropic Universe is defined as

$$H = \frac{\dot{a}}{a} = \frac{1}{3}\left(\frac{\dot{A}}{A} + \frac{\dot{B}}{B} + \frac{\dot{C}}{C}\right), \tag{1.10.4}$$

and the corresponding directional Hubble parameters are defined as

$$H_1 = \frac{\dot{A}}{A}, \quad H_2 = \frac{\dot{B}}{B}, \quad H_3 = \frac{\dot{C}}{C}. \tag{1.10.5}$$

1.10.3 Shear Scalar

In the case of the anisotropic Universe the shear is measured by the observations. It places a vital role in the study of the homogeneous and anisotropic Universe. It is denoted by σ^2 and is defined as

$$\sigma^2 = \frac{1}{2}\sigma_{ij}\sigma^{ij} = \frac{1}{2}\left[\left(\frac{\dot{A}}{A}\right)^2 + \left(\frac{\dot{B}}{B}\right)^2 + \left(\frac{\dot{C}}{C}\right)^2\right] - \frac{\theta^2}{6}, \tag{1.10.6}$$

where σ^{ij} is the shear tensor and is defined as $\sigma^{ij} = \frac{1}{2}(u_{\mu;\alpha}h^{\alpha}_{\nu} + u_{\nu;\alpha}h^{\alpha}_{\mu}) - \frac{1}{3}\theta h_{\mu\nu}$, where $h_{\mu\nu} = g_{\mu\nu} - u_{\mu}u_{\nu}$ is the projection tensor.

1.11 Geometrical Parameters

The study of cosmological parameters like the Hubble parameter H, the DP q and the EoS parameter ω have attracted a lot of attention in present day cosmology. Since different DE models give a positive Hubble parameter and a negative DP at the present epoch, we can clearly understand that H and q can not effectively discriminate the

different DE energy density models. Therefore, a higher order of time derivatives of $a(t)$ is then required if we want to have a better understanding of the DE model considered. Rapid advances in observational cosmology are leading to the establishment of the first precision cosmological model, with many of the key cosmological parameters. Geometrical parameters have traditionally played a key role in cosmology. Let us discuss some geometrical parameters here which are used to study the cosmological phenomena in this thesis.

1.11.1 Statefinder Parameter

Since a number of dynamical DE models have been proposed to explain the cosmic acceleration, a sensitive and diagnostic tool is required to discriminate these DE models with other existing DE models. In this context, Sahni et al. [174] and Alam et al. [175] proposed a new geometrical diagnostic parameter for DE, which is known as statefinder pair and is denoted as $\{r,s\}$. The statefinder parameter probes the expansion dynamics of the Universe through higher derivatives of the scale factor and is a geometrical diagnosis in the sense that it depends on the scale factor and hence describes the spacetime. The statefinder parameter can be defined as

$$r = \frac{\dddot{a}}{aH^3} \quad \text{and} \quad s = \frac{r-1}{3(q-1/2)}. \tag{1.11.1}$$

This diagnostic tool has been used to study the various DE models. It has been used to diagnose different cases of the model, like different model parameters and various spatial curvature contributions. The various DE models have different evolutionary trajectories in $r-s$ plane. For example, the well-known Lambda cold dark matter (ΛCDM) model corresponds to a fixed point $\{r,s\} = \{1,0\}$ and standard cold dark matter ($SCDM$) model corresponds to $\{r,s\} = \{1,1\}$ [174,175]. We may plot trajectories in the $r-s$ and $r-q$ planes to discriminate among DE models. In the present era where a number of DE model are available in the literature, the statefinder parameters $\{r,s\}$ play an important role to discriminate among the DE models.

1.11.2 *Om* Diagnostic

In addition to statefinder $\{r,s\}$, another diagnostic tool, *Om(z)* is widely used to discriminate DE density in DE models. It is a new geometrical diagnostic which combines Hubble parameter H and redshift z. Since it depends only on the first derivative

of scale factor so it is more convenient to find out *Om(z)* as compare to statefinder parameters. The *Om(z)* diagnostic [176] has been proposed to differentiate ΛCDM to other DE models. Many authors [177–179] have been studied the DE models based on *Om(z)* diagnostic. The constant value of $Om(z)$ tells that DE behaves as cosmological constant (ΛCDM), whereas its positive and negative slopes with respect to z shows that the DE behaves like phantom and quintessence, respectively. According to ref. [176], *Om(z)* parameter for spatially flat Universe is defined as

$$Om(z) = \frac{\frac{H^2(z)}{H_0^2} - 1}{(1+z)^3 - 1}. \tag{1.11.2}$$

It is easier to reconstruct $Om(z)$ than statefinder pair because it depends only on the first derivative of scale factor. As we know that the curvature of *Om(z)* can discriminate dynamical DE from the cosmological constant in a robust manner, both with and without the reference of matter density.

1.12 Motivation

Motivated by the discussion in previous Sections, in this thesis, we propose to investigate the isotropic and anisotropic cosmological models in general relativity and modified gravity theories to observe the accelerated expansion of the Universe.

In recent years, the holographic dark energy has been studied as a possible candidate for dark energy which is based on holographic principle. The holographic energy density is given by $(1.7.13)$, where L is the IR cutoff. There are various choices of IR cutoff for the cosmological length scale available in the literature, for instance, Hubble horizon $(L = H^{-1})$, particle horizon $(L = a(t)\int_0^t \frac{dt'}{a(t')})$, future event horizon. In recent studies, some new IR cutoffs have been proposed. Gao et al. [180] proposed IR cutoff as a function of Ricci scalar. So, the length L is given by the average radius of Ricci scalar curvature. This type of HDE is called Ricci dark energy (RDE). Granda and Oliveros [73] proposed a new IR cutoff for HDE, known as new holographic dark energy. However, in this thesis, we will consider two types of IR cutoff: future event horizon and new HDE proposed by Granda and Oliveros [73].

The introduction of a scalar field potential augmented by a scalar field dependent coupling constant solved many problems and provided hints to the solutions of many outstanding cosmological problems in Brans–Dicke (BD) theory. The relativistic the-

ory of gravity based on the Einstein's theory of general relativity was proposed by Brans and Dicke [100] in the early 1960s. In this gravity theory, first time the scalar field was used to describe the dynamics of gravity while the metric tensor was used to represent the dynamics of spacetime. The basic notion is that the BD scalar field plays the role of quintessence or K-essence and leads to cosmic acceleration.

Thus, we can conclude that scalar field may be considered as a candidate of DE in the BD gravity. In this context, we can relate the energy density of HDE (or, can say any other form of DE) and BD scalar field. The BD scalar ϕ plays a role of the inverse of Newtonian constant ($\phi \propto 1/G$). Thus, from Eq. (1.7.13), the relation of HDE with BD scalar field can be written as

$$\rho_d = 3d_1\phi L^{-2}. \tag{1.12.1}$$

Most of the authors have assumed the BD scalar field as a power-law form of scale factor in HDE models to explain the evolution of the Universe. They claimed that this assumption gives time-dependent DP which shows the transition from deceleration one to acceleration. However, some authors claimed that this relation gives the constant DP which does not show the phase transition. Now, the problem is that which physical interpretation is valid to explain the evolutionary phases of the Universe.

In a paper, Kumar and Singh [181, 182] analyzed this problem and found that field equations in BD theory always gives constant value of DP using BD scalar field as a power-law form of scale factor irrespective of the matter content. They have proposed the BD scalar field as a logarithmic form of scale factor which always gives time-dependent DP. In chapter 2, motivated by this work, we have studied non-interacting and interacting HDE models with future event horizon as an IR cutoff in BD theory with logarithmic form of BD scalar field. It not only describes the phase transition but also solves the coincidence problem.

The bulk viscous fluid is a well known concept to produce the accelerated expansion without the need of any cosmological constant or DE component. Even, this concept has been known since several years ago before of the discovery of the present accelerated expansion of the Universe. In a cosmological fluid, the bulk viscosity may arise when the fluid expands (or contracts) too fast so that the system does not have enough time to restore its local thermodynamic equilibrium. Initially, the bulk viscosity was proposed to explain an inflationary period occurred in the early Universe. Nowadays, it has been studied in the context of present day Universe. Therefore, it is natural to assume the possibility that the expansion process is actually a collection of states

out of thermal equilibrium in a small fraction of time giving rise to the existence of a bulk viscosity.

In chapters 3, 4 and 5, we have analyzed the new HDE models with bulk viscosity in general relativity and $f(R,T)$ gravity with reference to the question whether the bulk viscous fluid can cause the recent acceleration of the Universe. The New HDE model is composed of pressureless fluid (dust) with bulk viscosity of the form $\zeta = \zeta_0 + \zeta_1 H$, where ζ_0 and ζ_1 are constants and H stands for Hubble parameter. The simplest parametrization for the bulk viscosity is its constant value, i.e., the term "ζ_0" and the term "$\zeta_1 H$" characterizes the possibility of a bulk viscosity proportional to the expansion rate of the Universe.

The discovery of the accelerated expansion of the Universe has opened a new window in cosmological studies. An alternative method of describing the matter content of the Universe is to adopt the energy momentum tensor of a scalar field ϕ with the kinetic part and the potential $V = V(\phi)$. The energy-momentum tensor for scalar field is given by $(1.7.6)$. Within the framework of general relativity, scalar fields provide possible dark energy models which can describe, but not so far explain, this acceleration. Scalar field models require the choice of a self-interaction potential $V(\phi)$ for scalar field ϕ. Obviously it is important to proposed potentials which are realistic and at the same time lead to exactly soluble models in the FRW spacetime. Various candidates have been proposed in the literature, such as an inverse power law, exponential, hyperbolic and the list goes on to discuss the behavior of the models. In Chapters 6 and 7, we have studied scalar field cosmology with exponential potential in anisotropic Bianchi types I and V cosmological models.

At last, the summary and further scope of the work have been carried out. The bibliography and list of publications have been enlisted at the end of this thesis.

Chapter 2

Holographic dark energy model in Brans-Dicke theory

In this chapter[1]*, we study the dynamics of non-interacting and interacting holographic dark energy models in the framework of Brans–Dicke cosmology with future event horizon as an infrared cutoff. We consider the logarithmic form of Brans–Dicke scalar field to obtain the time-dependent value of equation of state parameter and deceleration parameter which describe the phase transition of the Universe. We observe that the model explains the early time inflation and late time acceleration. It is also observed that the EoS parameter may cross phantom divide line in late time evolution. The cosmic coincidence problem is also discussed for both the models. We observe that it is more appropriate to achieve a less acute coincidence problem in non-interacting model whereas a soft coincidence can be achieved if coupling parameter in interacting model has small value.*

---

[1]The result of this chapter has been published as a research paper "Cosmological evolution of non-interacting and interacting holographic dark energy model in Brans-Dicke theory, *International Journal of Geometric Methods in Modern Physics* **15**, 1850124 (2018)".

2.1 Introduction

It is well known that the observations from Supernovae Type Ia (SNeIa) provide strong evidence for an accelerating Universe. In relativistic cosmology, such a phenomenon is usually explained by the existence of a new dark components, an exotic fluid endowed with negative pressure called as DE. Many candidates for DE have been proposed in literature to describe this late time acceleration of the Universe. Holographic dark energy is one of the strong candidate of this DE. In recent years, the HDE [67–71, 182–187] has been studied as a possible candidate for DE.

HDE is a great arena for modified gravity for a few reasons. As a non-renormalizable theory, and currently the only known non-renormalizable theory, gravity is ultraviolet sensitive. In HDE the UV cutoff of the theory depends on the IR cutoff. The IR cutoff is set at the cosmological scale for the concern of DE. As a result, the UV cutoff is much affected. As we do not have a firm general relativity equation for quantum gravity, the best we can do is to take a modified gravity theory with the presence of HDE as a candidate of the infrared gravity theory. For this reason, actually, even if a modified theory is ruled out on earth, solar system or galactic scale experiments, it may still be considered together with HDE because cosmological scales is a completely different scale. For many modified models to work as DE, they still have to solve the old cosmological constant problem and coincidence problem of GTR. HDE solves the problem for this modified theories. Thus, the modified theory in HDE can focus on the naturalness from first principle, dynamics of DE, agreement with observations, etc.

In this chapter, we consider non-interacting and interacting HDE models with IR cutoff as future event horizon in BD theory. It is worthwhile to investigate the HDE density in the framework of the BD theory. Since HDE density belongs to a dynamical cosmological constant, we need a dynamical frame to accommodate it instead of GTR. It is well known that the BD theory explains the dynamics of gravity, described by a scalar field.

In the literature, almost all the models have been discussed in BD theory by assuming the power-law form of BD scalar field $\phi \propto a^n$, where a is the scale factor and n is a constant. Many authors [114, 118, 188, 189] have studied the evolution of the Universe in BD theory by assuming the above power-law relation of BD scalar field. They have observed that this assumption leads to a constant value of DP. The constant value of DP can be obtained irrespective of matter content of the Universe. If it is constant,

then it can not describe the phase transition of the Universe.

However, some authors [70, 183, 187, 190] have studied HDE model in BD theory with the same form of BD scalar field and have obtained a time-dependent DP, which describes the phase transition. Similarly, some authors [191–193] have studied the new agegraphic dark energy models in BD theory by assuming the same power-law form of BD scalar field. They have also claimed for a time-dependent DP.

Now, the question arises that why does the same form of BD scalar field lead to two different values of DP, constant and time-dependent for the same model? In a paper [181, 182], the authors have analyzed this problem and have concluded that one can always find constant DP irrespective of matter content with power-law scale factor. Therefore, the power-law assumption can not describe the phase transition of the Universe. Taking into consideration this problem, the authors [181] have proposed a logarithmic form of BD scalar field. Using the logarithmic form of BD scalar they have found the time-dependent DP which explains the transition phase. This model also solves the cosmic coincidence problem successfully. Further, in a paper [182] authors have considered this logarithmic form for the HDE model in BD theory with Hubble horizon as an IR cutoff and obtained the same type of results which explains the phase transition as well as the cosmic coincidence problem.

In the present chapter, we extend this work to non-interacting and interacting HDE models with future event horizon in BD theory. We revisit the Ref. [187] and consider HDE model in BD theory with logarithmic form of scalar field. We obtain the time-dependent DP and EoS parameter which describe the phase transition of the evolution of the Universe. We further discuss a cosmological model where the pressureless dark matter and HDE are not conserved separately but interact with each other. We also discuss the cosmic coincidence problem which has not been discussed in previous work [183, 187]. It is found that the HDE model successfully resolves the cosmic coincidence problem in BD theory with this logarithmic form of the scalar field.

2.2 Holographic dark energy in Brans-Dicke Theory

We consider a homogeneous and isotropic non-flat Friedmann-Robertson-Walker (FRW) Universe described by (1.3.7). We assume that the Universe is filled with perfect fluid containing pressureless dark matter (excluding baryonic matter) and HDE whose

energy-momentum tensor can be written as

$$T_{\mu\nu} = (\rho_m + \rho_h + p_h)\, u_\mu\, u_\nu - p_h\, g_{\mu\nu}, \tag{2.2.1}$$

where ρ_m is the energy density of dark matter and ρ_h and p_h are the energy density and pressure of HDE, respectively.

The field equations of Brans–Dicke for the line element (1.3.7) and energy-momentum tensor (2.2.1) yield

$$\frac{3}{4w}\left(H^2 + \frac{k}{a^2}\right) - \frac{1}{2}\frac{\dot{\phi}^2}{\phi^2} + \frac{3H}{2w}\frac{\dot{\phi}}{\phi} = \frac{\rho_m + \rho_h}{\phi^2}, \tag{2.2.2}$$

$$\frac{1}{4w}\left(2\frac{\ddot{a}}{a} + H^2 + \frac{k}{a^2}\right) + \frac{H}{w}\frac{\dot{\phi}}{\phi} + \frac{1}{2w}\frac{\ddot{\phi}}{\phi} + \frac{1}{2}\left(1 + \frac{1}{w}\right)\frac{\dot{\phi}^2}{\phi^2} = -\frac{p_h}{\phi^2}. \tag{2.2.3}$$

The wave equation (1.7.17) for the scalar field ϕ is given by

$$\ddot{\phi} + 3H\dot{\phi} - \frac{3}{2w}\left(\frac{\ddot{a}}{a} + H^2 + \frac{k}{a^2}\right)\phi = 0. \tag{2.2.4}$$

The HDE density defined in (1.7.13), can be written as

$$\rho_h = \frac{3d_1^2}{8\pi G}L^{-2}. \tag{2.2.5}$$

In canonical form $G_{eff}^{-1} = \frac{2\pi}{w}\phi^2$, the HDE density (2.2.5) now become as

$$\rho_h = \frac{3d_1^2\phi^2}{4wL^2}. \tag{2.2.6}$$

If the IR cutoff is taken as the radius of the Hubble horizon then the energy density of HDE and the critical density match identically. Generally, this condition arises in the inflationary scenarios where $L = H^{-1}$. Since, there are various other choices of IR cutoff for the cosmological length scale L available in the literature, such as particle horizon, event horizon, Ricci length, Granda-Oliveros cutoff, etc. However, particle horizon is not suitable to drive the acceleration. A suitable choice of future event horizon as an IR cutoff was suggested by Li et al. [194]. By this choice of system's IR cutoff, the cosmological length L for the event horizon is

$$L = ar(t), \tag{2.2.7}$$

where the function $r(t)$ can be obtained by the relation

$$\int_0^{r(t)} \frac{dr}{\sqrt{1-kr^2}} = \int_t^{\infty} \frac{dt}{a(t)} = \frac{R_E}{a(t)}, \tag{2.2.8}$$

where R_E is the event horizon, defined by

$$R_E = a\int_t^{\infty} \frac{dt}{a(t)} = a\int_a^{\infty} \frac{da}{Ha^2}. \tag{2.2.9}$$

The general solution of $r(t)$ from Eq.(2.2.8) for non-flat FRW model is given by

$$r(t) = \frac{1}{\sqrt{k}} \sin y, \tag{2.2.10}$$

where, $y = \frac{\sqrt{k}R_E}{a(t)}$. The critical energy density ρ_{cr} and the energy density of the curvature ρ_k are, respectively, defined as

$$\rho_{cr} = \frac{3\phi^2 H^2}{4w}, \tag{2.2.11}$$

$$\rho_k = \frac{3k\phi^2}{4wa^2}. \tag{2.2.12}$$

To analyse the results in a better way, we convert the quantities in terms of fractional energy densities. The fractional energy densities in their usual form are given by

$$\Omega_m = \frac{\rho_m}{\rho_{cr}} = \frac{4w\rho_m}{3\phi^2 H^2}, \tag{2.2.13}$$

$$\Omega_k = \frac{\rho_k}{\rho_{cr}} = \frac{k}{H^2 a^2}, \tag{2.2.14}$$

$$\Omega_h = \frac{\rho_h}{\rho_{cr}} = \frac{d_1^2}{H^2 L^2}. \tag{2.2.15}$$

We can also write the Eq. (2.2.15) as

$$HL = \frac{d_1}{\sqrt{\Omega_h}}. \tag{2.2.16}$$

On differentiating (2.2.7) with respect to the cosmic time t, and using (2.2.10) and (2.2.16), we obtain

$$\dot{L} = HL + ar\dot{(t)} = \frac{d_1}{\sqrt{\Omega_h}} - \cos y. \tag{2.2.17}$$

2.2.1 Non-interacting HDE model

Let us first consider the case where HDE and dark matter do not interact. In this case, the conservation equations for HDE and dark matter are respectively given by

$$\dot{\rho}_h + 3(1+\omega_h)\rho_h H = 0, \tag{2.2.18}$$

$$\dot{\rho}_m + 3\rho_m H = 0, \tag{2.2.19}$$

where $\omega_h = \frac{p_h}{\rho_h}$ is the EoS parameter of HDE.

To discuss the physical behaviors of HDE model, we assume the following logarithmic relation between BD scalar field and scale factor [181, 182], which is claimed that it may avoid a constant result for the DP.

$$\phi = \phi_0 \ ln(l_1 + m_1 a), \tag{2.2.20}$$

where $\phi_0 > 0$, $l_1 > 1$ and $m_1 > 0$ are some constants. If $m_1 = 0$, we have $\phi = const.$, thus it reduces to GTR case.

On taking the first and second order derivative of (2.2.20) with respect to time, we get

$$\dot{\phi} = \phi_0 \frac{m_1 a H}{(l_1 + m_1 a)}, \tag{2.2.21}$$

$$\ddot{\phi} = \phi_0 \left\{ \frac{m_1 a \dot{H}}{(l_1 + m_1 a)} + \frac{m_1 a H^2}{(l_1 + m_1 a)} - \frac{m_1^2 a^2 H^2}{(l_1 + m_1 a)^2} \right\}. \tag{2.2.22}$$

Using (2.2.17) and (2.2.21) into (2.2.6), we get

$$\dot{\rho}_h = 2H\rho_h \left(-1 + \frac{\sqrt{\Omega_h}}{d_1} \cos y + \frac{m_1 a}{(l_1 + m_1 a)\ ln(l_1 + m_1 a)} \right). \tag{2.2.23}$$

Using (2.2.23) into (2.2.18), we obtain the EoS parameter for HDE

$$\omega_h = -\frac{1}{3} - \frac{2m_1 a}{3(l_1 + m_1 a)\ ln(l_1 + m_1 a)} - \frac{2\sqrt{\Omega_h}}{3d_1} \cos y. \tag{2.2.24}$$

The EoS parameter ω_h is bounded from below by

$$\omega_h = -\frac{1}{3} - \frac{2m_1 a}{3(l_1 + m_1 a)\ ln(l_1 + m_1 a)} - \frac{2\sqrt{\Omega_h}}{3d_1}. \tag{2.2.25}$$

From (2.2.24), we observe that for $m_1 = 0$ the EoS parameter ω_h of HDE reduces to its

respective form of non-flat standard cosmology [195], which is given by

$$\omega_h = -\frac{1}{3} - \frac{2\sqrt{\Omega_h}}{3d_1}\cos y. \tag{2.2.26}$$

It is to be noted that for power-law form $\phi \propto a^n$ of BD scalar field [183, 187], the second term in the value of ω_h of Eq. (2.2.25) is a constant term $\frac{2n}{3}$ whereas we get a time-dependent term $\frac{2m_1 a}{3(l_1+m_1 a)\, ln(l_1+m_1 a)}$ due to logarithmic form of BD scalar field. Therefore, the value of ω_h in our model is more dynamic in comparison to power-law in BD theory.

From (2.2.25), it is clear that ω_h always has a negative value such that $\omega_h < -\frac{1}{3}$. The value of ω_h at the beginning of the evolution, i.e., $a = 0$ is same as in Eq. (2.2.26) for GTR because the second term is zero at $a = 0$. Thus, we find a negative value of ω_h in the very early Universe. It is observed that the second term attains its maximum value during the evolution and approaches to zero in late time evolution. The maximum value depends on sufficiently small values of l_1 and large values of m_1 during the process of evolution. However, the maximum value only depends on the parameter l_1 and it is found that $\max\left\{\frac{m_1 a}{(l_1+m_1 a)\, ln(l_1+m_1 a)}\right\} \to 1$ as $l_1 \to 1$, i.e., $\omega_h < -1$. Therefore, ω_h may cross phantom divide line for this condition. It may also possible that ω_h crosses the phantom divide line for $\sqrt{\Omega_h} > d_1[1 - \frac{m_1 a}{(l_1+m_1 a)\, ln(l_1+m_1 a)}]$, i.e., for both conditions HDE model may cross the phantom divide line ($\omega_h = -1$) and approaches to the phantom region.

It is also interesting to note that as the logarithmic term converges to zero in the late time of evolution and also $\cos y \to 1$ in late time as $a \to \infty$, the EoS parameter starts behaving like its respective form in standard GTR [195] and it will depend only on the values of Ω_h and d_1. The form of ω_h in the late time is given by

$$\omega_h = -\frac{1}{3} - \frac{2\sqrt{\Omega_h}}{3d_1}. \tag{2.2.27}$$

In this model, the value of parameter d_1 determines the property of HDE in late time. Since, the observation predicts $\Omega_h \to 1$ for the present time, therefore, at $d_1 = 1$, ω_h approaches to -1, i.e., our model behaves like cosmological constant. We get $\omega_h > -1$ but less than $-1/3$ at $d_1 > 1$, i.e., our model shows the quintessence region and if $d_1 < 1$, we get $\omega_h < -1$, i.e., the phantom type behaviour occur. Thus, we conclude that when $d_1 > 1$, $d_1 = 1$ and $d_1 < 1$, one can generate quintessence, cosmological constant and phantom, respectively, for non-interacting HDE model in BD theory.

In the study of the Universe, the DP place a very important role which is defined in section 1.9.4 by Eq. (1.9.5). The DP in terms of Hubble parameter can be represented as

$$q = -1 - \frac{\dot{H}}{H^2}. \tag{2.2.28}$$

Now dividing Eq. (2.2.3) by H^2 and using Eqs. (2.2.6), (2.2.14), (2.2.16), (2.2.21) and (2.2.22), we get

$$\frac{\dot{H}}{H^2} = \frac{-3 - \Omega_k - 3\Omega_h\omega_h - \frac{6m_1a}{(l_1+m_1a)\,ln(l_1+m_1a)} + \frac{2m_1^2a^2}{(l_1+m_1a)^2\,ln(l_1+m_1a)} - \frac{2(w+1)m_1^2a^2}{(l_1+m_1a)^2\,[ln(l_1+m_1a)]^2}}{2\left(1 + \frac{m_1a}{(l_1+m_1a)\,ln(l_1+m_1a)}\right)}. \tag{2.2.29}$$

On substituting the above value in the (2.2.28), we get the DP as

$$q = \frac{1 + \Omega_k + 3\omega_h\Omega_h + \frac{4m_1a}{(l_1+m_1a)\,ln(l_1+m_1a)} - \frac{2m_1^2a^2}{(l_1+m_1a)^2\,ln(l_1+m_1a)} + \frac{2(w+1)m_1^2a^2}{(l_1+m_1a)^2\,[ln(l_1+m_1a)]^2}}{2\left(1 + \frac{m_1a}{(l_1+m_1a)\,ln(l_1+m_1a)}\right)}. \tag{2.2.30}$$

The term $\frac{m_1^2a^2}{(l_1+m_1a)^2\,ln(l_1+m_1a)}$ has the same behaviour as the term $\frac{m_1a}{(l_1+m_1a)\,ln(l_1+m_1a)}$ except it has maximum value lies in (0, 0.41) depending on the value of l_1. The BD parameter w also plays an important role in the value of q. The solar system experiment Cassini gave a very high bound on w as $|w| > 40000$ [111, 196], whereas the cosmological observations provide the relatively lower bounds on $|w|$ [197–200]. The observations suggest that $|w|$ has large value so the last term of numerator of Eq.(2.2.30) containing w will dominate during the evolution of the Universe. This shows that q may attain some positive value, i.e., the decelerated expansion of the Universe may occur during the evolution. Thus, HDE model explains the matter-dominated phase of the Universe. As in the late time of evolution, $\omega_h \to -1$ and the terms $\frac{m_1a}{(l_1+m_1a)\,ln(l_1+m_1a)}$ and $\frac{m_1^2a^2}{(l_1+m_1a)^2\,ln(l_1+m_1a)}$ converge to zero as $a \to \infty$. Thus, the value of q in late time of evolution is obtained as

$$q \approx \frac{1 + \Omega_k - 3\Omega_h}{2}. \tag{2.2.31}$$

Since the observations indicate that our present Universe is almost flat, i.e., $k = 0$ ($\Omega_k = 0$), Eq.(2.2.31) gives $q \approx \frac{1-3\Omega_h}{2}$. Thus, it is observed that q is negative for $\Omega_h > 1/3$, i.e., the accelerated expansion is obtained for $\Omega_h > 1/3$. It can also be noticed that if we consider the open Universe, i.e., $k < 0$ ($\Omega_k < 0$), the accelerated expansion can be obtained more easily. Even for the closed geometry case of the Universe we can also get an accelerated expansion of the Universe but for this we must have a

very large value of Ω_h which will give a negative value of q. Thus, we can conclude that the HDE model describes the phase transition from early time inflation to the matter-dominated phase and then matter-dominated phase to late time accelerated phase.

Cosmic Coincidence Problem

Let us discuss the cosmological coincidence problem which were raised by Steinhardt and Zlatev et al. [26, 27]. The problem may be resolved by making the density ratio $r_1 = \frac{\rho_m}{\rho_h}$ is of order unity, i.e., $(r_1)_0 \sim \mathscr{O}(1)$ for a wide range of initial condition. The second way is that either r_1 converses to a constant value or evolves very slowly in late time of evolution. From (2.2.2), the energy density ratio is given by

$$r_1 = -1 + \frac{1}{\Omega_h}\left[\Omega_k + 1 - \frac{2\,wm_1^2a^2}{3(l_1+m_1a)^2\,[ln(l_1+m_1a)]^2} + \frac{2m_1a}{(l_1+m_1a)\,ln(l_1+m_1a)}\right]. \quad (2.2.32)$$

Therefore, we obtain a time-dependent value of r_1. At the beginning of evolution the value of r_1 is $\left\{-1+\frac{(\Omega_k+1)}{\Omega_h}\right\}$ as the last two terms vanish at $a=0$. In the late time of evolution we obtain the same expression of r_1 as the last two terms approach to zero as $a \to \infty$. Now, the evolution of energy density ratio r_1 can be obtained as

$$\dot{r}_1 = 3r_1H\omega_h. \quad (2.2.33)$$

According to ΛCDM model, r_1 evolves as $|\frac{\dot{r}_1}{r_1}|_0 = 3H_0$. Throughout the chapter the subscript zero represents the present value of the quantity. Since, for $d_1 = 1$ our model shows $\omega_{h0} = -1$ in late time, therefore, we get $|\frac{\dot{r}_1}{r_1}|_0 = 3H_0$, which is same as for ΛCDM model. This shows that there is no reduction in the acuteness of the coincidence problem. Since, the EoS parameter ω_h is time-dependent, therefore, the less acute coincidence problem can be obtained if we have a quintessence like EoS parameter ($\omega_h > -1$). Also, we may achieve $\omega_{h0} > -1$ for $\sqrt{\Omega_h} < \frac{d_1}{\cos y}[1 - \frac{m_1a}{(l_1+m_1a)\,ln(l_1+m_1a)}]$. Since, the second term converges to zero as $a \to \infty$, we can get quintessence like EoS parameter more conveniently due to the logarithmic form as compared to the power-law form of BD scalar field where we get second term as a constant. Thus, we can conclude that this logarithmic form of BD scalar field is more appropriate to achieve a less acute coincidence problem. Now, let us assume $\omega_{h0} = -2/3$, we obtained $|\frac{\dot{r}_1}{r_1}|_0 = 2H_0$. Clearly, it shows less acuteness in the coincidence problem as compared to the ΛCDM model. But, the problem is more acute in the case of phantom like EoS

parameter ($\omega_{h0} < -1$). This case shows the more complex condition of coincidence problem as compared to the ΛCDM model.

2.3 Interacting HDE model

In a paper, Amendola [201] showed that it is possible to find the attractor solutions in nonminimal coupling models. He found a class of models in which the dynamics of the system is independent of the coupling and of the potential, and depends only on their relation. In other paper, Amendola [202] investigated the cosmological consequences of a coupled quintessence model, assuming an exponential potential and a linear coupling. He tried to write in covariant form of interacting sources. He considered two components, a scalar field ϕ and ordinary matter described by the energy momentum tensor $T_{\mu\nu(\phi)}$ and $T_{\mu\nu(m)}$, respectively. General covariance requires the conservation of their sum, so that it is possible to consider a coupling such that, for instance,

$$T^{\mu}_{\nu(\phi);\mu} = CT_{(m)}\phi_{;\nu}, \tag{2.3.1}$$

$$T^{\mu}_{\nu(m);\mu} = -CT_{(m)}\phi_{;\nu}. \tag{2.3.2}$$

Such a coupling arises for instance in string theory, or after a conformal transformation of BD theory. The specific coupling (2.3.1) and (2.3.2) are only one of the possible forms, other forms may be possible. Zimdhal et al. [37] demonstrated that a suitable coupling between a quintessence scalar field and a pressureless cold dark matter fluid leads to a constant ratio of the energy densities of both components which is compatible with an accelerated expansion of the Universe. Zimdhal et al. [37] assumed the interaction described by a source (loss) term in energy balances. They found this attractor form in terms of density.

In this section, we extend our study to the case where both dark components, the pressureless dark matter and the HDE, interact with each other. If we proceed to consider a scenario of interacting dark energy, ρ_m and ρ_h do not satisfy independent conservation laws, they instead satisfy

$$\dot{\rho}_h + 3H(1+\omega_h)\rho_h = -Q, \tag{2.3.3}$$

and

$$\dot{\rho}_m + 3H\rho_m = Q, \tag{2.3.4}$$

where $Q = 3b^2H(\rho_m + \rho_h)$ is a particular interacting term [203] with the coupling constant b^2. This interacting term can be rewritten in terms of ratio of density parameter $r_1 = \rho_m/\rho_h$ as

$$Q = 3b^2H\rho_h(1+r_1). \tag{2.3.5}$$

Using (2.2.23) and (2.3.5) into (2.3.3), the EoS parameter of HDE is given by

$$\begin{aligned}\omega_h &= -\frac{1}{3} - \frac{2\sqrt{\Omega_h}}{3d_1}\cos y - \frac{2m_1 a}{3(l_1+m_1 a)\, ln(l_1+m_1 a)} \\ &- \frac{b^2}{\Omega_h}\left[1+\Omega_k + \frac{2m_1 a}{(l_1+m_1 a)\, ln(l_1+m_1 a)} - \frac{2wm_1^2 a^2}{3(l_1+m_1 a)^2\,[ln(l_1+m_1 a)]^2}\right],\end{aligned} \tag{2.3.6}$$

which is a time-dependent value. It is to be noted that the term $\frac{m_1 a}{(l_1+m_1 a)\, ln(l_1+m_1 a)}$ has the same behaviour as discussed earlier for non-interacting case. It is easy to find out that, in the limit of $m_1 \to 0$, the standard cosmology is recovered. In the beginning of the evolution, the term $\frac{m_1 a}{(l_1+m_1 a)\, ln(l_1+m_1 a)}$ is zero and hence the EoS parameter of HDE (2.3.6) gives

$$\omega_h = -\frac{1}{3} - \frac{2\sqrt{\Omega_h}}{3d_1}\cos y - \frac{b^2(1+\Omega_k)}{\Omega_h}, \tag{2.3.7}$$

which is same as the standard non-flat HDE model in BD theory. We find that ω_h is always negative and less than $-1/3$ in the early of the evolution which shows the inflation in early time. The solar system experiments [111] predict a very high bound value of w which is $|w| > 40000$. However, Acquaviva and Verde [204] found that $|w|$ may be smaller than 40000 in cosmological scale. Due to a large value of $|w|$ suggested by the experiments, the last term containing w will dominate during early phase of the evolution of the Universe. Thus, we observe a positive value of ω_h. Thus, the decelerated phase occurs during the evolution of the Universe. It means that the Universe passes through the matter-dominated phase. During the late time evolution, the EoS parameter of HDE becomes

$$\omega_h = -\frac{1}{3} - \frac{2\sqrt{\Omega_h}}{3d_1} - \frac{b^2(1+\Omega_k)}{\Omega_h}, \tag{2.3.8}$$

which gives a negative value. Analysing ω_h in (2.3.8), one can observe that ω_h will definitely cross the phantom divide line in the late time evolution. The late time value of ω_h depends on the values of coupling constant b^2, d_1, Ω_h and Ω_k.

Using (2.2.29) and (2.3.6) in the definition of DP, we get

$$q = \frac{(1+3b^2)(1+\Omega_k)-\Omega_h\left(1+\frac{2\sqrt{\Omega_h}}{d_1}\cos y\right)}{2\left(1+\frac{m_1 a}{(l_1+m_1 a)\,ln(l_1+m_1 a)}\right)} + \frac{\frac{2m_1 a(-\Omega_h+3b^2+2)}{(l_1+m_1 a)\,ln(l_1+m_1 a)}-\frac{2m_1^2a^2}{(l_1+m_1 a)^2\,ln(l_1+m_1 a)}+\frac{2(w+1-3wb^2)m_1^2a^2}{(l_1+m_1 a)^2\,[ln(l_1+m_1 a)]^2}}{2\left(1+\frac{m_1 a}{(l_1+m_1 a)\,ln(l_1+m_1 a)}\right)}. \quad (2.3.9)$$

From (2.3.9), we observe that the last term will dominate during the evolution due to the large value of the BD parameter w provided $(1+3b^2)>0$, which means that q becomes positive and hence it describes the decelerated phase. In the late time of the evolution, the terms $\frac{m_1 a}{(l_1+m_1 a)\,ln(l_1+m_1 a)}$, $\frac{m_1^2a^2}{(l_1+m_1 a)^2\,ln(l_1+m_1 a)}$ and $\frac{m_1^2a^2}{(l_1+m_1 a)^2\,[ln(l_1+m_1 a)]^2}$ converge to zero and $\cos y$ converges to 1. Then, the value of q is given by

$$q = \frac{(1+3b^2)(1+\Omega_k)-\Omega_h(1+\frac{2\sqrt{\Omega_h}}{d_1})}{2}. \quad (2.3.10)$$

From above equation we observe that q is negative for $b^2 < \frac{\Omega_h(1+\frac{2\sqrt{\Omega_h}}{d_1})}{3(1+\Omega_k)}-\frac{1}{3}$.

Cosmic Coincidence Problem

Let us discuss the coincidence problem in interacting HDE model. Using (2.2.23), (2.3.4) and (2.3.5), the evolution of r_1 can be expressed as

$$\dot{r}_1 = 3Hr_1\left[\omega_h+\frac{b^2(1+r_1)^2}{r_1}\right]. \quad (2.3.11)$$

In the above expression the value within the bracket can be positive or negative but for a suitable value of b^2, we can get $|\omega_h+\frac{b^2(1+r_1)^2}{r_1}| << |\omega_h|$. Thus, from Eqs. (2.2.33) and (2.3.11) we can conclude that the energy density ratio r_1 may evolve more slowly in interacting HDE model as compared to the non-interacting HDE model. This imply that the interaction between dark matter and HDE plays a vital role to discuss the coincidence problem. As we know that the model must satisfy the condition $|\frac{\dot{r}_1}{r_1}|_0 \leq H_0$ for getting the soft coincidence. In our model we can achieve the soft coincidence if b^2 satisfies the condition $b^2 \leq \frac{(1-3\omega_{h0})r_{10}}{3(1+r_{10})^2}$. According to the present observational values $r_{10}=3/7$ and $\omega_{h0}=-1$, we get $b^2 \leq \frac{7}{25}$. Thus, the soft coincidence can be achieved at present if $b^2 \leq \frac{7}{25}$. It can also be concluded that the smaller the value of b^2, the energy density ratio may evolve more slowly. This explanation can resolve the problem of cosmic coincidence and it can be checked by taking any suitable small

value of b^2 along with $\omega_{h0} = -1$. This represents that the variation in r_1 is more slow as compared to the conventional ΛCDM model. Thus, the coupling constant b^2 plays an important role to resolve the cosmic coincidence problem and also this small value of coupling constant is compatible with the observations. The same is also analyzed by Feng et al. [205]. Thus, we observe that interacting HDE along with the logarithmic form of BD scalar field in the framework of BD theory may capable to resolve the cosmic coincidence problem.

2.4 Conclusion

In this work, we have studied non-interacting and interacting HDE model with future event horizon as an IR cutoff in the framework of BD theory. Motivated by work [181, 182], we have considered the logarithmic form of BD scalar field to discuss the early and late time evolution of the Universe. We have discussed the dynamical view of early and late time evolution of the Universe with the help of EoS parameter and DP. We have also discussed the cosmic coincident problem. The result of both, non-interacting and interacting models are summarized below.

In non-interacting HDE model, we have observed that the EoS parameter starts behaving like in its respective form in GTR. In late time of evolution, our model behaves like cosmological constant at $d_1 = 1$, it shows the quintessence region at $d_1 > 1$, and it mimic like phantom type at $d_1 < 1$. Initially, the value of DP is negative but it may attain the positive value during the evolution when the very high bound on BD parameter w dominates the other terms, and it is also observed that it again attain a negative value in late time, i.e., it shows the phase transition from decelerated to accelerated Universe during the evolution. Further, we have shown that a less acute coincidence problem than conventional ΛCDM model may be achieved. Thus, the logarithmic form of BD scalar field is more suitable to achieve a less acute coincidence problem than the power-law form.

In the interacting HDE model, we have found a time-dependent value of EoS parameter which behaves same as its respective form of GTR in early time and late time evolution of the Universe. In the beginning, it gives a negative value which is $< -1/3$, this shows the early time inflation. Due to the presence of the BD parameter w, which have a very high positive value (according to the observations), in the EoS parameter the value of ω_h may get some positive value at any time during the evolution depending

upon the values of l_1, m_1 and w. This means that during the evolution the decelerated phase of the Universe may occur. In the late time of the evolution it again gives the negative value which is $< -1/3$. This shows that the Universe accelerates during late time. Also, in this case we have obtained a time-dependent DP. The presence of the BD coupling parameter shows that during the evolution of the Universe under the condition $(1+3b^2) > 0$, q may attain a positive value. In late time q will show the accelerated expansion of the Universe under the condition $b^2 < \frac{\Omega_h(1+\frac{2\sqrt{\Omega_h}}{d_1})}{3(1+\Omega_k)} - \frac{1}{3}$. Thus, we conclude that the interacting HDE case in our model shows the phase transition from deceleration to acceleration, which is a good harmony with the current observations. We have observed that the soft coincidence can be achieved if $b^2 \leq \frac{7}{25}$. Thus, we can conclude that in the framework of BD theory the interacting HDE with the logarithmic form of BD scalar field may resolve the cosmic coincidence problem.

Thus, we can say that the logarithmic form of BD scalar field is suitable to explain the recent accelerated expansion of the Universe in HDE model. This model shows that the phase transition of the evolution of the Universe. It may also resolves the cosmic coincidence problem effectively. Therefore, this form of BD scalar field may play an important role in explaining the present dat Universe.

Chapter 3

Viscous cosmology in new holographic dark energy model

In this chapter[1]*, we study some viscous new HDE model in the framework of flat FRW Universe. We assume the viscous coefficient as:* $\zeta = \zeta_0 + \zeta_1 H$*, where* ζ_0 *and* ζ_1 *are constants. We obtain all possible solutions with viscous term and analyzed the expansion history of the Universe. We graphically observe the evolutionary behaviour of the scale factor as well as the deceleration parameter. We observe that the Universe transits from deceleration to acceleration for small values of* ζ *in late time. We also discuss two independent geometrical diagnostics: statefinder and* Om *to compare the model with other available dark energy models. The* $r-s$*,* $r-q$ *and* $Om-z$ *trajectories are plotted to interpret the results.*

---

[1]The result of this chapter is based on a research paper "Viscous cosmology in new holographic dark energy model and the cosmic acceleration, *European Physical Journal C* **78**, 190 (2018)".

3.1 Introduction

Recent observations have strongly indicated that DE leads to the late time accelerated expansion of the Universe. Nevertheless, the nature of such a DE is still the source of debate. Many theoretical models have been proposed to describe this late time acceleration of the Universe. In recent years, the considerable interest has been noticed in the study of HDE model to explain the recent phase transition of the Universe. The idea of HDE is based on the holographic principle [64, 65, 206]. According to holographic principle a short distance (UV) cutoff Λ is related to the long distance (IR) cutoff L due to the limit set by the formation of a black hole [207]. The UV cutoff is related to the vacuum energy, and the IR cutoff is related to the large scale structure of the Universe, i.e., Hubble horizon, particle horizon, event horizon, Ricci scalar, etc. The HDE model faces the problem about the choice of IR cutoff. As the origin of the HDE is still unknown, Granda and Oliveros [73] proposed a new IR cutoff for HDE, known as new holographic dark energy (new HDE) as defined and explained in section 1.7.1.

In general, many cosmological models have been studied by considering that the Universe has to be filled with perfect fluid. Eventhough, it is most important to investigate more realistic models in which the dissipative processes due to viscosity have been taken into account. The theory of dissipation was proposed by Eckart [151] and the full causal theory was developed by Israel and Stewart [152]. The first suggestion was investigated by Misner [161] who proposed that the neutrino viscosity acting in the early era might have considerably reduced the present anisotropy of the black–body radiation during the process of evolution. Murphy [163] showed that the bulk viscosity can push the initial singularity in FRW model to the infinite past.

The main motive of the work of this chapter is to explain the accelerated expansion in the presence of bulk viscosity for new HDE in GTR which has not been studied sofar. The bulk viscosity introduces dissipation by only redefining the effective pressure, which is defined in section 1.8 by Eq. $(1.8.1)$. In this chapter, we are interested when the Universe is dominated by viscous HDE and dark matter with Granda- Oliveros IR cutoff to study the effects of bulk viscosity to the cosmic evolution. We consider the general form of bulk viscosity $\zeta = \zeta_0 + \zeta_1 H$, where ζ_0 and ζ_1 are the constants and H stands for Hubble parameter, see Ref. [153, 208].

Here, we study the non-viscous new HDE model to find out the exact solution of the

field equations and also study the constant and varying bulk viscous new HDE model. We find the exact forms of scale factor, DP and transition redshift and discuss the evolution through the graphs. We also study the geometrical diagnostics like statefinder parameter and Om to compare our model with ΛCDM. We plot the trajectories of these parameters and observe the effects of bulk viscous coefficient.

3.2 Non-Viscous new HDE model

We consider a spatially homogeneous and isotropic flat FRW spacetime, specified by the line element

$$ds^2 = dt^2 - a^2(t)\left[dr^2 + r^2(d\theta^2 + sin^2\theta d\phi^2)\right], \tag{3.2.1}$$

where (r,θ,ϕ) are the comoving coordinates and $a(t)$ has its usual meaning.

We consider that the Universe is filled with new HDE plus pressureless DM (excluding the contribution of the baryonic matter here for simplicity) whose energy-momentum tensor can be written as

$$T_{\mu\nu} = (\rho_m + \rho_d + p_d)\, u_\mu\, u_\nu - p_d\, g_{\mu\nu}. \tag{3.2.2}$$

For Einstein field equations $R_{\mu\nu} - g_{\mu\nu}R/2 = T_{\mu\nu}$ in the units where $8\pi G = c = 1$, we obtain the Friedmann equations for the metric (3.2.1) as

$$3H^2 = \rho_m + \rho_d, \tag{3.2.3}$$

$$2\dot{H} + 3H^2 = -p_d, \tag{3.2.4}$$

where ρ_m and ρ_d are the energy density of DM and new HDE, respectively, and p_d stands for the pressure of the new HDE. The EoS parameter for new HDE is $\omega_d = p_d/\rho_d$. An over dot has its usual meaning.

Using the energy density of new HDE defined by (1.7.14), Eqs. (3.2.3) and (3.2.4) give

$$\dot{H} + \frac{3(1+\alpha\ \omega_d)}{(2+3\beta\ \omega_d)}H^2 = 0. \tag{3.2.5}$$

The solution of (3.2.5) is given by

$$H = \frac{1}{c_0 + \frac{3(1+\alpha\ \omega_d)}{(2+3\beta\ \omega_d)}t}, \tag{3.2.6}$$

where c_0 is the constant of integration. The Hubble parameter (3.2.6) can be rewritten as

$$H = \frac{H_0}{\left\{1 + \frac{3H_0(1+\alpha\ \omega_d)}{(2+3\beta\ \omega_d)}(t-t_0)\right\}}, \tag{3.2.7}$$

where H_0 is the value of Hubble parameter at $t = t_0$, when new HDE starts to dominate. As we know $H = \dot{a}/a$, Eq. (3.2.7) gives the scale factor value as

$$a = a_0\left\{1 + \frac{3(1+\alpha\ \omega_d)H_0}{(2+3\beta\ \omega_d)}(t-t_0)\right\}^{\frac{(2+3\beta\ \omega_d)}{3(1+\alpha\ \omega_d)}},\ \text{for}\ \alpha \neq -1/\omega_d,\ \beta \neq -2/3\omega_d, \tag{3.2.8}$$

where a_0 is the present value of the scale factor at a cosmic time $t = t_0$. Equation (3.2.8) shows the power-law $a \propto t^n$, where n is a constant, type expansion of the scale factor. As we know that the Universe will undergo with decelerated expansion for $n < 1$, i.e., $(2+3\beta\omega_d) < (3+3\alpha\omega_d)$ in our case whereas it accelerates for $n > 1$, i.e., $(2+3\beta\omega_d) > (3+3\alpha\omega_d)$. For $n = 1$, i.e., $(2+3\beta\omega_d) = (3+3\alpha\omega_d)$, the Universe will show marginal inflation. In the absence of new HDE, i.e., for $\alpha = \beta = 0$, we get the dark matter dominated scale factor, $a = a_0(1+\frac{3}{2}H_0(t-t_0))^{2/3}$.

The DP which is very useful parameter to discuss the behaviour of the Universe. The sign (positive or negative) of DP explains whether the Universe decelerates or accelerates. On substituting the required values in the definition of DP (1.9.5), we get the DP for non-viscous new HDE model in the framework of GR

$$q = \frac{3(1+\alpha\omega_d)}{(2+3\beta\omega_d)} - 1, \tag{3.2.9}$$

which does not depend on time so it remains constant during the evolution of the Universe. The Universe will expand with decelerated rate for $q > 0$, i.e., $(2+3\beta\omega_d) < (3+3\alpha\omega_d)$, accelerated rate for $q < 0$, i.e., $(2+3\beta\omega_d) > (3+3\alpha\omega_d)$ and marginal inflation for $q = 0$, i.e., $(2+3\beta\omega_d) = (3+3\alpha\omega_d)$. One can explicitly observe the dependence of DP q on the model parameters α, β and EoS parameter ω_d under above constraints. Thus, the deceleration or acceleration of the Universe can be obtained depending on the suitable choices of these parameters. This non-viscous model does not show the phase transition due to power-law expansion or constant DP. The model shows marginal inflation, $q = 0$ when $\omega_d = 1/3(\beta - \alpha)$. Using Markov Chain Monte Carlo method on latest observational data, Wang and Xu [74] have constrained the new HDE model and obtained the best fit values of the parameters $\alpha = 0.8502^{+0.0984+0.1299}_{-0.0875-0.1064}$ and $\beta = 0.4817^{+0.0842+0.1176}_{-0.0773-0.0955}$ with 1σ and 2σ errors in flat model. In the best fit new

HDE models, they have obtained the EoS parameter $\omega_d = -1.1414 \pm 0.0608$. Putting these values of parameters (excluding the errors) in Eq. (3.2.9), we get $q = -0.7468$, which shows that our new HDE model is compatible with current observational data given in [74].

In order to discriminate among the available DE models, we use the geometrical parameters defined by Sahni et al. [174] and Alam et al. [175] as in Eq. (1.11.1), which is known as statefinder pair and is denoted as $\{r,s\}$. The statefinder probes the expansion dynamics of the Universe through higher derivatives of the scale factor and is a geometrical diagnosis in the sense that it depends on the scale factor and hence describes the spacetime. On substituting the required values into (1.11.1), we get

$$r = 1 - \frac{9(1+\alpha\omega_d)}{(2+3\beta\omega_d)} + \frac{18(1+\alpha\omega_d)^2}{(2+3\beta\omega_d)^2}, \tag{3.2.10}$$

and

$$s = \frac{2(1+\alpha\omega_d)}{2+3\beta\omega_d}. \tag{3.2.11}$$

From (3.2.10) and (3.2.11), we can observe that these statefinder parameters are constant whose values depend on α, β and ω_d. Putting the values of parameters [74] as mentioned above, we observe that this set of data do not favor the new HDE model over the ΛCDM as well as $SCDM$ model. However, new HDE model behaves like $SCDM$ model for $\alpha = 3\beta/2$. We can also observe that this model tends to $\{r,s\} \to \{1,0\}$ in the limiting case when $\alpha \to -1/\omega_d$ but no such fixed value of parameters exist for which it would clearly repesents the ΛCDM.

3.3 Viscous new HDE model

Since, non-viscous new HDE model gives constant DP which is unable to represent the phase transition. However, the observations show that the phase transition has a significant importance in describing the evolution of the Universe. Therefore, it will be interesting to explore the new HDE model with viscous to investigate either a viscous new HDE model with Granda-Oliveros IR cutoff would be able to find the phase transition or not.

In an isotropic and homogeneous FRW Universe, the dissipative effects arise due to the presence of bulk viscosity in cosmic fluids as shear viscosity plays no role. DE with bulk viscosity has a peculiar property to cause accelerated expansion of phantom type

in the late time evolution of the Universe [209–211]. It can also alleviate the problem like age problem and coincidence problem.

Let us consider that the effective pressure of new HDE is a sum of pressure of new HDE and bulk viscosity, i.e., the Universe is filled with bulk viscous new HDE plus pressureless DM whose energy-momentum tensor can be written as

$$T_{\mu\nu} = (\rho_m + \rho_d)u_\mu u_\nu - (g_{\mu\nu} + u_\mu u_\nu)\tilde{p_d}. \tag{3.3.1}$$

Then, the field equations (3.2.3) and (3.2.4) modify to

$$3H^2 = \rho_m + \rho_d, \tag{3.3.2}$$

$$2\dot{H} + 3H^2 = -\tilde{p_d}, \tag{3.3.3}$$

where $\tilde{p_d} = p_d - 3H\zeta$ is the effective pressure of new HDE. This form of effective pressure was originally proposed by Eckart [151] in the context of relativistic dissipative process occurring in thermodynamic systems went out of local thermal equilibrium. The term ζ is the bulk viscosity coefficient [37, 212, 213]. On the thermodynamical grounds, ζ is conventionally chosen to be a positive quantity and generically depends on the cosmic time t, or redshift z, or the scale factor a, or the energy density ρ_d, or a more complicated combination form. Maartens [214] assumed the bulk viscous coefficient as $\zeta \propto \rho^m$, where m is a constant. In the Refs. [153, 154, 208], the most general form of bulk viscosity has been considered with generalized EoS. Following [153, 154, 208, 215], we consider the bulk viscosity coefficient as

$$\zeta = \zeta_0 + \zeta_1 H, \tag{3.3.4}$$

where ζ_0 and ζ_1 are positive constants. The motivation for considering this bulk viscosity has been discussed in Refs. [153, 154, 208].

From the dynamical equations (3.3.2) and (3.3.3), we can obtain the single evolution equation for the Hubble parameter by using Eqs. (1.7.14) and (3.3.4) as,

$$\dot{H} + \frac{3(1+\alpha\omega_d)}{(2+3\beta\omega_d)}H^2 - \frac{3\zeta}{(2+3\beta\omega_d)}H = 0. \tag{3.3.5}$$

It can be observed that Eq. (3.3.5) reduces to the non-viscous equation (3.2.5) for $\zeta = 0$ as discussed in previous section.

Now, we classify different viscous new HDE models arises due to the constant and variable bulk viscous coefficient. We analyze the behavior of the scale factor, DP, statefinder parameter and *Om* diagnostic of these different cases.

3.3.1 New HDE Model with constant bulk viscosity

The simplest case of viscous new HDE model is to be taken with constant bulk viscous coefficient. Therefore, assuming $\zeta_1 = 0$ in Eq. (3.3.4), the bulk viscous coefficient reduces to

$$\zeta = \zeta_0 = \text{const.} \tag{3.3.6}$$

Using (3.3.6) into (3.3.5), we get

$$\dot{H} + \frac{3(1+\alpha\omega_d)}{(2+3\beta\omega_d)}H^2 - \frac{3\zeta_0}{(2+3\beta\omega_d)}H = 0. \tag{3.3.7}$$

The solution of (3.3.7) in terms of cosmic time t can be given by

$$H = e^{\frac{3\zeta_0 t}{(2+3\beta\omega_d)}}\left[c_1 + \frac{(1+\alpha\omega_d)}{\zeta_0}\, e^{\frac{3\zeta_0 t}{(2+3\beta\omega_d)}}\right]^{-1}, \tag{3.3.8}$$

where c_1 is the constant of integration. From (3.3.8), we get the evolution of the scale factor as

$$a = c_2\left[c_1 + \frac{(1+\alpha\omega_d)}{\zeta_0}\, e^{\frac{3\zeta_0 t}{(2+3\beta\omega_d)}}\right]^{\frac{(2+3\beta\omega_d)}{3(1+\alpha\omega_d)}}, \tag{3.3.9}$$

where c_2 is an integration constant. The above scale factor can be rewritten as

$$a = \left[1 + \frac{H_0(1+\alpha\omega_d)}{\zeta_0}\left\{e^{\frac{3\zeta_0(t-t_0)}{(2+3\beta\omega_d)}} - 1\right\}\right]^{\frac{(2+3\beta\omega_d)}{3(1+\alpha\omega_d)}}, \quad \text{for } \alpha \neq -1/\omega_d,\ \zeta_0 \neq 0 \tag{3.3.10}$$

where t_0 is the present cosmic time. Here, the scale factor is obtained as an exponential form which shows non-singular solution. Equation (3.3.10) shows that in early stages of the evolution, the scale factor can be approximated as $a(t) \sim \left[1 + \frac{3H_0(1+\alpha\omega_d)}{(2+3\beta\omega_d)}(t-t_0)\right]^{\frac{(2+3\beta\omega_d)}{3(1+\alpha\omega_d)}}$, and as $(t-t_0) \to \infty$, the scale factor approaches to a form like that of the de Sitter Universe, i.e., $a(t) \to \exp\left[\frac{3\zeta_0(t-t_0)}{(2+3\beta\omega_d)}\right]$. Thus, we observe that the Universe starts with a finite volume followed by an early decelerated epoch, then making a transition into the accelerated epoch in the late time of the evolution.

From (3.3.10), we can obtain the Hubble parameter in terms of scale factor a as

$$H(a)=\frac{H_0}{(1+\alpha\omega_d)}\left[\frac{\zeta_0}{H_0}+\left\{(1+\alpha\omega_d)-\frac{\zeta_0}{H_0}\right\}a^{-\frac{(3+3\alpha\omega_d)}{(2+3\beta\omega_d)}}\right], \tag{3.3.11}$$

where H_0 has its usual meaning and we have made the assumption that the present value of scale factor is $a_0=1$. The derivative of $\dot{a}$ with respect to a can be obtained as [215]

$$\frac{d\dot{a}}{da}=\frac{H_0}{(1+\alpha\omega_d)}\left[\frac{\zeta_0}{H_0}-\left\{(1+\alpha\omega_d)-\frac{\zeta_0}{H_0}\right\}\left(\frac{(1+3(\alpha-\beta)\omega_d)}{2+3\beta\omega_d}\right)a^{-\frac{3(1+\alpha\omega_d)}{(2+3\beta\omega_d)}}\right]. \tag{3.3.12}$$

Equating (3.3.12) to zero, the transition scale factor a_T can be obtained as

$$a_T=\left[\frac{(1+3(\alpha-\beta)\omega_d)\{(1+\alpha\omega_d)H_0-\zeta_0\}}{(2+3\beta\omega_d)\zeta_0}\right]^{\frac{(2+3\beta\omega_d)}{3(1+\alpha\omega_d)}}. \tag{3.3.13}$$

Using the relation $a=(1+z)^{-1}$, we can obtain the transition redshift z_T as

$$z_T=\left[\frac{(1+3(\alpha-\beta)\omega_d)\{(1+\alpha\omega_d)H_0-\zeta_0\}}{(2+3\beta\omega_d)\zeta_0}\right]^{-\frac{(2+3\beta\omega_d)}{3(1+\alpha\omega_d)}}-1. \tag{3.3.14}$$

From (3.3.13) or (3.3.14), we observe that for $\zeta_0=\frac{\{1+3(\alpha-\beta)\omega_d\}H_0}{3}$, the transition from deceleration to acceleration occurs at $a_T=1$ or $z_T=0$, i.e., at present time of the Universe. On taking the observed values of $\alpha=0.8502$ and $\beta=0.4817$ [74], $H_0=1$ and $\omega_d=-0.5$ in this expression of ζ_0, we get $\zeta_0=0.15$. Figure 3.1 represents the evolution of the scale factor $a(t)$ *versus* time $(t-t_0)$ for various values of $\zeta_0>0$. It is observed that the transition from decelerated to accelerated phase occure in late time for small values of ζ_0, i.e., in $0<\zeta_0<0.15$. The transition from deceleration to acceleration occurs at $a_T=1$, i.e., at present time for $\zeta_0=0.15$. However, the transition takes place at early stages of the evolution for large values of ζ_0, i.e., for $\zeta_0>0.15$. Thus, as the value of ζ_0 increases, the scale factor expands more rapidly with exponential rate.

The result regarding the transition of the Universe into the accelerated epoch discussed above can be further verified by studying the evolution of DP q. In this case, DP is given by

$$q(t)=\frac{3\left\{(1+\alpha\omega_d)-\frac{\zeta_0}{H_0}\right\}}{(2+3\beta\omega_d)}e^{-\frac{3\zeta_0(t-t_0)}{(2+3\beta\omega_d)}}-1. \tag{3.3.15}$$

Thus, we find a time-varying DP for the constant viscous new HDE model, which explains the transition of the evolutionary phases of the Universe. DP must change

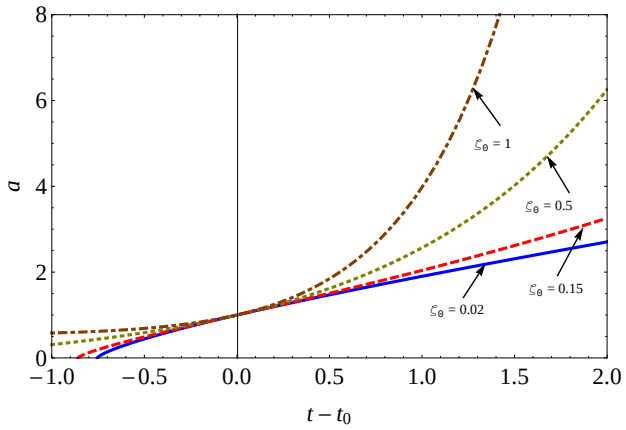

Figure 3.1: The evolution of the scale factor for $\zeta_0 > 0$ with $\omega_d = -0.5$, $\alpha = 0.8502$ and $\beta = 0.4817$.

its sign at $t = t_0$, i.e., the time at which the viscous new HDE begins to dominate. This time can be achieved if $[1+3(\alpha-\beta)\omega_d]H_0 = 3\zeta_0$. The Universe must decelerate for $t < t_0$ and accelerate for $t > t_0$ for any parametric values of α, β and ω_d.

From (3.3.15), DP in terms of scale factor is

$$q(a) = \frac{\{3(1+\alpha\omega_d)-3\zeta_0\}}{(2+3\beta\omega_d)}\left[\frac{(1+\alpha\omega_d)}{(a^{\frac{3+3\alpha\omega_d}{2+3\beta\omega_d}}-1)\zeta_0+(1+\alpha\omega_d)}\right]-1. \tag{3.3.16}$$

Now, the DP in terms of red shift z is

$$q(z) = \frac{\{3(1+\alpha\omega_d)-3\zeta_0\}}{(2+3\beta\omega_d)}\left[\frac{(1+\alpha\omega_d)}{\left((1+z)^{-\frac{3+3\alpha\omega_d}{2+3\beta\omega_d}}-1\right)\zeta_0+(1+\alpha\omega_d)}\right]-1. \tag{3.3.17}$$

In the absence of model parameter and viscosity coefficient, the value of DP(q) is $1/2$, which represents the decelerating matter-dominated Universe with null bulk viscosity. However, when only the bulk viscous term $\zeta_0 = 0$, the value of q is same as obtained in Eq. (3.2.9) for non-viscous new HDE model.

The present value of q corresponds to $z = 0$ or $a = 1$ is,

$$q_0 = q(a=1) = \frac{3(1+\alpha\omega_d)-3\zeta_0}{(2+3\beta\omega_d)}-1. \tag{3.3.18}$$

This equation shows that if $3\zeta_0 = [1+3(\alpha-\beta)\omega_d]$, the DP $q_0 = 0$. This implies that the transition from deceleration to acceleration takes place at the present time. The current DP $q_0 < 0$ if $3\zeta_0 > [1+3(\alpha-\beta)\omega_d]$, this shows that the transition from

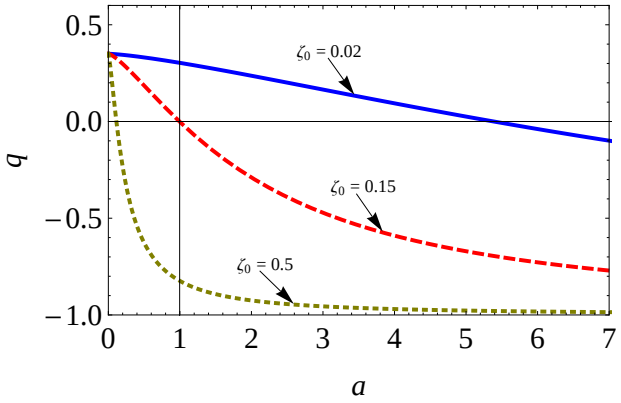

Figure 3.2: Plot of DP with respect to a for $\zeta_0 > 0$ taking $\omega_d = -0.5$, $\alpha = 0.8502$ and $\beta = 0.4817$.

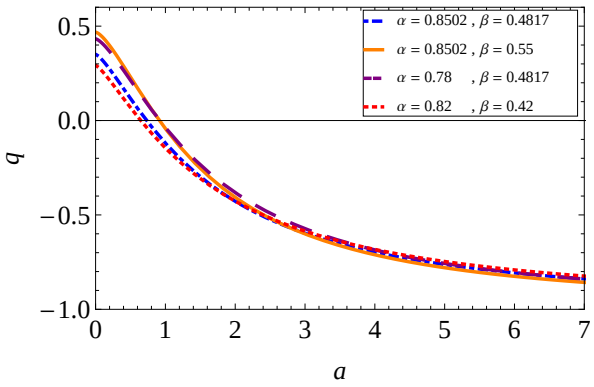

Figure 3.3: Plot of DP with respect to a for different combinations of α and β taking $\zeta_0 = 0.2$ and $\omega_d = -0.5$

deceleration to acceleration takes place at an early stage. But we observe that $q_0 > 0$ if $3\zeta_0 < [1 + 3(\alpha - \beta)\omega_d]$, this shows that the present time the Universe expand with decelerated rate and the transition from deceleration to acceleration takes place in a future time. The evolution of q with a is shown in Figs. 3.2 and 3.3 by taking fixed constant α and β (or ζ_0), from which we can see that the evolution of the Universe is from deceleration to acceleration. Figure 3.2 illustrates the evolutionary history of DP for different value of ζ_0 with $\omega_d = -0.5$, $\alpha = 0.8502$ and $\beta = 0.4817$. On considering $\alpha = 0.8502$, $\beta = 0.4817$ [74] and $\omega_d = -0.5$ in Eq. (3.3.18), we get $\zeta_0 = 0.15$ which gives $q_0 = 0$. Thus, the transition from deceleration to acceleration would take place at present time. For the large value $\zeta_0 > 0.15$, $q_0 < 0$, i.e., for this value of ζ_0 the Universe experience the acceleration at present time and the transition from deceleration to acceleration take place at an early stage. For the small value $\zeta_0 < 0.15$, $q_0 > 0$, i.e., for this value of ζ_0 the Universe experience the deceleration at present time and the transition from deceleration to acceleration take place in future. Thus, the larger the value ζ_0 is, the earlier acceleration occurs. The similar results for a fixed ζ_0 also

appear in Fig. 3.3. The larger the values α and β is, the earlier q changes it sign from $q>0$ to $q<0$ for a fixed ζ_0. In both Figs. 3.2 and 3.3, we observe that in late time the DP tends to -1.

Statefinder diagnostic

From above discussion we conclude that there is a phase transition from deceleration to acceleration in future for small bulk viscous coefficient, $0<\zeta_0<0.15$. It takes place to the present time for $\zeta=0.15$. However, the transition takes place in past for $\zeta>0.15$. The behavior of scale factor and DP shows that the constant bulk viscous coefficient plays the role of DE. In what follows, we will present the statefinder diagnostic of the viscous new HDE model. In this model, the statefinder parameters defined in $(1.11.1)$ can be obtained as

$$r=1+\frac{9\left(\frac{\zeta_0}{H_0}-(1+\alpha\omega_d)\right)\left(1-\frac{1+\alpha\omega_d}{(2+3\beta\omega_d)}\right)}{(2+3\beta\omega_d)}\,e^{-\frac{3\zeta_0(t-t_0)}{(2+3\beta\omega_d)}}+\frac{9\left(\frac{\zeta_0}{H_0}-(1+\alpha\omega_d)\right)^2}{(2+3\beta\omega_d)^2}\,e^{-\frac{6\zeta_0(t-t_0)}{(2+3\beta\omega_d)}}, \tag{3.3.19}$$

and

$$s=\frac{\frac{2\left(\frac{\zeta_0}{H_0}-(1+\alpha\omega_d)\right)\left(1-\frac{1+\alpha\omega_d}{(2+3\beta\omega_d)}\right)}{(2+3\beta\omega_d)}\,e^{-\frac{3\zeta_0(t-t_0)}{(2+3\beta\omega_d)}}+\frac{2\left(\frac{\zeta_0}{H_0}-(1+\alpha\omega_d)\right)^2}{(2+3\beta\omega_d)^2}\,e^{-\frac{6\zeta_0(t-t_0)}{(2+3\beta\omega_d)}}}{\frac{2\left((1+\alpha\omega_d)-\frac{\zeta_0}{H_0}\right)}{(2+3\beta\omega_d)}\,e^{-\frac{3\zeta_0(t-t_0)}{(2+3\beta\omega_d)}}-1}. \tag{3.3.20}$$

Here, these values of statefinder parameter are time-dependent due to the bulk viscous coefficient ζ_0. In the case of non-viscous new HDE model, we get the constant value of statefinder pair. As we can observe from the above two equations that in the limit of $(t-t_0)\to\infty$, the model corresponds to $\{r,s\}\to\{1,0\}$ and for this limit we get $q\to-1$. We draw the trajectories of the statefinder pair $\{r,s\}$ in $r-s$ plane for different values of constant ζ_0 with $\omega_d=-0.5$, $H_0=t_0=1$, $\alpha=0.8502$ and $\beta=0.4817$ as shown in Fig. 3.4. Here, we observe that the model tends to $\{r,s\}\to\{1,0\}$ for all positive values of ζ_0. In Fig. 3.4, the fixed point values of $SCDM$ model ($\{r,s\}=\{1,1\}$) and ΛCDM model ($\{r,s\}=\{1,0\}$) are shown by dots.

It is observed from figures that the statefinder diagnostic of our model can discriminate from other DE models. For example, in quiessence with constant EoS parameter [174,175] and the Ricci dark energy (RDE) model [216], the trajectory in $r-s$ plane is a vertical segment, i.e., s is constant during the evolution of the Universe whereas the trajectories for the chaplygin gas (CG) [217] and the quintessence (inverse power-law) models (Q) [174, 175] are similar to arcs of a parabola (downward and upward)

lying in the regions $s<0$, $r>1$ and $s>0$, $r<1$, respectively. In modified new HDE model [218], the trajectory in $r-s$ is from left to right. In HDE model with future event horizon [219, 220] its evolution starts from the point $s=2/3$, $r=1$ and ends at ΛCDM model fixed point in future.

In Fig. 3.4, the plot reveals that the $r-s$ plane can be divided into two regions $r<1, s>0$ and $r>1, s<0$ which are showing the similar characteristics to Q and CG models, respectively. The present model starts in both regions $r<1, s>0$ and $r>1, s<0$, and end on the ΛCDM point in the $r-s$ plane in far future. The trajectories in the right side of the vertical line correspond to the different values of ζ_0, i.e., $\zeta_0=0.02$, $\zeta_0=0.10$, $\zeta_0=0.15$ and $\zeta_0=0.30$ lying in the range $0<\zeta_0\leq 0.57$ whereas the trajectories to the left side of the vertical line correspond to $\zeta_0>0.57$, i.e., $\zeta_0=0.60$, $\zeta_0=0.70$, $\zeta_0=0.80$ and $\zeta_0=1.00$. This reveals that smaller values of ζ_0 give the model similar to Q model and larger values correspond to the CG model. We find that the evolutions are coinciding each other for all different values of ζ_0 in both regions.

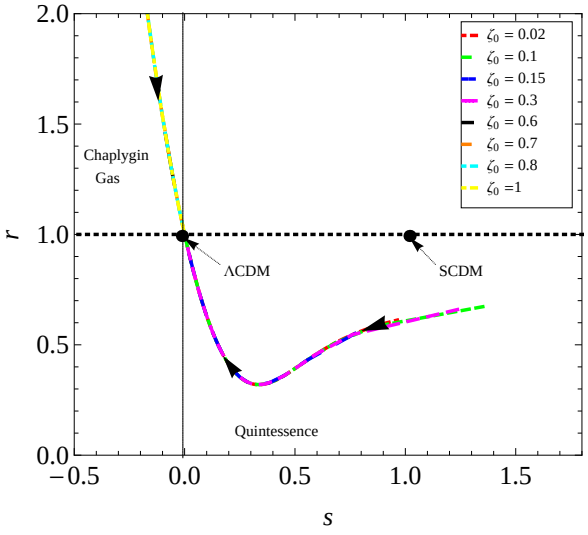

Figure 3.4: The $r-s$ trajectories are plotted in $r-s$ plane for $\zeta_0>0$ taking $\omega_d=-0.5$, $\alpha=0.8502$ and $\beta=0.4817$.

We also study the evolutionary behaviour of constant viscous new HDE model in $r-q$ plane. For different values of ζ_0, as taken in $\{r,s\}$, the trajectories are shown in Fig. 3.5 for $\omega_d=-0.5$, $H_0=t_0=1$, $\alpha=0.8502$ and $\beta=0.4817$. The fixed point values of $SCDM$ model ($\{r,q\}=\{1,0.5\}$) and steady state (SS) model ($\{r,q\}=\{1,-1\}$) are shown by dots in the figure. The sign change from $+ve$ to $-ve$ in the value of q shows the phase transition of the Universe which can be easily observed by the figure. The trajectories show that viscous new HDE models commence evolving from different

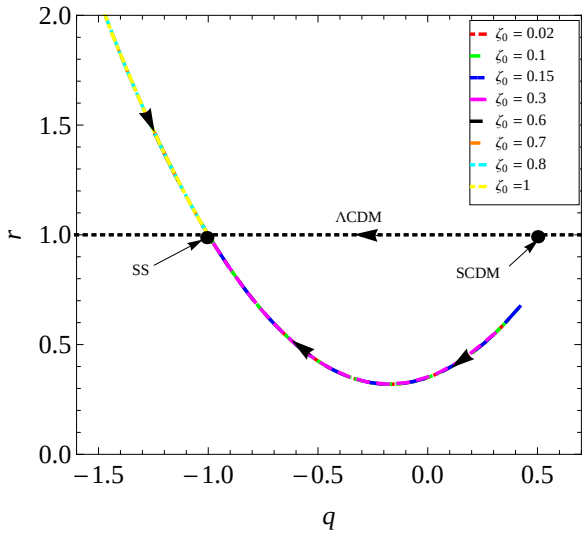

Figure 3.5: The $r-q$ trajectories are plotted in $r-q$ plane for $\zeta_0 > 0$ taking $\omega_d = -0.5$, $\alpha = 0.8502$ and $\beta = 0.4817$.

points for different values of ζ_0 with respect to ΛCDM which starts from $SCDM$ fixed point. We also observe that the viscous new HDE model always tends to SS model as ΛCDM, Q and CG models behaves in late time evolution of the Universe. Thus, this case is compatible with both Q and CG models.

The effect of constant viscous term in new HDE model is explained above. Now, we are interested to investigate the model behaviour in prospect of model parameters α and β. Figures 3.6 and 3.7 represents the $r-s$ trajectories in $r-s$ plane and $r-q$ trajectories in $r-q$ plane, respectively, for the various combinations of α and β with $\omega_d = -0.5$, $H_0 = t_0 = 1$ and $\zeta_0 = 0.02$. In the figures, the evolution direction of the statefinder trajectories and $r-q$ trajectories represented by arrows. From Fig. 3.6, we notice that for the fixed value of ζ_0 all the trajectories lie in the region $r < 1$ and $s > 0$, i.e., Q region. For some values of α and β, e.g., $(\alpha, \beta) = (0.8502, 0.55)$, the trajectory may start from the neighbourhood of $SCDM$ model in early time of evolution. For all values of α and β the constant bulk viscous new HDE model always tends to ΛCDM model in late time of the evolution.

Figure 3.7 represents the $r-q$ trajectories in $r-q$ plane for the various combinations of α and β with $\omega_d = -0.5$, $H_0 = t_0 = 1$ and $\zeta_0 = 0.02$. The time evolution of the ΛCDM model is represented by the horizontal line at $r = 1$. The sign change of the value of q from $+ve$ to $-ve$ shows that this model represents the phase transition of the Universe. The constant viscous new HDE model may start from the neighbourhood of the $SCDM$ model for some values of α and β (e.g., $\alpha = 0.8502, \beta = 0.55$). However, the

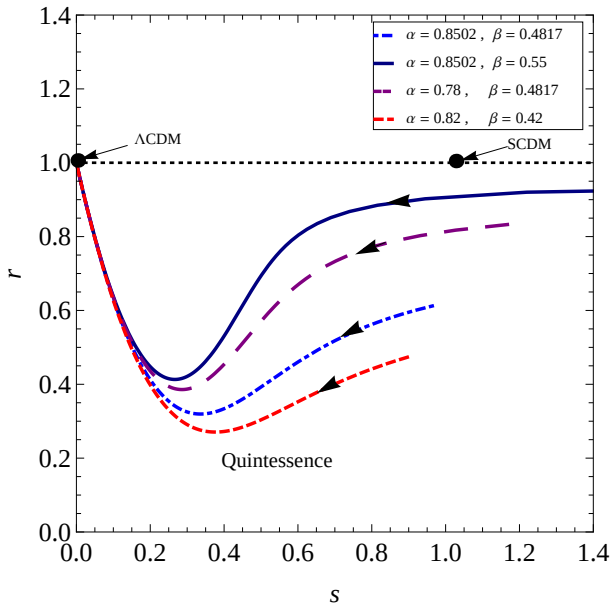

Figure 3.6: The $r-s$ trajectories are plotted in $r-s$ plane for various combinations of α and β taking $\omega_d = -0.5$ and $\zeta_0 = 0.02$.

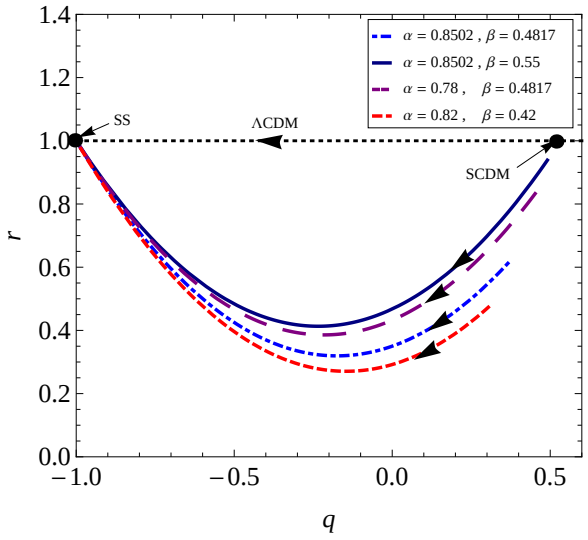

Figure 3.7: The $r-q$ trajectories are plotted in $r-q$ plane for various combinations of α and β taking $\omega_d = -0.5$ and $\zeta_0 = 0.02$.

constant viscous new HDE model tends to the SS model as the ΛCDM and Q models in future. Thus, the constant viscous new HDE model is compatible with the ΛCDM and Q models with variables model parameters and constant value of ζ_0.

Thus, we conclude that our model corresponds to both Q and CG models for the different values of viscous coefficient ζ_0 whereas for the different values of model parameters α and β with respect to the fixed value of ζ_0, our model only corresponds to Q model. Hence, we can conclude that due to the viscosity new HDE model is compatible with the Q and CG models. By above analysis, we can say that the bulk viscous coefficient and model parameters play the vital roles in the evolution of the Universe.

***Om* Diagnostic**:

In addition to statefinder $\{r,s\}$, another diagnostic, *Om(z)* is widely used to discriminate DE models. It is a new geometrical diagnostic which combines Hubble parameter H and redshift z. It is defined in section 1.11.2 by Eq. (1.11.2). It is easier to reconstruct it as compare to statefinder parameters. Since, the slope of *Om(z)* can distinguish dynamical DE from the cosmological constant in a robust manner, both with and without reference to the value of the matter density. Now, substituting the required value of $H(z)$ from (3.3.11) in (1.11.2), we get the value of *Om(z)* as

$$Om(z) = \frac{\left[\frac{\zeta_0}{H_0} + \{1+\alpha\omega_d - \frac{\zeta_0}{H_0}\}(1+z)^{\frac{3(1+\alpha\omega_d)}{2+3\beta\omega_d}}\right]^2 - (1+\alpha\omega_d)^2}{(1+\alpha\omega_d)^2[(1+z)^3-1]}. \tag{3.3.21}$$

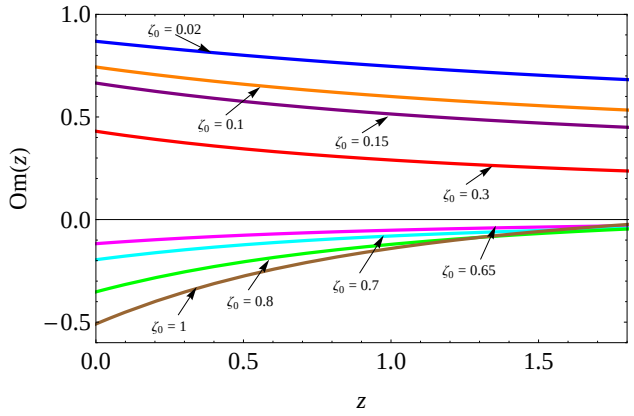

Figure 3.8: The *Om(z)* evolutionary diagram of viscous new HDE for different values of $\zeta_0 > 0$ with fixed $\omega_d = -0.5$, $\alpha = 0.8502$ and $\beta = 0.4817$.

For comparison, the evolutionary trajectories of *Om(z) versus* z have been plotted

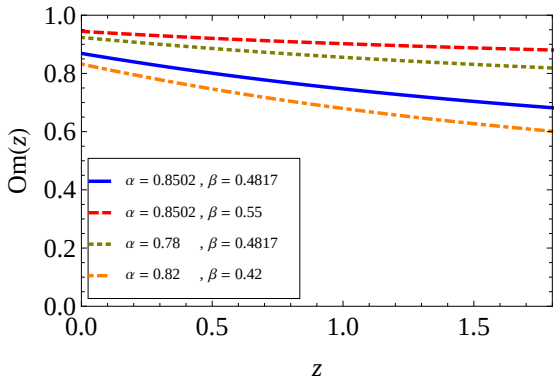

Figure 3.9: The *Om(z)* evolutionary diagram of viscous new HDE for different values of α and β with fixed $\zeta_0 = 0.02$ with $\omega_d = -0.5$.

in Figs. 3.8 and 3.9 for various values of $\zeta_0 > 0$ (or α and β) with fixed α and β (or ζ_0), with $H_0 = 1$ and $\omega_d = -0.5$. From Fig. 3.8, we observe that for $0 < \zeta_0 \leq 0.57$, the trajectory shows the negative slope, i.e., the DE behaves like quintessence and for $\zeta_0 > 0.57$, the positive slope of the *Om* trajectory is observed, i.e., the DE behaves as phantom. For the late future stage of evolution when $z = -1$, we get *Om(z)* $= 1 - \frac{\zeta_0^2}{H_0^2(1+\alpha\omega_d)^2}$, which is the constant value of *Om(z)*. Thus for $z = -1$, the DE will correspond to ΛCDM.

The Fig. 3.9 shows the *Om(z)* trajectory for different values of model parameters α and β with fixed $\zeta_0 = 0.02$, $\omega_d = -0.5$ and $H_0 = 1$. This trajectory only shows the negative curvature which imply that the DE behaves like quintessence.

From the above discussion with constant bulk viscous coefficient, we find that the constant ζ_0 (or cosmological parameters α and β) play an important roles in the evolution of the Universe, i.e., they both determine the evolutionary behavior as well as the ultimate fate of the Universe.

3.3.2 Solution with bulk viscosity

In this section, we consider two cases: **(i)** $\zeta_0 = 0$ and $\zeta_1 \neq 0$, and **(ii)** $\zeta_0 \neq 0$ and $\zeta_1 \neq 0$.

Case(i) $\zeta_0 = 0$ **and** $\zeta_1 \neq 0$:

In this case, the bulk viscosity coefficient given in (3.3.4) reduces to

$$\zeta = \zeta_1 H, \tag{3.3.22}$$

which shows that the bulk viscous coefficient is directly proportional to Hubble parameter.

Using (3.3.22) into (3.3.5), we get

$$\dot{H}+\frac{3(1-\zeta_1+\alpha\omega_d)}{(2+3\beta\omega_d)}H^2=0. \tag{3.3.23}$$

The above equation is similar to the Eq. (3.2.5) obtained in the case of non-viscous new HDE model in section 3.2. The solution of (3.3.23) for H in terms of t is given by

$$H=\frac{1}{c_3+\frac{3(1-\zeta_1+\alpha\omega_d)}{(2+3\beta\omega_d)}t}, \tag{3.3.24}$$

where c_3 represents the constant of integration. The scale factor can be obtained as

$$a=a_0\left[1+\frac{3(1-\zeta_1+\alpha\omega_d)H_0}{(2+3\beta\omega_d)}(t-t_0)\right]^{\frac{(2+3\beta\omega_d)}{3(1-\zeta_1+\alpha\omega_d)}},\quad \text{for } \zeta_1\neq(1+\alpha\omega_d),\ \beta\neq-\frac{2}{3\omega_d} \tag{3.3.25}$$

The scale factor varies as power-law expansion. Now, the DP is

$$q=\frac{3(1-\zeta_1+\alpha\omega_d)}{(2+3\beta\omega_d)}-1. \tag{3.3.26}$$

which is a constant value. Such form of ζ gives no transition phase. The positive or negative sign of q depends on whether $3\zeta_1<(1+3(\alpha-\beta)\omega_d)$ or $3\zeta_1>(1+3(\alpha-\beta)\omega_d)$, respectively.

Now, the statefinder pair is

$$r=1-\frac{9(1+\alpha\omega_d-\zeta_1)}{(2+3\beta\omega_d)}+\frac{18(1+\alpha\omega_d-\zeta_1)^2}{(2+3\beta\omega_d)^2}, \tag{3.3.27}$$

and

$$s=\frac{2(1+\alpha\omega_d-\zeta_1)}{(2+3\beta\omega_d)}. \tag{3.3.28}$$

In this case the constant value of statefinder parameter is obtained. In the limit of $\zeta_1\to(1+\alpha\omega_d)$, the statefinder pair $\{r,s\}\to\{1,0\}$ and for $\zeta_1=\frac{(2\alpha-3\beta)\omega_d}{2}$, this model has the fixed value $\{r,s\}=\{1,1\}$, i.e., it behaves as *SCDM* model.

Case(ii) $\zeta_0\neq0$ and $\zeta_1\neq0$:

Let us consider the more general form of the bulk viscous coefficient, i.e., $\zeta=\zeta_0+\zeta_1H$. Using (3.3.4) into (3.3.5), we get

$$\dot{H}+\frac{3(1-\zeta_1+\alpha\omega_d)}{(2+3\beta\omega_d)}H^2-\frac{3\zeta_0}{(2+3\beta\omega_d)}H=0. \tag{3.3.29}$$

Solving the above equation, we get the Hubble parameter in terms of t as

$$H = H_0 e^{\frac{3\zeta_0(t-t_0)}{(2+3\beta\omega_d)}} \left[1 + \frac{H_0(1-\zeta_1+\alpha\omega_d)}{\zeta_0}\left\{e^{\frac{3\zeta_0(t-t_0)}{(2+3\beta\omega_d)}} - 1\right\}\right]^{-1}, \tag{3.3.30}$$

where H_0 is the present value of the Hubble parameter and we have made the assumption that the present value of scale factor is $a_0 = 1$. The solution of (3.3.30) for the scale factor a in terms of t is given by

$$a = \left[1 + \frac{H_0(1-\zeta_1+\alpha\omega_d)}{\zeta_0}\left\{e^{\frac{3\zeta_0(t-t_0)}{(2+3\beta\omega_d)}} - 1\right\}\right]^{\frac{(2+3\beta\omega_d)}{3(1-\zeta_1+\alpha\omega_d)}}, \quad \text{for } \zeta_0 \neq 0,\ \zeta_1 \neq (1+\alpha\omega_d) \tag{3.3.31}$$

Here, we get an exponential type scale factor with the viscous terms. As $(t-t_0) \to 0$, the scale factor behaves as

$$a \to \left[1 + \frac{3H_0(1-\zeta_1+\alpha\omega_d)(t-t_0)}{(2+3\beta\omega_d)}\right]^{\frac{(2+3\beta\omega_d)}{3(1-\zeta_1+\alpha\omega_d)}}, \tag{3.3.32}$$

which shows power-law expansion in early time. On the other hand, if $\zeta_0 = H_0(1-\zeta_1+\alpha\omega_d)$ or $(t-t_0) \to \infty$, we obtain

$$a(t) = \exp\left(\frac{3\zeta_0(t-t_0)}{(2+3\beta\omega_d)}\right). \tag{3.3.33}$$

This case corresponds the de Sitter Universe which shows accelerated expansion in the later time of evolution.

Now, from (3.3.31), the Hubble parameter in terms of a can be written as

$$H(a) = \frac{H_0}{(1-\zeta_1+\alpha\omega_d)}\left[\frac{\zeta_0}{H_0} + \left\{(1-\zeta_1+\alpha\omega_d) - \frac{\zeta_0}{H_0}\right\} a^{-\frac{3(1-\zeta_1+\alpha\omega_d)}{(2+3\beta\omega_d)}}\right]. \tag{3.3.34}$$

This equations shows that if both ζ_0 and ζ_1 are zero, the Hubble parameter, $H = H_0 a^{\frac{-3(1+\alpha\omega_d)}{(2+3\alpha\omega_d)}}$, which corresponds to non-viscous new HDE model. When $\zeta_1 = 0$, H reduces to Eq. (3.3.11) which is the case of constant viscosity.

The derivative of $\dot{a}$ with respect to a can be obtained from (3.3.34), which is given by

$$\frac{d\dot{a}}{da} = \frac{H_0}{(1-\zeta_1+\alpha\omega_d)}\left[\frac{\zeta_0}{H_0} - \left\{(1-\zeta_1+\alpha\omega_d) - \frac{\zeta_0}{H_0}\right\}\left(\frac{(1+3(\alpha-\beta)\omega_d - 3\zeta_1)}{2+3\beta\omega_d}\right) a^{-\frac{3(1-\zeta_1+\alpha\omega_d)}{(2+3\beta\omega_d)}}\right]. \tag{3.3.35}$$

Equating (3.3.35) to zero to get the transition scale factor a_T as

$$a_T = \left[\frac{(1+3(\alpha-\beta)\omega_d - 3\zeta_1)\{(1-\zeta_1+\alpha\omega_d)H_0 - \zeta_0\}}{(2+3\beta\omega_d)\zeta_0}\right]^{\frac{(2+3\beta\omega_d)}{3(1-\zeta_1+\alpha\omega_d)}}. \tag{3.3.36}$$

The corresponding transition redshift z_T is

$$z_T = \left[\frac{(1+(\alpha-\beta)\omega_d - 3\zeta_1)\{(1-\zeta_1+\alpha\omega_d)H_0 - \zeta_0\}}{(2+3\beta\omega_d)\zeta_0}\right]^{-\frac{(2+3\beta\omega_d)}{3(1-\zeta_1+\alpha\omega_d)}} - 1. \tag{3.3.37}$$

It can be observed that for $(\zeta_0+\zeta_1 H_0) = \frac{\{1+3(\alpha-\beta)\omega_d\}H_0}{3}$, the transition from decelerated phase to accelerated phase occurs at $a_T = 1$ or $z_T = 0$, which corresponds to the present time of the Universe. By considering the observational value $\alpha = 0.8502$ and $\beta = 0.4817$ along with $\omega_d = -0.5$, $H_0 = 1$, we get $(\zeta_0+\zeta_1) = 0.15$. The evolution of the scale factor is represented by Fig. 3.10. We observe that the transition from deceleration to acceleration take place in later stage of the evolution for $0 < (\zeta_0+\zeta_1) \leq 0.15$. The transition from the deceleration to acceleration depends on the viscosity ζ_0 and ζ_1 as shown above. The transition from deceleration to acceleration take place at early time of the Universe for $(\zeta_0+\zeta_1) > 0.15$.

The DP is also a very vital parameter to explain the phase transition of the Universe.

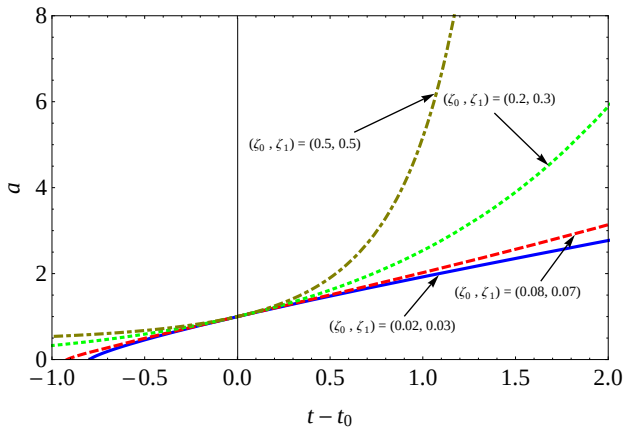

Figure 3.10: The evolution of a *versus* $(t-t_0)$ *for* $\zeta_0 > 0$ *and* $\zeta_1 > 0$ *with* $\omega_d = -0.5$, $\alpha = 0.8502$ *and* $\beta = 0.4817$.

Thus, in this case the DP is obtained as

$$q(t) = \frac{3\left\{(1-\zeta_1+\alpha\omega_d) - \frac{\zeta_0}{H_0}\right\}}{(2+3\beta\omega_d)} e^{-\frac{3\zeta_0(t-t_0)}{(2+3\beta\omega_d)}} - 1. \tag{3.3.38}$$

From (3.3.38), we observe that for this general case we get the time-dependent DP. Thus, it may be possible to explain the phase transition scenario of the Universe with

DP. It can be noticed that DP must change its sign at $t = t_0$ and this time can be achieved if $3(\zeta_0 + \zeta_1 H_0) = \{1 + 3(\alpha - \beta)\omega_d\}H_0$. The sign of q is positive for $t < t_0$ and it is negative for $t > t_0$. The values of ζ_0 and ζ_1 can be obtained for a given values of ω_d, α and β, which may be obtained from observation, or vice-versa.

From (3.3.38), DP can be written in terms of scale factor as

$$q(a) = \frac{\{3(1-\zeta_1+\alpha\omega_d)-3\zeta_0\}}{(2+3\beta\omega_d)}\left[\frac{(1-\zeta_1+\alpha\omega_d)}{(a^{\frac{3(1-\zeta_1+\alpha\omega_d)}{2+3\beta\omega_d}}-1)\zeta_0+(1-\zeta_1+\alpha\omega_d)}\right]-1. \quad (3.3.39)$$

The DP in terms of redshift z is

$$q(z) = \frac{\{3(1-\zeta_1+\alpha\omega_d)-3\zeta_0\}}{(2+3\beta\omega_d)}\left[\frac{(1-\zeta_1+\alpha\omega_d)}{\left((1+z)^{-\frac{3(1-\zeta_1+\alpha\omega_d)}{2+3\beta\omega_d}}-1\right)\zeta_0+(1-\zeta_1+\alpha\omega_d)}\right]-1. \quad (3.3.40)$$

In the absence of bulk viscous parameter and all other parameter, the DP q has value $1/2$, which represents a decelerating matter dominated Universe with null bulk viscosity. However, when only the bulk viscous term $\zeta_0 = 0$ and $\zeta_1 \neq 0$, the value of q is same as obtained in Eq. (3.3.26) for case (i) of variable viscous new HDE model, and when $\zeta_0 \neq 0$ and $\zeta_1 = 0$, Eq. (3.3.39) reduces to Eq. (3.3.16) of constant viscous coefficient.

The present value of q corresponds to $z = 0$ or $a = 1$ is,

$$q_0 = q(a=1) = \frac{3(1-\zeta_1+\alpha\omega_d)-3\zeta_0}{(2+3\beta\omega_d)}-1. \quad (3.3.41)$$

This equation implies that if $3(\zeta_0+\zeta_1) = [1+3(\alpha-\beta)\omega_d]$, the DP $q_0 = 0$. This shows that the phase transition from deceleration to acceleration take place at the present time. The DP $q_0 < 0$ if $3(\zeta_0+\zeta_1) > [1+3(\alpha-\beta)\omega_d]$, this shows that Universe experiencing the accelerating phase at present, i.e., the transition from deceleration to acceleration takes place at an early stage. But we observe that $q_0 > 0$ if $3(\zeta_0+\zeta_1) < [1+3(\alpha-\beta)\omega_d]$, this shows that the present time the Universe expand with decelerated rate and the transition from deceleration to acceleration takes place in a future time. For the observational value $\alpha = 0.8502$ and $\beta = 0.4817$ with $\omega_d = -0.5$ and $H_0 = 1$, we get $(\zeta_0+\zeta_1) = 0.15$ which gives $q_0 = 0$. Thus for this value set, the transition into accelerating phase would occur at present time. If $(\zeta_0+\zeta_1) > 0.15$, $q_0 < 0$, i.e., this shows that the present time the Universe experience the accelerating phase

and the transition from deceleration to acceleration takes place at an early stage. If $(\zeta_0+\zeta_1)<0.15$, $q_0>0$, i.e., this shows that the present time the Universe expand with decelerated rate and the transition from deceleration to acceleration takes place in a future time. This result is verified graphically which is represented by Fig. 3.11. Figure 3.12 shows the $q-a$ graph in $q-a$ plane to discuss the evolution of the Universe with respect to model parameters α and β. Here, the signature change in the value of DP can be seen by the figure. From above discussion we say that both viscous coefficient and model parameter have their own role in the evolution of the Universe. Some values of bulk viscous term gives the accelerated phase from the beginning and continues to be accelerated in late time.

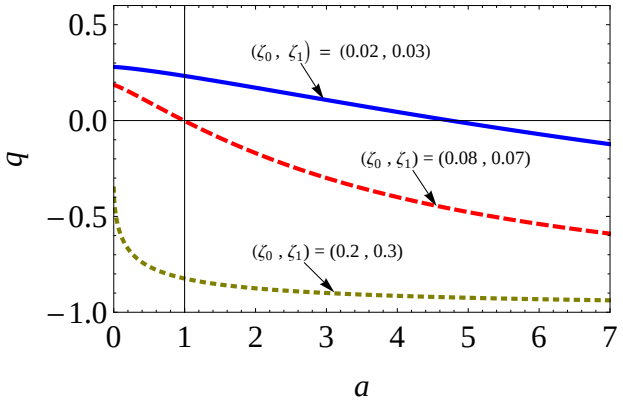

Figure 3.11: The $q-a$ graph in $q-a$ plane for $\zeta_0>0$ and $\zeta_1>0$ with $\omega_d=-0.5$, $\alpha=0.8502$ and $\beta=0.4817$.

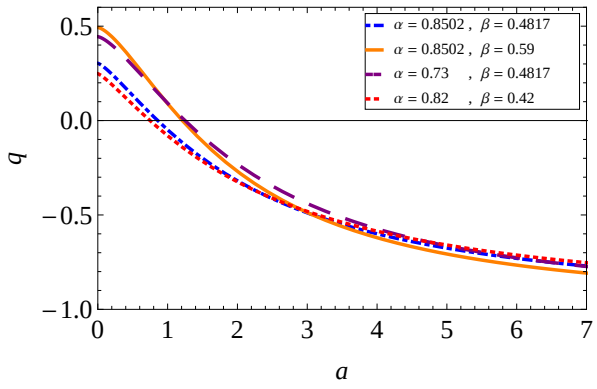

Figure 3.12: The $q-a$ graph in $q-a$ plane for different combinations of α and β with $\zeta_0=0.2$, $\zeta_1=0.3$ and $\omega_d=-0.5$.

Statefinder diagnostic:

As we have mentioned above, the scale factor and DP have been discussed to explain the accelerating Universe with viscous term or model parameters. So it is necessary to distinguish these models in a model-independent manner. In what follows we will

apply two geometrical approaches to viscous new HDE model, i.e., the statefinder and Om diagnostic from which we can compute the evolutionary trajectories with ones of the ΛCDM model to show the difference among them.

In this case, the statefinder parameters defined in Eq. (1.11.1) can be evaluated as

$$\begin{aligned} r &= 1+\frac{9\left(\frac{\zeta_0}{H_0}-(1-\zeta_1+\alpha\omega_d)\right)\left(1-\frac{(1-\zeta_1+\alpha\omega_d)}{(2+3\beta\omega_d)}\right)}{(2+3\beta\omega_d)}\, e^{-\frac{3\zeta_0(t-t_0)}{(2+3\beta\omega_d)}} \\ &\quad + \frac{9\left(\frac{\zeta_0}{H_0}-(1-\zeta_1+\alpha\omega_d)\right)^2}{(2+3\beta\omega_d)^2}\, e^{-\frac{6\zeta_0(t-t_0)}{(2+3\beta\omega_d)}}, \end{aligned} \tag{3.3.42}$$

and

$$s=\frac{\frac{2\left(\frac{\zeta_0}{H_0}-(1-\zeta_1+\alpha\omega_d)\right)\left(1-\frac{1-\zeta_1+\alpha\omega_d}{(2+3\beta\omega_d)}\right)}{(2+3\beta\omega_d)}\, e^{-\frac{3\zeta_0(t-t_0)}{(2+3\beta\omega_d)}}+\frac{2\left(\frac{\zeta_0}{H_0}-(1-\zeta_1+\alpha\omega_d)\right)^2}{(2+3\beta\omega_d)^2}\, e^{-\frac{6\zeta_0(t-t_0)}{(2+3\beta\omega_d)}}}{\frac{2\left((1-\zeta_1+\alpha\omega_d)-\frac{\zeta_0}{H_0}\right)}{(2+3\beta\omega_d)}\, e^{-\frac{3\zeta_0(t-t_0)}{(2+3\beta\omega_d)}}-1}. \tag{3.3.43}$$

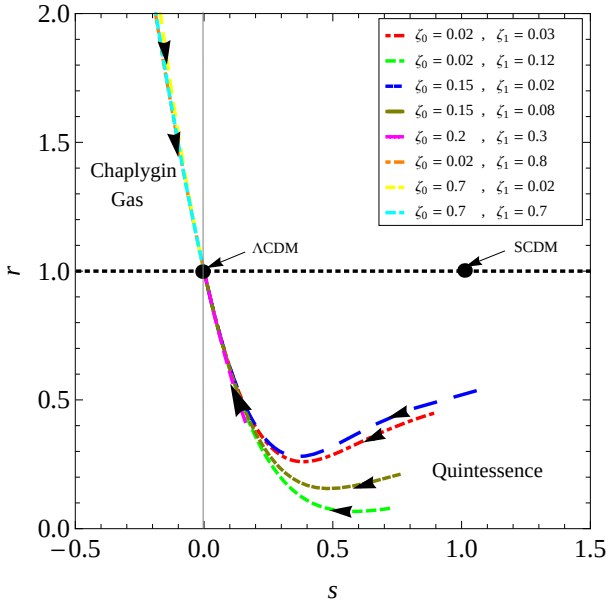

Figure 3.13: The $r-s$ trajectories are plotted in $r-s$ plane for $\zeta_0>0$ and $\zeta_1>0$ taking $\omega_d=-0.5$, $\alpha=0.8502$ and $\beta=0.4817$.

From (3.3.42) and (3.3.43) it can be observed that the viscous new HDE model converges to $\{r,s\}\to\{1,0\}$ in the limit of $(t-t_0)\to\infty$. This can also be achieved at $(\zeta_0+H_0\zeta_1)=H_0(1+\alpha\omega_d)$ but this is a very fixed point. Thus, the statefinder diagnostic fails to discriminate between ΛCDM and the new HDE model. Here, we obtain time-dependent statefinder pair which needs to study the general behavior. Let us see the

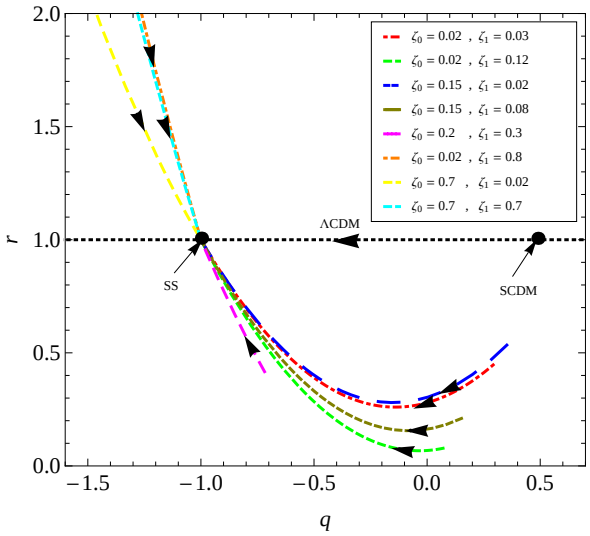

Figure 3.14: The $r-q$ trajectories are plotted in $r-q$ plane for $\zeta_0 > 0$ and $\zeta_1 > 0$ taking $\omega_d = -0.5$, $\alpha = 0.8502$ and $\beta = 0.4817$.

effect of viscosity coefficients ζ_0, ζ_1 and model parameters α, β for the general form of variable viscous new HDE model. Figure 3.13 shows the $r-s$ trajectory in $r-s$ plane for different values of ζ_0 and ζ_1 with $H_0 = t_0 = 1$, $\alpha = 0.8502$ and $\beta = 0.4817$. The model behaviors to Q models for $0 < (\zeta_0 + \zeta_1) \leq 0.57$ and CG models for $(\zeta_0 + \zeta_1) > 0.57$. The trajectories in Q-model and CG-model both converge to the ΛCDM model in late time of evolution.

Figure 3.14 shows the time evolution of $\{r, q\}$ pair in $r-q$ plane for different combinations of the values of ζ_0 and ζ_1 with $H_0 = t_0 = 1$, $\alpha = 0.8502$ and $\beta = 0.4817$. The fixed points $\{r, q\} = \{1, 0.5\}$ and $\{r, q\} = \{1, -1\}$ represents the $SCDM$ and SS models, respectively. Since q changes its sign from positive to negative with respect to time which shows the phase transition of the Universe from deceleration to acceleration. In beginning this model behaves different from the ΛCDM but in future it behaves same as ΛCDM which converges to SS model in late time. Hence the variable viscous new HDE model always converges to SS model as ΛCDM, Q and CG models in late time evolution of the Universe. For all the ranges of $(\zeta_0 + \zeta_1)$ the trajectories correspond to Q and CG models as in Fig. 3.13. Thus, the variable viscous new HDE model is compatible with both Q and CG models.

Thus, the viscosity coefficients are able to correspond to both Q and CG models for different combinations of ζ_0, ζ_1 and also explain the phase transition of the Universe.

Now, we are curious to know the behaviour of variable viscous new HDE model with respect to the model parameters α and β. Here, Figs. 3.15 and 3.16 represents the

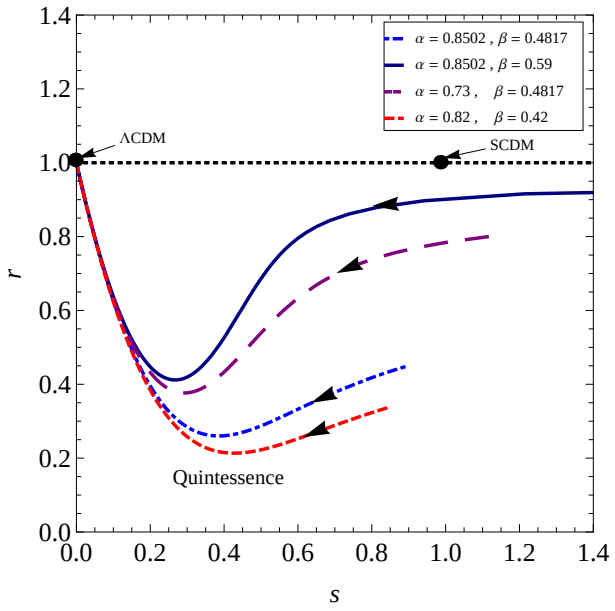

Figure 3.15: The $r-s$ trajectories are plotted in $r-s$ plane for various combinations of α and β taking $\omega_d = -0.5$, $\zeta_0 = 0.02$ and $\zeta_1 = 0.03$.

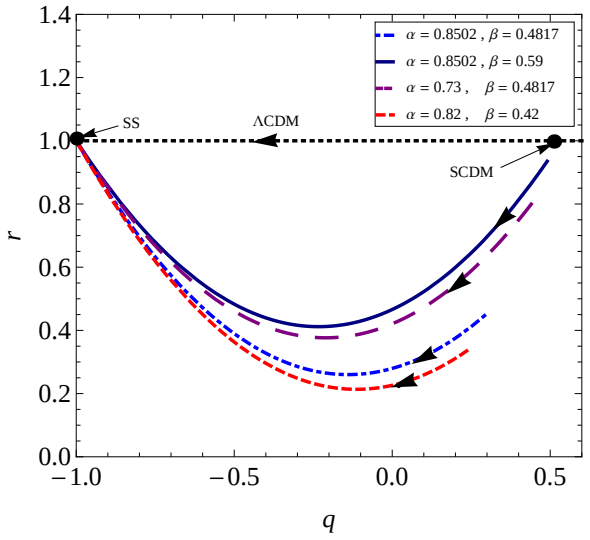

Figure 3.16: The $r-q$ trajectories are plotted in $r-q$ plane for various combinations of α and β taking $\omega_d = -0.5$, $\zeta_0 = 0.02$ and $\zeta_1 = 0.03$.

$r-s$ and $r-q$ trajectories in $r-s$ and $r-q$ plane, respectively, for the different values of α and β close to it's observational value with $\omega_d = -0.5$, $H_0 = t_0 = 1$, $\zeta_0 = 0.02$ and $\zeta_1 = 0.03$. The evolutionary directions of both the trajectories are shown in the figures by the arrows. In Fig. 3.15, we analysed that for this fixed value of ζ_0 and ζ_1 the $r-s$ trajectories are lying in the region corresponds to $r < 1$, $s > 0$ which shows that our model is similar to the Q model. It also starts from the vicinity of $SCDM$ model in early time of evolution for some values of α and β, e.g., $(\alpha, \beta) = (0.8502, 0.59)$. It is different from RDE model and quiessence model as it produces the curved trajectories for any values of (α, β) close to observational value which approach to ΛCDM in late time of evolution as the Q model tends to ΛCDM model in late time of evolution.

The $r-q$ trajectories in $r-q$ plane are shown by the Fig. 3.16. This model is also able to explain the phase transition of the Universe. It also starts from the neighbourhood of the $SCDM$ model for some values of α and β (e.g., $\alpha = 0.8502, \beta = 0.55$) and approaches to SS model in late time for any value of α and β close to the observational value. In future the variable viscous new HDE model approaches to the SS model same as the ΛCDM and Q models. Thus the viscous new HDE model is compatible with the ΛCDM and Q models.

Thus, we observed from Figs. 3.13–3.16 that viscous new HDE model is compatible to Q and CG models for different ranges of viscosity coefficients in the presence of the fixed observational value of model parameters whereas the model parameter in the presence of fixed value of viscosity coefficients approaches only to Q model.

***Om* Diagnostic**:

Let us discuss the another geometrical parameter, i.e., *Om(z)* diagnostic in viscous new HDE model. By substituting the required values in Eq. $(1.11.2)$, we get the *Om(z)* diagnostic for $\zeta = \zeta_0 + \zeta_1 H$ as

$$Om(z) = \frac{\left[\frac{\zeta_0}{H_0} + \left\{(1-\zeta_1+\alpha\omega_d) - \frac{\zeta_0}{H_0}\right\}(1+z)^{\frac{3(1-\zeta_1+\alpha\omega_d)}{2+3\beta\omega_d}}\right]^2 - (1-\zeta_1+\alpha\omega_d)^2}{(1-\zeta_1+\alpha\omega_d)^2[(1+z)^3-1]}. \quad (3.3.44)$$

Figure 3.17 shows the *Om(z)* trajectory with respect to z for different values of $\zeta_0 > 0$ and $\zeta_1 > 0$ corresponding to $\alpha = 0.8502$, $\beta = 0.4817$, $H_0 = 1$ and $\omega_d = -0.5$. Here, the trajectory represents the negative curvature, i.e., the viscous new HDE behaves as quintessence for the limit $0 < (\zeta_0 + \zeta_1) \leq 0.57$ and it shows the positive curvature, i.e., the viscous DE behaves as phantom, for $(\zeta_0 + \zeta_1) > 0.57$ whereas for $z = -1$, i.e., in

future time we get $Om(z) = 1 - \frac{\zeta_0^2}{H_0^2(1-\zeta_1+\alpha\omega_d)^2}$, which is the constant value of $Om(z)$. Thus, for $z = -1$, the viscous new HDE will correspond to ΛCDM.

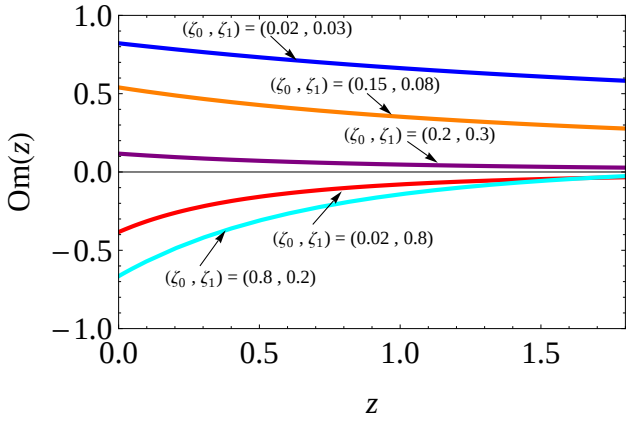

Figure 3.17: The $Om(z)$ evolutionary diagram of viscous new HDE for different values of $\zeta_0 > 0$ and $\zeta_1 > 0$ with $\omega_d = -0.5$, $\alpha = 0.8502$ and $\beta = 0.4817$.

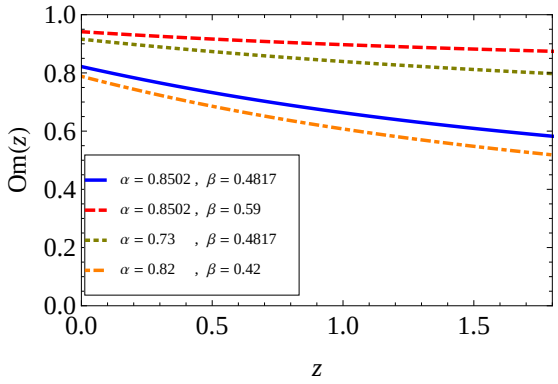

Figure 3.18: The $Om(z)$ evolutionary diagram of viscous new HDE for different values of α and β with $\zeta_0 = 0.02$, $\zeta_1 = 0.03$ and $\omega_d = -0.5$.

Figure 3.18 plot the $Om(z)$ versus z for different model parameters α and β correspond to fixed ζ_0 and ζ_1. The graph shows that there is always negative curvature for any values of model parameters. This shows that the model behaviors similar to quintessence model.

3.4 Conclusion

We have studied some viscous cosmological new HDE models on the evolution of the Universe, where the IR cutoff is given by the modified Ricci scalar, proposed by Granda and Olivers [73, 75]. It has been tried to demonstrate that the bulk viscosity can also play the role as a possible candidate of DE. We have performed a detailed study of both non-viscous and viscous new HDE models. The component of this

model is DE and pressureless DM. We have obtained the solutions for scale factor and DP. We have also studied these models from two independent geometrical point of view, namely the statefinder parameter and *Om* diagnostic. We have studied the different possible scenarios of viscous new HDE and analyzed the evolution of the Universe according to the assumption of bulk viscous coefficient ζ.

In section 3.2, we have investigated non-viscous new HDE in flat FRW Universe. We have obtained power-law form of scale factor for which the model may decelerate or accelerate depending on the constraint of model parameters. The DP is constant in this case. Therefore, the model can not describe the transition phase of the Universe. The statefinder parameters are also constant. We have observed that the observed set of data of model parameters do not favor the new HDE model over the ΛCDM as well as $SCDM$ model. However, new HDE model behaves like $SCDM$ model for $\alpha \to 3\beta/2$. It has been observed that this model approaches to $\{r,s\} \to \{1,0\}$ in the limit of $\alpha \to -1/\omega_d$ but there is no such value of parameters which would clearly show the ΛCDM.

In viscous new HDE model as discussed in section 3.3, we have considered that the matter consists of viscous holographic dark energy and pressureless DM. We have assumed a most general form $\zeta = \zeta_0 + \zeta_1 H$ to observe the effect of bulk viscous coefficient in the evolution of the Universe during early and late time. We have studied three cases: $(\zeta_0 \neq 0,\ \zeta_1 = 0)$; $(\zeta_0 = 0,\ \zeta_1 \neq 0)$ and $(\zeta_0 \neq 0,\ \zeta_1 \neq 0)$.

In the first case where we have constant bulk viscous coefficient, i.e., $\zeta = \zeta_0$, an exponential form of the scale factor is obtained. Therefore, the Universe starts from a finite volume followed by an early decelerated phase and then transits into an accelerated phase in late time of evolution. The evolution of scale factor has been shown is figure 3.1. The viscous new HDE model gives time-dependent DP which would describe the phase transition. We have obtained q in terms of a and z. The variation of q with a has been shown in Figs. 3.2 and 3.3 with varying ζ_0 and constant model parameters, and varying model parameters and constant ζ_0, respectively. Both the figures clearly show the phase transition of the Universe from deceleration to acceleration.

As the model predicts the late time acceleration, we have analyzed the model using statefinder parameter and *Om* diagnostic to distinguish it from other DE models especially from ΛCDM model. The evolution of the viscous new HDE model in the $r-s$ plane is shown in Fig. 3.4 with different values of ζ_0 with constant α and β. It shows that the evolution of $\{r,s\}$ parameter is in such a way that $r < 1$, $s > 0$, a feature

of quintessence (Q) model where as $r > 1,\ s < 0$ corresponds to the Chaplygin gas (CG) model. In both models, the trajectories are coinciding with each other for any value of ζ_0. The viscous new HDE model behaving Q and CG models in early time for different ζ_0 untimely approaches to ΛCDM model in late time. We have also discussed the evolutionary behavior of $\{r,q\}$ to discriminate the viscous new HDE model. The trajectory of $\{r,q\}$ has been plotted in Fig. 3.5 which shows the phase transition from decelerated to accelerated phase. If $0 < \zeta_0 \leq 0.57$, the transition takes place from quintessence region and approaches to SS model in late time as ΛCDM model approaches from $SCDM$. However, if $\zeta_0 > 0.57$, the transition starts from Chaplygin gas model and approaches to SS model in late time. Both the trajectories in Q model and CG model are coinciding on each other for any value of ζ_0.

A study of *Om* diagnostic of viscous new HDE model has been carried out in Fig. 3.3.21 for different values of ζ_0 and fixed α and β. The trajectory shows that if $0 < \zeta_0 \leq 0.57$, the *Om(z)* trajectory shows the negative slope which means viscous new HDE behaves like quintessence and if $\zeta_0 > 0.57$, the positive slope of the *Om(z)* trajectory is observed, i.e., the viscous new HDE behaves like phantom. In future as $z \to -1$, the *Om(z)* becomes constant, i.e, it may approach to ΛCDM model.

The above discussion shows that effect of bulk viscous coefficient on new HDE model with different values of ζ_0. We have also discussed the viscous new HDE model with varying model parameters α and β taking fixed ζ_0. The trajectory for q versus a as shown in Fig. 3.3 shows that the transition takes place from decelerated to accelerated phase in future for any values of α and β and approaches to $q = -1$ in late time. The trajectory for $\{r,s\}$ and $\{r,q\}$ have also been plotted respectively in Figs. 3.6 and 3.7 for different values of α and β with fixed value of ζ_0. The $r-s$ trajectory as shown in Fig. 3.6 shows that the trajectory starts from the quintessence region, even though some starts from the vicinity of $SCDM$ and approaches to ΛCDM in late time. The signature change of q from positive to negative has been observed in $r-q$ plane as shown in Fig. 3.7. The viscous new HDE model approaches to SS model in late time as ΛCDM does. The *Om* trajectory has been plotted in Fig. 3.9 for different values of α and β for fixed ζ_0. This trajectory only shows the negative curvature which imply that the viscous new HDE behaves like quintessence only.

From the above discussion with constant bulk viscous coefficient, we find that the constant ζ_0 (or cosmological parameters α and β) play important roles in the evolution of the Universe, i.e., they both determine the evolutionary behavior as well as the

ultimate fate of the Universe.

In second viscous new HDE model we have assumed $\zeta = \zeta_1 H$. The solution of this model is similar to the non-viscous new HDE one. We have obtained power-law form of scale factor which gives constant values of DP and statefinder pairs.

In last case, we have taken the most general form of bulk viscous coefficient $\zeta = \zeta_0 + \zeta_1 H$. The solution of this model is similar to the constant bulk viscous coefficient ζ_0. The effect of both non-zero values of ζ_0 and ζ_1 have been discussed. We have obtained exponential scale factor which gives time-dependent DP and statefinder pairs. The transition from decelerated to accelerated epoch has been discussed. The DP is time-dependent which shows phase transition from decelerated to accelerated phase. The DP has been written in terms of scale factor or redshift. We have calculated the present value q_0. We have plotted q versus a for different values of (ζ_0, ζ_1) with fixed model parameters and others as shown in Fig. 3.11. The Fig. 3.12 plots the $q-a$ for different models parameters α, β with fixed ζ_0, ζ_1 and others.

Figure 3.13 shows the $r-s$ trajectory in $r-s$ plane for different values of ζ_0 and ζ_1 with constant model parameters and others. The model behaviors to Q models for $0 < (\zeta_0 + \zeta_1) \leq 0.57$ and CG models for $(\zeta_0 + \zeta_1) > 0.57$. The trajectories in Q-model and CG model both converge to the ΛCDM model in late time of evolution. Figure 3.14 plots the trajectory of $r-q$ for different values of (ζ_0, ζ_1) with constant model parameters and others. The DP changes its sign from positive to negative with respect to time which shows the phase transition of the Universe from deceleration to acceleration. In beginning this model behaves different from the ΛCDM but in future it behaves same as ΛCDM which converges to SS model in late time. Thus, the variable viscous new HDE model is compatible with both Q and CG model. Figure 3.15 and 3.16 plot the trajectories of $r-s$ and $r-q$ for different model parameters (α, β) with fixed ζ_0, ζ_1 and others. In Fig. 3.15, we have analysed that for this fixed value of ζ_0 and ζ_1 the $\{r, s\}$ trajectories are lying in the region corresponds to $r < 1$, $s > 0$ which shows that our model is similar to the Q model. Figure 3.16 shows that this model is also able to explain the phase transition of the Universe. It also starts from the neighbourhood of the $SCDM$ model for some values of α and β. In future the variable viscous new HDE model approaches to the SS model same as the ΛCDM and Q models. Thus the viscous new HDE model is compatible with the ΛCDM and Q models.

We conclude that the trajectory of $r-s$ and $r-q$ suggest a different behavior as compare to Ricci dark energy done by Feng [221] where it was found that the $r-s$

trajectory is a vertical segment, i.e., s is constant during the evolution of the Universe. The trajectory in our viscous new HDE model is mostly confined a parabolic curve and approaches to $\{r,s\}=\{1,0\}$ in $r-s$ plane and $\{r,q\}=\{1,-1\}$ in $r-q$ plane.

From *Om* diagnostic we find that the trajectory represents the negative curvature, i.e, viscous new HDE behaves as a quintessence for $0<(\zeta_0+\zeta_1)\leq 0.57$ and it shows the positive curvature, i.e., the viscous DE behaves as phantom, for $(\zeta_0+\zeta_1)>0.57$, which is graphically represented by Fig. 3.17. We have also concluded that as $z\to -1$, we get the constant value of *Om*, which corresponds to ΛCDM model. However, plot of *Om* as shown in Fig. 3.18 for different model parameters with constant ζ_0 and ζ_1 reveal that there is always negative curvature for any values of model parameters. This shows that the viscous new HDE behaviors similar to quintessence.

In concluding remarks, we compare our work with respect to the earlier studied in this direction. Feng and Li [166] who investigated the viscous Ricci DE model by assuming bulk viscous coefficient proportional to the velocity vector of the fluid. Chattopadhyay [222] reported a study on modified Chaplygin gas based reconstructed scheme for extended HDE in the presence of bulk viscosity. In comparison to the said work, the present work lies not only in its choice of different bulk viscous coefficient but also in its different approach to discuss the evolution of the Universe. The present viscous new HDE model successfully describes the present accelerated epoch. The ΛCDM model is attainable by present model. The new HDE model behaves quintessence model and Chaplygin gas model in early time due to viscous effect. However, it behaves only quintessence if we consider the model parameters with fixed viscous coefficient. Our work implies the theoretical basis for future observations to constraint the viscous new HDE.

In concluding remark we can say that the bulk viscosity with new HDE in the framework of GTR plays a vital role to explain the accelerated expansion of the Universe.

Chapter 4

Constant bulk viscous new holographic dark energy model in $f(R,T)$ gravity

---

In this chapter[1]*, we extend the study of previous chapter in the modified* $f(R,T)$ *gravity theory within the framework of flat FRW model with constant bulk viscous matter content. The exact solution of field equations are obtained by assuming a particular form* $f(R,T) = R + \lambda T$ *and bulk viscosity as constant,* $\zeta = \zeta_0 = const$*. We obtain the time-dependent DP and classify all possible scenarios (deceleration, acceleration and their transition) with possible positive and negative ranges of* λ *over the constraint on* ζ_0 *to analyze the evolution of the Universe. We observe the finite-time singularities of type I and III at a finite time under certain constraints on* λ*. We also investigate the statefinder and* Om *diagnostics of the model to discriminate with other existing DE models. We also graphically describe it by plotting* $r-s$*,* $r-q$ *and* $Om-z$ *trajectories. At the end, we also discuss the thermodynamics and entropy of the model and find that it satisfy the second law of thermodynamics.*

---

[1]The content of this chapter is based on research paper "New holographic dark energy model with constant bulk viscosity in modified $f(R,T)$ gravity theory, *Astrophysics and Space Science* **363**, 117 (2018)".

4.1 Introduction

The modification in the geometrical part of Einstein-Hilbert action is very attractive way to resolve many problems in cosmology. The most famous modification of GTR is the $f(R)$ gravity in which the Ricci scalar R is replaced by a general function $f(R)$. This theory is consistent with the observations [91, 223]. In 2011, Harko et al. [108] proposed a new modified theory known as $f(R,T)$ gravity theory, where R is the Ricci Scalar and T stands for the trace of energy-momentum tensor. This modified theory presents a maximal coupling between geometry and matter. Many authors [130–148] have studied modified $f(R,T)$ theory in different context to explain early and late time evolution of the Universe. The new HDE model has not been yet discussed in detail in framework of $f(R,T)$ theory. Therefore, our aim is to study new HDE model with bulk viscosity in $f(R,T)$ gravity theory to explain the accelerated expansion of the Universe.

In chapter 3, we have investigated the effects of bulk viscosity in the GTR. In the present chapter, we extend our study in the $f(R,T)$ gravity with constant bulk viscosity. The purpose of this chapter is to observe the effect of constant bulk viscous coefficient on new HDE model in modified $f(R,T)$ gravity theory by considering the dark matter coupled with viscous fluid. We briefly discuss how the presence of viscous fluid could produce the late time acceleration. We present the solutions for non-viscous and constant viscous new HDE model in $f(R,T)$ gravity theory. The bulk viscous coefficient ζ is assumed to be a constant, i.e., $\zeta = \zeta_0 =$ const. as it is the simplest parametrization for the bulk viscosity.

The theoretical solutions of this model are analyzed in detail. We analyze the behaviour of the scale factor for the possible scenario that the model predicts for the Universe according to the value of ζ_0. The finite-time singularity are discussed for non-viscous and constant viscous new HDE models. The constant viscous new HDE model gives time-dependent DP which shows phase transition. We discuss the behavior of DP by constraining on ζ and gravity parameter λ which are given in table. We also find the two independent geometrical diagnostics, namely statefinder pair and *Om* to discriminate the new HDE model with other existing DE models.

4.2 Non-viscous new HDE model in $f(R,T)$ Gravity

We assume that the universe is filled with pressureless DM (excluding baryonic matter) and new HDE. Then the field equations (1.7.25) for the metric (3.2.1) yield

$$3H^2 = \rho_m + \rho_d + (\rho_m + \rho_d + p_d)f'(T) + \frac{1}{2}f(T), \tag{4.2.1}$$

$$2\dot{H} + 3H^2 = -p_d + \frac{1}{2}f(T), \tag{4.2.2}$$

where ρ_m, ρ_d, p_d and H have their usual meanings. An overdot represents the derivative with respect to the cosmic time t.

The field equations (4.2.1) and (4.2.2) are highly non-linear, therefore, let us assume $f(T) = \lambda T$ [108], where λ is a coupling parameter. Using this form, the field equations (4.2.1) and (4.2.2) reduce to

$$3H^2 = \rho_m + \rho_d + (\rho_m + \rho_d + p_d)\lambda + \frac{1}{2}\lambda T, \tag{4.2.3}$$

$$2\dot{H} + 3H^2 = -p_d + \frac{1}{2}\lambda T. \tag{4.2.4}$$

A relation between p_d and ρ_d is connected by EoS, $p_d = \omega_d \rho_d$, where ω_d is the EoS parameter of new HDE. The trace of energy-momentum tensor is given by $T = \rho_m + \rho_d - 3p_d$.

Now, Combining (4.2.3) and (4.2.4), a single evolution equation for H can be written as

$$2\dot{H} + (1+\lambda)[\rho_m + (1+\omega_d)\rho_d] = 0. \tag{4.2.5}$$

Using the energy density of new HDE defined by (1.7.14), into (4.2.3), the energy density ρ_m of DM can be obtained as

$$\rho_m = \frac{3[(2-2\alpha-3\lambda\alpha+\lambda\alpha\omega_d)H^2 - \beta(2+3\lambda-\lambda\omega_d)\dot{H}]}{2+3\lambda}. \tag{4.2.6}$$

4.2.1 Evolution of the scale factor

Using (1.7.14) and (4.2.6) into (4.2.5), we get

$$\dot{H} + (1+2\lambda\alpha\omega_d+\alpha\omega_d)XH^2 = 0, \tag{4.2.7}$$

where, $X = \frac{3(1+\lambda)}{[2+3\lambda+3\beta(1+\lambda)(1+2\lambda)\omega_d]}$.

On integration, we get

$$H(t) = \frac{1}{c_4 + (1+2\lambda\alpha\omega_d + \alpha\omega_d)X\,t}, \tag{4.2.8}$$

where c_4 is a constant of integration. Since $H = \dot{a}/a$, then the cosmic scale factor a can be obtained as

$$a(t) = c_5\Big[c_4 + (1+2\lambda\alpha\omega_d + \alpha\omega_d)X\,t\Big]^{\frac{2+3\lambda+3\beta(1+\lambda)(1+2\lambda)\omega_d}{3(1+\lambda)(1+2\lambda\alpha\omega_d+\alpha\omega_d)}}, \tag{4.2.9}$$

where c_5 is another constant of integration. Equation (4.2.8) can be rewritten as

$$H(t) = \frac{H_0}{1 + (1+2\lambda\alpha\omega_d + \alpha\omega_d)H_0\,X\,(t-t_0)}, \tag{4.2.10}$$

where H_0 has its usual meaning, and at $t = t_0$ the new HDE starts to dominate. Now, the scale factor (4.2.9) takes the form

$$a(t) = a_0\Big[1 + (1+2\lambda\alpha\omega_d + \alpha\omega_d)H_0\,X\,(t-t_0)\Big]^{\frac{2+3\lambda+3\beta(1+\lambda)(1+2\lambda)\omega_d}{3(1+\lambda)(1+2\lambda\alpha\omega_d+\alpha\omega_d)}}. \tag{4.2.11}$$

Here and there after, we assume $a_0 = 1$. Equation (4.2.11) shows power-law type scale factor, i.e., $a \propto t^n$, where n is a constant. The Universe corresponds to the decelerated expansion for $n < 1$, i.e., $1+3(1+\lambda)(1+2\lambda)(\alpha-\beta)\omega_d > 0$ and corresponds to the accelerated expansion for $n > 1$, i.e., $1+3(1+\lambda)(1+2\lambda)(\alpha-\beta)\omega_d < 0$ and for $n = 1$, i.e., $1+3(1+\lambda)(1+2\lambda)(\alpha-\beta)\omega_d = 0$, the Universe shows the marginal inflation. In the absence of $\alpha = \beta = 0$, we get the scale factor as

$$a(t) = \left[1 + \frac{3(1+\lambda)H_0}{(2+3\lambda)}(t-t_0)\right]^{\frac{(2+3\lambda)}{3(1+\lambda)}}, \tag{4.2.12}$$

In the absence of parameter λ, we get $a(t) = \left[1 + \frac{3H_0}{2}(t-t_0)\right]^{\frac{2}{3}}$, which is the case of matter-dominated phase.

4.2.2 Future finite-time singularity

Nojiri et al. [224], Nojiri and Odintsov [225], and Capozziello et al. [226] have classified the finite-time singularities into four classes. The classifications of the finite-time singularities was suggested in the following way:

(i) Type I (big rip): For $t \to t_s,\ a \to \infty,\ \rho \to \infty,\ \ |p| \to \infty$. This also includes the case of ρ, p being finite at t_s,

(ii) Type II (sudden): For $t \to t_s,\ a \to a_s,\ \rho \to \rho_s,\ \ |p| \to \infty$,

(iii) Type III : For $t \to t_s,\ a \to a_s,\ \rho \to \infty,\ \ |p| \to \infty$.

(iv) Type IV: For $t \to t_s,\ a \to \infty,\ \rho \to 0,\ \ |p| \to 0$, and higher derivatives of H diverge.

Here, t_s, a_s, and ρ_s are constants. Meng et al. [153], Sebastiani [171], Myrzakul et al. [227] and Khadekar et al. [228] studied finite-time singularity in viscous FRW models.

In the following, we show that the different choice of parameters may lead to different finite-time singularity.

The total energy density, i.e., $\rho = \rho_m + \rho_d$ is given by

$$\rho = \rho_0 \left[1 + (1 + 2\lambda\alpha\omega_d + \alpha\omega_d) H_0 X (t - t_0)\right]^{-2}, \tag{4.2.13}$$

where $\rho_0 = \frac{3H_0^2[2+\lambda\alpha\omega_d - \beta\lambda\omega_d X(1+2\lambda\alpha\omega_d+\alpha\omega_d)]}{(2+3\lambda)}$.

The total pressure is only the pressure of new HDE model which is given by

$$p = p_d = \frac{3H_0^2\omega_d\left[\alpha - \beta X(1 + 2\lambda\alpha\omega_d + \alpha\omega_d)\right]}{\left[1 + (1 + 2\lambda\alpha\omega_d + \alpha\omega_d) H_0 X (t - t_0)\right]^2}. \tag{4.2.14}$$

In the above equations, we assume $\alpha = 0.8502$, $\beta = 0.4817$ [74] and $\omega_d = -0.5$. Using these values we get the restriction on λ only. Therefore, if $-1 < \lambda < -0.69533$ or $0.676194 < \lambda < 1.27131$ (as calculated by Mathematica software), we find that as $t \to t_s$, $a \to \infty$, $\rho \to \infty$ and $|p| \to \infty$. Thus, we get Type I big-rip singularity at finite time

$$t_s = -\frac{1}{(1 + 2\lambda\alpha\omega_d + \alpha\omega_d) H_0\, X} + t_0. \tag{4.2.15}$$

It is also observed that for other values of λ which do not belong to the above ranges, $a \to 0$, $\rho \to \infty$ and $|p| \to \infty$, which gives Type III singularity.

In the absence of model parameters, i.e., $\alpha = 0$ and $\beta = 0$ we find that $a \to \infty$, $\rho \to \infty$ and $|p| \to \infty$ for $\lambda < -2/3$ at a finite time $t = t_s = -\frac{(2+3\lambda)}{3(1+\lambda)H_0} + t_0$ which shows big-rip singularity. It is to be noted that in the absence of λ too, we find there is no future singularity in this case. We get Big-Bang singularity as $a \to 0$ and $\rho \to \infty$. The elapsed time between the Big-Bang time till today is $t_b = t_0 - \frac{2}{3H_0}$.

4.2.3 Behavior of deceleration parameter

To discuss the transition phase, we consider one more parameter which depends only on the scale factor and its derivatives, known as DP. It is represented by q and is defined by (1.9.5). It gives a measure of the rate at which the expansion of the Universe is taking place. The positive value of DP shows that the Universe expands with decelerated rate and negative value of it imply that the Universe has accelerated expansion whereas the marginal inflation occurs at $q = 0$. Using (4.2.11) into (1.9.5), we get

$$q = (1 + 2\lambda\alpha\omega_d + \alpha\omega_d)\, X - 1, \tag{4.2.16}$$

which is a constant. Therefore, the DP is unable to explain the phase transition of the Universe. From (4.2.16), we observe that the Universe accelerates for $1 + 3(1 + \lambda)(1+2\lambda)(\alpha-\beta)\omega_d < 0$ and decelerates for $1+3(1+\lambda)(1+2\lambda)(\alpha-\beta)\omega_d > 0$ and has marginal inflation for $1+3(1+\lambda)(1+2\lambda)(\alpha-\beta)\omega_d = 0$.

4.2.4 Statefinder diagnostic

Now, we discuss this model on the context of geometrical parameter. A new geometrical diagnostic pair to discriminate among dark energy models has been introduced by Sahni et al. [174] and Alam et al. [175] and are defined by Eq. (1.11.1). These pair are known as statefinder parameters and are represented as $\{r, s\}$. Now, by substituting the required values in (1.11.1) we get the statefinder pair for non-viscous new HDE model as

$$r = 1 - 3(1 + 2\lambda\alpha\omega_d + \alpha\omega_d)\, X + 2(1 + 2\lambda\alpha\omega_d + \alpha\omega_d)^2\, X^2. \tag{4.2.17}$$

Similarly, the corresponding value of s can be obtained as

$$s = \frac{2(1 + 2\lambda\alpha\omega_d + \alpha\omega_d)\, X}{3}, \tag{4.2.18}$$

which are independent of the cosmic time and depend on λ, α, β and ω_d. This pair will correspond to the $SCDM$ model for the particular combination which satisfy the restriction $(2\alpha - 3\beta) = \frac{\lambda}{(1+\lambda)(1+2\lambda)\omega_d}$. There is no such values of the parameter which can directly corresponds to ΛCDM model but in the limiting case when $\lambda \to -1$, our model will approach to ΛCDM model.

Thus, we conclude that the non-viscous new HDE model in $f(R,T)$ theory is un-

able to explain the phase-transition. Therefore, to observe the possibility of phase transition, we extend our work to constant viscous new HDE model in $f(R,T)$ theory.

4.3 Bulk viscous new HDE model in $f(R,T)$ gravity

Now, we discuss bulk viscous new HDE model in $f(R,T)$ gravity theory. Because of the assumed isotropic and homogeneity of the model, the shear viscosity plays no role, and only the bulk viscosity ζ has to be considered. In general, the presence of ζ does not have any influence upon the (00)-component of the equations of motion. The only change in the formalism because of viscosity is that the thermodynamical pressure p replaced with the effective pressure $\tilde{p_d}$, defined as $\tilde{p_d} = p_d - 3\zeta H$, where ζ stands for bulk viscosity coefficient. This form was originally proposed by Eckart [151]. Many authors [155, 170, 229, 230] have used Eckart approach to explain the recent acceleration of the Universe with bulk viscous fluid. This motivates us to use Eckart formalism on viscous term, especially when one tries to look at recent acceleration of the Universe with $f(R,T)$ gravity.

In $f(R,T)$ theory when it is considered the effective pressure, the matter Lagrangian is $\mathscr{L}_m = -\tilde{p_d}$. Therefore, Eq. (1.7.22) gives $\ominus = -2T_{\mu\nu} - \tilde{p_d} g_{\mu\nu}$, where the trace T takes the form of $T = \rho_m + \rho_d - 3(p_d - 3\zeta H)$.

Using $f(T) = \lambda T$, the field equations (4.2.1) and (4.2.2) for the viscous new HDE model in $f(R,T)$ theory modify to

$$3H^2 = \rho_m + \rho_d + \lambda(\rho_m + \rho_d + p_d - 3\zeta H) + \frac{1}{2}\lambda T, \tag{4.3.1}$$

$$2\dot{H} + 3H^2 = -p_d + 3\zeta H + \frac{1}{2}\lambda T. \tag{4.3.2}$$

From dynamical equations (4.3.1) and (4.3.2), a single evolution equation for H can be obtained as

$$2\dot{H} + (1+\lambda)[\rho_m + (1+\omega_d)\rho_d] - 3(1+\lambda)\zeta H = 0. \tag{4.3.3}$$

Using Granda and Oliveros [73] new HDE density as defined in (1.7.14) into (4.3.1), we get

$$\rho_m = \frac{3}{(2+3\lambda)}\Big[(2 - 2\alpha - 3\lambda\alpha + \lambda\alpha\omega_d)H^2 - \lambda\zeta H - \beta(2 + 3\lambda - \lambda\omega_d)\dot{H}\Big]. \tag{4.3.4}$$

Using (4.3.4) into (4.3.3), we finally get

$$\dot{H} + (1+2\lambda\,\alpha\omega_d + \alpha\omega_d)\,X\,H^2 - (1+2\lambda)\zeta\,X\,H = 0. \tag{4.3.5}$$

4.4 Solution with constant bulk viscous new HDE model

In this section we solve (4.3.5) with constant bulk viscous coefficient ($\zeta = \zeta_0 = \text{const.}$) to get the solution for the scale factor, future finite-time singularity, DP, statefinder pair and *Om* diagnostic.

4.4.1 Evolution of the scale factor

On solving (4.3.5), we get the Hubble parameter H in terms of cosmic time t as

$$H(t) = \frac{H_0 e^{(1+2\lambda)\zeta_0 X(t-t_0)}}{1 + \frac{(1+2\lambda\,\alpha\omega_d+\alpha\omega_d)H_0}{(1+2\lambda)\zeta_0}\left\{e^{(1+2\lambda)\zeta_0 X(t-t_0)} - 1\right\}}. \tag{4.4.1}$$

The corresponding scale factor is obtained as

$$a(t) = \left[1 + \frac{(1+2\lambda\,\alpha\omega_d + \alpha\omega_d)H_0}{(1+2\lambda)\zeta_0}\left\{e^{(1+2\lambda)\zeta_0 X(t-t_0)} - 1\right\}\right]^{\frac{1}{(1+2\lambda\,\alpha\omega_d+\alpha\omega_d)\,X}}. \tag{4.4.2}$$

Here, in the flat case, we can safely choose $a_0 = 1$ as the present scale factor. From (4.4.2), it is observed that the scale factor is of the exponential form. We can observe the phase transition in the evolution of the Universe. In early stages of evolution of the Universe, the scale factor can be approximated as,

$$a(t) \to \left[1 + H_0(1+2\lambda\,\alpha\omega_d + \alpha\omega_d)X(t-t_0)\right]^{\frac{1}{(1+2\lambda\,\alpha\omega_d+\alpha\omega_d)X}}, \tag{4.4.3}$$

which shows a power-law expansion. As $(t-t_0) \to \infty$, the scale factor behaves as

$$a(t) \to \left[exp\left((1+2\lambda)\zeta_0 X(t-t_0)\right)\right]. \tag{4.4.4}$$

Thus, a de Sitter type Universe is obtained in late time evolution. Therefore, the scale factor is approximately power-law expansion at sufficiently early time, which corresponds to the decelerated epoch, and it evolves exponentially with time in future epoch, corresponding to the de Sitter phase. This asymptotic behavior indicates the transition from the early decelerated phase to a late time accelerated phase. The

behavior of scale factor with $(t-t_0)$ for best values of parameters is shown in Fig. 4.1. We consider the observational values of model parameters $\alpha = 0.8502$, $\beta = 0.4817$ [74], $\omega_d = -0.5$ and $\lambda = 0.06$. It is to be noted that if one can assume negative value of λ but the evolution of the scale factor is similar. The value of the scale factor at which the phase transition from deceleration to acceleration take place, is depend on the bulk viscous coefficient ζ_0.

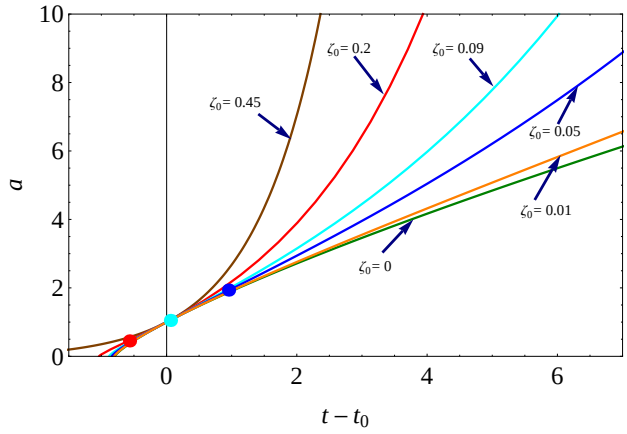

Figure 4.1: The evolution of the *a versus* $(t-t_0)$ *for* $\zeta_0 > 0$ *taking* $\alpha = 0.8502$, $\beta = 0.4817$, $\omega_d = -0.5$ *and* $\lambda = 0.06$. *The dot on each curve denotes the transition time.*

Now, for further analysis about the evolution, let us rewrite the Hubble parameter as

$$H(a) = \frac{(1+2\lambda)H_0}{(1+2\lambda\alpha\omega_d+\alpha\omega_d)}\left[\frac{\zeta_0}{H_0}+\left\{\frac{(1+2\lambda\alpha\omega_d+\alpha\omega_d)}{(1+2\lambda)}-\frac{\zeta_0}{H_0}\right\}a^{-(1+2\lambda\alpha\omega_d+\alpha\omega_d)X}\right]. \tag{4.4.5}$$

From (4.4.5), we can obtain $\frac{d\dot{a}}{da}$ as,

$$\frac{d\dot{a}}{da} = \frac{(1+2\lambda)H_0}{(1+2\lambda\alpha\omega_d+\alpha\omega_d)}\left[\frac{\zeta_0}{H_0}-\left\{\frac{(1+2\lambda\alpha\omega_d+\alpha\omega_d)}{(1+2\lambda)}-\frac{\zeta_0}{H_0}\right\}\right.$$
$$\left.\times\left(\frac{1+3(1+\lambda)(1+2\lambda)(\alpha-\beta)\omega_d}{2+3\lambda+3\beta(1+\lambda)(1+2\lambda)\omega_d}\right)a^{-(1+2\lambda\alpha\omega_d+\alpha\omega_d)X}\right]. \tag{4.4.6}$$

Equating to zero, we can obtain the transition scale factor a_T as

$$a_T = \left[\left\{\frac{\{1+3(1+\lambda)(1+2\lambda)(\alpha-\beta)\omega_d\}}{(1+2\lambda)\{2+3\lambda+3\beta(1+\lambda)(1+2\lambda)\omega_d\}\zeta_0}\right\}\right.$$
$$\left.\times\left\{(1+2\lambda\alpha\omega_d+\alpha\omega_d)H_0-(1+2\lambda)\zeta_0\right\}\right]^{\frac{1}{(1+2\lambda\alpha\omega_d+\alpha\omega_d)X}}. \tag{4.4.7}$$

where the subscript T stands for transition. Using the relation $a = (1+z)^{-1}$, we can

obtain the corresponding transition redshift z_T as

$$z_T = \left[\left\{ \frac{\{1+3(1+\lambda)(1+2\lambda)(\alpha-\beta)\omega_d\}}{(1+2\lambda)\{2+3\lambda+3\beta(1+\lambda)(1+2\lambda)\omega_d\}\zeta_0} \right\} \right.$$
$$\left. \times \left\{ (1+2\lambda\alpha\omega_d+\alpha\omega_d)H_0-(1+2\lambda)\zeta_0 \right\} \right]^{-\frac{1}{(1+2\lambda\alpha\omega_d+\alpha\omega_d)X}} - 1. \quad (4.4.8)$$

From (4.4.7) and (4.4.8), we observe that the phase transition from deceleration to acceleration occurs at present time ($a_T = 1$ or $z_T = 0$) for

$$\zeta_0 = \frac{\{1+3(1+\lambda)(1+2\lambda)(\alpha-\beta)\omega_d\}H_0}{3(1+\lambda)(1+2\lambda)}$$

The transition from deceleration to acceleration take place in late time ($a(t) > 1$) for

$$\zeta_0 < \frac{\{1+3(1+\lambda)(1+2\lambda)(\alpha-\beta)\omega_d\}H_0}{3(1+\lambda)(1+2\lambda)}$$

and it takes place in past ($0 < a(t) < 1$) for

$$\zeta_0 > \frac{\{1+3(1+\lambda)(1+2\lambda)(\alpha-\beta)\omega_d\}H_0}{3(1+\lambda)(1+2\lambda)}$$

As $\zeta_0 \to 0$, $a_T \to \infty$ in future.

The transition expression with respect to time can be obtained by equating the second derivative of a with respect to time. Then, the second derivative of (4.4.2) with respect t can be obtain as

$$\frac{d^2a}{dt^2} = H_0^2\left(e^{2(1+2\lambda)\zeta_0 X\,(t-t_0)}\right)\left[1+\frac{X[(1+2\lambda)\zeta_0-(1+2\lambda\alpha\omega_d+\alpha\omega_d)H_0]}{H_0\,e^{(1+2\lambda)\zeta_0 X\,(t-t_0)}}\right]$$
$$\times \left[1+\frac{(1+2\lambda\alpha\omega_d+\alpha\omega_d)H_0}{(1+2\lambda)\zeta_0}\left\{e^{(1+2\lambda)\zeta_0 X\,(t-t_0)}-1\right\}\right]^{\frac{1}{(1+2\lambda\alpha\omega_d+\alpha\omega_d)\,X}-2}. \quad (4.4.9)$$

Now, the transition cosmic time (t_{trans}) between decelerated to accelerated epochs is calculated by equating (4.4.9) to zero. Thus, we get

$$t_{trans} = t_0 + \frac{1}{X\,(1+2\lambda)\zeta_0}\ \ln\left\{\frac{X\,[(1+2\lambda\alpha\omega_d+\alpha\omega_d)H_0-(1+2\lambda)\zeta_0]}{H_0}\right\}. \quad (4.4.10)$$

Figure 4.1 shows that the acceleration can be achieved in future for the small values of ζ_0, however, it can be achieved in early for large values of ζ_0. It can be observed

that the scale factor begins to accelerate from infinite past for $\zeta_0 = 0.45$ and it begins to accelerate in very late time for $\zeta_0 = 0.01$. For $\zeta_0 > 0.45$, we have an Universe which expands forever. In the absence of viscous term, i.e., $\zeta_0 = 0$, the scale factor has the power-law form and the expansion takes place with decelerated rate as shown by the first trajectory in Fig. 4.1.

4.4.2 Future finite-time singularity

We have already defined the four types of singularities in subsection 4.2.2. Here, we will discuss these four singularities in case of constant viscous new HDE model in $f(R,T)$ gravity.

Let us find the total energy density which is given by

$$\rho = \frac{3H_0 e^{(1+2\lambda)\zeta_0 X (t-t_0)}}{(1+2\lambda)(2+3\lambda)}\Bigg[(2+3\lambda)H_0 e^{(1+2\lambda)\zeta_0 X (t-t_0)} - \lambda\{1-\alpha\beta X \omega_d(1+2\lambda)\} \times [(1+2\lambda)\zeta_0 - (1+2\lambda\alpha\omega_d+\alpha\omega_d)H_0]\Bigg] \times \left[1+\frac{(1+2\lambda\alpha\omega_d+\alpha\omega_d)H_0}{(1+2\lambda)\zeta_0}\left\{e^{(1+2\lambda)\zeta_0 X (t-t_0)}-1\right\}\right]^{-2}. \tag{4.4.11}$$

The total pressure of the new HDE in the presence of viscosity is $p_{eff} = \tilde{p_d} = p_d - 3\zeta H$, can be evaluated as

$$p_{eff} = \frac{3H_0 e^{(1+2\lambda)\zeta_0 X (t-t_0)}}{(1+2\lambda)}\Bigg[\{\beta X \omega_d(1+2\lambda)-1\}[(1+2\lambda)\zeta_0 - (1+2\lambda\alpha\omega_d+\alpha\omega_d)H_0] - H_0 e^{(1+2\lambda)\zeta_0 X (t-t_0)}\Bigg]\left[1+\frac{(1+2\lambda\alpha\omega_d+\alpha\omega_d)H_0}{(1+2\lambda)\zeta_0}\left\{e^{(1+2\lambda)\zeta_0 X (t-t_0)}-1\right\}\right]^{-2}. \tag{4.4.12}$$

On considering $\omega_d = -0.5$, $\alpha = 0.8502$, $\beta = 0.4817$ and $H_0 = 1$, we obtain that for $-1 < \lambda < -0.69533$ or $0.676194 < \lambda < 1.27131$ (as calculated by Mathematica software), we have $a \to \infty$, $\rho \to \infty$ and $|\tilde{p_d}| \to \infty$, which shows the Type I big-rip singularity at a finite time

$$t_s = \frac{1}{X\ \zeta_0(1+2\lambda)}\ \ln\left[1-\frac{(1+2\lambda)\zeta_0}{(1+2\lambda\alpha\omega_d\alpha\omega_d)H_0}\right]+t_0. \tag{4.4.13}$$

For other values of λ (excluding the mentioned interval), we obtain that at this finite time $a \to 0$, $\rho \to \infty$ and $|p_{eff}| \to \infty$, which shows the Type III singularity.

In the absence of model parameters α and β, the big-rip singularity depends on only λ. Thus, for $\lambda < -2/3$ we have $a \to \infty$, $\rho \to \infty$ and $|p_{eff}| \to \infty$ at finite-time

$$t_s = \frac{(2+3\lambda)}{3\zeta_0(1+\lambda)(1+2\lambda)} \ln\left(1 - \frac{(1+2\lambda)\zeta_0}{H_0}\right) + t_0. \tag{4.4.14}$$

The age of the Universe can be deduced from the scale factor (4.4.2) by equating it to zero. The time elapsed since the Big Bang is given by Eq. (4.4.13) replacing t_s by t_b. Hence the age of the Universe since Big bang is

$$\begin{aligned} Age &\equiv t_0 - t_b \\ &= -\frac{(2+3\lambda)}{3\zeta_0(1+\lambda)(1+2\lambda)} \ln\left(1 - \frac{(1+2\lambda)\zeta_0}{H_0}\right). \end{aligned} \tag{4.4.15}$$

4.4.3 Behavior of deceleration parameter

Now, we verify the results with the help of DP which is defined in (1.9.5). The DP for constant viscous new HDE model in $f(R,T)$ is calculated as

$$q(t) = \left\{\frac{\{(1+2\lambda\alpha\omega_d + \alpha\omega_d)H_0 - (1+2\lambda)\zeta_0\}\, X}{H_0}\right\} e^{-(1+2\lambda)\zeta_0 X\,(t-t_0)} - 1. \tag{4.4.16}$$

We observe that the DP is time-dependent when we include the constant bulk viscosity in the matter. It is now possible to describe the phase transition of the Universe.

The DP from Eq. (4.4.16) can be rewritten as

$$\begin{aligned} q(a) = X\,&[(1+2\lambda\alpha\omega_d + \alpha\omega_d)H_0 - (1+2\lambda)\zeta_0] \\ &\times \left[\frac{(1+2\lambda\alpha\omega_d + \alpha\omega_d)}{\left(a^{(1+2\lambda\alpha\omega_d+\alpha\omega_d)\,X} - 1\right)(1+2\lambda)\zeta_0 + (1+2\lambda\alpha\omega_d + \alpha\omega_d)H_0}\right] - 1. \end{aligned} \tag{4.4.17}$$

The DP in terms of redshift z is

$$\begin{aligned} q(z) = X\,&[(1+2\lambda\alpha\omega_d + \alpha\omega_d)H_0 - (1+2\lambda)\zeta_0] \\ &\times \left[\frac{(1+2\lambda\alpha\omega_d + \alpha\omega_d)}{\left((1+z)^{-(1+2\lambda\alpha\omega_d+\alpha\omega_d)\,X} - 1\right)(1+2\lambda)\zeta_0 + (1+2\lambda\alpha\omega_d + \alpha\omega_d)H_0}\right] - 1. \end{aligned} \tag{4.4.18}$$

In the absence of bulk viscous parameter and all other model parameters, the value of DP q is $1/2$, which corresponds to a decelerating matter-dominated Universe with null bulk viscosity. However, when only the bulk viscous term $\zeta_0 = 0$, the value of q is same as obtained in Eq. $(4.2.16)$ for non-viscous new HDE model.

The present value of q corresponds to $z = 0$ or $a = 1$ is,

$$q_0 = \frac{\{(1+2\lambda\alpha\omega_d + \alpha\omega_d)H_0 - (1+2\lambda)\zeta_0\}\, X}{H_0} - 1. \tag{4.4.19}$$

Note that when the whole fraction part on right hand side of $(4.4.19)$ equals to 1, the transition from decelerated to accelerated epochs takes place today. If the same term is less than one, we have an accelerated epoch while if it is greater than one, the decelerated epoch occurs.

We can observe the evolution of the Universe for different ranges of λ with respect to the viscous coefficient ζ_0 for $\omega_d > -1$, $\omega_d = -1$ and $\omega_d < -1$. We summarize the evolution in Tables 4.1– 4.3 for different ranges of λ which shows deceleration or acceleration or phase transition according to the constraint on the bulk viscous coefficient ζ_0. We assume the observational value of the model parameters $\alpha = 0.8502$ and $\beta = 0.4817$ [74].

In Table 4.1, we analyse the evolution of the Universe for $\omega_d = -0.5$ along with the observational values of model parameters $\alpha = 0.8502$ and $\beta = 0.4817$. We observe that for any positive value of ζ_0, i.e., $\zeta_0 > 0$, the model corresponds to the decelerated expansion throughout the evolution for $\lambda \geq 1.272$, $-0.69 \leq \lambda \leq -0.5$ and $\lambda < -1.73$, and the model corresponds to the accelerated expansion throughout the evolution for $0.24 \leq \lambda < 1.272$ and $-1 \leq \lambda < -0.69$. For smaller values of ζ_0, i.e., $0 < \zeta_0 < \frac{\{1-0.55275(1+\lambda)(1+2\lambda)\}H_0}{3(1+\lambda)(1+2\lambda)}$, the Universe shows the phase transition from positive to negative for $-0.5 < \lambda < 0.24$ and shows the phase transition from negative to positive for $-1.73 \leq \lambda < -1$. The larger values of ζ_0, i.e., $\zeta_0 \geq \frac{\{1-0.55275(1+\lambda)(1+2\lambda)\}H_0}{3(1+\lambda)(1+2\lambda)}$, shows that the Universe represents the accelerated expansion throughout the evolution for $-0.5 < \lambda < 0.24$ and represents the decelerated expansion throughout the evolution for $-1.73 \leq \lambda < -1$.

Table 4.2 represents the analysis of the evolution of the Universe for $\omega_d = -1$ along with the same observational values of model parameters. We observe that for any positive value of ζ_0, the model corresponds to the decelerated expansion throughout the evolution for $\lambda \geq 0.265$, $-0.727 < \lambda \leq -0.5$ and $\lambda < -1.46$ ranges

Table 4.1: Variation of q for $\omega_d = -0.5$, $\alpha = 0.8502$, $\beta = 0.4817$

λ	Constraints on ζ_0	q	Evolution of Universe
$\lambda \geq 1.272$	For all $\zeta_0 > 0$	Positive	Decelerated expansion
$0.24 \leq \lambda < 1.272$	For all $\zeta_0 > 0$	Negative	Accelerated expansion
$-0.5 < \lambda < 0.24$	$0 < \zeta_0 < \frac{\{1-0.55275(1+\lambda)(1+2\lambda)\}H_0}{3(1+\lambda)(1+2\lambda)}$	$+$ve to $-$ve	Trans. from dec. to acc.
	$\zeta_0 \geq \frac{\{1-0.55275(1+\lambda)(1+2\lambda)\}H_0}{3(1+\lambda)(1+2\lambda)}$	Negative	Accelerated expansion
$-0.69 \leq \lambda \leq -0.5$	For all $\zeta_0 > 0$	Positive	Decelerated expansion
$-1 \leq \lambda < -0.69$	For all $\zeta_0 > 0$	Negative	Accelerated expansion
$-1.73 \leq \lambda < -1$	$0 < \zeta_0 < \frac{\{1-0.55275(1+\lambda)(1+2\lambda)\}H_0}{3(1+\lambda)(1+2\lambda)}$	$-$ve to $+$ve	Trans. from acc. to dec.
	$\zeta_0 \geq \frac{\{1-0.55275(1+\lambda)(1+2\lambda)\}H_0}{3(1+\lambda)(1+2\lambda)}$	Positive	Decelerated expansion
$\lambda < -1.73$	For all $\zeta_0 > 0$	Positive	Decelerated expansion

of λ, and the model corresponds to the accelerated expansion throughout the evolution for $-0.032 \leq \lambda < 0.265$ and $-1 \leq \lambda \leq -0.727$. For smaller values of ζ_0, i.e., $0 < \zeta_0 < \frac{\{1-1.1055(1+\lambda)(1+2\lambda)\}H_0}{3(1+\lambda)(1+2\lambda)}$, the Universe shows the phase transition from deceleration to acceleration for $-0.5 < \lambda < -0.032$ and shows the phase transition from acceleration to deceleration for $-1.46 \leq \lambda < -1$. The larger values of ζ_0, i.e., $\zeta_0 \geq \frac{\{1-1.1055(1+\lambda)(1+2\lambda)\}H_0}{3(1+\lambda)(1+2\lambda)}$, shows that the Universe represents the accelerated expansion throughout the evolution for $-0.5 < \lambda < -0.032$ and represents the decelerated expansion throughout the evolution for $-1.46 \leq \lambda < -1$.

In Table 4.3, we consider the value of $\omega_d < -1$, e.g., $\omega_d = -1.1414$ and the same observational values of model parameters. In this we observe that for any positive value of ζ_0, the model shows the decelerated expansion throughout the evolution for $\lambda \geq 0.145$, $-0.735 \leq \lambda \leq -0.5$ and $\lambda < -1.42$, and the model corresponds to the accelerated expansion throughout the evolution for $-0.072 \leq \lambda < 0.145$ and $-1 \leq \lambda < -0.735$. The smaller values of ζ_0, i.e., $0 < \zeta_0 < \frac{\{1-1.26182(1+\lambda)(1+2\lambda)\}H_0}{3(1+\lambda)(1+2\lambda)}$, the Universe transits from decelerated to accelerated one for $-0.5 < \lambda < -0.072$ and transits from accelerated to decelerated one for $-1.42 \leq \lambda < -1$. For the larger values of ζ_0, i.e., $\zeta_0 \geq \frac{\{1-1.26182(1+\lambda)(1+2\lambda)\}H_0}{3(1+\lambda)(1+2\lambda)}$, the Universe represents the accelerated expansion throughout the evolution for $-0.5 < \lambda < -0.072$ and shows the decelerated expansion throughout the evolution for $-1.42 \leq \lambda < -1$.

Table 4.2: Variation of q for $\omega_d = -1$, $\alpha = 0.8502$, $\beta = 0.4817$

λ	Constraints on ζ_0	q	Evolution of Universe
$\lambda \geq 0.265$	For all $\zeta_0 > 0$	Positive	Decelerated expansion
$-0.032 \leq \lambda < 0.265$	For all $\zeta_0 > 0$	Negative	Accelerated expansion
$-0.5 < \lambda < -0.032$	$0 < \zeta_0 < \frac{\{1-1.1055(1+\lambda)(1+2\lambda)\}H_0}{3(1+\lambda)(1+2\lambda)}$	$+$ve to $-$ve	Trans. from dec. to acc.
	$\zeta_0 \geq \frac{\{1-1.1055(1+\lambda)(1+2\lambda)\}H_0}{3(1+\lambda)(1+2\lambda)}$	Negative	Accelerated expansion
$-0.727 < \lambda \leq -0.5$	For all $\zeta_0 > 0$	Positive	Decelerated expansion
$-1 \leq \lambda \leq -0.727$	For all $\zeta_0 > 0$	Negative	Accelerated expansion
$-1.46 \leq \lambda < -1$	$0 < \zeta_0 < \frac{\{1-1.1055(1+\lambda)(1+2\lambda)\}H_0}{3(1+\lambda)(1+2\lambda)}$	$-$ve to $+$ve	Trans. from acc. to dec.
	$\zeta_0 \geq \frac{\{1-1.1055(1+\lambda)(1+2\lambda)\}H_0}{3(1+\lambda)(1+2\lambda)}$	Positive	Decelerated expansion
$\lambda < -1.46$	For all $\zeta_0 > 0$	Positive	Decelerated expansion

Table 4.3: Variation of q for $\omega_d = -1.1414$, $\alpha = 0.8502$, $\beta = 0.4817$

λ	Constraints on ζ_0	q	Evolution of Universe
$\lambda \geq 0.145$	For all $\zeta_0 > 0$	Positive	Decelerated expansion
$-0.072 \leq \lambda < 0.145$	For all $\zeta_0 > 0$	Negative	Accelerated expansion
$-0.5 < \lambda < -0.072$	$0 < \zeta_0 < \frac{\{1-1.26182(1+\lambda)(1+2\lambda)\}H_0}{3(1+\lambda)(1+2\lambda)}$	$+$ve to $-$ve	Trans. from dec. to acc.
	$\zeta_0 \geq \frac{\{1-1.26182(1+\lambda)(1+2\lambda)\}H_0}{3(1+\lambda)(1+2\lambda)}$	Negative	Accelerated expansion
$-0.735 \leq \lambda \leq -0.5$	For all $\zeta_0 > 0$	Positive	Decelerated expansion
$-1 \leq \lambda < -0.735$	For all $\zeta_0 > 0$	Negative	Accelerated expansion
$-1.42 \leq \lambda < -1$	$0 < \zeta_0 < \frac{\{1-1.26182(1+\lambda)(1+2\lambda)\}H_0}{3(1+\lambda)(1+2\lambda)}$	$-$ve to $+$ve	Trans. from acc. to dec.
	$\zeta_0 \geq \frac{\{1-1.26182(1+\lambda)(1+2\lambda)\}H_0}{3(1+\lambda)(1+2\lambda)}$	Positive	Decelerated expansion
$\lambda < -1.42$	For all $\zeta_0 > 0$	Positive	Decelerated expansion

4.4.4 Statefinder diagnostic

In the presence of constant bulk viscous coefficient, we get the exponential form of scale factor and time-dependent value of the DP which explain the phase transition of the Universe. Let us evaluate the statefinder parameters for the constant viscous new HDE model to discriminate our model with respect to existing DE models. In this case, the statefinder parameters are calculated as

$$r = 1+\left[\left(1-\frac{X\,(1+2\lambda\,\alpha\omega_d+\alpha\omega_d)}{3}\right)\left(\frac{3\,X\,[(1+2\lambda)\zeta_0-(1+2\lambda\,\alpha\omega_d+\alpha\omega_d)H_0]}{H_0\,e^{(1+2\lambda)\zeta_0\,X\,(t-t_0)}}\right)\right] + \left[\frac{X^2[(1+2\lambda)\zeta_0-(1+2\lambda\,\alpha\omega_d+\alpha\omega_d)H_0]^2}{H_0^2\,e^{2(1+2\lambda)\zeta_0\,X\,(t-t_0)}}\right], \tag{4.4.20}$$

and

$$s=\frac{\frac{2\,X\left(1-\frac{X\,(1+2\lambda\,\alpha\omega_d+\alpha\omega_d)}{3}\right)[(1+2\lambda)\zeta_0-(1+2\lambda\,\alpha\omega_d+\alpha\omega_d)H_0]}{3H_0e^{(1+2\lambda)\zeta_0\,X\,(t-t_0)}}+\frac{2\,X^2[(1+2\lambda)\zeta_0-(1+2\lambda\,\alpha\omega_d+\alpha\omega_d)H_0]^2}{9H_0^2e^{2(1+2\lambda)\zeta_0\,X\,(t-t_0)}}}{\frac{2\,X\,[(1+2\lambda\,\alpha\omega_d+\alpha\omega_d)H_0-(1+2\lambda)\zeta_0]}{3H_0e^{(1+2\lambda)\zeta_0\,X\,(t-t_0)}}-1}. \tag{4.4.21}$$

From (4.4.20) and (4.4.21), it is clear that due to the presence of viscosity, we get the time-dependent values of the statefinder parameters. The trajectories in $r-s$ and $r-q$ planes for different values of ζ_0 and fixed positive value of λ are shown in Fig. 4.2 and Fig. 4.3, respectively. Similarly, the trajectories in $r-s$ and $r-q$ planes for different values of ζ_0 and fixed negative value of λ are shown in Fig. 4.4 and Fig. 4.5, respectively. In all figures we take $\alpha=0.8502$, $\beta=0.4817$, $\omega_d=-0.5$ and $H_0=1$.

If we look Fig. 4.2 and Fig. 4.4, we find that a vertical line passing through $(1,0)$ divides $r-s$ plane into two regions. The right side of the vertical region which is $r<1$, $s>0$, belongs to a model similar to quintessence(Q model) [174, 175]. The other region on left side of vertical line which has $r>1$, $s<0$, belongs to a model similar to Chaplygin gas (CG) model [217]. Fig. 4.2 and Fig. 4.4 represent the $r-s$ trajectories for $\lambda=0.06$ and $\lambda=-0.06$ for different values of ζ_0, respectively. In figures stars represent the fixed point values of the parameters, i.e., $\{r,s\}=\{1,1\}$ and $\{r,s\}=\{1,0\}$ with respect to $SCDM$ and ΛCDM, respectively and arrows show the direction of the trajectories. For the present Universe, the statefinder parameters take the form

$$r_0 = 1+\left[\left(1-\frac{X\,(1+2\lambda\alpha\omega_d+\alpha\omega_d)}{3}\right)\left(\frac{3\,X\,[(1+2\lambda)\zeta_0-(1+2\lambda\alpha\omega_d+\alpha\omega_d)H_0]}{H_0}\right)\right] + \left[\frac{X^2[(1+2\lambda)\zeta_0-(1+2\lambda\alpha\omega_d+\alpha\omega_d)H_0]^2}{H_0^2}\right], \tag{4.4.22}$$

and

$$s_0 = \frac{\frac{2\,X\left(1-\frac{X\,(1+2\lambda\alpha\omega_d+\alpha\omega_d)}{3}\right)[(1+2\lambda)\zeta_0-(1+2\lambda\alpha\omega_d+\alpha\omega_d)H_0]}{3H_0}+\frac{2\,X^2[(1+2\lambda)\zeta_0-(1+2\lambda\alpha\omega_d+\alpha\omega_d)H_0]^2}{9H_0^2}}{\frac{2\,X\,[(1+2\lambda\alpha\omega_d+\alpha\omega_d)H_0-(1+2\lambda)\zeta_0]}{3H_0}-1}. \tag{4.4.23}$$

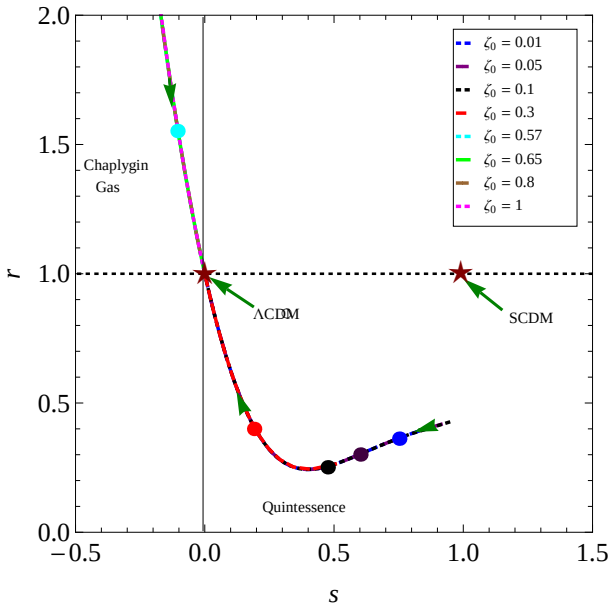

Figure 4.2: The $r-s$ trajectory of the bulk viscous new HDE model for $\zeta_0 > 0$ and fixed positive value $\lambda = 0.06$ and $\omega_d = -0.5$.

In Fig. 4.2, for $0 < \zeta_0 \leq 0.46$, the trajectories during the early time lie in the region $r < 1$, $s > 0$, which is the general behavior of any Q model and approaches to ΛCDM in late time. However, the trajectories lie in $r > 1$, $s < 0$ for $\zeta_0 > 0.46$, which is the general behavior of CG model and tends to ΛCDM in late time. Similarly, in Fig. 4.4 for $0 < \zeta_0 \leq 0.71$, the trajectory starts in Q region during early time and tends to ΛCDM in late time. It starts from CG region for $\zeta_0 > 0.71$ and approaches to ΛCDM in late time. Thus, the constant viscous new HDE model is compatible with Q model for small values of ζ_0 whereas it is compatible with CG model for large values of ζ_0, irrespective of values of λ, either positive or negative. It is to be noted that all the trajectories

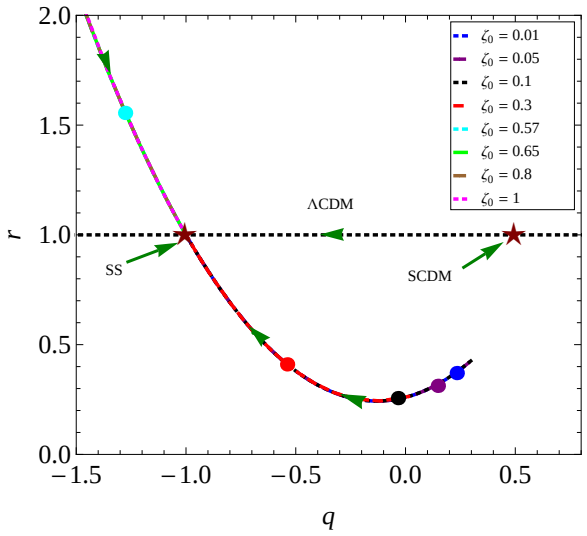

Figure 4.3: The $r-q$ trajectory of the bulk viscous new HDE model for $\zeta_0 > 0$ and fixed positive value $\lambda = 0.06$ and $\omega_d = -0.5$.

of Q and CG regions coincide on each other for any value of ζ_0 with $\lambda = 0.06$ and $\lambda = -0.06$, respectively.

In Fig. 4.4, we observe that for some small values of ζ_0 (e.g., $\zeta_0 = 0.05$) the trajectory starts from the vicinity of the $SCDM$ model. Our constant viscous new HDE model also discriminates from HDE model with event horizon as the IR cutoff in which the evolution starts in $r \sim 1$, $s \sim 2/3$ and ends on the ΛCDM model. This model is also discriminated from Ricci dark energy model [216], where the $r-s$ trajectory is a vertical segment, i.e., s is a constant during the evolution of the Universe.

The $r-q$ trajectories are plotted in Fig. 4.3 and Fig. 4.5 for $\lambda = 0.06$ and $\lambda = -0.06$, respectively, along with the observational value of model parameters $\alpha = 0.8502$ and $\beta = 0.4817$ for different values of ζ_0. Here, the stars represent the fixed point values $\{r,q\} = \{1, 0.5\}$ and $\{r,q\} = \{1,-1\}$ for $SCDM$ and Steady State (SS) models, respectively, and the horizontal line at $r = 1$ shows the time evolution of the ΛCDM. The direction of evolution is shown by arrow. In both the figures, there is the change of sign in q, i.e., from $+ve$ to $-ve$ in quintessence region for small values of ζ_0 and q transits from phantom region to SS for large values of ζ_0. This shows that the phase transition occurs for both positive and negative values of λ. In both cases, the model approaches to SS model in future time from both regions as ΛCDM, Q and CG models approach to SS model in late time. The trajectories for different values of ζ_0 coincide to each other. Some trajectories start earlier and some starts in later. From Fig. 4.5, we observe that for small values of ζ_0 (e.g., $\zeta_0 = 0.05$), the $r-q$ trajectory starts from

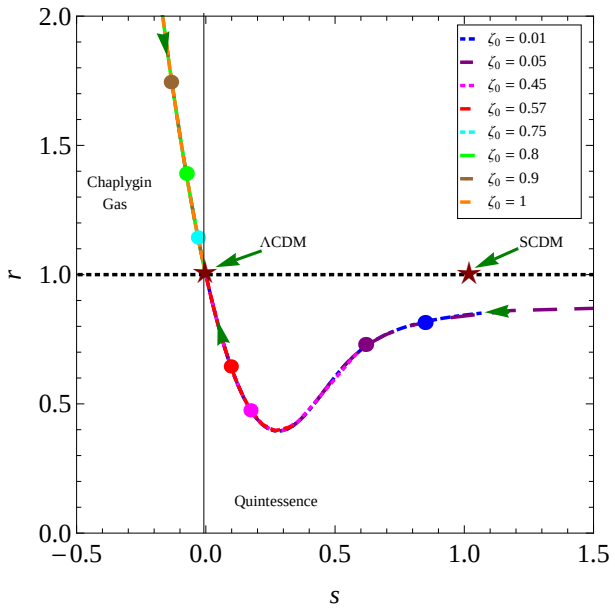

Figure 4.4: The $r-s$ trajectory of the bulk viscous new HDE model for $\zeta_0 > 0$ and fixed negative value $\lambda = -0.06$ and $\omega_d = -0.5$.

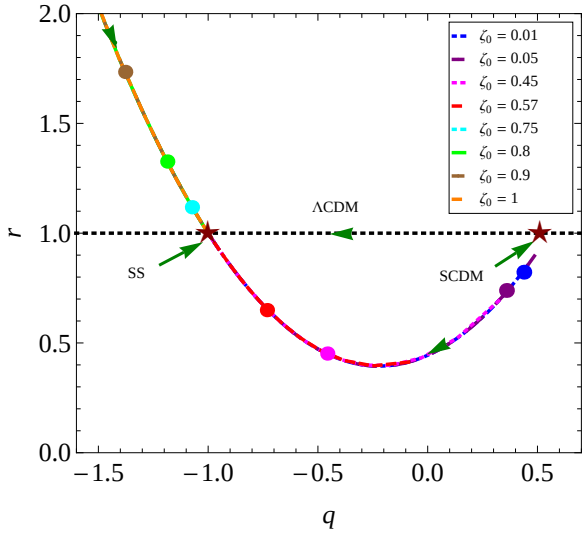

Figure 4.5: The $r-q$ trajectory of the bulk viscous new HDE model for $\zeta_0 > 0$ and fixed negative value $\lambda = -0.06$ and $\omega_d = -0.5$.

the neighbourhood of the $SCDM$ model in Q region.

4.4.5 *Om* diagnostic

Now, we discuss the nature of new HDE density with respect to a geometrical tool which is defined by (1.11.2) and known as *Om* diagnostic. By substituting the required values in (1.11.2), we get

$$Om(z) = \frac{\frac{(1+2\lambda)^2\left\{\frac{\zeta_0}{H_0}+\left(\frac{1+2\lambda\alpha\omega_d+\alpha\omega_d}{(1+2\lambda)}-\frac{\zeta_0}{H_0}\right)(1+z)^{X\,(1+2\lambda\alpha\omega_d+\alpha\omega_d)}\right\}^2}{(1+2\lambda\alpha\omega_d+\alpha\omega_d)^2}-1}{[(1+z)^3-1]}. \tag{4.4.24}$$

To analyze the behaviour of viscous new HDE, we plot the graph for *Om(z)* trajectory for different values of ζ_0 and fixed positive and negative values of λ with observational value of model parameters $\alpha = 0.8502$ and $\beta = 0.4817$. Fig. 4.6 represents the *Om(z)* trajectory with respect to redshift z for different values of ζ_0 and the fixed positive value of $\lambda = 0.06$, $H_0 = 1$, $\omega_d = -0.5$. It is observed that for $0 < \zeta_0 \leq 0.46$, the negative slope of *Om* trajectory is observed, i.e., the new HDE behaves as quintessence like for this range of ζ_0, whereas, the positive slope of the *Om* trajectory is observed for $\zeta_0 > 0.46$, i.e., in this range the new HDE mimic to the phantom like.

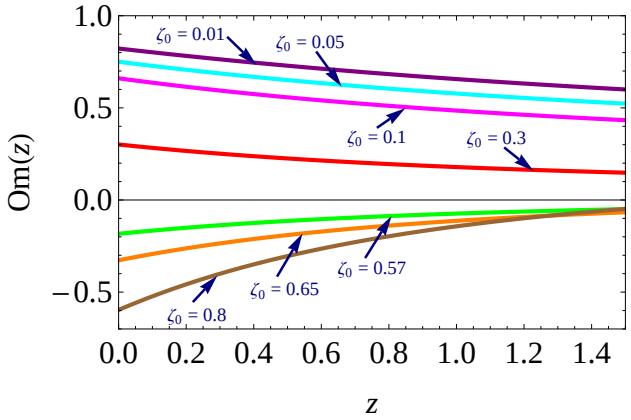

Figure 4.6: The *Om(z)* evolutionary diagram for $\zeta_0 > 0$ and fixed $\lambda = 0.06$

Fig. 4.7 shows the *Om(z)* trajectory for the negative value of λ (e.g., $\lambda = -0.06$), $H_0 = 1$ and $\omega_d = -0.5$. We observe that the *Om(z)* trajectory shows the negative curvature for $0 < \zeta_0 \leq 0.71$, i.e., the new HDE corresponds to the quintessence for this range and the positive curvature is observed for $\zeta_0 > 0.71$, i.e., the new HDE behaves as phantom. In the late time of evolution when $z = -1$, we get $Om(z) = 1 - \frac{(1+2\lambda)^2\zeta_0^2}{(1+2\alpha\lambda\omega_d+\alpha\omega_d)^2H_0^2}$, which is the constant value of *Om(z)*, i.e., zero curvature. Thus,

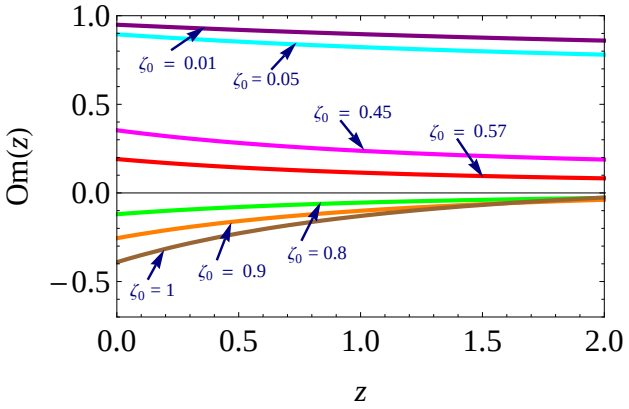

Figure 4.7: The *Om(z)* evolutionary diagram for $\zeta_0 > 0$ and fixed $\lambda = -0.06$

in late time the new HDE corresponds to ΛCDM.

4.4.6 Thermodynamics and local entropy

In the FRW line element, the law of generation of the local entropy is found to be [4, 231]

$$\mathbb{T}\nabla_\nu s^\nu = \zeta(\nabla_\nu u^\nu)^2 = 9H^2\zeta, \tag{4.4.25}$$

where $\mathbb{T}$ stands for temperature and $\nabla_\nu s^\nu$ represents the rate at which entropy is being generated in unit volume. The second law of thermodynamics is

$$\mathbb{T}\nabla_\nu s^\nu \geq 0, \tag{4.4.26}$$

which implies from (4.4.25) that $9H^2\zeta \geq 0$. Since for the expanding Universe, the value of Hubble parameter is positive, then to satisfy the second law of thermodynamics, the viscous coefficient ζ_0 must be positive. Therefore, Eq. (4.4.26) implies that

$$\zeta = \zeta_0 \geq 0. \tag{4.4.27}$$

Thus from Eq. (4.4.27), we observe that the viscous coefficient is always positive, i.e., $\zeta_0 > 0$ which shows the validity of the local second law of thermodynamics.

4.5 Conclusion

From the viewpoint of the fluid description and the current cosmological observational data, there is no reason for excluding the imperfect fluid due to the presence of a bulk viscosity. This bulk viscosity is introduced in energy-momentum tensor through an

additional term $-3\zeta H$, where the whole term represents the bulk viscous pressure of the fluid.

In this chapter, we have performed a detailed dynamical analysis for viscous cosmology in the Eckart's formalism. In our study we have considered the total cosmic fluid constituted by pressureless DM and viscous new HDE. The bulk viscous coefficient ζ is assumed as a constant, whereas the other components are assumed to behave as perfect fluids with constant EoS parameter. We have discussed the non-viscous and constant viscous cosmological new HDE model in $f(R,T)$ theory with new IR cutoff proposed by Granda and Oliveros [73]. Since this new HDE model depends only on local quantities, so it avoids the causality problem which occur while studying the HDE model based on event horizon. Thus, this new HDE model can be considered as a phenomenological model for HDE. We have investigated the actions of some viscous cosmology in new HDE model, with the hope to demonstrate that the bulk viscosity can also play the role as a possible candidate of DE. We have performed a detailed study of both non-viscous and constant viscous new HDE models. Some cosmological parameters and their evolution have been computed. Some geometrical parameters: statefinder and Om, have also been studies.

In section 4.2, we have presented a non-viscous new HDE model in $f(R,T)$ gravity theory. The scale factor has been obtained for this model which gives power-law expansion. The nature of the expansion depends on the constraint of parameters used in the model. The model decelerates, accelerates or show marginal expansion under the constraints. Type I (big-rip) and Type III singularities have been discussed which occur under certain constraints of λ. In the absence of all parameters the model behaves like matter-dominated which has big bang singularity at $t_b = t_0 - \frac{2}{3H_0}$. We could see that the model we discussed above falls basically into the Type I category, that is, the so-called "Big Rip" singularity. The DP comes out to be constant and hence the transition can not be observed for this case. However, the constant value of statefinder pair is obtained and there exist no such exact value of parameters which clearly represent the ΛCDM.

Section 4.3 provides the field equations of viscous new HDE model in $f(R,T)$ gravity theory. The bulk viscous coefficient is taken as a constant, i.e., $\zeta = \zeta_0 =$const.. In section 4.4, the solutions of different cosmological parameters have been obtained. We have found the scale factor as an exponential type which shows accelerated expansion of the Universe. The asymptotic behavior of the scale factor shows that the

transition from an early deceleration to late acceleration. This shows that the constant viscous new HDE model has an earlier decelerated phase followed by an accelerated phase in late time. The evolution of scale factor is shown in Fig. 4.1. In this case, we have discussed future finite-time singularity and observed the finite-time Type I (big-rip) and Type III singularities under the constraints on λ. The transition scale factor and redshift are obtained and transition at present time is calculated. We have also obtained the transition time between decelerated to accelerated epochs. Fig. 4.1 shows that for small values of ζ_0, we get late time acceleration for positive or negative value of λ. However, we get early acceleration for large values of ζ_0. The trend of the evolution of scale factor is: the larger the bulk viscosity, more early acceleration and smaller the value of ζ_0, late time acceleration occur during the evolution.

The evolution of DP is obtained, which is time-dependent and describes the phase transition of the Universe. We have expressed q in terms of a and z and have analyzed starting of the present time transition from decelerated to accelerated phase. We have observed the evolution of the Universe for different ranges of λ and corresponding constraints of ζ_0 for $\omega_d > -1$, $\omega_d = -1$ and $\omega_d < -1$ and $\alpha = 0.8502$ and $\beta = 0.4817$. The nature of q and its corresponding evolution of the Universe (deceleration, acceleration or transition between these two epochs) are summarized in tables 4.1–4.3.

We have studied this model from viewpoint of statefinder and *Om* diagnostics. As we know the statefinder diagnostic is a crucial tool for discriminating different DE models. We have calculated the evolution of new HDE model in the statefinder plane $r-s$ for different values of viscous coefficient ζ_0. The statefinder trajectory are dependent on viscous term ζ_0 and geometry term λ. We have plotted two $r-s$ planes in Fig. 4.2 and Fig.4.4 for positive and negative values of λ, respectively. We have obtained curved trajectory starting from both regions (quintessence and Chaplygin gas) depending on the values of ζ_0. The trajectory starts from quintessence region for the range $0 < \zeta_0 \leq 0.46$ and it starts from Chaplygin gas region for $\zeta_0 > 0.46$ as shown in Fig. 4.2. Similarly, in Fig. 4.4 the trajectory starts from quintessence region for the range $0 < \zeta_0 \leq 0.71$ and it starts from Chaplygin gas region for $\zeta_0 > 0.71$. The trajectories are coinciding with each other in both quintessence and Chaplygin gas regions. However, the trajectory approaches to ΛCDM in late time from both the regions. This constant viscous new HDE model discriminates from viscous Ricci dark energy [216] where the value of s is constant. It also discriminates from HDE model with event horizon as an IR cutoff.

We have also performed the statefinder diagnostic in $r-q$ plane for constant viscous new HDE model for different values of ζ_0 by taking positive and negative value of λ, which are shown in Figs. 4.3 and 4.5, respectively. The evolutionary trajectories in $r-q$ plane start from positive q in quintessence region and tend to $q=-1$, $r=1$ in late time for the range $0<\zeta_0\leq 0.46$, but the trajectories in $r-q$ plane start from negative q in phantom region and tend to $q=-1$, $r=1$ in late time for $\zeta_0>0.46$ as shown in Fig. 4.3. Similar trajectories can be seen in Fig. 4.5 for negative λ and $0<\zeta_0\leq 0.71$ and $\zeta_0>0.71$, respectively. The trajectory clearly shows that there is transition from decelerated phase to accelerated phase whereas some trajectories show that there is through out acceleration.

We have also studied *Om* for this model. We have plotted the trajectory in $Om-z$ plane as shown in Figs. 4.6 and 4.7 for different values of ζ_0 with fixed positive and negative values of λ, respectively. In Fig. 4.6, it is observed that for $0<\zeta_0\leq 0.46$, the $Om-z$ trajectory shows the negative slope, i.e., new HDE mimic like quintessence and for $\zeta_0>0.46$, we have observed the positive slope of *Om*, i.e., new HDE behaves as phantom. Similar trajectory can be observed in Fig. 4.7 for negative λ and $0<\zeta_0\leq 0.71$ and $\zeta_0>0.71$, respectively. In late time when $z\to -1$, *Om* tends to a constant value, i.e., zero curvature, which corresponds to ΛCDM.

Finally, the thermodynamics and the local entropy have been discussed for the model. It has been observed that the model preserves the validity of the second law of thermodynamics as ζ_0 remains positive through out the evolution of the Universe.

In conclusion, we can say that the constant bulk viscosity plays an important role in defining the DE. By addition of constant viscous term, one can observe that the Universe shows the transition from decelerated phase to accelerated phase. The viscous new HDE model is compatible with quintessence and Chaplygin gas like models for small and large values of ζ_0, but approaches to ΛCDM in late time. The model also discriminates with other model like Ricci dark energy and HDE with event horizon. Thus, the new HDE model suitably describes the DE concept in $f(R,T)$ in the presence of constant bulk viscosity.

Chapter 5

Thermodynamics of bulk viscous new holographic dark energy in $f(R,T)$ gravity

---

This chapter[1] *is the extension of the previous chapter for the most general form of bulk viscosity* $\zeta = \zeta_0 + \zeta_1 H$*, where* ζ_0 *and* ζ_1 *are constants, in* $f(R,T)$ *gravity. We obtain the scale factor and DP and classify all the possible scenarios (deceleration, acceleration and their transition) with different parameter regions chosen properly for positive and negative ranges of* λ*, and* ζ_0 *and* ζ_1 *to analyze the evolution of the Universe. We also graphically discuss the evolution of scale factor and obtained the transition from decelerated phase to accelerated phase. We investigate the statefinder pair* $\{r,s\}$ *and Om diagnostic for this viscous model to discriminate from other existing DE models. The model evolution behaviors are shown in the planes of* $r-s$*,* $r-q$ *and* $Om-z$*. The evolution of effective EoS parameter is also shown graphically. The entropy and generalized second law of thermodynamics are found to be valid for this model under some constraints on bulk viscous coefficient.*

---

[1]The work presented in this chapter comprises the results of a research paper entitled "Evolution and thermodynamics of bulk viscous new holographic dark energy in $f(R,T)$ gravity, Communicated in a journal, [arXiv:1804.05693 [gr-qc]], (2018)".

5.1 Introduction

In literature [130–148], a number of work has been done to explain the different phases of the Universe in the framework of the $f(R,T)$ theory. Modified gravity theories have rich dynamics. It is thus interesting to study reconstructing those modified gravity theories using the dynamics of HDE. Thus, here we study the new HDE model with variable bulk viscosity in the framework of the $f(R,T)$ theory to explain the different consequences of the expansion of the Universe.

In the previous work, we have studied new HDE with constant bulk viscosity in $f(R,T)$ gravity and have discussed the evolution of the Universe. In this chapter, a most general form of bulk viscous coefficient $\zeta = \zeta_0 + \zeta_1 H$, where ζ_0 and ζ_1 are constants, has been assumed to discuss the evolution of the Universe. The effect of time-dependent bulk viscous term in new HDE model within the context of $f(R,T)$ gravity, on the study of the evolution of the Universe is discussed in detail.

In this model, we discuss how the presence of viscous fluid could produce the late time acceleration. The viscous new HDE model gives time-dependent deceleration parameter which shows phase transition. We also frame table representation to explain all scenarios (deceleration or acceleration or phase transition) of the evolution of the Universe with respect to deceleration parameter by constraining the coefficient ζ_0. ζ_1 and coupling parameter λ. We also extend the work to discriminate the new HDE model with other existing DE models with the help of two independent geometrical diagnostics, namely statefinder pair and *Om*. The effective equation of state parameter, entropy and generalized second law of thermodynamics are also discussed.

5.2 Solution with variable bulk viscous new HDE model

We extend our study for the most general form of the bulk viscous coefficient in the framework of $f(R,T)$ gravity theory. We find the cosmological parameters, Hubble parameter, scale factor, DP in terms of cosmic time t and scale factor a and discuss the behavior in detail. We also discuss here the geometrical parameters and also discuss the thermodynamical validity of the model.

5.2.1 Field Equations

We consider that the contents of the Universe are bulk viscous new HDE fluid and dust dark matter. Using the predefined form of $f(R,T) = R + f(T)$ with $f(T) = \lambda T$, λ is a coupling parameter, the field equations (1.7.20) become as

$$R_{\mu\nu} - \frac{1}{2}R\, g_{\mu\nu} = T_{\mu\nu} - \lambda\, (T_{\mu\nu} + \ominus_{\mu\nu}) + \frac{1}{2}\lambda\, g_{\mu\nu}\, T, \tag{5.2.1}$$

Harko et al. [108], have suggested that the matter Lagrangian $\mathscr{L}_m$ is considered in such a way that $\mathscr{L}_m = -p$, where p stands as a thermodynamical pressure of matter of the universe. Then, Eq. (1.7.22) becomes as $\ominus_{\mu\nu} = -2T_{\mu\nu} - p\, g_{\mu\nu}$. Using this value into Eq. (5.2.1), we get

$$R_{\mu\nu} - \frac{1}{2}R\, g_{\mu\nu} = T_{\mu\nu} + \lambda\, (T_{\mu\nu} + p\, g_{\mu\nu}) + \frac{1}{2}\lambda T\, g_{\mu\nu}. \tag{5.2.2}$$

The stress-energy-momentum tensor in the presence of bulk viscous term is given by

$$T_{\mu\nu} = (\rho_m + \rho_d)u_\mu u_\nu + (g_{\mu\nu} + u_\mu u_\nu)\tilde{p_d}, \tag{5.2.3}$$

where, ρ_m, ρ_d and $\tilde{p_d}$ have their usual meanings and $\tilde{p_d} = p_d - 3\zeta H$.

Now, the field equations (5.2.2) for the spatially flat FRW metric (3.2.1) and the energy-momentum tensor (5.2.3) yield

$$3H^2 = \rho_m + \rho_d + \lambda\, (\rho_m + \rho_d + p_d - 3\zeta H) + \frac{1}{2}\lambda\, T, \tag{5.2.4}$$

$$2\dot{H} + 3H^2 = -p_d + 3\zeta H + \frac{1}{2}\lambda\, T, \tag{5.2.5}$$

where ζ is the bulk viscosity coefficient.

On considering the general form of bulk viscous coefficient as $\zeta = \zeta_0 + H\zeta_1$ in the field equations (5.2.4) and (5.2.5), we get the single evolution equation as

$$\dot{H} + \{1 + (1+2\lambda)(\alpha\omega_d - \zeta_1)\}\, X\, H^2 - (1+2\lambda)\zeta_0\, X\, H = 0, \tag{5.2.6}$$

where $X = [\frac{3(1+\lambda)}{2+3\lambda+3\beta(1+\lambda)(1+2\lambda)\omega_d}]$.

5.2.2 Evolution of the scale factor

On solving (5.2.6), we get

$$H=\frac{e^{(1+2\lambda)\,X\,\zeta_0 t}}{c_6+\frac{\{1+(1+2\lambda)(\alpha\omega_d-\zeta_1)\}}{(1+2\lambda)\zeta_0}\,e^{(1+2\lambda)\,X\,\zeta_0 t}}, \tag{5.2.7}$$

where c_6 is the constant of integration. Now, using $H=\dot{a}/a$, we can obtained the scale factor as

$$a=c_7\left[c_6+\frac{\{1+(1+2\lambda)(\alpha\omega_d-\zeta_1)\}}{(1+2\lambda)\zeta_0}e^{(1+2\lambda)\,X\,\zeta_0 t}\right]^{\frac{1}{X\,\{1+(1+2\lambda)(\alpha\omega_d-\zeta_1)\}}}, \tag{5.2.8}$$

where c_7 is another integration constant.

Eq. (5.2.7) can be written as

$$H(t)=H_0 e^{(1+2\lambda)\,X\,\zeta_0(t-t_0)}\left[1+\frac{\{1+(1+2\lambda)(\alpha\omega_d-\zeta_1)\}H_0}{(1+2\lambda)\zeta_0}\left(e^{(1+2\lambda)\,X\,\zeta_0(t-t_0)}-1\right)\right]^{-1}, \tag{5.2.9}$$

If we consider $a=a_0=1$ at $t=t_0$, then the scale factor (5.2.8) can be written as

$$a(t)=\left[1+\frac{\{1+(1+2\lambda)(\alpha\omega_d-\zeta_1)\}H_0}{(1+2\lambda)\zeta_0}\left(e^{(1+2\lambda)\zeta_0\,X\,(t-t_0)}-1\right)\right]^{\frac{1}{X\,\{1+(1+2\lambda)(\alpha\omega_d-\zeta_1)\}}}, \tag{5.2.10}$$

where $\lambda\neq-1/2$ and $\zeta_0\neq 0$. It is observed that the scale factor is of exponential form which can explain the phase transition. We can analyze the behavior of the scale factor in all possible combination of values of (ζ_0,ζ_1) and model parameter λ. Taking $a(t)=0$, we obtain the cosmic time when the Big-Bang happens

$$t(\text{at big-Bang})=t_0+\frac{1}{(1+2\lambda)\,X\,\zeta_0}\,\ln\left[1-\frac{(1+2\lambda)\zeta_0}{\{1+(1+2\lambda)(\alpha\omega_d-\zeta_1)\}H_0}\right] \tag{5.2.11}$$

In early time of evolution, the scale factor (5.2.10) can be approximated by

$$a\to\left[1+\frac{3H_0(1+\lambda)\{1+(1+2\lambda)(\alpha\omega_d-\zeta_1)\}}{2+3\lambda+3\beta(1+\lambda)(1+2\lambda)}(t-t_0)\right]^{\frac{1}{X\{1+(1+2\lambda)(\alpha\omega_d-\zeta_1)\}}}. \tag{5.2.12}$$

which shows that the decelerated expansion in early time. In late time of evolution, the scale factor behaves as

$$a(t)\to exp\left[(1+2\lambda)\zeta_0\,X\,(t-t_0)\right]. \tag{5.2.13}$$

which shows the de Sitter Universe, i.e., the Universe expands with accelerated rate in the late time of the evolution. This shows that the scale factor at the respective limits has an earlier decelerated phase followed by an accelerated phase in the later stage of the evolution.

Let us compute the second order derivatives of (5.2.10), which is given by

$$\begin{aligned}\frac{d^2a}{dt^2} &= H_0^2\Big(e^{2(1+2\lambda)\zeta_0 X (t-t_0)}\Big)\left[1+\frac{[(1+2\lambda)\zeta_0-\{1+(1+2\lambda)(\alpha\omega_d-\zeta_1)\}H_0]\,X}{H_0\,e^{(1+2\lambda)\zeta_0 X (t-t_0)}}\right]\\ &\times\left[1+\frac{\{1+(1+2\lambda)(\alpha\omega_d-\zeta_1)\}H_0}{(1+2\lambda)\zeta_0}\Big(e^{(1+2\lambda)\zeta_0 X (t-t_0)}-1\Big)\right]^{\frac{1}{X\{1+(1+2\lambda)(\alpha\omega_d-\zeta_1)\}}-2},\end{aligned} \tag{5.2.14}$$

Equating to zero the above equation to get the transition time t_{trans} between the decelerated to the accelerated expansion epochs, which is given by

$$t_{trans}=t_0+\frac{1}{X\,(1+2\lambda)\zeta_0}\ \ln\left\{\frac{X\,[\{1+(1+2\lambda)(\alpha\omega_d-\zeta_1)\}H_0-(1+2\lambda)\zeta_0]}{H_0}\right\}. \tag{5.2.15}$$

Using (5.2.10) into (5.2.9), the Hubble parameter in terms of the scale factor can be written as

$$\begin{aligned}H(a) &= \frac{(1+2\lambda)H_0}{[1+(1+2\lambda)(\alpha\omega_d-\zeta_1)]}\left[\frac{\zeta_0}{H_0}+\left\{\frac{[1+(1+2\lambda)(\alpha\omega_d-\zeta_1)]}{(1+2\lambda)}-\frac{\zeta_0}{H_0}\right\}\right.\\ &\left.\times\, a^{-X\{1+(1+2\lambda)(\alpha\omega_d-\zeta_1)\}}\right].\end{aligned} \tag{5.2.16}$$

Differentiating (5.2.16) with respect to a, we obtain

$$\begin{aligned}\frac{d\dot{a}}{da} &= \frac{(1+2\lambda)H_0}{[1+(1+2\lambda)(\alpha\omega_d-\zeta_1)]}\left[\frac{\zeta_0}{H_0}-\left(\frac{[1+(1+2\lambda)(\alpha\omega_d-\zeta_1)]}{(1+2\lambda)}-\frac{\zeta_0}{H_0}\right)\right.\\ &\left.\times\left(\frac{1+3(1+\lambda)(1+2\lambda)\{(\alpha-\beta)\omega_d-\zeta_1\}}{2+3\lambda+3\beta(1+\lambda)(1+2\lambda)\omega_d}\right)a^{-X\{1+(1+2\lambda)(\alpha\omega_d-\zeta_1)\}}\right].\end{aligned} \tag{5.2.17}$$

Equating (5.2.17) to zero, the transition between the decelerated to the accelerated

phase in terms of the scale factor can be written as

$$a_T = \left[\left\{\frac{1+3(1+\lambda)(1+2\lambda)[(\alpha-\beta)\omega_d-\zeta_1]}{(1+2\lambda)\{2+3\lambda+3\beta(1+\lambda)(1+2\lambda)\omega_d\}\zeta_0}\right\} \times\left\{[1+(1+2\lambda)(\alpha\omega_d-\zeta_1)]H_0-(1+2\lambda)\zeta_0\right\}\right]^{\frac{1}{X[1+(1+2\lambda)(\alpha\omega_d-\zeta_1)]}}. \quad (5.2.18)$$

and the corresponding transition redshift $z=a^{-1}-1$ is

$$z_T = \left[\left\{\frac{1+3(1+\lambda)(1+2\lambda)[(\alpha-\beta)\omega_d-\zeta_1]}{(1+2\lambda)\{2+3\lambda+3\beta(1+\lambda)(1+2\lambda)\omega_d\}\zeta_0}\right\} \times\left\{[1+(1+2\lambda)(\alpha\omega_d-\zeta_1)]H_0-(1+2\lambda)\zeta_0\right\}\right]^{-\frac{1}{X[1+(1+2\lambda)(\alpha\omega_d-\zeta_1)]}}-1. \quad (5.2.19)$$

Here, T stands for transition. From (5.2.18) and (5.2.19), we observe that the transi-

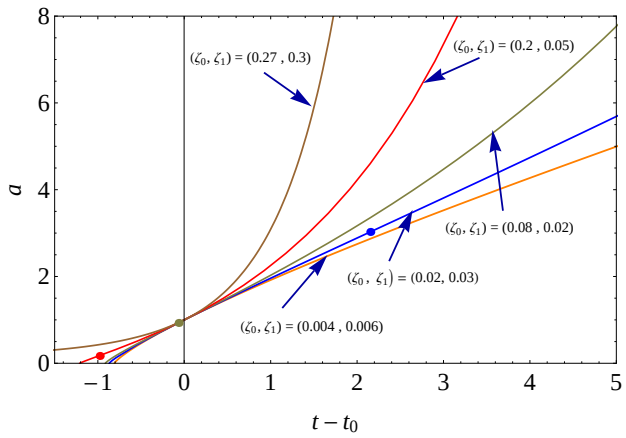

Figure 5.1: The evolution of *a versus* $(t-t_0)$ *for* $\zeta_0>0$ *and* $\zeta_1>0$ *taking* $\omega_d=-0.5$, $\lambda=0.06$, $\alpha=0.8502$ *and* $\beta=0.4817$.

tion from decelerated to accelerated epoch takes place at present time, i.e., at $a_T=1$ or $z_T=0$ for $(\zeta_0+H_0\zeta_1)=\frac{\{1+3(1+\lambda)(1+2\lambda)(\alpha-\beta)\omega_d\}H_0}{3(1+\lambda)(1+2\lambda)}$ depending on positive or negative value of λ. Especially, substituting the observational values of model parameters $\alpha=0.8502$ and $\beta=0.4817$ [74] along with $\omega_d=-0.5$, $H_0=1$, we get $\zeta_0+\zeta_1=0.096$ for positive value of $\lambda=0.06$ and $\zeta_0+\zeta_1=0.218$ for negative value of $\lambda=-0.06$, respectively. Thus, for the present time transition from deceleration to acceleration takes place at $\zeta_0+\zeta_1=0.096$ for positive values of $\lambda=0.06$ and for negative value of $\lambda=-0.06$, we get $\zeta_0+\zeta_1=0.218$. A plot of the evolution of the scale factor is given in Fig. 5.1 for different values of a combination of ζ_0 and ζ_1 and positive value of λ. For

$0 < (\zeta_0 + \zeta_1) < 0.096$, the scale factor has a decelerated phase followed by an accelerated phase in late time. For $(\zeta_0 + \zeta_1) = 0.096$, the transition takes place at present time and for $(\zeta_0 + \zeta_1) > 0.096$, the transition from decelerated phase to accelerated phase occurs at early time. For higher combination of (ζ_0, ζ_1), acceleration takes place in infinite past. Similar behavior can be observed for the negative value of λ. Fig. 5.1 plots the graph of the scale factor versus time for different combinations of (ζ_0, ζ_1). A dot on each trajectory denotes the present time transition from decelerated phase to accelerated phase.

5.2.3 Behavior of the deceleration parameter

Now, the evolutionary behavior of the Universe can also be discussed by the DP, which is defined by (1.9.5). Using (5.2.10), the DP can be obtained as

$$q(t) = \left\{ \frac{[\{1+(1+2\lambda)(\alpha\omega_d - \zeta_1)\}H_0 - (1+2\lambda)\zeta_0]\, X}{H_0} \right\} e^{-(1+2\lambda)\zeta_0 X\,(t-t_0)} - 1. \quad (5.2.20)$$

Equation (5.2.20) shows that the DP is time-dependent which may describe the phase transition. It can be observed that DP must change its sign at $t = t_0$. The sign of q is positive for $t < t_0$ and it is negative for $t > t_0$.

The DP in terms of a can be obtained as

$$q(a) = X\,[\{1+(1+2\lambda)(\alpha\omega_d - \zeta_1)\}H_0 - (1+2\lambda)\zeta_0] \times \left[\frac{[1+(1+2\lambda)(\alpha\omega_d - \zeta_1)]}{(1+2\lambda)\zeta_0 \left(a^{X\,[1+(1+2\lambda)(\alpha\omega_d - \zeta_1)]} - 1\right) + [1+(1+2\lambda)(\alpha\omega_d - \zeta_1)]H_0} \right] - 1. \quad (5.2.21)$$

In the terms of redshift, the DP is given by

$$q(z) = X\,[\{1+(1+2\lambda)(\alpha\omega_d - \zeta_1)\}H_0 - (1+2\lambda)\zeta_0] \times \left[\frac{[1+(1+2\lambda)(\alpha\omega_d - \zeta_1)]}{(1+2\lambda)\zeta_0 \left((1+z)^{-X\,[1+(1+2\lambda)(\alpha\omega_d - \zeta_1)]} - 1\right) + [1+(1+2\lambda)(\alpha\omega_d - \zeta_1)]H_0} \right] - 1. \quad (5.2.22)$$

The present value of q corresponds to $z = 0$ or $a = 1$ is,

$$q_0 = \frac{[\{1+(1+2\lambda)(\alpha\omega_d - \zeta_1)\}H_0 - (1+2\lambda)\zeta_0]\, X}{H_0} - 1. \quad (5.2.23)$$

Table 5.1: Variation of q for $\omega_d = -0.5$, $\alpha = 0.8502$, $\beta = 0.4817$

λ	Constraints on ζ_0 and ζ_1	q	Evolution of Universe
$\lambda \geq 1.272$	For all $\zeta_0 > 0$ and $\zeta_1 > 0$	Positive	Decelerated expansion
$0.24 \leq \lambda < 1.272$	For all $\zeta_0 > 0$ and $\zeta_1 > 0$	Negative	Accelerated expansion
$-0.5 < \lambda < 0.24$	$0 < (\zeta_0 + H_0\zeta_1) < \frac{\{1-0.55275(1+\lambda)(1+2\lambda)\}H_0}{3(1+\lambda)(1+2\lambda)}$	$+$ve to $-$ve	Trans. from dec. to acc.
	$(\zeta_0 + H_0\zeta_1) \geq \frac{\{1-0.55275(1+\lambda)(1+2\lambda)\}H_0}{3(1+\lambda)(1+2\lambda)}$	Negative	Accelerated expansion
$-0.69 \leq \lambda \leq -0.5$	For all $\zeta_0 > 0$ and $\zeta_1 > 0$	Positive	Decelerated expansion
$-1 \leq \lambda < -0.69$	For all $\zeta_0 > 0$ and $\zeta_1 > 0$	Negative	Accelerated expansion
$-1.73 \leq \lambda < -1$	$0 < (\zeta_0 + H_0\zeta_1) < \frac{\{1-0.55275(1+\lambda)(1+2\lambda)\}H_0}{3(1+\lambda)(1+2\lambda)}$	$-$ve to $+$ve	Trans. from acc. to dec.
	$(\zeta_0 + H_0\zeta_1) \geq \frac{\{1-0.55275(1+\lambda)(1+2\lambda)\}H_0}{3(1+\lambda)(1+2\lambda)}$	Positive	Decelerated expansion
$\lambda < -1.73$	For all $\zeta_0 > 0$ and $\zeta_1 > 0$	Positive	Decelerated expansion

Table 5.2: Variation of q for $\omega_d = -1$, $\alpha = 0.8502$, $\beta = 0.4817$

λ	Constraints on ζ_0 and ζ_1	q	Evolution of Universe
$\lambda \geq 0.265$	For all $\zeta_0 > 0$ and $\zeta_1 > 0$	Positive	Decelerated expansion
$-0.032 \leq \lambda < 0.265$	For all $\zeta_0 > 0$ and $\zeta_1 > 0$	Negative	Accelerated expansion
$-0.5 < \lambda < -0.032$	$0 < (\zeta_0 + H_0\zeta_1) < \frac{\{1-1.1055(1+\lambda)(1+2\lambda)\}H_0}{3(1+\lambda)(1+2\lambda)}$	$+$ve to $-$ve	Trans. from dec. to acc.
	$(\zeta_0 + H_0\zeta_1) \geq \frac{\{1-1.1055(1+\lambda)(1+2\lambda)\}H_0}{3(1+\lambda)(1+2\lambda)}$	Negative	Accelerated expansion
$-0.727 < \lambda \leq -0.5$	For all $\zeta_0 > 0$ and $\zeta_1 > 0$	Positive	Decelerated expansion
$-1 \leq \lambda \leq -0.727$	For all $\zeta_0 > 0$ and $\zeta_1 > 0$	Negative	Accelerated expansion
$-1.46 \leq \lambda < -1$	$0 < (\zeta_0 + H_0\zeta_1) < \frac{\{1-1.1055(1+\lambda)(1+2\lambda)\}H_0}{3(1+\lambda)(1+2\lambda)}$	$-$ve to $+$ve	Trans. from acc. to dec.
	$(\zeta_0 + H_0\zeta_1) \geq \frac{\{1-1.1055(1+\lambda)(1+2\lambda)\}H_0}{3(1+\lambda)(1+2\lambda)}$	Positive	Decelerated expansion
$\lambda < -1.46$	For all $\zeta_0 > 0$ and $\zeta_1 > 0$	Positive	Decelerated expansion

This equation shows that if $(\zeta_0 + H_0\zeta_1) = \frac{\{1+3(1+\lambda)(1+2\lambda)(\alpha-\beta)\omega_d\}H_0}{3(1+\lambda)(1+2\lambda)}$, the value of $q_0 = 0$. Thus, the transition into accelerating phase would occur at present time for this combination of (ζ_0, ζ_1). Especially, taking $\alpha = 0.8502$, $\beta = 0.4817$, $\omega_d = -0.5$, $H_0 = 1$ and $\lambda = 0.06$ in above expression, we get $\zeta_0 + \zeta_1 = 0.096$, which gives $q_0 = 0$.

Tables 5.1– 5.3 discuss the behavior of DP and corresponding evolution for different ranges of λ under constraints on $(\zeta_0 + H_0\zeta_1)$. We consider three different values of ω_d of three different phases, e.g., $\omega_d = -0.5,\ -1$ and -1.1414, respectively. We assume the observational values of the model parameters are $\alpha = 0.8502$ and $\beta = 0.4817$ [74].

Table 5.3: Variation of q for $\omega_d = -1.1414$, $\alpha = 0.8502$, $\beta = 0.4817$

λ	Constraints on ζ_0 and ζ_1	q	Evolution of Universe
$\lambda \geq 0.145$	For all $\zeta_0 > 0$ and $\zeta_1 > 0$	Positive	Decelerated expansion
$-0.072 \leq \lambda < 0.145$	For all $\zeta_0 > 0$ and $\zeta_1 > 0$	Negative	Accelerated expansion
$-0.5 < \lambda < -0.072$	$0 < (\zeta_0 + H_0\zeta_1) < \frac{\{1-1.26182(1+\lambda)(1+2\lambda)\}H_0}{3(1+\lambda)(1+2\lambda)}$	$+$ve to $-$ve	Trans. from dec. to acc.
	$(\zeta_0 + H_0\zeta_1) \geq \frac{\{1-1.26182(1+\lambda)(1+2\lambda)\}H_0}{3(1+\lambda)(1+2\lambda)}$	Negative	Accelerated expansion
$-0.735 \leq \lambda \leq -0.5$	For all $\zeta_0 > 0$ and $\zeta_1 > 0$	Positive	Decelerated expansion
$-1 \leq \lambda < -0.735$	For all $\zeta_0 > 0$ and $\zeta_1 > 0$	Negative	Accelerated expansion
$-1.42 \leq \lambda < -1$	$0 < (\zeta_0 + H_0\zeta_1) < \frac{\{1-1.26182(1+\lambda)(1+2\lambda)\}H_0}{3(1+\lambda)(1+2\lambda)}$	$-$ve to $+$ve	Trans. from acc. to dec.
	$(\zeta_0 + H_0\zeta_1) \geq \frac{\{1-1.26182(1+\lambda)(1+2\lambda)\}H_0}{3(1+\lambda)(1+2\lambda)}$	Positive	Decelerated expansion
$\lambda < -1.42$	For all $\zeta_0 > 0$ and $\zeta_1 > 0$	Positive	Decelerated expansion

In table 5.1, we analyse that for any positive value of ζ_0 and ζ_1, the model shows only the decelerated expansion of the Universe in the complete evolution for $\lambda \geq 1.272$, $-0.69 \leq \lambda \leq -0.5$ and $\lambda < -1.73$, and the model represents the Universe accelerate exponentially throughout the evolution for $0.24 \leq \lambda < 1.272$ and $-1 \leq \lambda < -0.69$. If we choose the small values of ζ_0 and ζ_1, i.e., $0 < (\zeta_0 + H_0\zeta_1) < \frac{\{1-0.55275(1+\lambda)(1+2\lambda)\}H_0}{3(1+\lambda)(1+2\lambda)}$, the phase transition occurs from $+ve$ to $-ve$ for $-0.5 < \lambda < 0.24$ and from $-ve$ to $+ve$ for $-1.73 \leq \lambda < -1$. As we go for the higher values of ζ_0 and ζ_1, i.e., $(\zeta_0 + H_0\zeta_1) \geq \frac{\{1-0.55275(1+\lambda)(1+2\lambda)\}H_0}{3(1+\lambda)(1+2\lambda)}$, the Universe accelerate exponentially throughout the evolution for $-0.5 < \lambda < 0.24$ and decelerate for the complete evolution for $-1.73 \leq \lambda < -1$.

In Table 5.2, the evolution of the Universe is analysed for $\omega_d = -1$. We analyse that for any positive value of ζ_0 and ζ_1, the model shows the expansion of the Universe with decelerated rate in the complete evolution for $\lambda \geq 0.265$, $-0.727 < \lambda \leq -0.5$ and $\lambda < -1.46$, and the model represents the expansion of the Universe with accelerated rate throughout the evolution for $-0.032 \leq \lambda < 0.265$ and $-1 \leq \lambda \leq -0.727$. If we go with the small values of ζ_0 and ζ_1, i.e., $0 < (\zeta_0 + H_0\zeta_1) < \frac{\{1-1.1055(1+\lambda)(1+2\lambda)\}H_0}{3(1+\lambda)(1+2\lambda)}$, it shows the phase transition of the Universe from $+ve$ to $-ve$ for $-0.5 < \lambda < -0.032$ and phase transition from $-ve$ to $+ve$ for $-1.46 \leq \lambda < -1$. If we go with the higher values of ζ_0 and ζ_1, i.e., $(\zeta_0 + H_0\zeta_1) \geq \frac{\{1-1.1055(1+\lambda)(1+2\lambda)\}H_0}{3(1+\lambda)(1+2\lambda)}$, it represents that the Universe always accelerate for $-0.5 < \lambda < -0.032$ and always decelerate for $-1.46 \leq \lambda < -1$.

In Table 5.3, the evolution of the Universe is discussed with $\omega_d < -1$, e.g., $\omega_d = -1.1414$. We analyse that for any positive value of ζ_0 and ζ_1, the model represents the decelerated expansion of the Universe throughout the evolution for $\lambda \geq 0.145$, $-0.735 \leq \lambda \leq -0.5$ and $\lambda < -1.42$, and the expansion of the Universe with accelerated rate in the complete evolution for $-0.072 \leq \lambda < 0.145$ and $-1 \leq \lambda < -0.735$. If we consider the small values of ζ_0 and ζ_1 , i.e., $0 < (\zeta_0 + H_0\zeta_1) < \frac{\{1-1.26182(1+\lambda)(1+2\lambda)\}H_0}{3(1+\lambda)(1+2\lambda)}$,

represents phase transition of the Universe from $+ve$ to $-ve$ for $-0.5 < \lambda < -0.072$ and phase transition from $-ve$ to $+ve$ for $-1.42 \leq \lambda < -1$. On considering the high values of ζ_0 and ζ_1, i.e., $(\zeta_0 + H_0\zeta_1) \geq \frac{\{1-1.26182(1+\lambda)(1+2\lambda)\}H_0}{3(1+\lambda)(1+2\lambda)}$, the Universe always accelerate for $-0.5 < \lambda < -0.072$ and always decelerate for $-1.42 \leq \lambda < -1$.

5.2.4 Statefinder diagnostic

Let us evaluate the statefinder parameters for the viscous new HDE model to discriminate our model with respect to existing DE models. In this general case, the statefinder parameters are calculated as

$$\begin{aligned} r &= 1+\left[\frac{3\,X\left\{1-\frac{X\,[(1+(1+2\lambda)(\alpha\omega_d-\zeta_1)]}{3}\right\}[(1+2\lambda)\zeta_0-\{(1+(1+2\lambda)(\alpha\omega_d-\zeta_1)\}H_0]}{H_0\;e^{(1+2\lambda)\zeta_0\,X\,(t-t_0)}}\right] \\ &+ \left[\frac{X^2[(1+2\lambda)\zeta_0-\{(1+(1+2\lambda)(\alpha\omega_d-\zeta_1)\}H_0]^2}{H_0^2\;e^{2(1+2\lambda)\zeta_0\,X\,(t-t_0)}}\right], \end{aligned} \tag{5.2.24}$$

and

$$\begin{aligned} s &= \left[\frac{2\,X\left\{1-\frac{X\,[(1+(1+2\lambda)(\alpha\omega_d-\zeta_1)]}{3}\right\}[(1+2\lambda)\zeta_0-\{(1+(1+2\lambda)(\alpha\omega_d-\zeta_1)\}H_0]}{3H_0\;\;e^{(1+2\lambda)\zeta_0\,X\,(t-t_0)}}\right. \\ &\left.+\;\frac{2X^2[(1+2\lambda)\zeta_0-\{(1+(1+2\lambda)(\alpha\omega_d-\zeta_1)\}H_0]^2}{9H_0^2\;\;e^{2(1+2\lambda)\zeta_0\,X\,(t-t_0)}}\right] \\ &\Big/\left[\frac{2\,X\,[\{(1+(1+2\lambda)(\alpha\omega_d-\zeta_1)\}H_0-(1+2\lambda)\zeta_0]}{3H_0\;\;e^{(1+2\lambda)\zeta_0\,X\,(t-t_0)}}-1\right], \end{aligned} \tag{5.2.25}$$

which are time-dependent due to the presence of bulk viscosity coefficient. Equations (5.2.24) and (5.2.25) show that in the limit $(t-t_0) \to \infty$, the statefinder parameters $\{r,s\} \to \{1,0\}$, a value corresponding to the ΛCDM model. Hence, the viscous new HDE model resembles the ΛCDM model in future. Now, we can plot the $r-s$ trajectory in $r-s$ plane and $r-q$ trajectory in $r-q$ plane to analyse viscous new HDE model in the framework of $f(R,T)$ theory. It can be observed that the values of $\{r,s\}$ depend on the choice of coupling parameter λ and the viscosity coefficients (ζ_0,ζ_1). We consider the observational values of model parameters $\alpha = 0.8502$, $\beta = 0.4817$ and $H_0 = 1$, $t_0 = 1$, $\omega_d = -0.5$ to plot these trajectories for positive and negative value of λ along with the different combinations of (ζ_0,ζ_1). The $r-s$ and $r-q$ trajectories for different

combinations of (ζ_0, ζ_1) and positive value of λ (e.g., $\lambda = 0.06$) are shown in Figs. 5.2 and 5.3, respectively. Figs. 5.4 and 5.5 show the respective $r-s$ and $r-q$ trajectories for different combinations of (ζ_0, ζ_1) and negative value of λ (e.g., $\lambda = -0.06$). The present value of the statefinder pair are

$$r_0 = 1 + \left[\frac{3\,X\left\{1 - \frac{X[(1+(1+2\lambda)(\alpha\omega_d - \zeta_1)]}{3}\right\}[(1+2\lambda)\zeta_0 - \{(1+(1+2\lambda)(\alpha\omega_d - \zeta_1)\}H_0]}{H_0}\right] + \left[\frac{X^2[(1+2\lambda)\zeta_0 - \{(1+(1+2\lambda)(\alpha\omega_d - \zeta_1)\}H_0]^2}{H_0^2}\right], \tag{5.2.26}$$

and

$$s_0 = \left[\frac{2\,X\left\{1 - \frac{X[(1+(1+2\lambda)(\alpha\omega_d - \zeta_1)]}{3}\right\}[(1+2\lambda)\zeta_0 - \{(1+(1+2\lambda)(\alpha\omega_d - \zeta_1)\}H_0]}{3H_0} + \frac{2X^2[(1+2\lambda)\zeta_0 - \{(1+(1+2\lambda)(\alpha\omega_d - \zeta_1)\}H_0]^2}{9H_0^2}\right] \Bigg/ \left[\frac{2\,X\,[\{(1+(1+2\lambda)(\alpha\omega_d - \zeta_1)\}H_0 - (1+2\lambda)\zeta_0]}{3H_0} - 1\right], \tag{5.2.27}$$

In Figs. 5.2 and 5.4, stars represent the fixed point values of ΛCDM and $SCDM$

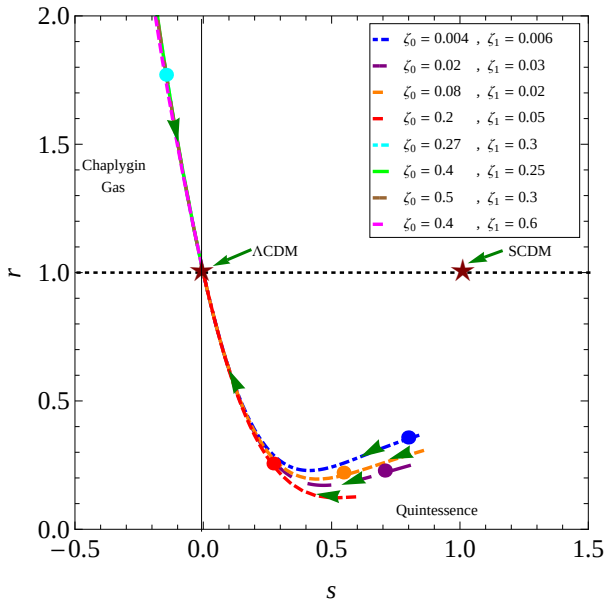

Figure 5.2: The $r-s$ trajectories are plotted in $r-s$ plane for $\zeta_0 > 0$ and $\zeta_1 > 0$ taking $\omega_d = -0.5$, $\alpha = 0.8502$, $\beta = 0.4817$ and $\lambda = 0.06$.

models, dots represent the present time values of $\{r,s\} = \{r_0, s_0\}$ and $\{r,q\} = \{r_0, q_0\}$, and the arrows represent the direction of the trajectories. The $r-s$ planes in Figs.

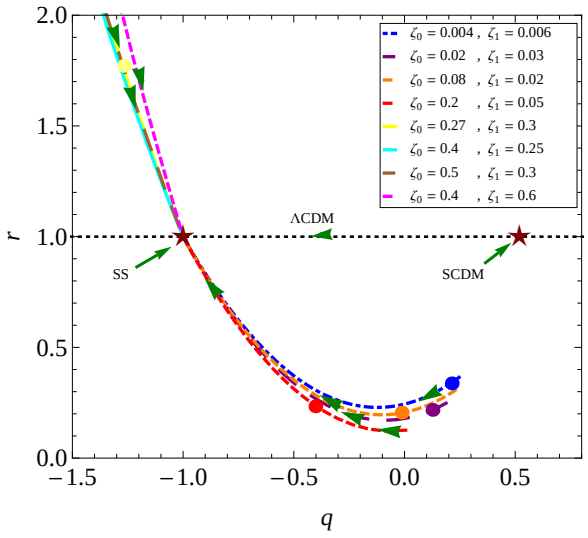

Figure 5.3: The $r-q$ trajectories are plotted in $r-q$ plane for $\zeta_0 > 0$ and $\zeta_1 > 0$ taking $\omega_d = -0.5$, $\alpha = 0.8502$, $\beta = 0.4817$ and $\lambda = 0.06$.

5.2 and 5.4 are divided into two regions $r < 1$, $s > 0$ and $r > 1$, $s < 0$ by a vertical line passing through the point (1,0). The trajectories in the $r-s$ planes lying in the region $r < 1$, $s > 0$, a feature similar to the Q model of DE [174, 175]. The trajectories in the $r-s$ planes lying in the region $r > 1$, $s < 0$, a feature similar to the CG model of DE [217]. Here, we obtain a parabolic trajectory for both cases on λ. From Fig. 5.2, for $\lambda = 0.06$ we notice that the model behaves like Q model for $0 < (\zeta_0 + \zeta_1) \leq 0.46$, whereas for $(\zeta_0 + \zeta_1) > 0.46$ the model mimic like CG model. The trajectories in both the regions converge to ΛCDM model in late time of evolution. In the case $\lambda = -0.06$, we observe from Fig. 5.4 that all the $r-s$ trajectories lie in the region $(r < 1, s > 0)$ for $0 < (\zeta_0 + \zeta_1) \leq 0.71$ which imply that the viscous new HDE model corresponds to Q model while the trajectories lie in $(r > 1, s < 0)$ region for $(\zeta_0 + \zeta_1) > 0.71$, i.e., the model behaves like CG model. In late time the viscous new HDE model approaches to ΛCDM. For some combinations like $(\zeta_0, \zeta_1) = (0.08, 0.02)$, the trajectory starts in the vicinity of the $SCDM$ model and approaches to ΛCDM. Thus, we can conclude that for any value of λ (either positive or negative), our viscous new HDE model in the framework of $f(R,T)$ theory mimic like Q and CG models for specific range of viscosity coefficients and in late time of evolution it always converges to ΛCDM model.

The $r-q$ trajectories in $r-q$ plane for positive and negative values of λ and for different combinations of (ζ_0, ζ_1) are shown in Figs 5.3 and 5.5, respectively. Here, in both the figures stars represent the fixed point values $\{r, q\} = \{1, 0.5\}$ for $SCDM$ model and $\{r, q\} = \{1, -1\}$ for Steady State (SS) model. In figures arrows are used to show the direction of the trajectories and the time evolution of the ΛCDM model

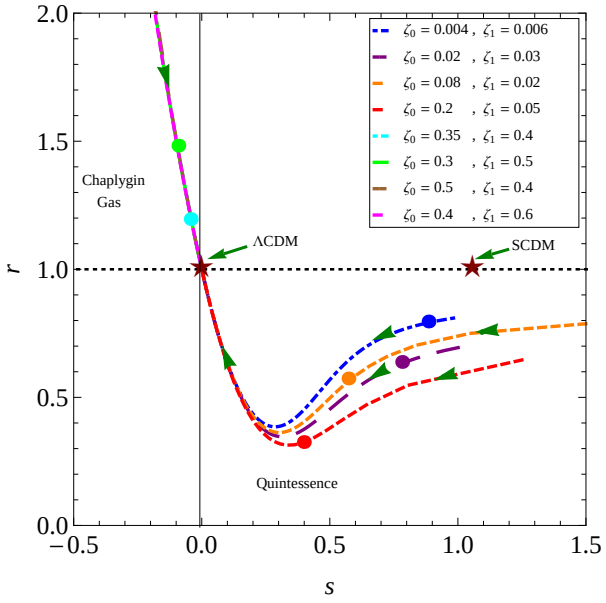

Figure 5.4: The $r-s$ trajectories are plotted in $r-s$ plane for $\zeta_0 > 0$ and $\zeta_1 > 0$ taking $\omega_d = -0.5$, $\alpha = 0.8502$, $\beta = 0.4817$ and $\lambda = -0.06$.

is represented by the horizontal line at $r = 1$. It can be observed that q changes its sign from positive to negative with respect to time in case of $\lambda = 0.06$ as well as for $\lambda = -0.06$, which show the Universe transits from decelerated to accelerated phase. For $(\zeta_0 + \zeta_1) > 0.46$ when $\lambda = 0.06$ and $(\zeta_0 + \zeta_1) > 0.71$ when $\lambda = -0.06$, q is always negative showing behavior of phantom. In the beginning this model behaves different from ΛCDM model but in late time it behaves the same as ΛCDM which converges to SS model in late time evolution. From Fig. 5.5, we analyse that for some small values of (ζ_0, ζ_1), like $(\zeta_0, \zeta_1) = (0.08, 0.02)$, the $r-q$ trajectory starts in the neighbourhood of the $SCDM$ model. The present position of $\{r,s\} = \{r_0, s_0\}$ and $\{r,q\} = \{r_0, q_0\}$ is indicated by dot in the plot. This means that the present viscous new HDE model is distinguishably different from the ΛCDM model but in late time it converges to SS model.

The present viscous new HDE model can also be discriminated from the holographic dark energy model with event horizon as the IR cut–off, in which the $r-s$ evolution starts from a region $r \sim 1$, $s \sim 2/3$ and ends on the ΛCDM point [232]. It can also be discriminated from Ricci dark energy model in which $r-s$ trajectory is a vertical segment, i.e., s is a constant during the evolution of the Universe [216].

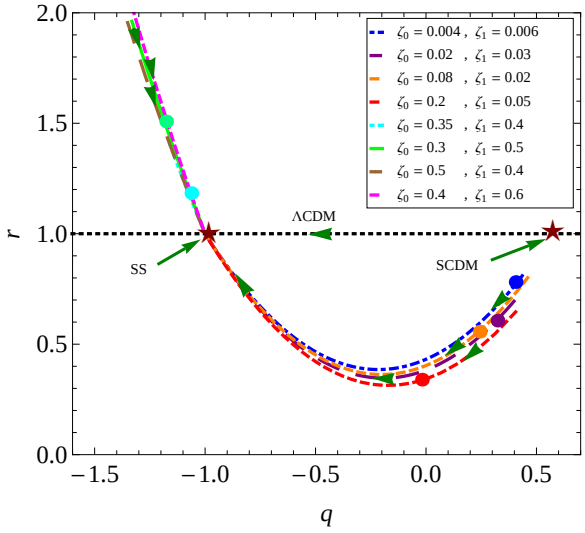

Figure 5.5: The $r-q$ trajectories are plotted in $r-q$ plane for $\zeta_0 > 0$ and $\zeta_1 > 0$ taking $\omega_d = -0.5$, $\alpha = 0.8502$, $\beta = 0.4817$ and $\lambda = -0.06$.

5.2.5 *Om* diagnostic

Further, we investigate the viscous new HDE behaviour with respect to *Om* diagnostic. This tool was proposed by Sahni et al. [176] in 2008. It is defined by Eq. 1.11.2 and for this viscous new HDE model the $Om(z)$ is obtained as

$$Om(z) = \frac{\frac{(1+2\lambda)^2}{[1+(1+2\lambda)(\alpha\omega_d-\zeta_1)]^2}\left[\frac{\zeta_0}{H_0}+\left\{\frac{[1+(1+2\lambda)(\alpha\omega_d-\zeta_1)]}{(1+2\lambda)}-\frac{\zeta_0}{H_0}\right\}(1+z)^{X[1+(1+2\lambda)(\alpha\omega_d-\zeta_1)]}\right]^2-1}{[(1+z)^3-1]}. \tag{5.2.28}$$

Now, we plot the $Om(z)-z$ trajectories to discuss it graphically. In Fig. 5.6, we plot the evolution of *Om(z)* against redshift z corresponding to different values of a combination of (ζ_0, ζ_1), $\alpha = 0.8502$, $\beta = 0.4817$, $\omega_d = -0.5$ $H_0 = 1$ and $\lambda = 0.06$. Similarly, in Fig. 5.7, we plot the evolution of *Om(z)* against redshift z corresponding to different values of a combination of (ζ_0, ζ_1), $\alpha = 0.8502$, $\beta = 0.4817$, $\omega_d = -0.5$ $H_0 = 1$ and $\lambda = -0.06$. The trajectory in Fig. 5.6 is divided horizontally into two regions. In lower region, it may be seen that *Om(z)* decreases as z decreases for $(\zeta_0+\zeta_1) > 0.46$, so positive slope of *Om(z)* suggests phantom $(\omega_d < -1)$ like behavior in the presence of viscosity with positive values of $\lambda = 0.06$. However, in upper region, *Om(z)* increases as z decreases for $0 < (\zeta_0+\zeta_1) \leq 0.46$, so negative slope of *Om(z)* indicating quintessence like behavior in the presence of viscosity.

Similarly, the trajectory in Fig. 5.7 is divided horizontally into two regions. In lower region, it may be seen that *Om(z)* decreases as z decreases for $(\zeta_0+\zeta_1) > 0.71$, so

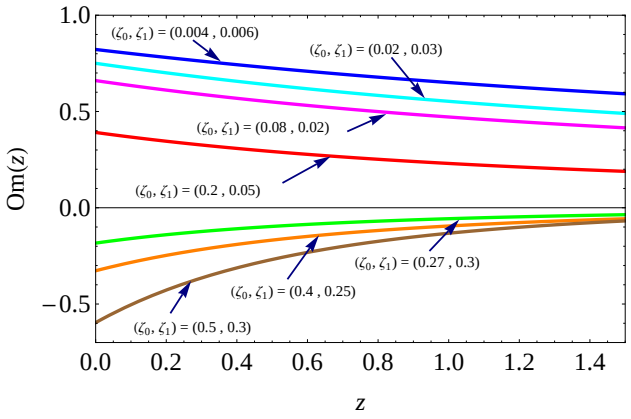

Figure 5.6: The *Om(z)* evolutionary diagram for $\zeta_0 > 0$ and $\zeta_1 > 0$ taking $\omega_d = -0.5$ and $\lambda = 0.06$ along with the observational value of $\alpha = 0.8502$ and $\beta = 0.4817$.

positive slope of *Om(z)* suggests phantom $(\omega_d < -1)$ like behavior in the presence of viscosity with positive values of $\lambda = -0.06$. However, in upper region, *Om(z)* increases as z decreases for $0 < (\zeta_0 + \zeta_1) \leq 0.71$, so negative slope of *Om(z)* indicating quintessence like behavior in the presence of viscosity. In the late time of evolution when $z = -1$, we get $Om(z) = 1 - \frac{(1+2\lambda)^2\zeta_0^2}{[1+(1+2\lambda)(\alpha\omega_d-\zeta_1)]^2H_0^2}$, which is the constant value of *Om(z)*, i.e., zero curvature. Thus, in late time the variable viscous new HDE corresponds to ΛCDM.

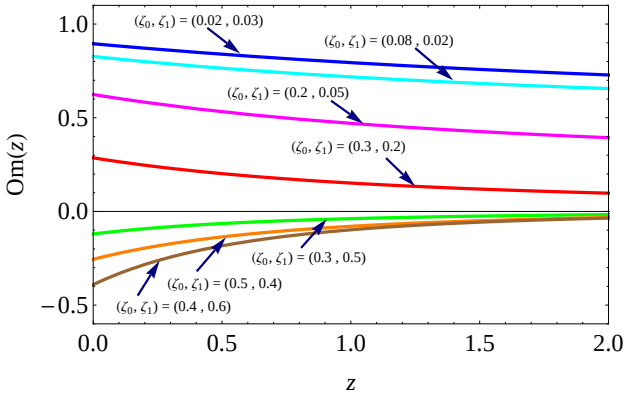

Figure 5.7: The *Om(z)* evolutionary diagram for $\zeta_0 > 0$ and $\zeta_1 > 0$ taking $\omega_d = -0.5$ and $\lambda = -0.06$ along with the observational value of $\alpha = 0.8502$ and $\beta = 0.4817$.

5.2.6 Effective Equation of state parameter

Let us discuss the bulk viscous effect on effective EoS parameter, ω_{eff} which is given by

$$\omega_{eff} = \frac{p_d - 3\zeta H}{\rho_m + \rho_d}, \tag{5.2.29}$$

where $p_m = 0$. On substituting the values of p_d, ζ, H, ρ_m and ρ_d in Eq. 5.2.29, we get

$$\omega_{eff} = \frac{(2+3\lambda)\left[\frac{\{(1+2\lambda)\,X\,\beta\omega_d - 1\}[(1+2\lambda)\zeta_0 - \{1+(1+2\lambda)(\alpha\omega_d - \zeta_1)\}H_0]}{e^{(1+2\lambda)\,X\,\zeta_0(t-t_0)}} - H_0\right]}{\left[\frac{\{(1+2\lambda)\,X\,\beta\omega_d - 1\}[(1+2\lambda)\zeta_0 - \{1+(1+2\lambda)(\alpha\omega_d - \zeta_1)\}H_0]\lambda}{e^{(1+2\lambda)\,X\,\zeta_0(t-t_0)}} + (2+3\lambda+\alpha\lambda+2\alpha\lambda^2)H_0\right]}. \tag{5.2.30}$$

The evolutions of ω_{eff} versus t are shown in Figs. 5.8 and 5.9 for different pairs of

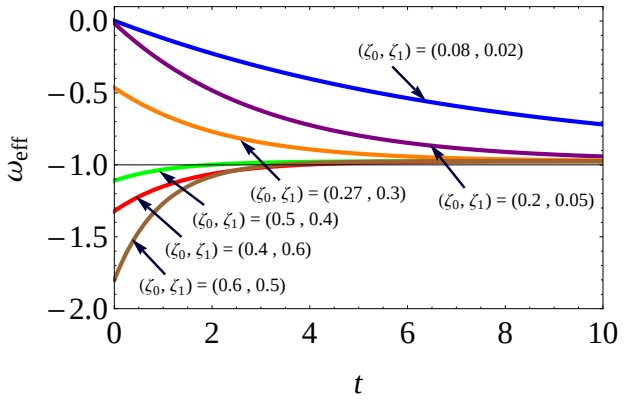

Figure 5.8: The evolution of ω_{eff} for different combinations of (ζ_0, ζ_1) in respect of $\lambda = 0.06$. We take $H_0 = 1$, $\omega_d = -0.5$, $\alpha = 0.8502$ and $\beta = 0.4817$.

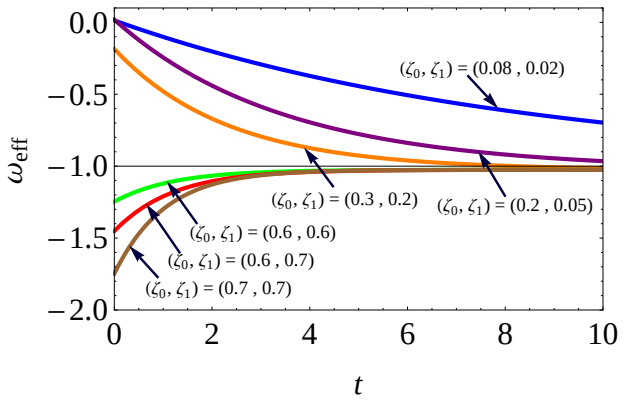

Figure 5.9: The evolution of ω_{eff} for different combinations of (ζ_0, ζ_1) in respect of $\lambda = -0.06$. We take $H_0 = 1$, $\omega_d = -0.5$, $\alpha = 0.8502$ and $\beta = 0.4817$.

(ζ_0, ζ_1) in respect of $\lambda = 0.06$ and $\lambda = -0.06$, respectively. Figure 5.8 shows that the trajectories of ω_{eff} start from $\omega_{eff} > -1$ (it may also start from matter-dominated era) for small values and $\omega_{eff} < -1$ for large values of (ζ_0, ζ_1) in respect of $\lambda = 0.06$. As $t \to \infty$, ω_{eff} approaches to a constant for all values of (ζ_0, ζ_1), i.e., $\omega_{eff} \to -0.9745$. There is no $\omega_{eff} = -1$ crossing for small values of (ζ_0, ζ_1) but for large values of (ζ_0, ζ_1) it will cross the $\omega_{eff} = -1$. In Fig. 5.9 where we have $\lambda = -0.06$, we can observe the similar evolution of ω_{eff}. However, $\omega_{eff} \to -1.0252$ in late times, i.e., it crosses $\omega_{eff} = -1$ for small values of (ζ_0, ζ_1) but it will not cross for large values of (ζ_0, ζ_1). Thus, the effective EoS parameter for both models shows consistency with the

observational data given in Ref. [233]. We can say that the dark energy phenomena may be obtained in the presence of viscous fluid.

5.2.7 Entropy and second law of thermodynamics

The local entropy production for a fluid on a flat FRW spacetime is expressed as [4]

$$\mathbb{T}\nabla_{\nu}s^{\nu} = \zeta(\nabla_{\nu}u^{\nu})^2 = 9H^2\zeta, \tag{5.2.31}$$

where $\mathbb{T}$ is the temperature, $\nabla_{\nu}s^{\nu}$ is the rate at which entropy is being generated in unit volume, and ζ is the total bulk viscosity.

The second law of thermodynamics can be stated as

$$\mathbb{T}\nabla_{\nu}s^{\nu} \geq 0. \tag{5.2.32}$$

Since the Hubble parameter H is positive in an expanding Universe, then ζ has to be positive in order to preserve the validity of the second law of thermodynamics. Thus, equation (5.2.32) implies that

$$\zeta \geq 0. \tag{5.2.33}$$

Thus, for the present model the inequality (5.2.33) can be written as

$$\zeta = \zeta_0 + \zeta_1 H \geq 0. \tag{5.2.34}$$

Using (5.2.16), we find the expression for the total bulk viscosity $\zeta(a)$ as

$$\begin{aligned}\zeta(a) &= \zeta_0 + \zeta_1\left[\frac{(1+2\lambda)H_0}{[1+(1+2\lambda)(\alpha\omega_d-\zeta_1)]}\left(\frac{\zeta_0}{H_0}+\left\{\frac{[1+(1+2\lambda)(\alpha\omega_d-\zeta_1)]}{(1+2\lambda)}-\frac{\zeta_0}{H_0}\right\}\right.\right.\\ &\left.\left.\times\ a^{-X\{1+(1+2\lambda)(\alpha\omega_d-\zeta_1)\}}\right)\right].\end{aligned} \tag{5.2.35}$$

The value of the scale factor, at which the transition of the total bulk viscosity from negative to positive values happen, is

$$a_{np} = \left[\frac{\{1+(1+2\lambda)\alpha\omega_d\}\zeta_0}{\{(1+2\lambda)(\zeta_0+\zeta_1H_0-\alpha\omega_d)-1\}\zeta_1}\right]^{-\frac{1}{X[1+(1+2\lambda)(\alpha\omega_d-\zeta_1)]}}, \tag{5.2.36}$$

where, the subscript “np” stands for “negative to positive” values. In late time of evo-

lution, i.e., at $a \to \infty$ the total bulk viscosity is $\zeta(a) = \frac{\{1+(1+2\lambda)\alpha\omega_d\}\zeta_0}{\{1+(1+2\lambda)(\alpha\omega_d-\zeta_1)\}}$.

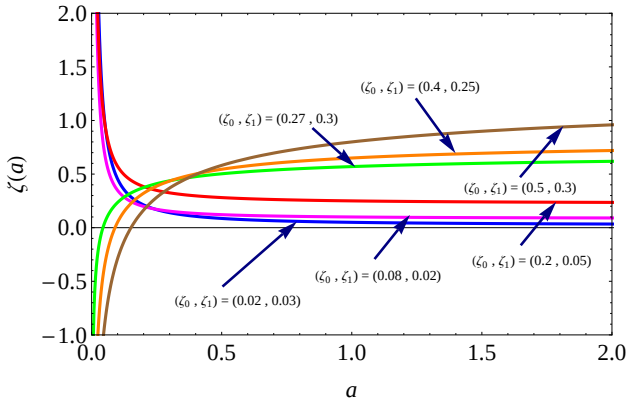

Figure 5.10: The evolution of $\zeta(a)$ for different combination of ζ_0 and ζ_1 with $\omega_d = -0.5$, $\lambda = 0.06$, $\alpha = 0.8502$ and $\beta = 0.4817$.

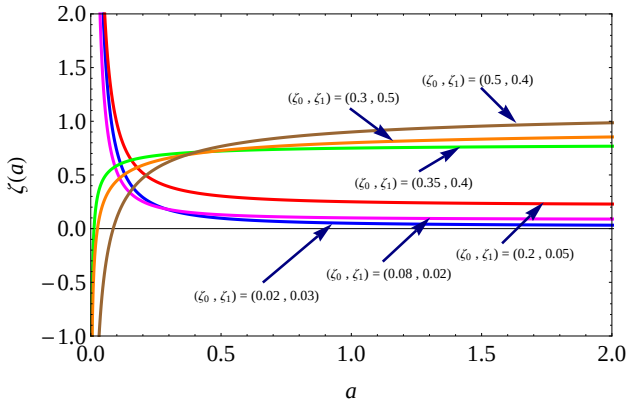

Figure 5.11: The evolution of $\zeta(a)$ for different combination of ζ_0 and ζ_1 with $\omega_d = -0.5$, $\lambda = -0.06$, $\alpha = 0.8502$ and $\beta = 0.4817$.

Figures 5.10 and 5.11 represent the evolution of the total bulk viscous coefficient ζ with respect to the scale factor for the different combinations of the (ζ_0, ζ_1) with positive ($\lambda = 0.06$) and negative ($\lambda = -0.06$) values of the coupling parameter, respectively. The Figs. 5.10 and 5.11 show that the total bulk viscosity is positive throughout the evolution of the Universe for $0 < (\zeta_0 + \zeta_1) \leq 0.46$ with $\lambda = 0.06$, and $0 < (\zeta_0 + \zeta_1) \leq 0.71$ with $\lambda = -0.06$, respectively. These curves have been shown above the line (0,0). Therefore, the model does not violate the entropy law for these ranges. The figures also show that the total bulk viscous coefficient is evolving from negative to positive value for $(\zeta_0 + \zeta_1) \geq 0.46$ and $(\zeta_0 + \zeta_1) \geq 0.71$, respectively. Thus, the rate of entropy production is negative for large values of $(\zeta_0 + \zeta_1)$ in early epoch and positive in the later epoch. Hence the entropy law violates in the early epoch and obeys in the later epoch for these values of $(\zeta_0 + \zeta_1)$.

In an absolute way the status of the second law of thermodynamics should be considered along with the accounting of the entropy generation from the horizon. In those circumstances, the second law becomes the generalised second law (GSL) of thermodynamics, according to which the total sum of the entropies of the fluid components of the Universe plus that of the horizon entropy should never decrease [234, 235]. In the present model this means the rate of change of complete entropy along with horizon must be greater than or equal to 0. Mathew et al. [235] have discussed the status of GSL for flat FRW Universe with matter and cosmological vacuum. Karami et al. [236] have discussed the status of GSL in a flat Universe with viscous dark energy and have shown that the GSL is valid in FRW Universe with apparent horizon as the boundary. Many authors [172, 237] have verified the status of GSL with apparent horizon as the boundary. The status of GSL in the modified gravity theories have also been discussed by many authors [132, 238–240] with the apparent horizon as the boundary.

Let us verify the GSL of thermodynamics for this model. As stated above we consider the apparent horizon as the boundary of the Universe. Then, the GSL can be stated as

$$\frac{d}{dt}(S_{tot}) = \frac{d}{dt}(S_m + S_d + S_p + \tilde{S_h}) \geq 0, \tag{5.2.37}$$

where S_m, S_d, S_p and $\tilde{S_h}$ are the entropies of the dark matter, dark energy, the entropy production and the entropy of the apparent horizon, respectively.

From the first law of thermodynamics the change of entropy of the viscous matter inside the apparent horizon can be obtained using Gibbs equation

$$\mathbb{T}_i dS_i = d(\rho_i V) + p_i dV, \tag{5.2.38}$$

where $\mathbb{T}_i$ is the temperature and $S_i = S_m + S_d$, is the sum of the entropies of the dark matter and dark energy, ρ_i represents the sum of the densities of the dark matter and dark energy, $V = \frac{4\pi \tilde{r_h}^3}{3}$ is the volume of the apparent horizon with $\tilde{r_h}$ as a radius of the apparent horizon and $p_i = \tilde{p_d} = p_d - 3\zeta H$ as the effective pressure.

In the present viscous model the above Gibbs equation modifies to [132, 239, 240]

$$\mathbb{T}_i dS_i = d(\rho_i V) + p_i dV - T_i dS_p. \tag{5.2.39}$$

The radius $\tilde{r_h}$ of the apparent horizon for a flat FRW Universe, is defined as [240]

$$\tilde{r_h} = \frac{1}{H}. \tag{5.2.40}$$

In the $f(R,T)$ theories the entropy associated with the apparent horizon is defined as

$$\tilde{S_h} = \frac{\tilde{A_h}}{4}\frac{f_R(R,T)}{\left(\frac{1}{8\pi}+\frac{f_T(R,T)}{8\pi}\right)} = \frac{2\pi\tilde{A_h}}{(1+\lambda)} = \frac{8\pi^2\tilde{r_h}^2}{(1+\lambda)}, \tag{5.2.41}$$

where $\tilde{A_h} = 4\pi\tilde{r_h}^2$ is the area of the apparent horizon. Here, we have taken $8\pi G = 1$. Taking the derivative of Eq. (5.2.41) with respect to time t, we get

$$\dot{\tilde{S}}_h = \frac{16\pi^2\tilde{r_h}\dot{\tilde{r}}_h}{(1+\lambda)} = \frac{16\pi^2}{(1+\lambda)H}\left(-\frac{\dot{H}}{H^2}\right). \tag{5.2.42}$$

Now, from (5.2.39) we have

$$\mathbb{T}_i(\dot{S}_m+\dot{S}_d+\dot{S}_p) = 4\pi\tilde{r_h}^2(\dot{\tilde{r}}_h-1)\{\rho_m+(1+\omega_d)\rho_d-3\zeta_0 H-3\zeta_1 H^2\}. \tag{5.2.43}$$

Under the thermal equilibrium conditions between the fluids and the horizon, we have $\mathbb{T}_i = \tilde{\mathbb{T}}_h$. We take the temperature $\tilde{\mathbb{T}}_h = \frac{H}{2\pi}$, which is equal to the Hawking temperature of the horizon with the assumption that the fluid within the horizon is in equilibrium with the horizon, so there is no effective flow of the fluid toward the horizon [241]. Now, Eq. (5.2.43) become as

$$\dot{S}_m+\dot{S}_d+\dot{S}_p = \frac{8\pi^2}{H^3}\left(-\frac{\dot{H}}{H^2}-1\right)\{\rho_m+(1+\omega_d)\rho_d-3\zeta_0 H-3\zeta_1 H^2\}. \tag{5.2.44}$$

Now, using the definition of DP $q = \left(-\frac{\dot{H}}{H^2}-1\right)$ and Eqs. (5.2.42) and (5.2.44) into (5.2.37), we get the change of the sum of all the entropies as

$$\begin{aligned}\dot{S}_{tot} &= \dot{S}_m+\dot{S}_d+\dot{S}_p+\dot{\tilde{S}}_h \\ &= \frac{8\pi^2 q}{H^3}\{\rho_m+(1+\omega_d)\rho_d-3\zeta_0 H-3\zeta_1 H^2\}+\frac{16\pi^2(q+1)}{(1+\lambda)H}.\end{aligned} \tag{5.2.45}$$

On substituting the required values in above equation and simplifying, we get the

change in total entropy as

$$\dot{S}_{tot} = \left[\frac{16\pi^2[\{1+(1+2\lambda)(\alpha\omega_d-\zeta_1)\}H_0-(1+2\lambda)\zeta_0]\left\{1+\frac{\{1+(1+2\lambda)(\alpha\omega_d-\zeta_1)\}H_0\left(e^{(1+2\lambda)\,X\,\zeta_0(t-t_0)}-1\right)}{(1+2\lambda)\zeta_0}\right\}}{H_0^2 e^{2(1+2\lambda)\zeta_0\,X\,(t-t_0)}}\right]$$
$$\times\left[\frac{X}{(1+\lambda)}+\frac{3\{1-(1+2\lambda)\,X\,\beta\omega_d\}}{(2+3\lambda)H_0}\left\{\frac{[\{1+(1+2\lambda)(\alpha\omega_d-\zeta_1)\}H_0-(1+2\lambda)\zeta_0]\,X}{e^{(1+2\lambda)X\,\zeta_0(t-t_0)}}-H_0\right\}\right]. \quad (5.2.46)$$

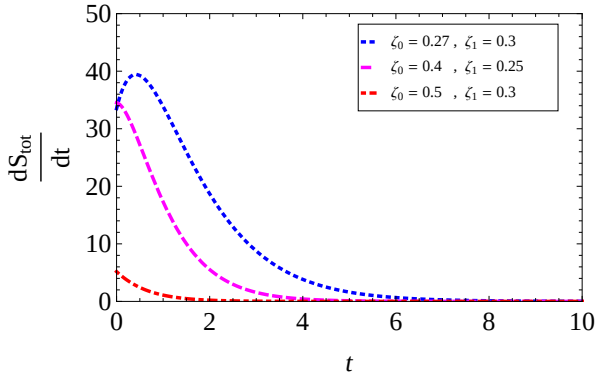

Figure 5.12: The change in total entropy *versus t for various combination of* ζ_0 *and* ζ_1 *with* $\omega_d = -0.5$, $\lambda = 0.06$, $\alpha = 0.8502$ *and* $\beta = 0.4817$.

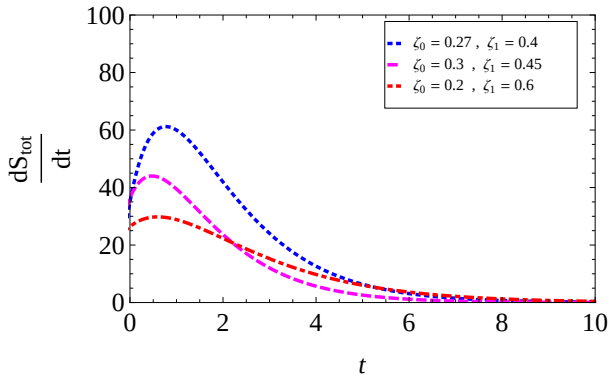

Figure 5.13: The change in total entropy *versus t for various combination of* ζ_0 *and* ζ_1 *with* $\omega_d = -0.5$, $\lambda = -0.06$, $\alpha = 0.8502$ *and* $\beta = 0.4817$.

From Eq. (5.2.46), it is noticed that the rate of change of entropy can not clearly state either the change in entropy is greater than and equal to zero. We plot the evolution of $\dot{S}$ in Figs. 5.12 and 5.13, respectively for positive and negative values of the λ (e.g., $\lambda = 0.06$, $\lambda = -0.06$) taking $\alpha = 0.8502$, $\beta = 0.4817$, $\omega_d = -0.5$, $H_0 = 1$ and $t_0 = 1$ for different values of viscosity coefficients (ζ_0, ζ_1). Figure 5.12 shows that the GSL is always valid for $\zeta_0 > 0$ and $0.27 \leq \zeta_1 \leq 0.85$ whereas it holds for $\zeta_0 > 0$ and $0.39 \leq \zeta_1 \leq 1$ in Fig. 5.12. We also notice that in both the cases, the total entropy corresponds to

zero in late time of the evolution.

5.3 Conclusion

In this Chapter, we have explored the new HDE model in modified $f(R,T)$ gravity with bulk viscosity of the form $\zeta = \zeta_0 + \zeta_1 H$. We have considered that the Universe is filled with the pressureless DM and the new HDE proposed by Granda and Oliveros [73]. We have analyzed the different possible phases of the Universe according to the bulk viscous parameters ζ_0 and ζ_1.

The field equations of viscous new HDE model in modified $f(R,T)$ gravity have been solved for a most general bulk viscous coefficient. The scale factor has been obtained in the form of exponential which describes the phase transition of the Universe. We have analyzed the behavior of the scale factor for all possible combination of (ζ_0, ζ_1) and model parameter λ. We have obtained that the scale factor at the respective limits has an earlier decelerated phase followed by an accelerated phase in the later stage of the evolution. We have calculated the transition time between decelerated to accelerated epoch. We have expressed Hubble parameter in terms of scale factor to get the transition between decelerated to accelerated epoch in terms of scale factor a_T and redshift z_T. A plot of the evolution of the scale factor is given in Fig. 5.1 for difference values of a combination of ζ_0 and ζ_1 and positive value of λ. Similar behavior can be observed for the negative value of λ. We have also studied the evolution of the DP q. We have obtained time-dependent DP. As $(t-t_0) \to \infty$, we get $q \to -1$, which shows that the model accelerates in late time. We have discussed the behavior of q and corresponding evolution for different ranges of coupling parameter λ and constraints on $(\zeta_0 + H_0\zeta_1)$. The results are summarized in tables 5.1– 5.3 for $\omega_d = -0.5$, $\omega_d = -1$ and $\omega_d = -1.1414$, and model parameters $\alpha = 0.8502$, $\beta = 0.4817$. The tables show that the deceleration or acceleration or their transition depend on the values of ζ_0, ζ_1 and λ.

We have discussed two geometrical diagnostics, namely statefinder and *Om* to observe the discrimination with the other existing DE models. We have obtained the time-dependent value of the statefinder parameter for viscous new HDE model. In the late time as $(t-t_0) \to \infty$, the statefinder pair $\{r,s\}$ for the viscous new HDE model tends to $\{1,0\}$, a value corresponding to ΛCDM model. We have plotted the trajectory of statefinder pair $\{r,s\}$ in $r-s$ plane for different combinations of (ζ_0, ζ_1) as shown

in Fig. 5.2 and Fig. 5.4 for positive and negative values of coupling parameter λ, respectively. It has been observed that for any value of λ (either positive or negative), our viscous new HDE model in the framework of $f(R,T)$ theory mimics like Q and CG models for specific range of viscosity coefficients and in late time of evolution it always converges to ΛCDM model.

We have also plotted the trajectory of $\{r,q\}$ for different combinations of (ζ_0,ζ_1) and positive and negative values of λ as shown in Fig. 5.3 and Fig. 5.5. It can be observed that q changes its sign from positive to negative with respect to time in both the cases $\lambda = 0.06$ and $\lambda = -0.06$, which show the phase transition from decelerated phase to accelerated phase. For $(\zeta_0+\zeta_1) > 0.46$ when $\lambda = 0.06$ and $(\zeta_0+\zeta_1) > 0.71$ when $\lambda = -0.06$, q is always negative showing behavior of phantom. Thus, in the beginning this model behaves different from ΛCDM model but in late time it behaves the same as ΛCDM which converges to SS model in late time evolution. The present viscous new HDE model can also be discriminated from the HDE model with event horizon as the IR cut–off, in which the $r-s$ evolution starts from a region $r \sim 1$, $s \sim 2/3$ and ends on the ΛCDM point [232]. It can also be discriminated from Ricci dark energy model in which $r-s$ trajectory is a vertical segment, i.e., s is a constant during the evolution of the Universe [216].

The second geometrical diagnostic, namely *Om* has been carried out in section 5.2.5 . We have plotted the *Om(z)*$-z$ trajectories for different combinations of (ζ_0,ζ_1) in respect of positive and negative values of λ as shown in Fig. 5.6 and Fig. 5.7, respectively. We have observed two types of trajectory, one has the positive curvature which suggests the phantom like behavior and second has the negative curvature which suggests the quintessence like behavior.

We have calculated the effective EoS parameter for this model and analyzed the evolution of it graphically for different suitable values of viscosity coefficients. We have observed that $\omega_{eff} \to -0.9745$ and -1.0252, respectively as $t \to \infty$ in case positive and negative values of λ which is very close to -0.93 predicted in the Ref. [242].

At the end, we have discussed the entropy and second law of thermodynamics for viscous new HDE model. Figures 5.10 and 5.11 plot the evolution of the total bulk viscous coefficient. It has been observed that the total bulk viscosity is positive throughout the evolution of the Universe for $0 < (\zeta_0+\zeta_1) \leq 0.46$ with $\lambda = 0.06$, and $0 < (\zeta_0+\zeta_1) \leq 0.71$ with $\lambda = -0.06$, respectively. Therefore, the model does not violate the entropy law for these ranges. The figures also show that $\zeta(a)$ is evolving from

negative to positive value for $(\zeta_0+\zeta_1)>0.46$ and $(\zeta_0+\zeta_1)>0.71$, respectively. Thus, the rate of entropy production is negative for large values of $(\zeta_0+\zeta_1)$ in early epoch and positive in the later epoch. Hence the entropy law violates in the early epoch and obeys in the later epoch for these values of $(\zeta_0+\zeta_1)$. We have also studied the generalized second law of thermodynamics. It has been observed that it is always valid for $\zeta_0>0$ and $0.27\leq\zeta_1\leq0.85$ when λ is positive whereas it holds for $\zeta_0>0$ and $0.39\leq\zeta_1\leq1$ when λ is negative which are shown in Figs. 5.12 and 5.13, respectively. We have also noticed that in both the cases, the total entropy corresponds to zero in late time of the evolution.

Let us Summarize the results with the outcome of this work. In cosmology, the idea of viscous dark energy models has been presented in different ways to understand the evolution of the Universe. The notion of bulk viscosity has also been extensively studied in modified theories. This paper has explored the behavior of viscosity by considering dust matter and new HDE in the background of modified $f(R,T)$ gravity. The above investigations show that this model predicts an early deceleration followed by late time acceleration. We can conclude that the dark energy era may be obtained in the presence of bulk viscous fluid.

Chapter 6

Scalar field cosmology in Bianch I anisotropic model

In this chapter[1], we study scalar field cosmology in a spatially homogeneous and anisotropic cosmological model within the framework of Einstein gravitational theory. We consider non-interacting scalar field and perfect fluid as the source of matter components. We obtain the exact solution of the field equations under the assumption on relation between average scale factor and scalar field potential as $a = a_0\, e^{l_2\phi(t)}$, where a_0 represents the present average scale factor and l_2 is an arbitrary positive constant. We consider the solution for two cases: flat potential, i.e., $V(\phi) = 0$ and exponential potential, i.e., $V(\phi) = V_0\, e^{-m_2\phi}$, where V_0 and m_2 are non-negative constants. We obtain that the zero-rest-mass model expands with decelerated rate and behaves like a stiff matter. In case of exponential potential function, the model expands with decelerated, accelerated or shows the transition depending on the parameters. The isotropization is observed at late-time evolution of the Universe in exponential potential model.

---

[1]The work presented in this chapter comprises the results of a research paper "Minimally coupled Scalar field cosmology in anisotropic cosmological model, *Pramana Journal of Physics* **88**, 22 (2017)".

6.1 Introduction

It is assumed that the Universe is filled with a perfect fluid. But the observations suggest that the cosmological dynamics can not be fully explained by this standard matter. The observational results lead to the search of some kinds of exotic matter which would generate sufficient negative pressure to drive the late time cosmic acceleration. One of such exotic matter is the scalar field which provides the necessary negative pressure causing acceleration [32, 43]. Thus, the cosmological models with scalar field play a vital role in the current modern cosmology to explain the early inflation and the late time acceleration. The recent discovery of cosmic acceleration [6, 16, 17, 19, 243] has stimulated the interest to study the cosmological models based on scalar fields. The cosmological models based on scalar fields have been discussed by many authors for explaining the possible early inflationary scenarios [11] as well as for describing the dark energy [63].

The dynamics of the evolution of the Universe is often realized by scalar field with a proper scalar potential. The self-interacting potential can act like an effective cosmological constant which drives a period of inflation. It depends on the specific form of the potential as a function of scalar field. Many authors [40, 41, 244–252] have studied the scalar field cosmology in FRW model with different forms of scalar potential like flat, constant and exponential potentials.

The simplest field having the property to provide an accelerated expansion at late time, is a canonical scalar field with a scalar potential. It is well known that the evolution of the Universe admits a scenario of anisotropic expansion and gains a lot of interest, under the light of the recently announced Planck Probe results [19]. The Bianchi models, which describe homogeneous but anisotropic space times, have been discussed to explain the significance of anisotropy in the cosmic microwave background (CMB) and large scale structures (LSS) [242, 253, 254]. Therefore, motivated by the anomalies found in the CMB anisotropies [255], which violate the statistical isotropy [256], and on the increasing interest on Bianchi cosmologies [7, 257], we are interested to investigate the dynamics of a perfect fluid anisotropic Bianchi-I (B-I) cosmological model with a scalar field minimally coupled with gravity. Demianski et al. [258] have studied the dynamics of anisotropic model filled with scalar field minimally coupled to gravity. Saha and Boyadjiev [259] have considered a self-consistent system of interacting spinor and scalar fields within the framework of a B-I cosmolog-

ical model filled with perfect fluid. Do et al. [260] have studied anisotropic power-law inflation for a two scalar fields model. Sharif and Zubair [145] have studied the behavior of perfect fluid and massless scalar field for homogeneous and anisotropic B-I Universe model in $f(R,T)$ gravity.

The exact solutions of the field equations play a very important role in cosmology, because these allow us to analyze the qualitative and quantitative behavior of the Universe as a whole. The number of exact solutions based on scalar field with various form of scalar potential are limited. It has been observed that in a cosmological model the scalar potential has very important role as it radically affects the cosmological behavior.

Therefore, in the present chapter, our motivation is to find the exact cosmological solutions for a totally homogeneous and anisotropic perfect fluid B-I model with scalar field for various forms of scalar potential. We calculate the various observable cosmological parameters like expansion scalar, DP, anisotropy parameter, shear scalar, EoS parameters of scalar field and perfect fluid matter, and the isotropization measure to analysis the dynamics of the evolution of the Universe. We observe that the perfect fluid anisotropic models behave like an isotropic one with the inclusion of exotic matter like scalar field at late time of evolution. Fadragas et al. [261] have performed an analysis of anisotropic locally-rotationally-symmetric Bianchi models with scalar field for a wide range of potentials. We extend this work for a totally anisotropic and homogeneous B-I model by assuming two different forms of scalar potential.

6.2 Field equations

We consider the B-I cosmological model (1.3.8), which is spatially homogeneous and anisotropic. Let us consider that the Universe is filled with ordinary matter as a perfect fluid (1.4.4) and a scalar field (ϕ) with potential ($V(\phi)$) minimally coupled with gravity (1.7.6).

The Einstein field equations (1.7.5) yield the following equations

$$\frac{\ddot{B}}{B}+\frac{\ddot{C}}{C}+\frac{\dot{B}\dot{C}}{BC}=-\left(p_m+p_\phi\right), \tag{6.2.1}$$

$$\frac{\ddot{A}}{A}+\frac{\ddot{C}}{C}+\frac{\dot{A}\dot{C}}{AC}=-\left(p_m+p_\phi\right), \tag{6.2.2}$$

$$\frac{\ddot{A}}{A}+\frac{\ddot{B}}{B}+\frac{\dot{A}\dot{B}}{AB}=-\left(p_m+p_\phi\right), \tag{6.2.3}$$

$$\frac{\dot{A}\dot{B}}{AB}+\frac{\dot{B}\dot{C}}{BC}+\frac{\dot{C}\dot{A}}{CA}=\left(\rho_m+\rho_\phi\right), \tag{6.2.4}$$

where A, B, C, ρ_m, p_m and an overdot have there usual meanings and $\omega_m = p_m/\rho_m$ is the EoS parameter of DM. Here, ρ_ϕ and p_ϕ are respectively the energy density and pressure for the canonical scalar field. The EoS parameter ω_ϕ is represented by $\omega_\phi = \frac{\dot{\phi}^2-2V(\phi)}{\dot{\phi}^2+2V(\phi)}$.

The quintessence cosmological model accommodates a late time cosmic acceleration in the case of $\omega_\phi < -1/3$ which implies that $\dot{\phi}^2 < V(\phi)$. On the other hand, if the kinetic term of the scalar field is negligible with respect to the potential energy, i.e., $\dot{\phi}^2 \ll 2V(\phi)$ then the EoS is $\omega_\phi = -1$. It is important to notice that the usual relation $T^{ij}_{;j} = 0$, establishing the conservation laws satisfied by the matter fields, hold true. In this model the conservation equation for a perfect fluid and the corresponding evolution equation of the scalar field (1.7.7) is represented by (1.7.9) and (1.7.10), respectively.

For an anisotropic model, the average scale factor can be defined as [262, 263]

$$a(t) = (ABC)^{1/3}. \tag{6.2.5}$$

Using the definitions of Hubble parameter (H), DP (q) and shear scalar (σ^2) from Eqs. (1.10.2)–(1.10.6), (2.2.28), (6.2.5), the field Eqs. (6.2.1)–(6.2.4) can be rewritten in terms of H, q and σ^2 as

$$\rho_m = 3H^2 - \sigma^2 - \rho_\phi, \tag{6.2.6}$$

$$p_m = H^2(2q-1) - \sigma^2 - p_\phi. \tag{6.2.7}$$

6.3 Solution of Field Equations

Following the method described in [264, 265], Eq. (6.2.1) and Eq. (6.2.2) gives

$$\frac{\dot{A}}{A}-\frac{\dot{B}}{B}=\frac{x_1}{ABC}, \tag{6.3.1}$$

where x_1 is a constant of integration. The solution of (6.3.1) can be written as

$$\frac{A}{B} = k_1 \exp\left(x_1 \int (ABC)^{-1} dt\right), \tag{6.3.2}$$

where k_1 is an another constant of integration. Analogously, from Eq. (6.2.1) and Eq. (6.2.3), and Eq. (6.2.2) and Eq. (6.2.3), we get

$$\frac{A}{C} = k_2 \exp\left(x_2 \int (ABC)^{-1} dt\right), \tag{6.3.3}$$

$$\frac{B}{C} = k_3 \exp\left(x_3 \int (ABC)^{-1} dt\right), \tag{6.3.4}$$

where k_2, k_3 and x_2, x_3 are constants of integration.

Using Eq. (6.2.5) into Eqs.(6.3.2)–(6.3.4), we get the metric functions as

$$A(t) = b_1\, a(t) \exp\left(a_1 \int a^{-3} dt\right), \tag{6.3.5}$$

$$B(t) = b_2\, a(t) \exp\left(a_2 \int a^{-3} dt\right), \tag{6.3.6}$$

$$C(t) = b_3\, a(t) \exp\left(a_3 \int a^{-3} dt\right), \tag{6.3.7}$$

where

$a_1 = \frac{x_1+x_2}{3}$, $a_2 = \frac{x_3-x_1}{3}$, $a_3 = -\frac{x_3+x_2}{3}$,

and

$b_1 = \sqrt[3]{k_1 k_2}$, $b_2 = \sqrt[3]{k_1^{-1} k_3}$, $b_3 = \sqrt[3]{k_2 k_3^{-1}}$.

The constants $a_1,\ a_2,\ a_3$, and $b_1,\ b_2,\ b_3$ satisfy the following relations

$$a_1 + a_2 + a_3 = 0 \qquad \text{and} \qquad b_1 b_2 b_3 = 1. \tag{6.3.8}$$

The unknown quantities of the problem are A, B, C, p_m, ρ_m, ϕ and $V(\phi)$ whereas we have only five equations available namely Eqs. (6.2.1)–(6.2.4) and (1.7.10). Therefore, in order to solve the system of differential equations we need to assume two more relations among the unknown quantities. Thus, for any arbitrary average scale factor a and scalar field potential $V(\phi)$, Eq. (1.7.10) gives $\phi(t)$ and Eqs. (6.3.5)–(6.3.7) give $A(t)$, $B(t)$ and $C(t)$.

In general, the cosmological expansion will vary as the scalar field ϕ evolves along the potential $V(\phi)$. A convenient approach to the more general case is to express the cosmological expansion directly as a function of scalar field ϕ instead of the function of time, $a = a(\phi)$. This involves the use of the inflation as an effective time coordinate and allows the full dynamical behavior of the field to be investigated (see ref., [266]).

Also, in BD theory [100], many authors [118, 267, 268] have solve the field equations by assuming a relation between scale factor and scalar field. Here, in this chapter we adopt a similar assumption between scale factor and scalar field. For this, let us assume that the average scale factor a is an exponential functions of scalar field ϕ, which is given as [269, 270]

$$a = a_0 e^{l_2 \phi(t)}, \tag{6.3.9}$$

where a_0 represents the average scale factor at present time and l_2 is an arbitrary positive constant.

Thus, the Hubble parameter simply gives

$$H = l_2 \dot{\phi}(t). \tag{6.3.10}$$

To illustrate our analysis, we assume a specific forms of $V(\phi)$. In the literature, due to the unknown nature of DE, there are various forms of this potential (for a detail review, see [28,271–277]) which describes the physical features of the scalar field cosmology. Therefore, as long as potential $V(\phi)$ is given, we can solve other geometrical and physical parameters correspondingly. Thus, here we consider two most common and genuine form of scalar potential, which are discussed in following subsections.

6.3.1 Solution with zero potential

First, we consider the case where the scalar potential is zero [275, 276], that is,

$$V(\phi) = 0, \tag{6.3.11}$$

Using (6.3.10) and (6.3.11), Eq. (1.7.10) reduces to

$$\ddot{\phi} + 3 l_2 \dot{\phi}^2 = 0. \tag{6.3.12}$$

The solution of (6.3.12) is given by

$$\phi = \frac{1}{3 l_2} \ln[3\, l_2 (c_8 t + t_0)], \tag{6.3.13}$$

where c_8 is a positive constant of integration. We observe that at the beginning, i.e., at $t = -\frac{t_0}{c_8}$, $\phi \to -\infty$. It increases with time and it tends to $+\infty$ at $t \to \infty$. Thus, the kinetic energy vanishes at the end of the evolution (an infinite expansion).

Using (6.3.13) into (6.3.9), the average scale factor in terms of t for an expanding Universe is given by

$$a = a_0[3\, l_2(c_8 t + t_0)]^{1/3}. \tag{6.3.14}$$

This is of the power-law form $a \propto t^n$ which represents a generalized inflation for $n > 1$. But, in our case we have $n = 1/3 < 1$, therefore, the model will expand with decelerated rate.

Using (6.3.14) into the metric functions (6.3.5)–(6.3.7), we get

$$A(t) = a_0 b_1 [3l_2(c_8 t + t_0)]^{\frac{1}{3}\left(1+\frac{a_1}{l_2 c_8 a_0^3}\right)}, \tag{6.3.15}$$

$$B(t) = a_0 b_2 [3l_2(c_8 t + t_0)]^{\frac{1}{3}\left(1+\frac{a_2}{l_2 c_8 a_0^3}\right)}, \tag{6.3.16}$$

$$C(t) = a_0 b_3 [3l_2(c_8 t + t_0)]^{\frac{1}{3}\left(1+\frac{a_3}{l_2 c_8 a_0^3}\right)}. \tag{6.3.17}$$

Equations (6.3.15)–(6.3.17) show that the directional scale factors have power-law expansion form. These three spatial scale factors are zero at $t = -\frac{t_0}{c_8}$ and all tend to infinity at $t \to \infty$. The model has a point singularity at $t = -\frac{t_0}{c_8}$. The directional Hubble parameters have the expressions

$$H_i = l_2 c_8 \left(1 + \frac{a_i}{l_2 c_8 a_0^3}\right) [3l_2(c_8 t + t_0)]^{-1}, \quad (i = 1, 2, 3). \tag{6.3.18}$$

Using the constraint $a_1 + a_2 + a_3 = 0$, the generalized mean Hubble's parameter is given by

$$H = \frac{c_8}{3(c_8 t + t_0)}. \tag{6.3.19}$$

As H is a function of time, the model is not a steady-state model. The DP, defined in (2.2.28), gives

$$q = 2, \tag{6.3.20}$$

which shows that the model expands with decelerated rate.

Now, the kinematical quantities for this model can be obtained by substituting the required values in Eqs. (1.10.2), (1.10.3) and (1.10.6). Thus, we have the following values of physical quantities

$$\theta = c_8(c_8 t + t_0)^{-1}, \tag{6.3.21}$$

$$A_p = \frac{2M}{3l_2^2 c_8^2 a_0^6}, \tag{6.3.22}$$

$$\sigma^2 = \frac{M}{9l_2^2 a_0^6} \frac{1}{(c_8 t + t_0)^2}, \tag{6.3.23}$$

where, $M = \frac{a_1^2 + a_2^2 + a_3^2}{2}$.

The values of ρ_ϕ and p_ϕ are given by

$$\rho_\phi = \frac{c_8^2}{2}[3l_2(c_8 t + t_0)]^{-2} = p_\phi, \tag{6.3.24}$$

which gives $\omega_\phi = 1$ throughout the evolution and this is the case of stiff-matter state. We observe that θ, σ, ρ_ϕ and p_ϕ are decreasing functions of time which have infinite value at $t = -\frac{t_0}{c_8}$ but tend to zero in late time evolution. The anisotropy parameter is constant, which shows that the nature of the model is always anisotropy throughout the evolution. Also, $\lim_{t\to\infty} \frac{\sigma}{\theta} =$ const., i.e., the measure of shear scalar to expansion rate is constant and continues through out the evolution, which shows that the shear does not tend to zero faster than the expansion scalar and hence the model has anisotropy behavior.

Now, Eqs. (6.2.6) and (6.2.7) give

$$\rho_m = \left(3l_2^2 c_8^2 - \frac{M}{a_0^6} - \frac{c_8^2}{2}\right)[3l_2(c_8 t + t_0)]^{-2} = p_m. \tag{6.3.25}$$

For energy density to be positive we must have the positive value within the first bracket, i.e., $6l_2^2 c_8^2 a_0^6 - c_8^2 a_0^6 - 2M > 0$. From Eq.(6.3.25), we get $\omega_m = 1$, which is again the case of stiff-matter. The effective density $(\rho_{eff} = \rho_m + \rho_\phi)$ and pressure $(p_{eff} = p_m + p_\phi)$ are respectively given by

$$\rho_{eff} = \left(3l_2^2 c_8^2 - \frac{M}{a_0^6}\right)[3l_2(c_8 t + t_0)]^{-2} = p_{eff}. \tag{6.3.26}$$

From (6.3.26), we find that $\omega_{eff} = 1$. Thus, the Universe is filled with stiff-matter in the presence of scalar field with zero potential and gives decelerating Universe as $q > 0$.

6.3.2 Solution with exponential potential

Let us assume the exponential potential of the form [41, 271, 273]

$$V(\phi) = V_0\, e^{-m_2 \phi}, \tag{6.3.27}$$

where V_0 and m_2 are non-negative constants.

Using (6.3.10) and (6.3.27), Eq.(1.7.10) reduces to

$$\ddot{\phi} + 3l_2\,\dot{\phi}^2 - V_0\,m_2\,e^{-m_2\phi} = 0. \tag{6.3.28}$$

The solution of Eq.(6.3.28) is given by

$$\phi = \frac{2}{m_2}\left[\ln\left(\frac{m_2}{2}\,c_9 + \frac{m_2\sqrt{D}}{2}\,t\right)\right], \tag{6.3.29}$$

where $c_9 > 0$ is a constant of integration and $D = \frac{2V_0 m_2}{(6l_2 - m_2)}$. The real solution of ϕ exists provided $D > 0$, i.e., $0 < m_2 < 6l_2$. We shall choose the positive sign within the bracket, without loosing any generality to obtain an expanding model. We find that ϕ is time-dependent and is increasing function of cosmic time. Therefore, during the evolution the scalar field is growing and hence kinetic energy vanishes at late time evolution.

Using (6.3.29) into (6.3.9), the solution of the average scale factor for an expanding Universe is given by

$$a = a_0\left[\frac{m_2}{2}\,c_9 + \frac{m_2\sqrt{D}}{2}\,t\right]^{2l_2/m_2}. \tag{6.3.30}$$

In this case we again get the power-law form $a \propto t^n$. The model will accelerate or decelerate according as $0 < m_2 \leq 2l_2$ or $2l_2 < m_2 < 6l_2$. From Eq. (6.3.27) and (6.3.29), the potential turns out to be

$$V(\phi) = V_0\left(\frac{m_2}{2}\,c_9 + \frac{m_2\sqrt{D}}{2}\,t\right)^{-2}, \tag{6.3.31}$$

which shows that V decreases with time and vanishes as $t \to \infty$.

By use of Eq. (6.3.30) in Eqs. (6.3.5)–(6.3.7), the spatial scale factors can be obtained as

$$A(t) = a_0 b_1\left(\frac{m_2}{2}\,c_9 + \frac{m_2\sqrt{D}}{2}\,t\right)^{2l_2/m_2}\exp\left[-\frac{2a_1}{a_0^3\sqrt{D}(6l_2 - m_2)}\,\frac{1}{\left(\frac{m_2}{2}\,c_9 + \frac{m_2\sqrt{D}}{2}\,t\right)^{\left(\frac{6l_2 - m_2}{m_2}\right)}}\right], \tag{6.3.32}$$

$$B(t) = a_0 b_2 \left(\frac{m_2}{2}\, c_9 + \frac{m_2\sqrt{D}}{2}\, t \right)^{2l_2/m_2} \exp\left[-\frac{2a_2}{a_0^3\sqrt{D}(6l_2 - m_2)} \frac{1}{\left(\frac{m_2}{2}\, c_9 + \frac{m_2\sqrt{D}}{2}\, t \right)^{\left(\frac{6l_2 - m_2}{m_2}\right)}} \right], \tag{6.3.33}$$

$$C(t) = a_0 b_3 \left(\frac{m_2}{2}\, c_9 + \frac{m_2\sqrt{D}}{2}\, t \right)^{2l_2/m_2} \exp\left[-\frac{2a_3}{a_0^3\sqrt{D}(6l_2 - m_2)} \frac{1}{\left(\frac{m_2}{2}\, c_9 + \frac{m_2\sqrt{D}}{2}\, t \right)^{\left(\frac{6l_2 - m_2}{m_2}\right)}} \right]. \tag{6.3.34}$$

Equations (6.3.32)–(6.3.34) show that the scale factors have hybrid (a combination of power-law and exponential) type expansion. As we know that the power-law behaviour dominates in the early phase of the cosmic evolution where as the exponential factor dominates at late phase. Therefore, this form of scale factor describes both types of expansion depending on the dominating factor. The model has a point singularity at $t = -\frac{c_9}{\sqrt{D}}$. This solution describes an evolution from a point singularity to an infinite expansion. The directional Hubble parameters in this model are given by

$$H_i = l_2\sqrt{D} \left(\frac{m_2}{2}\, c_9 + \frac{m_2\sqrt{D}}{2}\, t \right)^{-1} + \frac{a_i}{a_0^3} \left(\frac{m_2}{2}\, c_9 + \frac{m_2\sqrt{D}}{2}\, t \right)^{-6l_2/m_2}, \quad (i = 1,2,3). \tag{6.3.35}$$

Now, the generalized mean Hubble's parameter is obtained as

$$H = l_2\sqrt{D} \left(\frac{m_2}{2}\, c_9 + \frac{m_2\sqrt{D}}{2}\, t \right)^{-1}, \quad (a_1 + a_2 + a_3 = 0). \tag{6.3.36}$$

For this case the DP can be evaluated as

$$q = \frac{m_2}{2l_2} - 1. \tag{6.3.37}$$

Equation (6.3.37) clearly shows that q is constant and therefore, its nature ($q < 0$, $q = 0$, or $q > 0$) depends on the values of l_2 and m_2. Therefore, for an accelerating Universe where $-1 < q < 0$, we must have $0 < m_2 < 2l_2$, for marginal inflation where $q = 0$, we have $m_2 = 2l_2$ and for a decelerating Universe where $q > 0$, we must have the constraints $2l_2 < m_2 < 6l_2$. It is to be noted that $m_2 > 6l_2$ gives the imaginary value.

The scalar field density and pressure are respectively given by

$$\rho_\phi = \frac{6l_2V_0}{(6l_2-m_2)}\left(\frac{m_2}{2}\,c_9+\frac{m_2\sqrt{D}}{2}\,t\right)^{-2}, \tag{6.3.38}$$

$$p_\phi = \frac{2V_0(m_2-3l_2)}{(6l_2-m_2)}\left(\frac{m_2}{2}\,c_9+\frac{m_2\sqrt{D}}{2}\,t\right)^{-2}. \tag{6.3.39}$$

We observe that ρ_ϕ is always positive as $m_2 < 6l_2$, and both ρ_ϕ and p_ϕ are decreasing functions of time. The corresponding EoS parameter is given by

$$\omega_\phi = \frac{m_2}{3l_2} - 1 = \frac{2q-1}{3}. \tag{6.3.40}$$

As we know that the EoS parameter to a quintessence region is $-1 < \omega_\phi < -\frac{1}{3}$, and this can be achieved when $0 < m_2 < 2l_2$. Also, $2l_2 < m_2 < 6l_2$ gives the EoS parameter $-\frac{1}{3} < \omega_\phi < 1$.

For this case, the kinematical parameters θ, A_p and σ^2 are respectively obtained as

$$\theta = 3l_2\sqrt{D}\left(\frac{m_2}{2}\,c_9+\frac{m_2\sqrt{D}}{2}\,t\right)^{-1}, \tag{6.3.41}$$

$$A_p = \frac{2M}{3l_2^2D\,a_0^6}\left(\frac{m_2}{2}\,c_9+\frac{m_2\sqrt{D}}{2}\,t\right)^{(-12\,l_2/m_2)+2}, \tag{6.3.42}$$

$$\sigma^2 = \frac{M}{a_0^6}\left(\frac{m_2}{2}\,c_9+\frac{m_2\sqrt{D}}{2}\,t\right)^{-12\,l_2/m_2}. \tag{6.3.43}$$

From Eqs. (6.3.41)–(6.3.43), we observe that θ, A_p and σ^2 are infinite at the point of singularity but they decrease with time and all tend to zero in late time evolution. Thus, the Universe is expanding with the increase of time but the rate of expansion, measure of anisotropy and shear scalar decrease to zero and becomes isotropic in late time. It is also observed that $\lim_{t\to\infty}\frac{\sigma}{\theta}=0$ for $m_2 < 6l_2$ which shows that the model approaches to isotropy in late time. Therefore, the anisotropy of the Universe damp out during the course of evolution which is consistent with the present observation.

Now, Eqs. (6.2.6) and (6.2.7) give

$$\rho_m = \frac{6l_2V_0(l_2m_2-1)}{(6l_2-m_2)}\left(\frac{m_2}{2}\,c_9+\frac{m_2\sqrt{D}}{2}\,t\right)^{-2} - \frac{M}{a_0^6}\left(\frac{m_2}{2}\,c_9+\frac{m_2\sqrt{D}}{2}\,t\right)^{-12\,l_2/m_2}, \tag{6.3.44}$$

$$p_m = \frac{2V_0(l_2m_2-1)(m_2-3l_2)}{(6l_2-m_2)}\left(\frac{m_2}{2}\,c_9+\frac{m_2\sqrt{D}}{2}\,t\right)^{-2} - \frac{M}{a_0^6}\left(\frac{m_2}{2}\,c_9+\frac{m_2\sqrt{D}}{2}\,t\right)^{-12\,l_2/m_2}. \tag{6.3.45}$$

The condition $\rho_m \geq 0$ gives $t \geq (\frac{2d_2}{m_2\sqrt{D}} - \frac{c_9}{\sqrt{D}})$, where $d_2 = \left[\frac{M(6\,l_2-m_2)}{6\,l_2\,V_0\,a_0^6\,(l_2\,m_2-1)}\right]^{\frac{m_2}{2(6\,l_2-m_2)}}$ with $l_2\,m_2 \geq 1$.

The corresponding perfect fluid EoS parameter ω_m is given by

$$\omega_m = \frac{\frac{2V_0(l_2\,m_2-1)(m_2-3l_2)\left(\frac{m_2}{2}\,c_9+\frac{m_2\sqrt{D}}{2}\,t\right)^{-2}}{(6\,l_2-m_2)} - \frac{M\left(\frac{m_2}{2}\,c_9+\frac{m_2\sqrt{D}}{2}\,t\right)^{-12\,l_2/m_2}}{a_0^6}}{\frac{6\,l_2V_0(l_2\,m_2-1)\left(\frac{m_2}{2}\,c_9+\frac{m_2\sqrt{D}}{2}\,t\right)^{-2}}{(6\,l_2-m_2)} - \frac{M\left(\frac{m_2}{2}\,c_9+\frac{m_2\sqrt{D}}{2}\,t\right)^{-12\,l_2/m_2}}{a_0^6}}. \tag{6.3.46}$$

From the EoS parameter (6.3.46), it is obvious that as long as both ρ_m and p_m are positive, $0 < \omega_m < 1$ only when $3l_2 < m_2 < 6l_2$ and as p_m is negative, $-1 \leq \omega_m \leq 0$ only when $0 < m_2 \leq 3l_2$. We can also calculate $\rho_{eff} = \rho_\phi + \rho_m$ and $p_{eff} = p_\phi + p_m$ but we avoid here to write the expressions of these quantities. The effective EoS parameter is calculated as

$$\omega_{eff} = \frac{\frac{2V_0l_2\,m_2(m_2-3l_2)\left(\frac{m_2}{2}\,c_9+\frac{m_2\sqrt{D}}{2}\,t\right)^{-2}}{(6\,l_2-m_2)} - \frac{M\left(\frac{m_2}{2}\,c_9+\frac{m_2\sqrt{D}}{2}\,t\right)^{-12\,l_2/m_2}}{a_0^6}}{\frac{6\,l_2^2\,m_2\,V_0\left(\frac{m_2}{2}\,c_9+\frac{m_2\sqrt{D}}{2}\,t\right)^{-2}}{(6\,l_2-m_2)} - \frac{M\left(\frac{m_2}{2}\,c_9+\frac{m_2\sqrt{D}}{2}\,t\right)^{-12\,l_2/m_2}}{a_0^6}}. \tag{6.3.47}$$

Here, we can give the similar interpretation. As long as both ρ_{eff} and p_{eff} are positive, $0 < \omega_{eff} < 1$ only when $3l_2 < m_2 < 6l_2$ and as p_{eff} is negative, $-1 \leq \omega_{eff} \leq 0$ only when $0 < m_2 \leq 3l_2$.

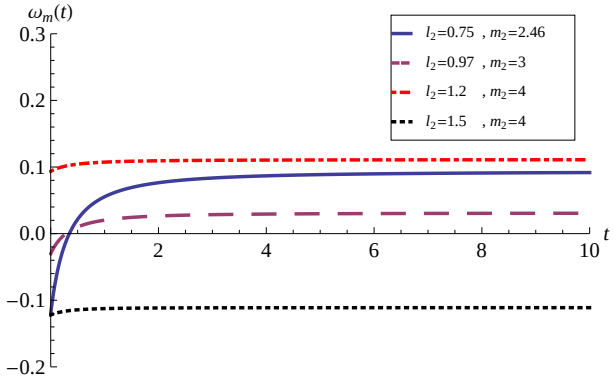

Figure 6.1: ω_m versus t for $c_9 = 1$, $V_0 = 1$ and some values of l_2 and m_2.

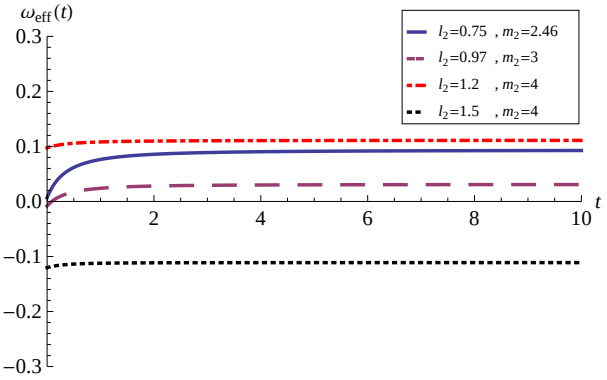

Figure 6.2: ω_{eff} versus t for $c_9 = 1$, $V_0 = 1$ and some values of l_2 and m_2.

Figures 6.1 and 6.2 plot the graphs of ω_m and ω_{eff}, respectively with respect to time t for some values of l_2 and m_2 satisfying the above mentioned constraints. It is to be noted that one can take those values of l_2 and m_2 which make ρ_m and ρ_{eff} to be positive. We observe that for some values of parameters, e.g., $l_2 = 0.97$ and $m_2 = 3$, both ω_m and ω_{eff} show a transition from negative value to positive one. Therefore, the model shows transition from early inflationary phase to decelerated phase. There are some values like $l_2 = 0.75$ and $m_2 = 2.46$, where ω_m shows the transition from negative to positive but ω_{eff} is always positive. However, there are some values of l_2 and m_2 for which ω_m and ω_{eff} are only positive or negative. Thus, for any arbitrary values of l_2 and m_2 we can observe any one of the behavior in EoS parameters: ω_m and ω_{eff} may be only positive or negative throughout the evolution or may vary from negative to positive.

6.4 Conclusion

In this chapter, we have presented a detailed discussion on the evolution of a homogeneous and anisotropic B-I Universe with a perfect fluid and a scalar field. We have studied two types of models, namely, zero potential and an exponential potential respectively. Exact solutions of the field equations for the both models have been obtained by assuming the average scale factor as an exponential function of scalar field.

In the first model, we have considered a mass-less scalar field by assuming the average scale factor as an exponential function of scalar field. In this case the average scale factor as well as the directional scale factors have power-law expansion which expand with decelerated rate. The model has a point singularity at $t = -\frac{t_0}{c_8}$. At the

beginning of the evolution, i.e., at $t = -\frac{t_0}{c_8}$, the scalar field $\phi \to -\infty$. During the evolution, ϕ increases and at the end of the evolution (an infinite expansion) when $t \to \infty$, it tends to $+\infty$. The kinetic energy vanishes at $t \to \infty$. The positive constant value of DP shows that the model expands but with decelerated rate. The nature of the model is always anisotropic throughout the evolution because of the constant behaviour of anisotropy parameter. All the physical parameters like energy density, pressure, expansion scalar and shear scalar are decreasing functions of time. The measure of shear scalar to expansion scale is constant throughout the evolution. Thus, the shear scalar does not tend faster than the expansion scalar. The EoS parameters of scalar field and perfect fluid come out to be one. Hence, we have found that the anisotropic perfect fluid model behaves like stiff-matter in the presence of scalar field.

In the second model, we have considered an exponential potential. We have obtained the logarithmic form of scalar field and power-law form of average scale factor. The directional scale factors have hybrid type expansion which is a combination of power-law and exponential forms. This form of scale factor describes both types of expansion depending on the dominating factor. The model has a point singularity at $t = -\frac{c_9}{\sqrt{D}}$. It has been observed that at the beginning of the evolution, i.e., at $t = -\frac{c_8}{\sqrt{D}}$, ϕ tends to $-\infty$ while $V(\phi)$ tends to $+\infty$. During the evolution ϕ increases where as $V(\phi)$ decreases and at late time evolution ϕ tends to $+\infty$ while $V(\phi)$ vanishes. The kinetic energy and potential energy tend to $+\infty$ at the beginning but both vanish at the end of evolution. This means that the Universe is born from the singularity at $t = -\frac{c_9}{\sqrt{D}}$. The DP is constant whose nature depends on the values of l_2 and m_2. The physical quantities like θ, A_p, σ^2, ρ_m, p_m, ρ_ϕ, p_ϕ are decreasing functions of time and tend to zero in late time evolution. The model approaches isotropy in late time. The EoS parameter of matter and the effective EoS parameter of matter plus scalar field are time dependent which show the deceleration or acceleration or transition from one phase to other depending on the constraint $0 < m_2 \leq 3l_2$ or $3l_2 < m_2 < 6l_2$ which have been shown in Figs. 6.1 and 6.2. We have find out that the physically valid range for m_2 is $0 < m_2 < 6l_2$, where l_2 is any positive constant.

Chapter 7

Dynamics of Bianchi V anisotropic model

This chapter[1] is the extension of the previous chapter. It deals with the dynamical evolution of a homogeneous and anisotropic Bianchi type-V model filled with perfect fluid and scalar field. The two sources are assumed to be non-interacting. The average scale factor and scalar potential are assumed to be the exponential functions of the scalar field, i.e., $a = a_0\, e^{l_2\phi(t)}$ and $V = V_0\, e^{-m_2\phi(t)}$, where l_2, V_0, and m_2 are arbitrary constants. We use the observational data to find the parameters l_2 and m_2. The role of scalar field through the variable EoS parameters are studied. It is also observed that EoS parameters change from phantom region to quintessence region for small values of l_2 and m_2, respectively. We conclude that the model shows phantom behavior during early time and quintessence in late time evolution. For large values of l_2 and m_2 it varies in quintessence region only. We also study the statefinder parameters and found that the model behaves like ΛCDM or $SCDM$ depending on the values of l_2 and m_2.

---

[1]The work presented in this chapter comprises the results of a research paper entitled "Dynamics of Bianchi V anisotropic model with perfect fluid and scalar field, *Indian Journal of Physics* **91**, 1645 (2017)".

7.1 Introduction

In the present chapter, we extend the work carried out in chapter 6 for the Bianchi type-V (B-V) homogeneous and anisotropic Universe filled with ordinary matter as a perfect fluid and a scalar field (ϕ) with potential ($V(\phi)$) minimally coupled with gravity. In the last few years, there has been considerable interest, primarily due to the observations of distant supernovae, in the possibility that a significant fraction of the energy of the Universe today is in a coherent zero mode of a very weakly coupled scalar field. The scalar fields are being used for exploration of possible inflationary scenario [13] and for description of DE [63].

It has been observed that the scalar potential $V(\phi)$ in a scalar field cosmology has very important role as it radically affects the cosmological behavior. There are a number of quintessence models which have been put forward in recent years. These fields involve a scalar field rolling down its potential dominating over the kinetic energy of the field. A purely exponential potential $V(\phi) = V_0 e^{m_2\phi}$ is one of the widely studied case [278]. Some other forms of the scalar potential have been assumed to describe the early and late time evolution of the Universe.

The standard Friedmann cosmology which is isotropic and homogeneous has been very successful in describing the evolution of the Universe. The present Universe, however, is not as simple as the Universe was in the early epoch. The large scale matter distribution in the observable Universe, largely manifested in the form of discrete structures, does not exhibit a high degree of homogeneity. Recent space investigations detect anisotropy in the cosmic microwave background. The Cosmic Background Explorers differential radiometer has detected and measured cosmic microwave background anisotropies at different angular scales. The theoretical arguments [161] and recent experimental data that support the existence of an anisotropic phase approaches to the isotropic phase. It leads one to consider Universe models with an anisotropic background.

In the last few years, observational results indicate that anisotropic Bianchi type models play the vital role in cosmology. Many authors [279–283] have studied the anisotropic models and found that the situation observed by the FRW model remains unchanged in the anisotropic model before the inflationary period. That's why the anisotropic Bianchi models have become more interesting. Spatially homogeneous Bianchi type models are more general than the FRW models and have anisotropic

spatial sections. These models provide an opportunity to consider asymmetric expansion along different spatial sections.

Bianchi type-I (B-I) is the simplest generalization of isotropic and homogeneous flat FRW models. The Bianchi type-V (B-V) model is the natural generalization of the open FRW model, which finally becomes isotropic. B-V cosmological models have been discussed by many authors (see, refs. [284–294]). Pradhan and Amirhashchi [295], Kumar and Yadav [296], Kumar [297], Chandel and ShriRam [298], and Farajollahi and Tayebi [299] have studied B-V models with dark energy component in different physical context.

Fadragas et al. [261] have studied anisotropic locally-rotationally-symmetric (LRS) B-I with scalar field for a wide range of potentials. The effect of the scalar fields with exponential potential in anisotropic cosmology is of interest. We have extended this work in the previous chapter to totally anisotropic B-I model and discussed the effect of scalar field [300].

In the present chapter, we find out the exact solutions of the Einstein field equations with the help of an exponential form of the scalar potential in B-V cosmological model to discuss the early and late time evolution of the Universe. We desire to impose observational constraints on scalar field cosmology along with the matter fluid in which the average scale factor is an exponential function of scalar field. We use the observational data from SNe Ia (Gold Sample) and H(z)+SNe Ia [301] in order to find the suitable values of model parameters. We discuss the behavior of various cosmological parameters, like shear scalar, anisotropy parameter and expansion scalar. We also discuss the statefinder parameter to observe the behavior of the anisotropic model.

7.2 The Field Equations

Let us consider a spatially homogeneous and anisotropic B-V line element, defined by (1.3.9). We consider that the Universe is filled with perfect fluid and scalar field where energy-momentum tensors are given by (1.4.4) and (1.7.6) respectively.

The Einstein field equations (1.7.5) for the B-V metric (1.3.9) and energy-momentum tensor (1.4.4) and (1.7.6) yield

$$\frac{\ddot{A}}{A}+\frac{\ddot{B}}{B}+\frac{\dot{A}\dot{B}}{AB}-\frac{m^2}{A^2}=-(p_m+p_\phi), \tag{7.2.1}$$

$$\frac{\ddot{A}}{A}+\frac{\ddot{C}}{C}+\frac{\dot{A}\dot{C}}{AC}-\frac{m^2}{A^2}=-(p_m+p_\phi), \tag{7.2.2}$$

$$\frac{\ddot{B}}{B}+\frac{\ddot{C}}{C}+\frac{\dot{B}\dot{C}}{BC}-\frac{m^2}{A^2}=-(p_m+p_\phi), \tag{7.2.3}$$

$$\frac{\dot{A}\dot{B}}{AB}+\frac{\dot{B}\dot{C}}{BC}+\frac{\dot{A}\dot{C}}{AC}-\frac{3m^2}{A^2}=(\rho_m+\rho_\phi), \tag{7.2.4}$$

$$2\frac{\dot{A}}{A}-\frac{\dot{B}}{B}-\frac{\dot{C}}{C}=0, \tag{7.2.5}$$

where, ρ_m, ρ_ϕ, p_m and p_ϕ have their usual meaning as defined in Chapter 6. We assume that there are no interaction between matter and the scalar field, so that they separately obey the energy conservation and Klein-Gordon equations, respectively as

$$\dot{\rho_m}+3H(1+\omega_m)\rho_m=0, \tag{7.2.6}$$

$$\ddot{\phi}+3H\dot{\phi}+\frac{dV(\phi)}{d\phi}=0. \tag{7.2.7}$$

The field equations (7.2.1)–(7.2.4) can be rewritten in terms of H, q, σ^2 as

$$\rho_m=3H^2-\sigma^2-\frac{3m^2}{A^2}-\rho_\phi, \tag{7.2.8}$$

$$p_m=H^2(2q-1)-\sigma^2+\frac{m^2}{A^2}-p_\phi, \tag{7.2.9}$$

where, σ^2 is the shear scalar.

7.3 Solution of the Field Equations

We follow the approaches of [291, 292, 302–304] to solve the field equations (7.2.1)–(7.2.5). Considering (6.2.5), from (7.2.1)–(7.2.4), we have the following metric potentials

$$A(t)=b_4\,a(t)\exp\left(a_4\int a^{-3}dt\right), \tag{7.3.1}$$

$$B(t)=b_5\,a(t)\exp\left(a_5\int a^{-3}dt\right), \tag{7.3.2}$$

$$C(t)=b_6\,a(t)\exp\left(a_6\int a^{-3}dt\right), \tag{7.3.3}$$

where the constants a_4, a_5, a_6 and b_4, b_5, b_6 are chosen in such a way that they must satisfy the constraints

$$a_4 + a_5 + a_6 = 0 \qquad \text{and} \qquad b_4 b_5 b_6 = 1. \tag{7.3.4}$$

Integrating (7.2.5) and absorbing the integration constant into B or C without loss of generality, we obtain

$$A^2 = BC. \tag{7.3.5}$$

Using (7.3.1)–(7.3.3) with the relations (7.3.4) into (7.3.5), we obtain $a_4 = 0$, $a_5 = -a_6 = d_3(say)$, $b_4 = 1$, $b_5 = b_6^{-1}$, where d_3 is another constant. Finally, using above relations, Eqs. (7.3.1)–(7.3.3) can be written as

$$A(t) = a(t), \tag{7.3.6}$$

$$B(t) = b_5 a(t) exp\left(d_3 \int a^{-3} dt\right), \tag{7.3.7}$$

$$C(t) = b_5^{-1} a(t) exp\left(-d_3 \int a^{-3} dt\right). \tag{7.3.8}$$

Thus, we get the metric potentials explicitly in terms of the average scale factor a. It is very obvious from the Eqs. (7.3.6)–(7.3.8) and (7.2.7) that if once we get the average scale factor and scalar field potential then we can compute the metric functions $A(t)$, $B(t)$, $C(t)$, scalar field (ϕ), and with the help of these parameters we can also compute all other remaining quantities, such as ρ_m, and p_m. Here, in this chapter we adopt a similar assumption between scale factor and scalar field. For this, let us assume that the average scale factor a is an exponential functions of scalar field ϕ, which is given as in Eq. (6.3.9) [269, 270].

Let us address the question of choice of potential of the scalar field which would lead to a viable cosmological model. The obvious restriction on the evolution is that, starting from Planck's time, the scalar field should survive till today (to account for the observed late time accelerated expansion) without interfering with the nucleosynthesis of the standard model.

Exponential potentials lead to the solutions which are the attractors of evolution equations and provide backdrop for the understanding of the dynamics in our case. The potential of this form is of interest because it arrives generally in a number of circumstances. Although, it does not possess minima, it can model the gradient of a potential

which possess a minimum in an orthogonal degree of freedom. Halliwell [305] has also pointed out that most theories undergoing dimensional reduction to an effective four dimensional theory result in a combination of exponential potentials and one of these will always dominate asymptotically. It is also known that an analogous structure exist in quadratic Lagrange's theories of gravity, which are conformally equivalent to a general relativity plus a scalar field which asymptotically tends to an exponential form. Let us assume scalar field potential V as [41, 271, 273] defined in the previous chapter by (6.3.27).

Using (6.3.9), the Hubble parameter is obtained as

$$H = \frac{\dot{a}}{a} = l_2\dot{\phi}. \tag{7.3.9}$$

Solving the Eq. (1.7.10), for the ansatz (6.3.9) and (6.3.27), we get the scalar field in terms of time t which is same as obtained in chapter 6, Eq. (6.3.29). Using this value of scalar field, the average scale factor and scalar field potential is obtained same as in chapter 6 by Eqs. (6.3.30) and (6.3.31), respectively.

If we insert the value of $a(t)$ from (6.3.30) into (7.3.6)–(7.3.8), we get the following metric potentials in terms of t

$$A(t) = a_0\left(\frac{m_2}{2}\,c_9 + \frac{m_2\sqrt{D}}{2}\,t\right)^{2\,l_2/m_2}, \tag{7.3.10}$$

$$B(t) = b_5 a_0\left(\frac{m_2}{2}\,c_9 + \frac{m_2\sqrt{D}}{2}\,t\right)^{2l_2/m_2} exp\left[-\frac{2d_3}{a_0^3\sqrt{D}(6l_2-m_2)}\left(\frac{m_2}{2}\,c_9 + \frac{m_2\sqrt{D}}{2}\,t\right)^{-\frac{6l_2}{m_2}+1}\right], \tag{7.3.11}$$

$$C(t) = b_5^{-1} a_0\left(\frac{m_2}{2}\,c_9 + \frac{m_2\sqrt{D}}{2}\,t\right)^{2\,l_2/m_2} exp\left[\frac{2d_3}{a_0^3\sqrt{D}(6\,l_2-m_2)}\left(\frac{m_2}{2}\,c_9 + \frac{m_2\sqrt{D}}{2}\,t\right)^{-\frac{6l_2}{m_2}+1}\right]. \tag{7.3.12}$$

where, $c_9 > 0$ is a constant of integration and $D = \frac{2V_0 m_2}{(6l_2-m_2)}$. From Eqs. (7.3.10)–(7.3.12), we can observe that only scale factor $A(t)$ is of the form of power-law expansion type whereas the other two scale factors $B(t)$ and $C(t)$ have hybrid (a combination of the power-law and exponential) type expansions. So the dominating factor decides the expansion. The scalar functions $A(t)$, $B(t)$ and $C(t)$ tend to infinity as $t \to \infty$.

The physical parameters such as directional Hubble's parameters (H_1, H_2, H_3), Hubble's parameter (H), DP (q), expansion scalar (θ), shear scalar (σ^2) and anisotropy parameter (A_p) for the model are respectively calculated as

$$H_1 = l_2\sqrt{D}\left(\frac{m_2}{2}\,c_9 + \frac{m_2\sqrt{D}}{2}\,t\right)^{-1}, \tag{7.3.13}$$

$$H_2 = l_2\sqrt{D}\left(\frac{m_2}{2}\,c_9 + \frac{m_2\sqrt{D}}{2}\,t\right)^{-1} + \frac{d_3}{a_0^3}\left(\frac{m_2}{2}\,c_9 + \frac{m_2\sqrt{D}}{2}\,t\right)^{-\frac{6\,l_2}{m_2}}, \tag{7.3.14}$$

$$H_3 = l_2\sqrt{D}\left(\frac{m_2}{2}\,c_9 + \frac{m_2\sqrt{D}}{2}\,t\right)^{-1} - \frac{d_3}{a_0^3}\left(\frac{m_2}{2}\,c_9 + \frac{m_2\sqrt{D}}{2}\,t\right)^{-\frac{6\,l_2}{m_2}}, \tag{7.3.15}$$

$$H = l_2\sqrt{D}\left(\frac{m_2}{2}\,c_9 + \frac{m_2\sqrt{D}}{2}\,t\right)^{-1}, \tag{7.3.16}$$

$$q = \frac{m_2}{2l_2} - 1, \tag{7.3.17}$$

$$\theta = 3l_2\sqrt{D}\left(\frac{m_2}{2}\,c_9 + \frac{m_2\sqrt{D}}{2}\,t\right)^{-1}, \tag{7.3.18}$$

$$\sigma^2 = \frac{d_3^2}{a_0^6}\left(\frac{m_2}{2}\,c_9 + \frac{m_2\sqrt{D}}{2}\,t\right)^{-\frac{12\,l_2}{m_2}}, \tag{7.3.19}$$

$$A_p = \frac{2d_3^2}{3a_0^6\,l_2^2 D}\left(\frac{m_2}{2}\,c_9 + \frac{m_2\sqrt{D}}{2}\,t\right)^{-\left(\frac{12\,l_2}{m_2}-2\right)}. \tag{7.3.20}$$

From Eq. (7.3.17), we can analyse that DP remains constant throughout the evolution and its sign depends on the values of the constants l_2 and m_2. For the considered model the Universe accelerates, i.e., $-1 < q < 0$ for $0 < m_2 < 2l_2$, the Universe has marginal inflation, i.e., $q = 0$ for $m_2 = 2l_2$ and the Universe decelerates, i.e., $q > 0$ for $2l_2 < m_2 < 6l_2$.

We observe that A_p is decreasing function of time in interval $0 < m_2 < 6l_2$ and tends to zero as $t \to \infty$. This indicates that our model has transition from initial anisotropy to isotropy at present epoch which is in good harmony with current observations. Thus, observed isotropy of the Universe can be achieved in our model at present epoch. The parameters, such as H_1, H_2, H_3, H, θ, σ^2 also decrease with time and all tend to zero at $t \to \infty$, which indicate that the model tends to isotropic at large time. It is also observed that $\lim_{t\to\infty} \frac{\sigma}{\theta} = 0$ for $0 < m_2 < 6l_2$, which indicates that in late time the model

damp out the anisotropy of the Universe and approaches to isotropy.

The scalar field energy density and pressure are respectively evaluated as

$$\rho_\phi = \frac{6l_2V_0}{(6l_2-m_2)}\left(\frac{m_2}{2}\,c_9+\frac{m_2\sqrt{D}}{2}\,t\right)^{-2}, \tag{7.3.21}$$

$$p_\phi = \frac{2V_0(m_2-3l_2)}{(6l_2-m_2)}\left(\frac{m_2}{2}\,c_9+\frac{m_2\sqrt{D}}{2}\,t\right)^{-2}. \tag{7.3.22}$$

It is clear from Eqs. (7.3.21) and (7.3.22) that ρ_ϕ is always positive for $0<m_2<6l_2$ which is the viable range for the existence of the solution as discussed above. We find that ρ_ϕ and p_ϕ tend to zero as $t\to\infty$. The EoS parameter gives

$$\omega_\phi = \frac{m_2}{3l_2}-1 = \frac{2q-1}{3}. \tag{7.3.23}$$

The model behaves as quintessence ($-1<\omega_\phi\leq\frac{1}{3}$) for $0<m_2\leq 2l_2$, whereas it goes from accelerated phase to decelerated phase ($-\frac{1}{3}<\omega_\phi<1$) for $2l_2<m_2<6l_2$.

From (7.2.8) and (7.2.9), we get

$$\begin{aligned}\rho_m &= \frac{6l_2\,V_0(l_2m_2-1)}{(6l_2-m_2)}\left(\frac{m_2}{2}\,c_9+\frac{m_2\sqrt{D}}{2}\,t\right)^{-2}-\frac{d_3^2}{a_0^6}\left(\frac{m_2}{2}\,c_9+\frac{m_2\sqrt{D}}{2}\,t\right)^{-\frac{12\,l_2}{m_2}}\\ &\quad-\frac{3m^2}{a_0^2}\left(\frac{m_2}{2}\,c_9+\frac{m_2\sqrt{D}}{2}\,t\right)^{-\frac{4\,l_2}{m_2}},\end{aligned} \tag{7.3.24}$$

and

$$\begin{aligned}p_m &= \frac{2V_0(l_2m_2-1)(m_2-3l_2)}{(6l_2-m_2)}\left(\frac{m_2}{2}\,c_9+\frac{m_2\sqrt{D}}{2}\,t\right)^{-2}-\frac{d_3^2}{a_0^6}\left(\frac{m_2}{2}\,c_9+\frac{m_2\sqrt{D}}{2}\,t\right)^{-\frac{12\,l_2}{m_2}}\\ &\quad+\frac{m^2}{a_0^2}\left(\frac{m_2}{2}\,c_9+\frac{m_2\sqrt{D}}{2}\,t\right)^{-\frac{4\,l_2}{m_2}}.\end{aligned} \tag{7.3.25}$$

For reality of ρ_m, we must have $m_2>\sqrt{6}$ and $m_2<6l_2$. The corresponding EoS parameter for the perfect fluid is

$$\omega_m = \frac{\frac{2V_0(l_2m_2-1)(m_2-3l_2)}{(6l_2-m_2)}\left(\frac{m_2}{2}\,c_9+\frac{m_2\sqrt{D}}{2}\,t\right)^{-2}-\frac{d_3^2}{a_0^6}\left(\frac{m_2}{2}\,c_9+\frac{m_2\sqrt{D}}{2}\,t\right)^{-\frac{12\,l_2}{m_2}}+\frac{m^2}{a_0^2}\left(\frac{m_2}{2}\,c_9+\frac{m_2\sqrt{D}}{2}\,t\right)^{-\frac{4\,l_2}{m_2}}}{\frac{6l_2V_0(l_2m_2-1)}{(6l_2-m_2)}\left(\frac{m_2}{2}\,c_9+\frac{m_2\sqrt{D}}{2}\,t\right)^{-2}-\frac{d_3^2}{a_0^6}\left(\frac{m_2}{2}\,c_9+\frac{m_2\sqrt{D}}{2}\,t\right)^{-\frac{12\,l_2}{m_2}}-\frac{3m^2}{a_0^2}\left(\frac{m_2}{2}\,c_9+\frac{m_2\sqrt{D}}{2}\,t\right)^{-\frac{4\,l_2}{m_2}}}. \tag{7.3.26}$$

Table 7.1: The constraints on ω_m and ω_{eff} for different values of l_2 and m_2 using observational data.

Data	$1/1+q$	$2l_2/m_2$	$m_2 > \sqrt{6}$	l_2	ω_m	ω_{eff}
SNe Ia (Gold Sample)	$1.04^{+0.07}_{-0.06}$	$1.04^{+0.07}_{-0.06}$	2.3	1.196	$---$	$-1.92369 \leq \omega_{eff} \leq -0.358974$
			2.6	1.352	$-1.55876 \leq \omega_m \leq -0.358974$	$-0.632776 \leq \omega_{eff} \leq -0.358974$
			3.351	**1.74252**	$-0.413721 \leq \omega_m \leq -0.358974$	$\mathbf{-0.39934 \leq \omega_{eff} \leq -0.358974}$
			3.502	**1.82104**	$\mathbf{-0.399347 \leq \omega_m \leq -0.358974}$	$-0.390097 \leq \omega_{eff} \leq -0.358974$
			4	2.08	$-0.377332 \leq \omega_m \leq -0.358974$	$-0.374444 \leq \omega_{eff} \leq -0.358974$
			5	2.6	$-0.365668 \leq \omega_m \leq -0.358974$	$-0.365064 \leq \omega_{eff} \leq -0.358974$
$H(z)$+SNe Ia	$1.31^{+0.06}_{-0.05}$	$1.31^{+0.06}_{-0.05}$	2.3	1.5065	$---$	$-1.24084 \leq \omega_{eff} \leq -0.491094$
			2.54	1.6637	$-1.01038 \leq \omega_m \leq -0.491094$	$-0.764679 \leq \omega_{eff} \leq -0.491094$
			4	2.62	$-0.52214 \leq \omega_m \leq -0.491094$	$-0.518695 \leq \omega_{eff} \leq -0.491094$
			4.266	**2.79423**	$-0.515664 \leq \omega_m \leq -0.491094$	$\mathbf{-0.513327 \leq \omega_{eff} \leq -0.491094}$
			4.39	**2.87545**	$\mathbf{-0.513338 \leq \omega_m \leq -0.491094}$	$-0.511359 \leq \omega_{eff} \leq -0.491094$
			5	3.275	$-0.505636 \leq \omega_m \leq -0.491094$	$-0.504673 \leq \omega_{eff} \leq -0.491094$

To observe the behaviour of ω_m, we need the values of parameters l_2 and m_2. From (7.3.17), we get $\frac{2l_2}{m_2} = (1+q)^{-1}$. On using the constraints on $(q+1)^{-1}$ from the SNe Ia (Gold Sample) and H(z)+ SNe Ia [301], respectively in this relation, we get the values of l_2 and m_2 keeping the constraints $m_2 > \sqrt{6}$ and $m_2 < 6l_2$, which are necessary for the existence of model and positivity of energy density. It is to be noted that these two constraints of l_2 and m_2 are obtained from Eq. (7.3.24) to make the energy density as positive quantity. Some values of l_2 and m_2 are listed in table 7.1.

Substituting these values of l_2 and m_2 and taking other parameters as unity in Eq. (7.3.26), we get different ranges of ω_m which are listed in table 7.1. We plot the graphs ω_m versus t for these values of l_2 and m_2 which are shown in Fig. 7.1 corresponding to SNe Ia (Gold sample) and in Fig. 7.2 with respect to H(z)+SNe Ia. It is observed that the EoS parameter varies from phantom phase to quintessence phase crossing the dividing line $\omega_m = -1$ for smaller values of l_2 and m_2, say $m_2 = 2.6$ and $l_2 = 1.352$ with respect to SNe Ia and $l_2 = 2.54$ and $m_2 = 1.6637$ corresponding to H(z)+ SNe Ia, respectively. Thus, the model shows phantom behavior in early time and quintessence in late time evolution. However, it shows quintessence to quintessence for larger values of l_2 and m_2 during whole evolution. The SNe Ia (Gold Sample) data suggests that $-0.3993994 \leq \omega_{de} \leq -0.3197279$ while the limit imposed by a combination of H(z)+SNe Ia data is $-0.513382 \leq \omega_{de} \leq -0.4708995$ for open model. The table 7.1 clearly shows that our result for ω_m evolves within a range of SNe Ia (Gold Sample) at $m_2 = 3.502$ and $l_2 = 1.82104$ whereas a range of ω_m as per H(z)+SNe Ia is obtained at $m_2 = 4.39$

and $l_2 = 2.87545$ which are nice agreement with both observational data.

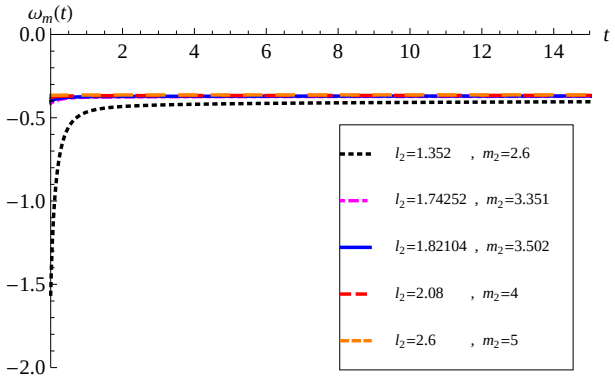

Figure 7.1: The evolution of EoS parameter of matter vs. time with $d_3 = 1$, $a_0 = 1$, $V_0 = 1$ using SNe Ia(Gold Sample) data.

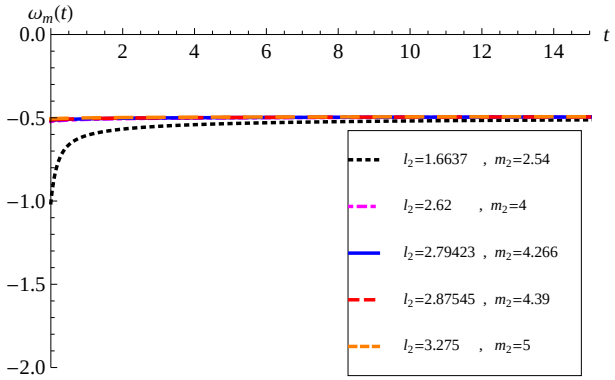

Figure 7.2: The evolution of EoS parameter of matter vs. time with $d_3 = 1$, $a_0 = 1$, $V_0 = 1$ using H(z)+SNe Ia data.

Now, we compute the effective density $(\rho_{eff} = \rho_m + \rho_\phi)$, the effective pressure $(p_{eff} = p_m + p_\phi)$ and the effective EoS parameter $(\omega_{eff} = p_{eff}/\rho_{eff})$ for the model. These quantities have the following forms, respectively

$$\begin{aligned}\rho_{eff} &= \frac{6l_2^2\, m_2\, V_0}{(6l_2 - m_2)}\left(\frac{m_2}{2}\, c_9 + \frac{m_2\sqrt{D}}{2}\, t\right)^{-2} - \frac{d_3^2}{a_0^6}\left(\frac{m_2}{2}\, c_9 + \frac{m_2\sqrt{D}}{2}\, t\right)^{-\frac{12\, l_2}{m_2}} \\ &\quad - \frac{3m^2}{a_0^2}\left(\frac{m_2}{2}\, c_9 + \frac{m_2\sqrt{D}}{2}\, t\right)^{-\frac{4\, l_2}{m_2}}, \end{aligned} \tag{7.3.27}$$

$$\begin{aligned}p_{eff} &= \frac{2V_0 l_2 m_2(m_2 - 3l_2)}{(6l_2 - m_2)}\left(\frac{m_2}{2}\, c_9 + \frac{m_2\sqrt{D}}{2}\, t\right)^{-2} - \frac{d_3^2}{a_0^6}\left(\frac{m_2}{2}\, c_9 + \frac{m_2\sqrt{D}}{2}\, t\right)^{-\frac{12\, l_2}{m_2}} \\ &\quad + \frac{m^2}{a_0^2}\left(\frac{m_2}{2}\, c_9 + \frac{m_2\sqrt{D}}{2}\, t\right)^{-\frac{4\, l_2}{m_2}}, \end{aligned} \tag{7.3.28}$$

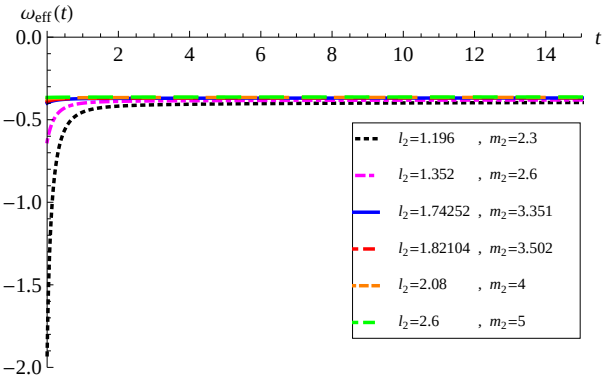

Figure 7.3: The evolution of effective EoS parameter vs. time with $d_3 = 1$, $a_0 = 1$, $V_0 = 1$ using SNe Ia(Gold Sample) data.

$$\omega_{eff} = \frac{\frac{2V_0\, l_2 m_2 (m_2 - 3l_2)}{(6l_2 - m_2)} \left(\frac{m_2}{2}\, c_9 + \frac{m_2\sqrt{D}}{2}\, t\right)^{-2} - \frac{d_3^2}{a_0^6}\left(\frac{m_2}{2}\, c_9 + \frac{m_2\sqrt{D}}{2}\, t\right)^{-\frac{12\, l_2}{m_2}} + \frac{m^2}{a_0^2}\left(\frac{m_2}{2}\, c_9 + \frac{m_2\sqrt{D}}{2}\, t\right)^{-\frac{4\, l_2}{m_2}}}{\frac{6\, l_2^2\, m_2\, V_0}{(6l_2 - m_2)}\left(\frac{m_2}{2}\, c_9 + \frac{m_2\sqrt{D}}{2}\, t\right)^{-2} - \frac{d_3^2}{a_0^6}\left(\frac{m_2}{2}\, c_9 + \frac{m_2\sqrt{D}}{2}\, t\right)^{-\frac{12\, l_2}{m_2}} - \frac{3m^2}{a_0^2}\left(\frac{m_2}{2}\, c_9 + \frac{m_2\sqrt{D}}{2}\, t\right)^{-\frac{4\, l_2}{m_2}}}. \tag{7.3.29}$$

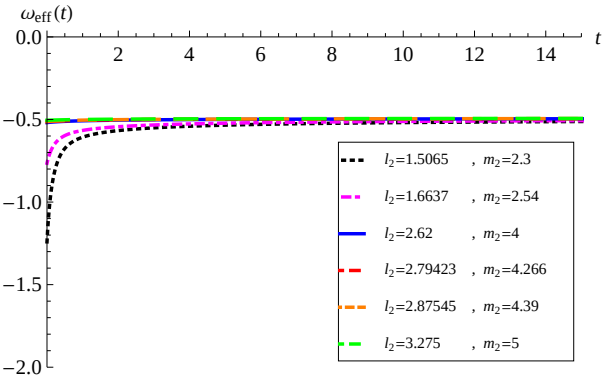

Figure 7.4: The evolution of effective EoS parameter vs. time with $d_3 = 1$, $a_0 = 1$, $V_0 = 1$ using H(z)+ SNe Ia data.

The constraints on ω_{eff} are calculated and listed in table 7.1 for the values of l_2 and m_2, obtained from the data of SNe Ia(Gold Sample) and H(z)+SNe Ia [301]. In this case, $m_2 > 0$ and $l_2 > m_2/6$ must have the constraints to make the effective density to be positive. We plot ω_{eff} versus t in Figs. 7.3 and 7.4 corresponding to the data of SNe Ia(Gold Sample) and H(z)+ SNe Ia, respectively. The Universe starts from phantom region and approaches to $\omega_{eff} = -\frac{1}{3}$ in late time evolution for the small values of l_2 and m_2, say, $m_2 = 2.3$ and $l_2 = 1.196$ with SNe Ia data and $m_2 = 2.3$ and $l_2 = 1.5065$ with H(z)+SNe Ia data, respectively. It means that there is a transition from phantom region to quintessence region corresponding to the both observational data. For the large values of l_2 and m_2, ω_{eff} varies in the quintessence region only.

We find that $m_2 = 3.351$ and $l_2 = 1.74252$ gives the range of effective EoS parameter of SNe Ia and $m_2 = 4.266$ and $l_2 = 2.79423$ gives the range of ω_{eff} of H(z)+SNe Ia. Thus, we find that our model is best fitted corresponding to these two observational data for the above values of l_2 and m_2.

Let us discuss the anisotropy parameter in term of redshift z. The relation between scale factor a and redshift z is given by

$$\frac{a_0}{a} = 1 + z. \tag{7.3.30}$$

Now, the anisotropy parameter A_p given in Eq. (7.3.20) in terms of z can be written as

$$A_p = \frac{2d_3^2}{3a_0^6\, l_2^2\, D}\,(1+z)^{\frac{6l_2-m_2}{l_2}}, \text{ where } 6l_2 > m_2 \tag{7.3.31}$$

Using the suitable values of l_2 and m_2 given in table 7.1 as obtained through the observations SNe Ia and H(z)+SNe Ia, we can obtain the constraint for A_p. We have observed that the suitable values of l_2 and m_2 are 2.79423 and 4.266, respectively for H(z)+SNe Ia data. Therefore, from Eq. (7.3.31) the constraint for A_p comes to $0.183925 \leq A_p \leq 11.5473$ with $0.09 \leq z \leq 1.75$ [301]. It means that at early time the measure of anisotropy was very high at the redshift of $z = 1.75$ but ultimately it decreases during the process of evolution. If we consider the present value, i.e., at $z = 0$, we find $A_p = 0.12509$ and at late time, i.e, $z \to -1$, we get $A_p \to 0$. Therefore, the anisotropic model behaves as isotropic.

Statefinder Parameter

Now, we discuss our model with another important parameter known as statefinder parameter. In this model, we obtain the statefinder parameters r and s as

$$r = \frac{(2l_2 - m_2)(l_2 - m_2)}{2\, l_2^2}, \tag{7.3.32}$$

and

$$s = \frac{m_2}{3\, l_2}. \tag{7.3.33}$$

It has been observed that our model approaches from initial anisotropic to isotropic state at late time. Therefore it is worthwhile to compare the statefinder parameters of our model with the ΛCDM model, available to an isotropic and homogeneous geometry. Now, from (7.3.32) and (7.3.33), we observe that the state finder parameters are

constants and the values of these parameters depend on the parameters l_2 and m_2. With the help of Eq. (7.3.32), we get $m_2 = 0$ or $m_2 = 3l_2$ for $r = 1$. Also from Eq. (7.3.23), we observe that at $m_2 = 0$ the scalar field behaves like a cosmological constant. For $m_2 = 0$, we get $s = 0$, i.e., $r = 1, s = 0$ which shows the ΛCDM behaviour of the model. For $m_2 = 3l_2$, we get $s = 1$, i.e., $r = 1, s = 1$ which shows the $SCDM$ behaviour of the model. Also, from Eqs. (7.3.22), (7.3.23) and (7.3.17), we observe that at $m_2 = 3l_2$ we get $p_\phi = 0$, $\omega_\phi = 0$ and $q = 0.5$, respectively which shows that scalar field anisotropic model behaves like $SCDM$ model at $m_2 = 3l_2$.

7.4 Conclusion

In this chapter, we have discussed the physical and geometrical behaviors of homogeneous and anisotropic B-V Universe with perfect fluid and scalar field. The exact solutions of Einstein's field equations have been obtained by taking the assumptions on scalar potential and scale factor. We have assumed an average scale factor and scalar potential as an exponential functions of scalar field.

We have found that the scalar field increases with time and tends to infinity as $t \to \infty$. The scalar potential decreases with time and tends to zero in late time evolution. The average scale factor is power-law form and the Universe accelerates for $m_2 \leq 2l_2$. The directional scale factors showed power-law expansion in only x-direction but in y-direction and z-direction it shows the hybrid expansion. Thus, the dominating one decides the behaviour of the expansion of the Universe. The anisotropy parameter A_p depends on cosmic time. It decreases with time and it tends to zero at late time evolution. Thus, our model approaches to isotropy state from initial anisotropy at present epoch which shows the good harmony with the current observations. We have observed that $\lim_{t\to\infty} \frac{\sigma}{\theta} = 0$ for $6l_2 - m_2 > 0$ which also indicates that in late time the anisotropic Universe approaches to an isotropic one. The other parameters such as H_1, H_2, H_3, H, θ, σ^2 etc. are decreasing functions of time, they all are tending to zero at $t \to \infty$. We have observed that the conservation equation is satisfied provided $a_1 = 0$.

In this model, the DP is independent of time, so it remains constant throughout the evolution and its value depends on the parameters l_2 and m_2. We have calculated the EoS parameter of perfect fluid and effective EoS parameter which are time-dependent. We have used observational data such as SNe Ia (Gold sample) and

H(z)+ SNe Ia to observe the behavior of ω_m and ω_{eff}. Using this observational data we have found the values of parameters l_2 and m_2 and then the values of ω_m and ω_{eff} as given in table 7.1. For these values of l_2 and m_2, the energy density is found to be positive and pressure is negative. We have also plotted the graphs for ω_m and ω_{eff} as shown in Figs. 7.1–7.4. We have observed that during the evolution of the Universe the EoS parameter ω_m varies from phantom region to quintessence region for some small values of l_2 and m_2. Thus, the model shows phantom behavior during early time and quintessence in late time evolution. The EoS parameter also has the value $\omega_m > -1$ and $\omega_{eff} > -1$ for the large values of l_2 and m_2, which show that the model behaviors like quintessence for these values of arbitrary parameters. We have listed some values of l_2 and m_2 which give the ranges of ω_m and ω_{eff} of SNe Ia (Gold Sample) and H(z)+ SNe Ia observational data, respectively. Very recently, Berezhiani et al. [306] have presented a research paper on "Universe without dark energy: cosmic acceleration from dark matter-Baryon interactions". They have presented a new idea for generating for cosmic acceleration without a source of negative pressure and without new degree of freedom beyond of Einstein gravity. The mechanism relies on the coupling between dark matter and baryons through an effective metric. We have discussed the statefinder parameters to test the viability of our model. We have found that the model would behavior like ΛCDM model for $m_2 = 0$, i.e., for constant potential. However, the scalar field model behaviors like $SCDM$ model for $m_2 = 3l_2$.

It can be concluded that the model presented in this chapter is very crucial for further investigations as the issue of accelerated expansion of the Universe has been discussed through anisotropic scalar field model along with perfect fluid.

Summary and Future Scope

Summary

In the thesis, we have carried out a dark energy phenomena of the Universe which has been predicted by many cosmological observations. In chapter 2, we have studied HDE model in well motivated and established BD theory. We have assumed a logarithmic form of BD scalar field, proposed by Kumar and Singh [181]. We have extended our study to HDE model with future event horizon as an IR cutoff and have shown that this model explains the evolution and solve the coincidence problem more effectively with the logarithmic form of BD scalar field in comparison of power-law form.

In chapter 3, the concept of bulk viscosity with new HDE has been analysed to explain the recent accelerated expansion of the Universe. It is thought that the negative pressure caused by the bulk viscosity can play the role of dark energy component and drive the accelerated expansion of the Universe. We have observed that the accelerated expansion may be possible for non-viscous case but the phase transition is not possible. It has been tried to demonstrate that the bulk viscosity can play the role as a possible candidate of dark energy. Using statefinder parameters and Om diagnostic, it has been found that our model shows the similar behavior as quintessence model and Chaplygin gas model for different values of the viscosity coefficient.

Chapter 4 is the extension of the work carried out in chapter 3, in $f(R,T)$ gravity theory. We have studied new HDE model with constant bulk viscosity in $f(R,T)$ gravity theory. We have observed that the accelerated expansion may be possible for non-viscous case in $f(R,T)$ gravity but does not show phase transition. The introduction of bulk viscosity not only makes the phase transition possible but also presents a wide range of possible evolutions of the Universe depending on parameters of the model. We have also distinguished this model from other existing dark energy models using two geometrical diagnostics: statefinder parameter and Om diagnostic. The ther-

modynamics and the local entropy have been discussed for this model. The model preserves the validity of the second law of thermodynamics as bulk viscous coefficient remains positive through the evolution of the Universe. Big-Rip and Type III singularities are obtained depending on values of model parameter.

In chapter 5, we have generalised the previous work for more general form of the bulk viscous coefficient with new HDE in the framework of $f(R,T)$ gravity theory. We have classified all possible scenarios (deceleration, acceleration and their transition) with different parameter regions chosen properly for positive and negative ranges of model parameter and viscosity coefficients to analyze the evolution of the Universe. We have also investigated the statefinder pair and Om diagnostic for this viscous model to discriminate from other existing DE models. The model evolution behaviors are shown by plotting the statefinder and $Om-z$ trajectories. The evolution of effective EoS parameter is also shown graphically. The entropy and generalized second law of thermodynamics are found to be valid for this model under some constraints on bulk viscous coefficients.

Thus, we have observed that GTR as well as $f(R,T)$ gravity have potential to explain the recent accelerated expansion of the Universe in the presence of bulk viscosity with new HDE. The concept of bulk viscosity presents a mechanism to observe accelerated expansion as well as phase transition of the Universe.

The spatially homogeneous and anisotropic Bianchi-I and Bianchi-V models with the scalar field have been studied in the chapter 6 and 7. In chapter 6, we have investigated the effect of non-interacting scalar field in the framework of Bianchi-I. We have assumed the average scale factor as an exponential function of scalar field. We have considered the solution for two cases: flat potential and exponential potential. We have obtained that the zero-rest-mass model expands with decelerated rate and behaves like a stiff matter. In case of exponential potential function, the model expands with decelerated, accelerated or shows the transition depending on the model parameters. The isotropization is observed at late-time evolution of the Universe in exponential potential model.

Chapter 7 is the extension of the previous chapter for homogeneous and anisotropic Bianchi-V model filled with perfect fluid and scalar field. The two sources have been assumed to be non-interacting. The average scale factor and scalar potential have been considered as an exponential functions of the scalar field. The observational data has been used here to find out the values of model parameters. The model

behaves like ΛCDM or $SCDM$ depending on the values of model parameters. The anisotropic models explains that in late time of evolution the anisotropic behaviour is damped out and the Universe become isotropic one which is the good harmony with the current observational data.

Future Scope

Our motive is to develop some cosmological models in the framework of BD, GTR and $f(R,T)$ theories of gravity which may be helpful in order to explain accelerated expansion of the Universe. We have considered BD theory which is a simple extension of GTR to discuss accelerated expansion. We have studied HDE model in this theory. The concepts of bulk viscosity, HDE and new HDE have been analyzed in GTR as well as in $f(R,T)$ theory.

The BD theory is an important scalar-tensor theory which provides a natural extension of GTR. We have used a logarithmic form of BD scalar field and have shown that HDE model with the future event horizon and this form of BD scalar field provides some significant results in BD theory. It may be interesting to study the behavior of perturbation of BD theory with this form of BD scalar field. It will be worthwhile to analyze whether this form of BD scalar field may provide a mechanism for structure formation to take place. There are many other area like Black hole study, DM problem etc. to discuss with this form of BD scalar field in BD theory.

As the $f(R,T)$ theory of gravitation presents a maximal coupling between matter and geometry of the Universe, therefore, it has potential to explain the problems of modern cosmology. Although, a wide range of models have been studied in this theory but still there is a good scope to do work. We have studied only first order Eckart theory of bulk viscosity in GTR and $f(R,T)$ gravity, therefore, it may be worthy to discuss the full causal theory of bulk viscosity which may provide better and more general results. The observational cosmology have not been studied considerably in this theory, therefore, there is a lot of scope in this area. The study of structure formation and perturbation theory are another main fields where a considerable work can be done.

We have assumed bulk viscous coefficient as $\zeta = \zeta_0 + \zeta_1 H$, however a second order bulk viscous coefficient as $\zeta = \zeta_0 + \zeta_1 H + \zeta_2(\frac{\dot{H}}{H^2} + H)$ may be considered to describe the late time evolution. In forthcoming paper, we will try to assume such form of ζ in GTR as well as in $f(R,T)$ gravity theory. We will also try to observationally fit these parameters and provide the best fit values to the parameters.

In case of anisotropic models, we can extend the concept of scalar field for other Bianchi models and can also do observational study to conclude more about the anisotropic behaviour of the Universe.

Bibliography

[1] E.P. Hubble; *A relation between distance and radial velocity among extra-galactic nebulae*, Proc. Nat. Acad. of Sci. USA **15**, 168 (1929).

[2] A. Einstein; *The foundation of the general theory of relativity*, Annalen Phys. **49**, 769 (1916); Sitz. Preuss. Akad. Wiss. Phys. **1**, 142 (4) (1917); Annalen Phys. **69**, 436 (1922).

[3] A. Friedmann; *Über die Krümmung des Raumes*, Zeitschriftfür Physik **10**, 377 (1922).

[4] S. Weinberg; *Gravitation and Cosmology: Principles and applications of the General Theory of Relativity*, John Wiley & Sons, ISBN-13: 978-0471925675, ISBN-10: 0471925675 (1972).

[5] C.B. Netterfield et al.; *A measurement by Boomerang of multiple peaks in the angular power spectrum of the cosmic microwave background (Boomerang Collaboration)*, Astrophys. J. **571**, 604 (2002); [arXiv:astro-ph/0104460].

[6] G. Hinshaw et al.; *Nine-Year Wilkinson Microwave Anisotropy Probe (WMAP) observations: Cosmological parameter results*, Astrophys. J. Suppl., **208**, 19 (2013); [arXiv:astro-ph/1212.5226].

[7] G.F.R. Ellis, M.A.H. MacCallum; *A class of homogeneous cosmological models*, Comm. Math. Phys. **12**, 108 (1969).

[8] S. Prakash; *Relativistic Mechanics (Theory of Relativity)*, Pragati Prakashan Meerut, ISBN- 978-93-5140-202-2, SEventeenth Edition (2015).

[9] G. Lemaître; *Un Univers homogène de masse constante et de rayon croissant rendant compte de la vitesse radiale des nébuleuses extra-galactiques*, Annales de la Société Scientifique de Bruxelles **47**, 49 (1927).

[10] A.S. Eddington; *The Mathematical Theory of Relativity*, Cambridge University Press, (1923).

[11] A.H. Guth; *Inflationary Universe: A possible solution to the horizon and flatness problems*, Phys. Rev. D **23**, 347 (1981).

[12] A.D. Linde; *Chaotic inflation*, Phys. Lett. B **129**, 177 (1983)

[13] A.D. Linde; *Particle Physics and inflationary cosmology*, Contemp. Concepts Phys. **5**, 1 (2005); [arXiv:hep-th/0503203].

[14] A. Albrecht, P.J. Steinhardt; *Cosmology for grand unified theories with radiatively induced symmetry breaking*, Phys. Rev. Lett. **48**, 1200 (1982).

[15] A. Albrecht et al.; *Reheating an inflationary universe*, Phys. Rev. Lett. **48**, 1437 (1982).

[16] S. Perlmutter et al.; *Measurements of Omega and Lambda from 42 high redshift supernovae (The Supernova Cosmology Project)*, Astrophys. J. **517**, 565 (1999); [arXiv:astro-ph/9812133].

[17] A.G. Riess et al.; *Observational evidence from supernovae for an accelerating Universe and a cosmological constant (Supernova Search Team Collaboration)*, Astron. J. **116**, 1009 (1998); [arXiv:astro-ph/9805201].

[18] C.L. Bennett et al.; *Nine-Year Wilkinson Microwave Anisotropy Probe (WMAP) Observations: Final maps and results (WMAP Collaboration)* Astrophys. J. Suppl., **208**, 20 (2013); [arXiv:astro-ph/1212.5225].

[19] P.A.R. Ade et al.; *Planck 2013 results. I. Overview of products and scientific results (Planck Collaboration)*, Astron. Astrophys. **571**, A1 (2014); [arXiv:astro-ph/1303.5062].

[20] L. Anderson et al.; *The clustering of galaxies in the SDSS-III Baryon Oscillation Spectroscopic Survey: Baryon Acoustic Oscillations in the data release 9 spectroscopic galaxy sample*, Mon. Not. Roy. Astron. Soc. **427**, 3435 (2013); [arXiv:astro-ph/1203.6594].

[21] L.M. Krauss, M. Turner; *The cosmological constant is back*, Gen. Rel. Grav. **27**, 1137 (1995); [arXiv:astro-ph/9504003].

[22] V. Sahni, A.A. Starobinsky; *The case for a positive cosmological Λ-term*, Int. J. Mod. Phys. D **9**, 373 (2000); [arXiv:astro-ph/9904398].

[23] S.M. Carroll; *The cosmological constant*, Living Rev. Rel. **4**, 1 (2001); [arXiv:astro-ph/0004075].

[24] P.J.E. Peebles, B. Ratra; *The Cosmological constant and dark energy*, Rev. Mod. Phys. **75**, 559 (2003); [arXiv:astro-ph/0207347].

[25] T. Padmanabhan; *Cosmological constant: The weight of the vacuum*, Phys. Rept. **380**, 235 (2003); [arXiv:hep-th/0212290].

[26] P. Steinhardt; *Critical Problems in Physics*, edited by V.L. Fitch, D.R. Marlow (Princeton University Press, Princeton, NJ, 1997).

[27] I. Zlatev, L.M. Wang, P.J. Steinhardt; *Quintessence, cosmic coincidence, and the cosmological constant*, Phys. Rev. Lett. **82**, 896 (1999); [arXiv:astro-ph/9807002].

[28] E.J. Copeland, M. Sami, S. Tsujikawa; *Dynamics of dark energy*, Int. J. Mod. Phys. D **15**, 1753 (2006); [arXiv:hep-th/0603057].

[29] P.J. Peebles, R. Ratra; *Cosmology with a time-variable cosmological "constant"*, Astrophys J. **325**, L17 (1988).

[30] C. Wetterich; *The cosmon model for an asymptotically vanishing time-dependent cosmological "constant"*, Astron. and Astrophys. **301**, 321 (1995); [arXiv:hep-th/9408025].

[31] L.H. Ford; *Cosmological-constant damping by unstable scalar fields*, Phys. Rev. D **35**, 2339 (1987).

[32] R.R. Caldwell, R. Dave, P.J. Steinherdt; *Cosmological imprint of an energy component with general equation of state*, Phys. Rev. Lett. **80**, 1582 (1998).

[33] E.J. Copeland, A.R. Liddle, D. Wands; *Exponential potentials, scaling solutions and inflation*, Ann. N. Y. Acad. Sci. **688**, 647 (1993).

[34] P.J. Steinhardt, L.M. Wang, I. Zlatev; *Cosmological tracking solutions*, Phys. Rev. D **59**, 123504 (1999); [arXiv:astro-ph/9812313].

[35] T. Chiba; *Quintessence, the gravitational constant, and gravity*, Phys. Rev. D **60**, 083508 (1999); [arXiv:gr-qc/9903094].

[36] L. Wang, R.R. Caldwell, J.P. Ostriker, P.J. Steinhardt; *Cosmic concordance and quintessence*, Astrophys J. **530**, 17 (2000); [arXiv:astro-ph/9901388].

[37] W. Zimdahl, D. Pavón, L.P. Chimento; *Interacting Quintessence*, Phys. Lett. B **521**, 133 (2001).

[38] J. Martin; *Quintessence: a mini-review*, Mod. Phys. Lett. A **23**, 1252 (2008); [arXiv:astro-ph/0803.4076].

[39] R. Ratra, P.J. Peebles; *Cosmological consequences of a rolling homogeneous scalar field*, Phys. Rev. D **37**, 3406 (1988).

[40] J.D. Barrow, P. Saich; *Scalar field cosmologies*, Class. Quantum Grav. **10**, 279 (1993).

[41] A.B. Burd, J.D. Barrow; *Inflationary models with exponential potentials*, Nucl. Phys. B **308**, 929 (1988).

[42] J.W. Lee, I.G. Koh; *Galactic halos as boson stars*, Phys. Rev. D **53**, 2236 (1996); [arXiv:hep-ph/9507385].

[43] V. Sahni; *Dark matter and dark energy*, Lect. Notes Phys. **653**, 141 (2004); [arXiv:astro-ph/0403324].

[44] V. Sahni, A. Starobinsky; *Reconstructing dark energy*, Int. J. Mod. Phys. D **15**, 2105 (2006); [arXiv:astro-ph/0610026].

[45] A. Melchiorri et al.; *The state of the dark energy equation of state*, Phys. Rev. D **68**, 043509 (2003); [arXiv:astro-ph/0211522].

[46] B.A. Bassett, P.S. Corasaniti, M. Kunz; *The essence of quintessence and the cost of compression*, Astrophys. J. **617**, L1 (2004); [arXiv:astro-ph/0407364].

[47] U. Alam et al.; *Is there Supernova evidence for dark energy metamorphosis ?*, Mon. Not. Roy. Astron. Soc. **354**, 275 (2004); [arXiv:astro-ph/0311364].

[48] D. Huterer, A. Cooray; *Uncorrelated estimates of dark energy evolution*, Phys. Rev. D **71**, 023506 (2005); [arXiv:astro-ph/0404062].

[49] G.B. Zhao, X. Zhang; *Probing dark energy dynamics from current and future cosmological observations*, Phys. Rev. D **81**, 043518 (2010); [arXiv:astro-ph/0908.1568].

[50] R.R. Caldwell; *A Phantom Menace? Cosmological consequences of a dark energy component with super-negative equation of state*, Phys. Lett. B **545**, 23 (2002); [arXiv:astro-ph/9908168].

[51] V. Faraoni; *Superquintessence*, Int. J. Mod. Phys. D **11**, 471 (2002).

[52] R.R. Caldwell, M. Kamionkowski, N.N. Weinberg; *Phantom energy and Cosmic Doomsday*, Phys. Rev. Lett. **91**, 071301 (2003); [arXiv:astro-ph/0302506].

[53] Z.K. Guo, Y.S. Piao, X.M. Zhang, Y.Z. Zhang; *Cosmological evolution of a quintom model of dark energy*, Phys. Lett. B **608**, 177 (2005); [arXiv: astro-ph/0410654].

[54] T. Padmanabhan; *Accelerated expansion of the Universe driven by tachyonic matter*, Phys. Rev. D **66**, 021301 (2002); [arXiv:hep-th/0204150].

[55] G.W. Gibbons; *Cosmological evolution of the rolling tachyon*, Phys. Lett. B **537**, 1 (2002); [arXiv:hep-th/0204008].

[56] S. Tsujikawa, M. Sami; *A unified approach to scaling solutions in a general cosmological background*, Phys. Lett. B **603**, 113 (2004); [arXiv:hep-th/0409212].

[57] T. Chiba, T. Okabe, M. Yamaguchi; *Kinetically driven quintessence*, Phys. Rev. D **62**, 023511 (2000); [arXiv:astro-ph/9912463].

[58] C. Armendariz-Picon, V.F. Mukhanov, P.J. Steinhardt; *Essentials of k-essence*, Phys. Rev. D **63**, 103510 (2001); [arXiv:astro-ph/0006373].

[59] A. Kamenshchik, U. Moschella, V. Pasquier; *An alternative to quintessence*, Phys. Lett. B **511**, 265 (2001); [arXiv:gr-qc/0103004].

[60] M.C. Bento, O. Bertolami, A.A. Sen; *Generalized Chaplygin gas, accelerated expansion and dark energy-matter unification*, Phys. Rev. D **66**, 043507 (2002); [arXiv:gr-qc/0202064].

[61] M. Sami, A. Toporensky; *Phantom field and the fate of Universe*, Mod. Phys. Lett. A **19**, 1509 (2004); [arXiv:gr-qc/0312009].

[62] E. Elizalde, S. Nojiri, S.D. Odintsov; *Late-time cosmology in (phantom) scalar-tensor theory: dark energy and the cosmic speed-up*, Phys. Rev. D **70**, 043539 (2004); [arXiv:hep-th/0405034].

[63] J.A. Frieman, I. Waga; *Constraints from high redshift supernovae upon scalar field cosmologies*, Phys. Rev. D **57**, 4642 (1998).

[64] G. 't Hooft; *Dimensional reduction in quantum gravity*, [arXiv:gr-qc/9310026].

[65] L. Susskind; *The world as a hologram*, J. Math. Phys. **36**, 6377 (1995).

[66] J.M. Maldacena; *The Large N limit of superconformal field theories and supergravity*, Int. J. Theor. Phys. **38**, 1113 (1999).

[67] M. Li; *A model of holographic dark energy*, Phys. Lett. B **603**, 1 (2004).

[68] S.D.H. Hsu; *Entropy bounds and dark energy*, Phys. Lett. B **594**, 13 (2004).

[69] Q. Wu, Y. Gong, A. Wang, J.S. Alcaniz; *Current constraints on interacting holographic dark energy*, Phys. Lett. B **659**, 34 (2008).

[70] L. Xu, W. Li, J. Lu; *Holographic dark energy in Brans-Dicke theory*, Eur. Phys. J. C **60**, 135 (2009).

[71] D. Pavón, W. Zimdahl; *Holographic dark energy and cosmic coincidence*, Phys. Lett. B **628**, 206 (2005).

[72] S. Nojiri, S.D. Odintsov; *Unifying phantom inflation with late-time acceleration: scalar phantomŰnon-phantom transition model and generalized holographic dark energy*, Gen. Relativ. Gravit. **38**, 1285 (2006).

[73] L.N. Granda, A. Oliveros; *Infrared cut-off proposal for the holographic density*, Phys. Lett. B **669**, 275 (2008).

[74] Y. Wang, L. Xu; *Current observational constraints to the holographic dark energy model with a new infrared cutoff via the Markov chain Monte Carlo method*, Phys. Rev. D **81**, 083523 (2010).

[75] L.N. Granda, A. Oliveros; *New infrared cut-off for the holographic scalar fields models of dark energy*, Phys. Lett. B **671**, 199 (2009).

[76] K. Karami, J. Fehri; *New holographic scalar field models of dark energy in non-flat universe*, Phy. Lett. B **684**, 61 (2010).

[77] M. Malekjani, A. Khodam-Mohammadi, N. Nazari-pooya; *Cosmological evolution and statefinder diagnostic for new holographic dark energy model in non flat universe*, Astrophys. Space Sci. **332**, 515 (2011).

[78] M. Sharif, A. Jawad; *Cosmological evolution of interacting new holographic dark energy in non-flat universe*, Eur. Phys. J. C **72**, 2097 (2012); [arXiv: gr-qc/1212.0129].

[79] U. Debnath, S. Chattopadhyay; *Statefinder and Om diagnostics for interacting new holographic dark energy model and generalized second law of thermodynamics*, Int. J. Theo. Phys. **52**, 1250 (2013); [arXiv: Phys-gen-ph/1102.009v2].

[80] A. Oliveros, M.A. Acero; *New holographic dark energy model with non-linear interaction*, Astrophys. Space Sci. **357**, 12 (2015).

[81] H. Weyl; *A new extension of Relativity Theory (In German)*, Annalen Phys. **59**, 101 (1919); Surveys High Energy Phys. **5**, 237 (1986); Annalen Phys. **364**, 101 (1919).

[82] T. Kaluza; *Zum Unitätsproblem der Physik*, Sitz. Preuss. Akad. Wiss. Phys. Math. **K1**, 966 (1921); T. Appelquist, A. Chodos, P.G.O. Freund; *Modern Kaluza-Klein theories*, Addison-Wesley, (1987).

[83] O. Klein; *Quantentheorie und fünfdimensionale Relativitätstheorie*, Zeits. Phys. **37**, 895 (1926); Nature **118**, 516 (1926); T. Appelquist, A. Chodos, P.G.O. Freund; *Modern Kaluza-Klein theories*, Addison-Wesley, (1987).

[84] E. Witten; *String theory dynamics in various dimensions*, Nucl. Phys. B **443**, 85 (1995); [arXiv:hep-th/9503124].

[85] K. Becker, M. Becker, J.H. Schwarz; *String theory and M-theory: A modern introduction*, Cambridge University Press, ISBN: 978-0-512-86069-7 (2007).

[86] P.G. Bergmann; *Unified field theory with fifteen variables*, Ann. Math **49**, 225 (1948).

[87] G.W. Horndeshe; *Second order scalar tensor field equations in a four-dimensional space*, Int. J. Theor. Phys. **10**, 363 (1974).

[88] R. Utiyama, B. S. DeWitt; *Renormalization of a classical gravitational field interacting with quantized matter fields*, J. Math. Phys. **3**, 608 (1962).

[89] A. Starobinsky; *A new type of isotropic cosmological models without singularity*, Phys. Lett. B **91**, 99 (1980).

[90] H.A. Buchdahl; *Non-linear Lagrangians and cosmological theory*, Mon. Not. Roy. Astron. Soc. **150**, 1 (1970).

[91] S. Nojiri, S.D. Odintsov; *Unified cosmic history in modified gravity: From $f(R)$ theory to Lorentz non-invariant models*, Phys. Rept. **505**, 59 (2011); [arXiv:gr-qc/1011.0544].

[92] A.A. Starobinsky; *Disappearing cosmological constant in $f(R)$ gravity*, JETP Lett. **86**, 157 (2007); [arXiv:astro-ph/0706.2041].

[93] T.P. Sotiriou, V. Faraoni; *$f(R)$ theories of gravity*, Rev. Mod. Phys. **82**, 451 (2010); [arXiv:gr-qc/0805.1726].

[94] S. Capozziello, V.F. Cardone, S. Carloni, A. Troisi; *Quintessence without scalar fields*, Rec. Res. Dev. Astron. Astrophys. **1**, 625 (2003); [arXiv:astro-ph/0303041].

[95] S. Capozziello, M. Francaviglia; *Extended theories of gravity and their cosmological and astrophysical applications*, Gen. Rel. Grav. **40**, 357 (2008); [arXiv:astro-ph/0706.1146].

[96] A. De Felice, S. Tsujikawa; *$f(R)$ theories*, Living Rev. Rel. **13**, 3 (2010); [arXiv:gr-qc/1002.4928].

[97] S. Nojiri, S.D. Odintsov; *Introduction to modified gravity and gravitational alternative for dark energy*, Int. J. Geom. Math. Mod. Phys. **4**, 115 (2007); [arXiv:hep-th/0601213].

[98] G. Cognola et al.; *Dark energy in modified Gauss-Bonnet gravity: Late-time acceleration and the hierarchy problem*, Phys. Rev. D **73**, 084007 (2006); [arXiv:hep-th/0601008].

[99] S. Nojiri, S.D. Odintsov; *Modified Gauss-Bonnet theory as gravitational alternative for dark energy*, Phys. Lett. B **631**, 1 (2005); [arXiv:hep-th/0508049].

[100] C. Brans, R.H. Dicke; *Mach's principle and a relativistic theory of gravitation*, Phys. Rev. **124**, 925 (1961).

[101] D. La, P.J. Steinhardt; *Extended infationary cosmology*, Phys. Rev. Lett. **62**, 376 (1989).

[102] Z. Berezhiania et al.; *Vanishing of cosmological constant and fully localized gravity in a brane world with extra time(s)*, Phys. Lett. B **517**, 387 (2001).

[103] R. Maartens, K. Koyama; *Brane-world gravity*, Living Rev. Rel. **13**, 5 (2010).

[104] P. Horava; *Quantum gravity at a Lifshitz point*, Phys. Rev. D **79**, 084008 (2009); [arXiv:hep-th/0901.3775].

[105] P. Horava; *Membranes at quantum criticality*, JHEP **0903**, 020 (2009); [arXiv:hep-th/0812.4287].

[106] Y. Zhang et al.; *Notes on f(T) theories*, J. Cosmol. Astropart. Phys **07**, 015 (2011).

[107] E.V. Linder; *Einstein's other gravity and the acceleration of the Universe*, Phys. Rev. D **81**, 127301 (2010); [arXiv:astro-ph/1005.3039].

[108] T. Harko et al.; *f(R, T) gravity*, Phys. Rev. D **84**, 024020 (2011).

[109] A. Pasqua, S. Chattopadhyay, I. Khomenkoc; *A reconstruction of modified holographic Ricci dark energy in $f(R,T)$ gravity*, Canadian J. Phys. **91**, 632 (2013); [arXiv:gen-ph1305.1873].

[110] T.P. Sotiriou, V. Faraoni, S. Liberati; *Theory of gravitation theories: A no-progress report*, Int. J. Mod. Phys. D **17**, 399 (2008); [arXiv:gr-qc/0707.2748].

[111] B. Bertotti, L. Iess, P. Tortora; *A test of general relativity using radio links with the Cassini spacecraft*, Nature **425**, 374 (2003).

[112] C. Mathiazhagen, V.B. Johri; *An infationary universe in Brans-Dicke theory: A hopeful sign of theoretical estimation of the gravitational constant*, Class. Quantum Grav. **1**, L29 (1984).

[113] A.D. Linde; *Extended chaotic inflation and spatial variations of the gravitational constant*, Phys. Lett. B **238**, 160 (1990).

[114] N. Banerjee, A. Beesham; *Brans-Dicke cosmology with causal viscous fluid*, Aust. J. Phys. 49, 899 (1996).

[115] S. Ram, C.P. Singh; *Early Cosmological Models with Bulk Viscosity in Brans-Dicke Theory*, Astrophys. Space Sci. **254**, 143 (1997); *Early universe in Brans-Dicke cosmology*, Nuovo Cim. B **114**, 245 (1999).

[116] A.R. Liddle, A. Mazumdar, J.D. Barrow; *The radiation-matter transition in Jordan-Brans-Dicke theory*, Phys. Rev. D **58**, 027302 (1998).

[117] S. de Campo, R. Herrera, P. Labrãna; *Emergent Universe in a Jordan-Brans-Dicke theory*, J. Cosm. Aastropart. Phys. **030**, 0711 (2007); [arXiv:gr-qc/0711.1559]

[118] C.P. Singh; *FRW models with particle creation in Brans-Dicke theory*, Astrophys. Space Sci. **338**, 411 (2012).

[119] M. Campanelli, C.O. Lousto; *Are black holes in Brans-Dicke theory precisely the same as in general relativity?*, Int. J. Mod. Phys. D **02**, 451 (1993).

[120] G. Kang; *Black hole area in Brans-Dicke theory*, Phys. Rev. D **54**, 7483 (1996).

[121] T. Tamaki, T. Torii, K. Maeda; *Non-abelian black holes in Brans-Dicke theory*, Phys. Rev. D **57**, 4870 (1998).

[122] H. Kim; *New black hole solutions in Brans-Dicke theory of gravity*, Phys. Rev. D **60**, 024001 (1999).

[123] H. Maeda, G. Giribet; *Lifshitz black holes in Brans-Dicke theory*, JHEP **11**, 015 (2011); [arXiv: gr-qc/1105.1331].

[124] H. Kim; *Brans-Dicke theory as a unified model for dark matter-dark energy*, Mon. Not. R. Astron. Soc. Lett. **364**, 813 (2005).

[125] T. Clifton, J.D. Barrow; *Decaying gravity*, Phys. Rev. D **73**, 104022 (2006).

[126] O. Bertolami, P.J. Martins; *Nonminimal coupling and quintessence*, Phys. Rev. D **61**, 064007 (2000).

[127] T. Harko; *Modified gravity with arbitrary coupling between matter and geometry*, Phys. Lett. B **669**, 376 (2008).

[128] T. Harko, F.S.N. Lobo; $f(R, L_m)$ gravity, Eur. Phys. J. C **70**, 373 (2010).

[129] L.D. Landau, E.M. Lifshitz; *The classical theory of field*, Butterwash Heinemann, Oxford (1998).

[130] T. Harko; *Thermodynamic interpretation of the generalized gravity models with geometry-matter coupling*, Phys. Rev. D **90**, 044067 (2014).

[131] M.J.S. Houndjo, C.E.M. Batista, J.P. Campos, O.F. Piattella; *Finite-time singularities in $f(R,T)$ gravity and the effect of conformal anomaly*, Canadian J. Phys. **91**, 548 (2013); [arXiv:gr-qc/1203.6084].

[132] M. Sharif, M. Zubair; *Thermodynamics in $f(R,T)$ theory of gravity*, J. Cosmo. Astropart. Phys. **03**, 028 (2012); [arXiv:gr-qc/1204.0848].

[133] T. Azizi; *Wormhole geometries in $f(R,T)$ gravity*, Int. J. Theor. Phys. **52**, 3486 (2013); [arXiv:gr-qc/1205.6957].

[134] S. Chakraborty; *An alternative $f(R,T)$ gravity theory and the dark energy problem*, Gen. Rel. Grav. **45**, 2039 (2013); [arXiv:gen-ph/1212.3050].

[135] F.G. Alvarenga et al.; *Dynamics of scalar perturbations in $f(R,T)$ gravity*, Phys. Rev. D **87**, 103526 (2013); [arXiv:gr-qc/1302.1866].

[136] E.H. Baffou et al.; *Cosmological viable f(R,T) dark energy model: dynamics and stability*, Astrophys. Space Sci. **356**, 173 (2015).

[137] H. Shabani, M. Farhoudi; *Cosmological and solar system consequences of $f(R,T)$ gravity models*, Phys. Rev. D **90**, 044031 (2014).

[138] V. Fayaz et al.; *Anisotropic cosmological models in $f(R,T)$ gravity according to holographic and new agegraphic dark energy*, Astrophys. space Sci. **353**, 301 (2014).

[139] M. Jamil, D. Momeni, M. Raza, R. Myrzakulov; *Reconstruction of some cosmological models in $f(R,T)$ gravity*, Eur. Phys. J. C **72**, 1999 (2012); [arXiv:gen-ph/1107.5807].

[140] M.J.S. Houndjo; *Reconstruction of $f(R,T)$ gravity describing matter-dominated and accelerated phases*, Int. J. Mod. Phys. D **21**, 1250003 (2012); [arXiv:astro-ph/1107.3887].

[141] M.J.S. Houndjo, O.F. Piattella; *Reconstructing $f(R,T)$ gravity from holographic dark energy*, Int. J. Mod. Phys. D **2**, 1250024 (2012); [arXiv:gr-qc/1111.4275].

[142] C.P. Singh, V. Singh; *Reconstruction of modified $f(R,T)$ gravity with perfect fluid cosmological models*, Gen. Relativ. Gravit. **46**, 1696 (2014).

[143] M. Sharif, S. Rani, R. Myrzakulov; *Analysis of $f(R,T)$ gravity models through energy conditions*, Eur. Phys. J. Plus **128**, 123 (2013); [arXiv:gr-qc/1210.2714].

[144] F.G. Alvarenga, M.J. Houndjo, A.V. Monwanou, J.B. Chabi Oron; *Testing some $f(R,T)$ gravity models from energy conditions*, J. Mod. Phys. **4**, 130 (2013); [arXiv:gr-qc/1205.4678].

[145] M. Sharif, M. Zubair; *Anisotropic Universe models with perfect fluid and scalar field in $f(R,T)$ gravity*, J. Phys. Soc. Jpn. **81**, 114005 (2012); [arXiv:gr-qc/1301.2251].

[146] K.S. Adhav; *LRS Bianchi type-I cosmological model in $f(R,T)$ theory of gravity*, Astrphys. Space Sci. **339**, 365 (2012).

[147] M. Sharif, M. Zubair; *Energy conditions constraints and stability of power law solutions in $f(R,T)$ gravity*, J. Phys. Soc. Jpn. **82**, 014002 (2013); [arXiv:gr-qc/1210.3878].

[148] H. Shabani, M. Farhoudi; *$f(R,T)$ cosmological models in phase space*, Phys. Rev. D **88**, 044048 (2013); [arXiv:gr-qc/1306.3164].

[149] V.U.M. Rao, D. Neelima; *Bianchi type-VI_0 perfect fluid cosmological model in a modified theory of gravity*, Astrophys. Space Sci. **345**, 427 (2013).

[150] N. Ahmed, A. Pradhan; *Bianchi Type-V cosmology in $f(R,T)$ gravity with $\Lambda(T)$*, Int. J. Theor. Phys. **53**, 289 (2014); [arXiv:.gen-ph/1303.3000].

[151] C. Eckart; *The thermodynamics of irreversible processes. III. relativistic theory of the simple fluid*, Phys. Rev. **58**, 919 (1940).

[152] W. Israel, J. Stewart; *Transient relativistic thermodynamics and kinetic theory*, Ann. Phys. **118**, 341 (1979).

[153] X.H. Meng, J. Ren, M.G. Hu; *Friedmann cosmology with a generalized equation of state and bulk viscosity*, Commun. Theor. Phys. **47**, 379 (2007).

[154] J. Ren, X.H. Meng; *Cosmological model with viscosity media (dark fluid) described by an effective equation of state*, Phys. Lett. B **633**, 1 (2006).

[155] M.G. Hu, X.H. Meng; *Bulk viscous cosmology: Statefinder and entropy*, Phys. Lett. B **635**, 186 (2006).

[156] C.P. Singh, S. Kumar, A. Pradhan; *Early viscous universe with variable gravitational and cosmological constants*, Class. Quantum Grav. **24**, 455 (2007).

[157] C.P. Singh; *Bulk viscous cosmology in early universe*, Pramana J. Phys. **71**, 33 (2008).

[158] C.P. Singh; *Viscous FRW models with particle creation in early universe*, Mod. Phys. Lett. A **27**, 1250070 (2012).

[159] C.P. Singh, P. Kumar, *Friedmann model with viscous cosmology in modified $f(R,T)$ gravity theory*, Eur. Phys. J. C **74**, 3070 (2014).

[160] P. Kumar, C.P. Singh; *Viscous cosmology with matter creation in modified $f(R,T)$ gravity*, Astrophys. Space Sci. **357**, 120 (2015).

[161] C.W. Misner, *The Isotropy of the Universe*, Astrophysical J. **151**, 431 (1968).

[162] R. Maarten; *Dissipative cosmology*, Class. Quantum Phys. **12**, 1455 (1995).

[163] G.L. Murphy; *Big-Bang model without singularities*, Phys. Rev. D **8**, 4231 (1973).

[164] J.D. Barrow; *String-driven inflationary and deflationary cosmological models*, Nucl. Phys. B **310**, 743 (1988).

[165] Y.D. Xu, Z.G. Huang, X.H. Zhai; *Generalized Chaplygin gas model with or without viscosity in the $w-w'$ plane*, Astrophys. Space Sci. **337**, 493 (2012).

[166] C.J. Feng, X.Z. Li; *Viscous Ricci dark energy*, Phys. Lett. B **680**, 355 (2009).

[167] S. Nojiri, S.D. Odintsov; *Inhomogeneous equation of state of the universe: Phantom era, future singularity, and crossing the phantom barrier*, Phys. Rev. D **72**, 023003 (2005).

[168] S. Capozziello et al.; *Observational constraints on dark energy with generalized equations of state*, Phys. Rev. D **73**, 043512 (2006).

[169] N. Cruz, S. Lepe, F. Peña; *Dissipative generalized Chaplygin gas as phantom dark energy*, Phys. Lett. B **646**, 177 (2007).

[170] M. Cataldo, N. Cruz, S. Lepe; *Viscous dark energy and phantom evolution*, Phys. Lett. B **619**, 5 (2005).

[171] L. Sebastiani; *Dark viscous fluid coupled with dark matter and future singularity*, Eur. Phys. J. C **69**, 547 (2010).

[172] M.R. Setare, A. Sheykhi; *Viscous dark energy and generalized second law of thermodynamics*, Int. J. Mod. Phys. D **19**, 1205 (2010).

[173] J.N. Grieb et al.; *The clustering of galaxies in the completed SDSS-III Baryon Oscillation Spectroscopic Survey: Cosmological implications of the Fourier space wedges of the final sample*; [arXiv:astro-ph/1607.03143].

[174] V. Sahni, T.D. Saini, A.A. Starobinsky, U. Alam; *Statefinder-A new geometrical diagnostic of dark energy*, JETP Lett. **77**, 201 (2003).

[175] U. Alam, V. Sahni, T.D. Saini, A.A. Starobinsky; *Exploring the expanding universe and dark energy using the statefinder diagnostic*, Mon. Not. R. Astron. Soc. **344**, 1057 (2003).

[176] V. Sahni, A. Shafieloo, A.A. Starobinsky; *Two new diagnostics of dark energy*, Phys. Rev. D **78**, 103502 (2008).

[177] M.L. Tong, Y. Zhang; *Cosmic age, statefinder, and Om diagnostics in the decaying vacuum cosmology*, Phys. Rev. D **80**, 023503 (2009).

[178] J.B. Lu, L.X. Xu; *Geometrical diagnostic for the generalised chaplygin gas model*, Int. J. Mod. Phys. D **18**, 1741 (2009).

[179] Z.G. Huang, H.Q. Lu, K. Zhang; *Om diagnostic for dilaton dark energy*, Astrophys. Space Sci. **331**, 331 (2011).

[180] C. Gao, F. Wu, X. Chen; *Holographic dark energy model from Ricci scalar curvature*, Phys. Rev. D **79**, 043511 (2009).

[181] P. Kumar, C.P. Singh; *New agegraphic dark energy model in Brans-Dicke theory with logarithmic form of scalar field*, Astrophys. Space Sci. **362**, 52 (2017).

[182] C.P. Singh, P. Kumar; *Holographic dark energy in Brans-Dicke theory with logarithmic form of scalar field*, Int. J. Theor. Phys. **56**, 3297 (2017).

[183] M.R. Setare; *The holographic dark energy in non-flat Brans-Dicke cosmology*, Phy. Lett. B **644**, 99 (2007).

[184] M.R. Setare; *Interacting holographic phantom*, Eur. Phys. J. C **50**, 991 (2007).

[185] N. Cruz, S. Lepe, F. Peña, J. Saavedra; *Holographic dark energy interacting with dark matter in a closed universe*, Phys. Lett. B **669**, 271 (2008).

[186] J. Zhang, X. Zhang, H. Liu; *Statefinder diagnosis for the interacting model of holographic dark energy*, Phys. Lett. B **659**, 26 (2008).

[187] A. Sheykhi; *Interacting holographic dark energy in Brans-Dicke theory*, Phys. Lett. B **681**, 205 (2009).

[188] V.B. Johri, K. Desikan; *Cosmological models with constant deceleration parameter in Brans-Dicke theory*, Gen. Relativ. Gravit. **26**, 1217 (1994).

[189] V.B. Johri, R. Sudharsan; *BD-FRW cosmology with bulk viscosity*, Aust. J. Phys. **42**, 215 (1989).

[190] N. Banerjee, D. Pavón; *Holographic dark energy in Brans-Dicke theory*, Phys. Lett. B **647**, 477 (2007).

[191] X.L. Liu, X. Zhang; *New Agegraphic Dark Energy in Brans-Dicke Theory*, Comm. Theor. Phys. **52**, 761 (2009).

[192] A. Sheykhi; *Interacting new agegraphic dark energy in non-flat Brans-Dicke cosmology*, Phys. Rev. D **81**, 023525 (2010).

[193] S. Chattopadhyay, A. Pasqua, M. Khurshudayan; *New holographic reconstruction of scalar-field dark-energy models in the framework of chameleon Brans-Dicke cosmology*, Eur. Phys. J. C **74**, 3080 (2014).

[194] M. Li, X.D. Li, S. Wang, X. Zhang; *Holographic dark energy models: a comparison from the latest observational data*, JCAP **06**, 036 (2009).

[195] Q.G. Huang, M. Li; *The holographic dark energy in a non-flat universe*, JCAP **08**, 013 (2004).

[196] C. Will; *The Confrontation between general relativity and experiment*, Living Rev. Relativity **9**, 3 (2006).

[197] L. Xu et al.; *Cosmic constraints on holographic dark energy in Brans-Dicke theory via Markov-chain Monte-Carlo method*, Mod. Phys. Lett. A **25**, 1441 (2010).

[198] V. Acquaviva et al.; *Structure formation constraints on the Jordan-Brans-Dicke theory*, Phys. Rev. D **71**, 104025 (2005).

[199] F.Q. Wu, X. Chen; *Cosmic microwave background with Brans-Dicke gravity. II. Constraints with the WMAP and SDSS data*, Phys. Rev. D **82**, 083003 (2010).

[200] Y.C. Li, F.Q. Wu, X. Chen; *Constraints on the Brans-Dicke gravity theory with the Planck data*, Phys. Rev. D **88**, 084053 (2013).

[201] L. Amendola; *Scaling solutions in general nonminimal coupling theories*, Phys. Rev. D **60**, 043501 (1999).

[202] L. Amendola; *Coupled quintessence*, Phys. Rev. D **62**, 043511 (2000).

[203] K. Karwan; *The coincidence problem and interacting holographic dark energy*, JCAP **05**, 011 (2008).

[204] V. Acquaviva, L. Verde; *Observational signatures of Jordan-Brans-Dicke theories of gravity*, JCAP **12**, 001 (2007).

[205] C. Feng et al.; *Observational constraints on the dark energy and dark matter mutual coupling*, Phys. Lett. B **665**, 111 (2008).

[206] R. Bousso; *The holographic principle for general backgrounds*, Class. quantum Grav. **17**, 997 (2000).

[207] A.G. Cohen, D.B. Kaplan, A.E. Nelson; *Effective field theory, black holes, and the cosmological constant*, Phys. Rev. Lett. **82**, 4971 (1999).

[208] X.H. Meng, X. Duo; *Friedmann Cosmology with Bulk Viscosity: A Concrete Model for Dark Energy*, Commun. Theor. Phys. **52**, 377 (2009).

[209] I. Brevik, O. Gorbunova, Y.A. Shaido; *Viscous FRW Cosmology in Modified Gravity*, Int. J. Mod. Phys. D **14**, 1899 (2005).

[210] I. Brevik, O. Gorbunova; *Viscous Dark Cosmology with Account of Quantum Effects*, Eur. Phys. J. C **56**, 425 (2008).

[211] I. Brevik, O. Gorbunova, D.S. Gomez; *Casimir effects near the big rip singularity in viscous cosmology*, Gen. Relativ. Gravit. **42**, 1513 (2010).

[212] W. Zimdahl, D. Pavón; *Scaling Cosmology*, Gen. Relativ. Gravit. **35**, 413 (2003).

[213] L.P. Chimento, A.S. Jakubi, D. Pavón, W. Zimdahl; *Interacting quintessence solution to the coincidence problem*, Phys. Rev. D **67**, 083513 (2003).

[214] R. Maartens; *Dissipative cosmology*, Class. Quantum Gravity **12**, 1455 (1995).

[215] A. Avelino, U. Nucamendi; *Exploring a matter-dominated model with bulk viscosity to drive the accelerated expansion of the Universe*, J. Cosmol. Astropart. Phys. **08**, 009 (2010).

[216] C.J. Feng; *Statefinder diagnosis for Ricci dark energy*, Phys. Lett. B **670**, 231 (2008).

[217] Y.B. Wu, S. Li, M.H. Fu, J. He; *A modified Chaplygin gas model with interaction*, Gen. Relativ. Grav. **39**, 653 (2007).

[218] T.K. Mathew, J. Suresh, D. Divakaran; *Modified holographic Ricci dark enegy model and statefinder diagnosis for flat universe*, Int. J. Mod. Phys. D **22**, 1350056 (2013).

[219] Z.G. Huang, X.M. Song, H.Q. Lu, W. Fang; *Statefinder diagnostic for dilaton dark energy*, Astrophys. Space Sci. **315**, 175 (2008).

[220] B. Wang, Y. Gong, E. Abdalla; *Thermodynamics of an accelerated expanding universe*, Phys. Rev. D **74**, 083520 (2006).

[221] B. Feng et al.; *Dark energy constraints from the cosmic age and supernova*, Phys. Lett. B **607**, 35 (2005)

[222] S. Chattopadhyay; *Modified Chaplygin gas equation of state on viscous dissipative extended holographic Ricci dark energy and the cosmological consequences*, Int. J. Mod. Phys. D **26**, 1750042 (2017)

[223] K. Bamba, S. Capozziello, S. Nojiri, S.D. Odintsov; *Dark energy cosmology: the equivalent description via different theoretical models and cosmography tests*, Astrophys. Space Sci. **342**, 155 (2012).

[224] S. Nojiri, S.D. Odintsov, S. Tsujikawa; *Properties of singularities in the (phantom) dark energy universe*, Phys. Rev. D **71**, 063004 (2005).

[225] S. Nojiri, S.D. Odintsov; *Future evolution and finite-time singularities in F(R) gravity unifying inflation and cosmic acceleration*, Phys. Rev. D **78**, 046006 (2008).

[226] S. Capozziello, M.De. Laurentis, S. Nojiri, S.D. Odintsov; *Classifying and avoiding singularities in the alternative gravity dark energy models*, Phys. Rev D **79**, 124007 (2009).

[227] S. Myrzakul, R. Myrzakulov, L. Sebastiani; *Inhomogeneous viscous fluids in FRW universe and finite-future time singularities*, Astrophys. Space Sci. **350**, 845 (2014).

[228] G.S. Khadekar, D. Raut, V.G. Miskin; *FRW viscous cosmology with inhomogeneous equation of state and future singularity*, Mod. Phys. Lett. A **29**, 1550144 (2015).

[229] G.M. Kremer, F.P. Devecchi; *Viscous cosmological models and accelerated universes*, Phys. Rev. D **67**, 047301 (2003).

[230] J.C. Fabris, S.V.B. Goncalves, R. de S*á* Ribeiro; ***, Gen. Relativ. Gravit. **38**, 495 (2006).

[231] C.W. Misner, K.S. Thorne, J.A. Wheeler; *Gravitation*, Freeman, New York (1973).

[232] D.J. Liu, W.Z. Liu; *Statefinder diagnostic for cosmology with the abnormally weighting energy hypothesis*, Phys. Rev. D **77**, 027301 (2008).

[233] P.A.R. Ade et al.; *Planck 2015 results*, Astron. Astrophys. **594**, A13 (2016).

[234] G.W. Gibbons, S.W. Hawking; *Cosmological event horizon, thermodynamics, and particle creation*, Phy. Rev. D **15**, 2738 (1977).

[235] T.K. Mathew, R. Aiswarya, K.S. Vidya; *Cosmological horizon entropy and generalized second law for flat Friedmann universe*, Eur. Phys. J. C **73**, 2619 (2013).

[236] K. Karami, A. Sheykhi, N. Sahraei, S. Ghaffari; *Generalized second law of thermodynamics in modified FRW cosmology with corrective entropy- area relation*, Europhys. Lett. **93**, 29002 (2011).

[237] A. Sasidharan, T.K. Mathew; *Bulk viscous matter and recent acceleration of the Universe*, Eur. Phys. J. C **75**, 348 (2015); [arXiv:gr-qc/1411.5154].

[238] S.F. Wu, B. Wang, G.H. Yang, P.M. Zhang; *The generalised second law of thermodynamics in generalized gravity theories*, Class. Quantum Grav. **25**, 235018 (2008).

[239] M. Sharif, M. Zubair; *Thermodynamic behavior of particular $f(R,T)$ gravity model*, J. Exper. Theor. Phys. **117**, 248 (2013).

[240] D. Momeni, P.H.R.S. Moraes, R. Myrzakulov; *Generalized second law of thermodynamics in $f(R,T)$ theory of gravity*, Atro. Space Sci. **361**, 228 (2016).

[241] T.K. Mathew, M.B. Aswathy, M. Manoj; *Cosmology and thermodynamics of FLRW universe with bulk viscous stiff fluid*, Eur. Phy. J. C **74**, 3188 (2014).

[242] E. Komatsu et al.; *$WMAP$ Collaboration, Seven-year Wilkinson Microwave Anisotropy Probe (WMAP) observations: Cosmological interpretation*, Astrophys. J. Suppl. **192**, 18 (2011).

[243] N. Suzuki et al.; *The Hubble Space Telescope Cluster Supernova Survey. v. Improving the Dark-Energy Constraints Above $z > 1$ and Building an Early-Type-Hosted Supernova Sample*, Astrophys. J. **746**, 85 (2012).

[244] J.D. Barrow; *Cosmic no-hair theorems and inflation*, Phys. Lett. B **187**, 12 (1987).

[245] J.D. Barrow; *Exact inflationary universes with potential minima*, Phys. Rev D, **49**, 3055 (1994).

[246] G.F.R. Ellis, M.S. Madsen; *Exact scalar field cosmologies*, Class. Quantum Grav. **8**, 667 (1991).

[247] J.D. Barrow, P. Parsons; *Inflationary models with logarithmic potentials*, Phys. Rev. D **52**, 5576 (1995).

[248] P. Parsons, J.D. Barrow; *Generalized scalar field potentials and inflation*, Phys. Rev. D **51**, 6757 (1995).

[249] A.A. Coley, J. Ibanez, R.J. Van de Hoogen; *Homogeneous scalar field cosmologies with an exponential potential*, J. Math. Phys. **38**, 5256 (1997).

[250] E.J. Copeland, A.R. Liddle, D. Wands; *Exponential potentials and cosmological scaling solutions*, Phys. Rev. D **57**, 4686 (1998).

[251] I.P.C. Heard, D. Wands; *Cosmology with positive and negative exponential potentials*, Class. Quantum Grav. **19**, 5435 (2002).

[252] E.J. Copenland, S. Mizuno, M. Shaeri; *Dynamics of a scalar field in Robertson-Walker spacetimes*, Phy. Rev. D **79**, 103515 (2009).

[253] M. Tegmark et al.; *(SDSS Collaboration), Cosmological parameters from SDSS and WMAP*, Phys. Rev. D **69**, 103501 (2004).

[254] J. Donkley et al.; *(WMAP Collaboration), Five-Year Wilkinson Microwave Anisotropy Probe (WMAP) Observations: Likelihoods and Parameters from the WMAP data*, Astrophys. J. Suppl. **180**, 306 (2009).

[255] C.J. Copi, D. Huterer, G.D. Starkman; *Multipole vectors: A new representation of the CMB sky and evidence for statistical anisotropy or non-Gaussianity at* $2 \leq l \leq 8$, Phys. Rev. D **70**, 043515 (2004).

[256] A. Bernui, B. Mota, M.J. Reboucas, R. Tavakol; *A note on the large-angle anisotropies in the WMAP cut-sky maps*, Int. J. Mod. Phys. D **16**, 411 (2007).

[257] G.F.R. Ellis; *The Bianchi models: Then and now*, Gen. Rel. Grav. **38**, 1003 (2006).

[258] M. Demianski, R. De Ritis, C. Rubano, P. Scudellaro; *Scalar fields and anisotropy in cosmological models*, Phys. Rev. D **46**, 1391 (1992).

[259] B. Saha, T. Boyadjiev; *Bianchi type-I cosmology with scalar and spinor fields*, Phys. Rev. D **69**, 124010 (2004).

[260] T.Q. Do, W.F. Kao, I.C. Lin; *Anisotropic power-law inflation for a two scalar fields model*, Phys. Rev. D **83**, 123002 (2011).

[261] C.R. Fadragas, G. Leon, E.N. Saridakis; *Dynamical analysis of anisotropic scalar-field cosmologies for a wide range of potentials*, Class. Quantam Grav. **31**, 075018 (2014); [arXiv:gr-qc/1308.1658].

[262] Ø. Grøn; *Expansion isotropization during the inflationary era*, Phys. Rev. D, **32**, 2522 (1985).

[263] Ø. Grøn; *Viscous inflationary universe models*, Astrophys. space Sci. **173**, 191 (1990).

[264] B. Saha, V. Rikhvitsky; *Bianchi type I universe with viscous fluid: A qualitative analysis*, Physica D **219**, 168 (2006).

[265] S. Kumar, C.P. Singh; *Anisotropic Bianchi type-I models with constant deceleration parameter in general relativity*, Astrophys. Space Sci. **312**, 57 (2007).

[266] B.J. Carr, J.E. Lidsey; *Primordial black holes and generalized constraints on chaotic inflation*, Phys. Rev. D **48**, 543 (1993).

[267] M.S. Berman, F.M. Gomide; *Cosmological models with constant deceleration parameter*, Gen. Relativ. Gravit. **20**, 191 (1988).

[268] V.B. Johri, D. Kalyani; *Cosmological models with constant deceleration parameter in Brans-Dicke theory*, Gen. Relativ. Gravit. **26**, 1217 (1994).

[269] S. Sen, N. Banerjee; *Exact Scalar Field Cosmology with Causal Viscous Fluid*, Astrophys. Space Sci. **254**, 133 (1997).

[270] C.P. Singh, V. Singh; *FRW models with perfect fluid and scalar field in higher derivative theory*, Mod. Phys. Lett. A **26**, 1495 (2011).

[271] L.P. Chimento; *Isotropic and anisotropic N-dimensional cosmologies with exponential potentials*, Class. Quantum Grav. **15**, 965 (1998).

[272] J.W. Van Holten; *Cosmic scalar fields with flat potential*, Mod. Phys. Lett. A **17**, 1383 (2002).

[273] J.G. Russo; *Exact solution of scalar field cosmology with exponential potentials and transient acceleration*, Phys. Lett. B **600**, 185 (2004); [arXiv : hep-th /0403010].

[274] R.R. Caldwell, M. Kamionkowski; *The Physics of Cosmic Acceleration*, Annu. Rev. Nucl. Part. Sci. **59**, 397 (2009).

[275] S.V. Sushkov; *Exact cosmological solutions with nonminimal derivative coupling*, Phys. Rev. D **80**, 103505 (2009).

[276] E.N. Saridakis, S.V. Sushkov; *Quintessence and phantom cosmology with nonminimal derivative coupling*, Phys. Rev. D **81**, 083510 (2010); [arXiv : gr-qc /1002.3478].

[277] V. Singh, C.P. Singh; *Modified $f(R,T)$ Gravity Theory and Scalar Field Cosmology*, Astrophys. Space Sci. **355**, 2183 (2014).

[278] P.G. Ferreira, M. Joyce; *Cosmology with a primordial scaling field*, Phys. Rev. D **58**, 023503 (1998).

[279] J.D. Barrow, M.S. Turner; *Inflation in the Universe*, Nature **292**, 35 (1981).

[280] G. Steigman, M.S. Turner; *Inflation in a shear- or curvature-dominated universe*, Phys. Lett. B **128**, 295 (1983).

[281] Ø, Grøn; *Expansion isotropization during the inflationary era*, Phys. Rev. D **32**, 2522 (1985).

[282] Ø, Grøn; *Transition of rotating Bianchi type-IX cosmological model into an inflationary era*, Phys. Rev. D **33**, 1204 (1986).

[283] E. Martinez-Gonzalez, B.J.T. Jones; *Primordial shear and the question of inflation*, Phys. Lett. B **167**, 37 (1986).

[284] S.D. Maharaj, A. Beesham; ***, S. Afr. J. Phys. **17**, 34 (1988).

[285] C.G. Hewitt, J. Wainwright; *Dynamical systems approach to titled Bianchi cosmologies: Irrotational models of type V*, Phys. Rev. D **46**, 4242 (1992).

[286] U. Camci, I. Yavuz, H. Baysal, I. Tahran, I. Yilmaz; *Generation of Bianchi Type V Universes Filled with A Perfect Fluid*, Astrophys. Space Sci. **275**, 391 (2001).

[287] R. Bali, B.L. Meena; *Conformally flat tilted Bianchi Type-V cosmological models in general relativity*, Pramana J. Phys. **62**, 1007 (2004).

[288] A. Pradhan, A. Rai; *Tilted bianchi type V bulk viscous cosmological models in general relativity*, Astrophys. Space Sci. **291**, 149 (2004).

[289] A. Pradhan, L. Yadav, A.K. Yadav; *Viscous fluid cosmological models in LRS Bianchi type V universe with varying ?*, Czech. J. Phys. **54**, 487 (2004).

[290] O. Aydogdu, M. Salti; *The momentum 4-vector in bulk viscous Bianchi type-V space-time*, Czech. J. Phys. **56**, 789 (2006).

[291] C.P. Singh, S. Ram, M. Zeyauddin; *Bianchi type-V perfect fluid space-time models in general relativity*, Astrophys. Space Sci. **315**, 181 (2008).

[292] C.P. Singh, M. Zeyauddin, S. Ram; *Some Exact Bianchi Type V Perfect Fluid Solutions with Heat Flow*, Int. J. Theor. Phys. **47**, 3162 (2008).

[293] C.P. Singh, A. Beesham; *Anisotropic Bianchi- Perfect Fluid space–time with variables G and ?*, Int. J. Mod. Phys. A **25**, 3825 (2010).

[294] C.P. Singh; *Bianchi -V Space -Time with Anisotropic Dark Energy in General Relativity*, Braz. J. Phys. **41**, 323 (2011).

[295] A. Pradhan, H. Amirhashchi; *Accelerating Dark Energy Models in Bianchi Type-V Spacetime*, Mod. Phys. Lett. A **26**, 2261 (2011).

[296] S. Kumar, A. Yadav; *Some Bianchi Type-v Models of Accelerating Universe With Dark Energy*, Mod. Phys. Lett. A **26**, 647 (2011).

[297] S. Kumar; *Anisotropic model of a dark energy dominated universe with hybrid expansion law*, Grav. and Cosmo. **19**, 284 (2013).

[298] S. Chandel, S. Ram; *Bianchi type-V early-decelerating and late-time-accelerating cosmological model with a perfect fluid and heat conduction*, Can. J. Phys. **93**, 632 (2015).

[299] H. Farajollahi, F. Tayebi; *Varying Alpha in Bianchi type-V universe*, Astrophys. Space Sci. **359**, 28 (2015).

[300] C.P. Singh, M. Srivastava; *Minimally coupled scalar field cosmology in anisotropic cosmological model*, Pramana J. Phys. **88**, 22 (2017).

[301] B. Gumjudpai; *Quintessential Power-law Cosmology: Dark Energy equation of state*, Mod. Phys. Lett. A **28**, 1350122 (2013).

[302] B. Saha; *Bianchi Type-V Dark Energy Model with Varying EoS Parameter*, Int. J. Theor. Phys. **52**, 1314 (2013).

[303] T. Singh, R. Chaubey; *Bianchi type-V model with a perfect fluid and A-term*, Pramana J. Phys. **67**, 415 (2006).

[304] B. Saha; *Nonlinear Spinor Fields in Bianchi Type-V Spacetime*, Chinese J. Phys. **53**, 110114 (2015).

[305] J.J. Halliwell; *Scalar fields in cosmology with an exponential potential*, Phys. Lett. B **185**, 341 (1987).

[306] L. Berezhiani, J. Khoury, J. Wang; *Universe without dark energy: Cosmic acceleration from dark matter-baryon interactions*, Phys. Rev. D **95**, 123530 (2017); [arXiv:1612.00453/hep-th]

List of Publications

1. **Milan Srivastava** and C. P. Singh; *Cosmological evolution of non-interacting and interacting holographic dark energy model in Brans-Dicke theory*, International Journal of Geometric Methods in Modern Physics **15**, 1850124 (2018). **Impact Factor (1.068)**

2. C. P. Singh and **Milan Srivastava**; *Viscous cosmology in new holographic dark energy model and the cosmic acceleration*, European Physical Journal C **78**, 190 (2018). **Impact Factor (5.331)**

3. **Milan Srivastava** and C. P. Singh; *New holographic dark energy model with constant bulk viscosity in modified $f(R,T)$ gravity theory*, Astrophysics and Space Science **363**, 117 (2018). **Impact Factor (1.885)**

4. **Milan Srivastava** and C. P. Singh; *Evolution and thermodynamics of bulk viscous new holographic dark energy in $f(R,T)$ gravity*, Communicated in a journal; [arXiv:1804.05693 [gr-qc]].

5. C. P. Singh and **Milan Srivastava**; *Miminally coupled scalar field cosmology in anisotropic cosmological model*, Pramana Journal of Physics **88**, 22 (2017). **Impact Factor (0.699)**

6. C. P. Singh and **Milan Srivastava**; *Dynamics of Bianchi V anisotropic model with perfect fluid and scalar field*, Indian Journal of Physics **91**, 1645 (2017). **Impact Factor (0.988)**
